Regulation of platelet production and function by ITIM-containing receptors

By

CHRISTOPHER WILLIAM SMITH

A thesis submitted to the University of Birmingham for the degree of DOCTOR OF PHILOSOPHY

Institute of Cardiovascular Sciences
College of Medical and Dental Sciences
University of Birmingham
October 2018

Abstract

Platelets are small highly reactive anucleate cells that circulate in the blood and regulate haemostasis and thrombosis. Understanding the mechanisms regulating platelet function has implications for health and disease. Immunoreceptor tyrosine-based inhibition motif (ITIM)-receptors regulate megakaryocyte and platelet function. The aim of this thesis was to determine the role of ITIM-receptors LAIR-1 and TLT-1 in platelet production and function. LAIR-1 ablation in megakaryocytes results in enhanced SFK activity which is transferred to platelets, rendering them hyper-reactive. LAIR-1 deficient mice exhibit enhanced ferric chloride, but not laser-induced thrombosis *in vivo*, correlating with GPVI hyper-reactivity observed *in vitro*. LAIR-1/PECAM-1 double deficient (DKO) mice were mildly thrombocythemic, with platelets hyper-responsive to GPVI activation *in vitro*. Interestingly, DKO mice lacked the enhanced SFK activity and *in vivo* thrombosis phenotype of single KO mice. TLT-1 deficient mice exhibit mild thrombocytopenia, with normal aggregation responses to ITAM-receptor and GPCR activation *in vitro,* and haemostatic response *in vivo*. Reduced thrombus stability was observed following laser, but not ferric chloride-injury in deficient mice, due to marked reduction in α-granule secretion. In addition, TLT-1 was described as a highly sensitive platelet activation marker *in vivo*, rapidly detected and present throughout core and shell of thrombi.

Publications arising from this thesis

Smith CW, Thomas SG, Raslan Z, Patel P, Byrne M, Lordkipanidzé M, Bem D, Meyaard L, Senis YA, Watson SP, Mazharian A. Mice lacking the inhibitory collagen receptor LAIR-1 exhibit a mild thrombocytosis and hyperactive platelets. ***Arteriosclerosis, Thrombosis, and Vascular Biology***. 2017; 37:823-835

Smith CW, Raslan Z, Parfitt L, Kahn AO, Patel P, Senis YA, Mazharian A. TREM-like transcript 1: a more sensitive marker of platelet activation than P-selectin in humans and mice. ***Blood Advances***. 2018; 2(16):2072-2078

Smith CW, Patel P, Geer MJ, Pike JA, Senis YA, Mazharian A. LAIR-1 and PECAM-1 function via the same pathway to mediate inhibition of platelet aggregation. ***Arteriosclerosis, Thrombosis, and Vascular Biology***. (Submitted)

Smith CW, Washington AV, Mazharian A. TREM-like transcript-1 a non-conventional ITIM-containing receptor. ***Journal of Thrombosis and Haemostasis***. (Invited review in preparation)

Smith CW, Raslan Z, Patel P, Mori J, Senis YA, Mazharian A. TLT-1 deficient mice display reduced α-granule secretion and thrombus stability. ***Blood***. (In preparation)

Acknowledgements

Firstly, I would like to thank my supervisor Alexandra Mazharian for giving me the opportunity to do my PhD in her lab, and for all her help and guidance throughout. I would also like to thank my co-supervisor Yotis Senis for his advice and necessary ‘training’. Thanks to the University of Birmingham Biomedical Services Unit for their help and support with animal work and the College for funding.

I would like to thank all members of the Birmingham Platelet Group past and present for putting up with me for the last 3 years, I know it cannot have been easy. Particularly; Abs for the nonsense, Annabel for eating all my biscuits, Elizabeth for the group emails, Mitch and his winning smile for the constant help, Natalie for the tea and Pip for his medical advice and failure to make me a believer. Also Stef, Beata and Gayle for keeping track of the lab, and Pushpa for all the genotyping. Finally, thank you to Jun and Deano, for training me and fixing all my intravital issues.

‘‘Yippee-ki-yay, motherfucker!’’

John McClane

Table of contents

Chapter 1

Chapter 2

Chapter 6

Chapter 7

List of figures

Chapter 1

Chapter 2

Chapter 3

Chapter 4

Chapter 5

Chapter 6

List of tables

Chapter 2

Chapter 3

Chapter 4

Chapter 6

Abbreviations

ADP	Adenosine diphosphate
ATP	Adenosine triphosphate
AUC	Area under the curve
BSA	Bovine serum albumin
CEACAM1	Carcinoembryonic antigen related cell adhesion molecule 1
CEACAM2	Carcinoembryonic antigen related cell adhesion molecule 2
CLEC-2	C-type lectin 2
CRP	Collagen related peptide (cross-linked)
Csk	C-terminal Src kinase
ECM	Extracellular matrix
ER	Endoplasmic reticulum
ERK	Extracellular signal-regulated kinase
FAK	Focal adhesion kinase
FcR	Fc receptor
GP	Glycoprotein
GPCR	G-protein coupled receptor
HSC	Haematopoietic stem cell
Ig	Immunoglobulin
ITAM	Immunoreceptor tyrosine-based activation motif
ITIM	Immunoreceptor tyrosine-based inhibition motif
ITSM	Immunoreceptor tyrosine-based switch motif
kDa	Kilodalton
KO	Knock-out
LAIR-1	Leukocyte associated inhibitory receptor-1
LAT	Linker of activated T-cells
LILRB2	Leukocyte immunoglobulin-like receptor B2
MAPK	Mitogen-activated protein kinase
MFI	Median fluorescence intensity
PAR	Protease-activated receptor
PCR	Polymerase chain reaction
PECAM-1	Platelet endothelial cell adhesion molecule-1
PGI2	Prostaglandin I2
PI3K	Phosphoinositide 3-kinase
PIR-B	Paired immunoglobulin-like receptor B
PLC	Phospholipase C
PRP	Platelet rich plasma
PRR	Proline rich region
PS	Phosphatidylserine
PTK	Protein tyrosine kinase
PTP	Protein tyrosine phosphatase

p-Tyr	Phosphor-tyrosine
RT	Room temperature
SAC	surface area coverage
SCF	Stem cell factor
SDF1α	Stromal cell derived factor 1α
SDS-PAGE	Sodium dodecyl sulfate-polyacrilamide electrophoresis
SEM	Standard error of the mean
SFK	Src family kinase
SH2	Src homology 2 domain
SH3	Src homology 3 domain
SHIP	SH2 domain containing inositol phosphatase
Shp	SH2 domain containing PTP
Syk	Spleen tyrosine kinase
TLT-1	Triggering receptor expressed on myeloid cells-like transcript-1
TPO	Thrombopoietin
TxA2	Thromboxane A2
vWF	von Willebrand factor
WCL	Whole cell lysate
WT	Wild type

CHAPTER 1

General Introduction

1.1. Platelets

Platelets are small highly reactive anucleic cells that circulate in the blood and are critically important in maintaining vascular integrity and preventing blood loss. Although their primary role is maintaining haemostasis, platelets also contribute to pathophysiological processes including atherogenesis, cancer metastasis and inflammation, as well as playing a central role in wound healing (Li et al., 2010, Engelmann and Massberg, 2013, Franco et al., 2015, Menter et al., 2017). These processes are dependent on the transition of platelets to an activated state. Surface proteins on circulating resting platelets bind their respective ligands, inducing intracellular signalling pathways producing rapid platelet activation. Understanding the modulation of platelet activity by inhibitory signals is therefore critical in order to target the pathophysiological functions of platelets.

1.1.1. Thrombosis and haemostasis

Platelets have been known to play a role in haemostasis and thrombosis for over 130 years. In 1882, Bizzozero observed disk shaped platelets circulating in guinea pig mesenteric venules that formed aggregates at sites of vascular damage and also observed leukocyte recruitment to the platelet aggregates. (Bizzozero, 1882). Thrombus formation is the best characterised function of platelets, essential to prevent blood loss at sites of vascular damage (Clemetson, 2012). Inappropriate activation of platelets through the same mechanisms at sites of vascular inflammation, such as atherosclerotic plaques, however can obstruct blood flow (Franco et al., 2015, Lindemann et al., 2007, Lievens and von Hundelshausen, 2011). Directly, by forming an occlusive thrombus, or indirectly by occluding smaller vessels downstream following clot embolization. The subsequent ischemia caused can result in myocardial infarction or stroke, which account for 26% of UK deaths in 2015 (BHF 2017).

1.1.2. Non-canonical roles

Primarily known for their role in haemostasis and thrombosis, growing evidence suggests this is only one of many important roles platelets play in both health and disease (Franco et al., 2015, Morrell et al., 2014). Increasing evidence has shown an important role of platelets in inflammation, angiogenesis and wound healing (Kubes, 2016, Walsh et al., 2015, Nurden et al., 2008).

Platelets act as immune sensing cells, able to detect, bind and retain pathogens such as bacteria and viruses on their plasma membrane or internally (Flaujac et al., 2010, Assinger, 2014, Yeaman, 2010b, Yeaman, 2010a, Kapur and Semple, 2016, Jenne and Kubes, 2015). Activated platelets also release antimicrobial mediators eliminating pathogens directly (Jenne and Kubes, 2015). Through binding or release of chemoattractants and soluble mediators such as CD40L platelets are able to recruit and activate leukocytes at sites of inflammation and infection(Andre et al., 2002). Platelet binding to adherent neutrophils also induces NET release, which capture and kill pathogens (Kim and Jenne, 2016). Various pro- and anti-inflammatory cytokines and chemokines are released by platelets which also affect wound repair (Mazzucco et al., 2010). In addition, studies have shown an important role of platelets in maintaining mature blood vessels (Ho-Tin-Noe et al., 2011), as well as a role facilitating cancer metastasis, shielding cancerous cells from the immune response and assisting their adhesion to endothelium (Leblanc and Peyruchaud, 2016, Franco et al., 2015). All these functions are dependent on platelet activation; therefore the ability to effect platelet activation has various implications in health and disease.

1.2. Platelet physiology

1.2.1. Structure

Typically 2-5 µm in diameter and 6-10 fl in volume, platelets are the smallest cells in the blood (mouse platelets: mean diameter 0.5µm and mean volume 3-4 fl) (White, 2013, Schmitt et al., 2001). Resting platelets are discoid in shape, which becomes irregular upon activation (Packham, 1994, Schmitt et al., 2001). Platelets are terminally differentiated anucleic cell fragments of megakaryocytes. All other organelles (mitochondria, endoplasmic reticulum, golgi apparatus and lysosomes) are present (White, 2013). The platelet plasma membrane is relatively smooth with small randomly dispersed openings to the surface connected open canalicular system (OCS), the chief source of membrane for surface area expansion during activation and spreading (White, 2013).

Platelets contain extensive cytoskeletal networks made up of actin, tubulin and their associated binding proteins (Sorrentino et al., 2015). In flowing blood the discoid shape and size of resting platelets means they are pushed to the vessel edge, allowing them to detect vascular damage to endothelium surface rapidly (Hartwig, 2013). Responsible for this shape is the marginal coil, a long microtubule encircling the platelet perimeter (8-12 times) just below the plasma membrane (Sorrentino et al., 2015, Hartwig, 2013). The most abundant protein in platelets, actin, forms filaments (F-actin) which are cross linked by the actin binding proteins filamin and α-actinin into a framework supporting the platelet. Via spectrin tetramers and several binding proteins, actin is able to interact with the plasma membrane and integrins (Sorrentino et al., 2015). Upon activation, platelets rapidly lose the discoid shape. This morphological transformation results from disassembly of the marginal microtubule coil, and greater assembly of F-actin creating filopodia and lamellipodia (Sorrentino et al., 2015, Aslan et al., 2012).

1.2.2. Granules

Alpha

Platelets also contain granules, of which α-granules are the largest (0.2-0.5 nm diameter) and most abundant. Containing both membrane bound and soluble proteins, α-granules following activation fuse with the platelet membrane and facilitate platelet adhesion by releasing their soluble cargo (fibrinogen, fibronectin, thrombospondin, vitronectin and Von Willebrand factor [vWF]) and exposing their membrane bound receptors on the platelet surface (Flaumenhaft, 2013, Handagama et al., 1990). Most of the membrane bound α-granule proteins (αIIbβ3 and GPIb-IX-V) are already present on the platelet surface. P-selectin however is absent, and only expressed on the surface following α-granule secretion (Harrison and Cramer, 1993, Whiteheart, 2011).

Dense

Dense granules, characterised by an electron dense matrix, are fewer and smaller (0.15 nm diameter) than α-granules. Containing high concentrations of the secondary mediators ADP and ATP as well as serotonin, dense granule secretion supports thrombus growth through local activation of platelets (Flaumenhaft, 2013, White, 1969, Whiteheart, 2011).

Lysosomes

Also present in platelets are lysosomes, containing acid hydrolases involved in the degradation of proteins, carbohydrates and lipids (Flaumenhaft, 2013). Although the function of platelet lysosomes are not well studied, secretion of their contents upon strong activation has been shown, and may play important extracellular roles such as receptor cleavage, fibrinolysis and ECM degradation (Heijnen and van der Sluijs, 2015).

1.3. Platelet production and clearance

1.3.1. Megakaryocyte development

In adults, megakaryocytes are derived from haematopoietic stem cells (HSCs), residing primarily in the bone marrow, which undergo long-term self-renewal (Machlus and Italiano, 2013). Classically HSCs gradually develop into multipotent progenitors (MPP) before becoming lineage committed able to give rise to either myeloid or lymphoid cells. Following commitment to the myeloid lineage, common myeloid progenitors (CMPs) develop into bipotent megakaryocyte-erythrocyte (MEP) and granulocyte-macrophage progenitors (GMP) and then unipotent progenitors which develop into mature progeny (Laurenti and Gottgens, 2018, Hunt, 1995, Debili et al., 1996).

Recently however, this classical model has been challenged by the identification of new progenitor populations. Lymphoid-primed multipotent progenitors (LMPPs) were identified as a population retaining high proliferative and lympho-myeloid differentiation potential, but unable to take on erythroid of megakaryocyte lineage fates (Adolfsson et al., 2001). A megakaryocyte -biased HSC population expressing vWF has also been discovered, as well as a subpopulation of HSCs, stem-like megakaryocyte-committed progenitors (SL-MkPs) which are activated upon inflammatory stress, but remain quiescent during homeostasis, although primed to megakaryocyte-commitment (Haas et al., 2015, Sanjuan-Pla et al., 2013).

Studies utilizing clonal tracking have also distinguished restricted megakaryocyte potential in HSCs or their direct progeny, resulting in a new model of megakaryocyte development, with heterogeneous HSCs that bypass classical intermediate progenitors and give rise to MK progenitors directly (Shin et al., 2014, Grinenko et al., 2014). Yet classical megakaryocyte-committed pathways can also occur in parallel (Woolthuis and Park, 2016).

1.3.2. Megakaryocyte Maturation and Differentiation

Megakaryocytes become polyploid through endomitosis – repeated cycles (2-6) of DNA replication without cellular division – resulting in cells of up to 64N in humans (and 128N in rodents) (Vitrat et al., 1998, Nagata et al., 1997). Polyploidization increases protein synthesis in parallel with enlargement of the cell (Raslova et al., 2003, Ravid et al., 2002). Following endomitosis is a maturation stage where the cytoplasm is filled with platelet specific proteins and organelles ready for packaging and subdivision into platelets. It is during this stage that granules are formed along with the invaginated membrane system (IMS) and dense tubular system (Kahr et al., 2013).

The IMS is formed progressively through maturation from the plasma membrane which enfolds forming tubular invaginations which permeate the cytoplasm but are still in contact with the external milieu. The primary function of the IMS is as a membrane reservoir for proplatelet formation (Eckly et al., 2014, Eckly et al., 2012, Radley and Haller, 1982, Schulze et al., 2006). The primary driver of megakaryocyte differentiation is the cytokine thrombopoietin (TPO). Discovered along with its receptor c-Mpl in the early 1990s (Zeigler et al., 1994, de Sauvage et al., 1994), TPO facilitated the development of cell culture systems that reconstitute megakaryocyte differentiation and proplatelet formation *in vitro*, enabling these mechanisms to be studied (Machlus et al., 2014, Cramer et al., 1997, Lecine et al., 1998). Binding of TPO to c-Mpl results in receptor dimerization and downstream signalling (Kaushansky, 2005). c-Mpl expression is restricted to megakaryocytes and platelets, with elimination of either leading to sever thrombocytopenia, due to reduced progenitor and mature megakaryocyte numbers, and decreased megakaryocyte maturation (Machlus et al., 2014, Gurney et al., 1994). Produced by the liver, the circulating plasma concentration of TPO varies inversely to platelet number (Machlus et al., 2014). This is due to platelet c-Mpl receptors binding and removing TPO from

the plasma, thus increasing platelet number increases removal of circulating TPO. Accordingly during thrombocytopenia, elevated TPO levels drive platelet production (Machlus et al., 2014, Hitchcock and Kaushansky, 2014).

Dimerization of c-Mpl upon TPO binding enables associated janus activated kinase-2 (JAK2) trans-autophosphorylation, and leads to signalling of phosphoinositide 3-kinase (PI3K) and the mitogen activated protein kinases (MAPKs) extracellular signal-regulated kinases 1 and 2 (ERK1/2) and p38 downstream (Kaushansky, 2005). Interaction of these with transcription factors alters gene expression to increase HSC proliferation and megakaryocyte maturation (Kaushansky, 2005).

1.3.3. Proplatelet formation and platelet release

Once mature, megakaryocytes extend long thin branching cytoplasmic processes, termed proplatelets, into the sinusoidal blood vessels of the bone marrow, where they fragment releasing platelets into the circulation (Tavassoli and Aoki, 1989, Dutting et al., 2017). The process of proplatelet formation originates with pseudopod formation which then elongates from the plasma membrane. This elongation is dependent on and powered by the microtubule cytoskeleton, which undergoes dramatic reorganization, lining the entire length of proplatelet extensions and looping at the distal end to form tear shaped platelet size structures (Bender et al., 2015). The motor protein dynein is also critical to this process, driving elongation through microtubule sliding (Machlus et al., 2014, Patel et al., 2005, Tanenbaum et al., 2013).

Actin also plays a role, forcing the proplatelet shafts to bend, kink and bifurcate amplifying the number of extensions and therefore number of sites platelets can be formed (Italiano et al., 1999). Although the proplatelet shaft has multiple platelet sized swellings, fragmentation and release only occurs from the tips of proplatelets as the swellings along the shaft lack

microtubule coils (Italiano et al., 1999, Radley and Hartshorn, 1987). The anucleic fragments released from the ends of proplatelets are typically larger than platelets, these barbell shaped preplatelets undergo fission in the circulation, dividing into platelets **(Figure 1. 1)** (Thon et al., 2012, Thon et al., 2010). Multiphoton microscopy has enabled visualisation of this process in the intact bone marrow of mice, with proplatelets seen to provide and release fragments which typically exceed platelet dimensions into the marrow vasculature (Junt et al., 2007). This also demonstrated the importance of the hydrodynamic shear stress from flowing blood on release of intravascular extensions into peripheral blood.

During proplatelet formation the megakaryocytes entire intracellular contents, is trafficked along the microtubules and concentrated within the platelet swellings along the proplatelet shaft (Richardson et al., 2005). The exception to this is the multi-lobed nucleus which is retained within the cell body before being extruded from the cell and degraded (McArthur et al., 2018). Recently it has been proposed that the lung is the primary site of thrombopoiesis. Using multiphoton intravital microscopy Lefrancais et al observed large circulating megakaryocytes pass through the microcirculation of the lung and produce proplatelet extensions in a flow dependent manner (Lefrancais et al., 2017). Following a single lung transplant model they found the platelet releasing megakaryocytes in the lung circulation originated extrapulmonarily, mostly from bone marrow (Lefrancais et al., 2017). This model is however controversial with multiple previous reports using intravital microscopy failing to observe large megakaryocytes migrating out of the bone marrow and entering the blood stream (Zhang et al., 2012, Stegner et al., 2017).

The trigger for proplatelet formation is currently not known, with the signals leading to this event still a significant gap in our understanding. Megakaryocytes reside in the bone marrow, an environment rich in ECM proteins including collagens, laminins and fibronectin. Collagen

type-I has been shown to inhibit megakaryocyte proplatelet formation preventing premature platelet release (Semeniak et al., 2016, Sabri et al., 2004, Sabri et al., 2006, Zou et al., 2009). Whereas collagen type-IV and laminins support proplatelet formation at the sinusoids (Balduini et al., 2008). GPVI and α2β1 the major activating collagen receptors on platelets are also expressed early in megakaryocyte differentiation. Recent work by the Schulze group has shown in megakaryocytes collagen type-I mediates inhibition by GPVI, however this inhibition is diminished at the vascular niche where collagen type-IV displaces type-I, thus promoting proplatelet formation (Semeniak et al., 2016). No positive enhancement of proplatelet formation was observed by bone marrow laminins or fibrinectin (Semeniak et al., 2016). Rather results suggest active inhibition of proplatelet formation is required instead of stimulatory signals (Semeniak et al., 2016).

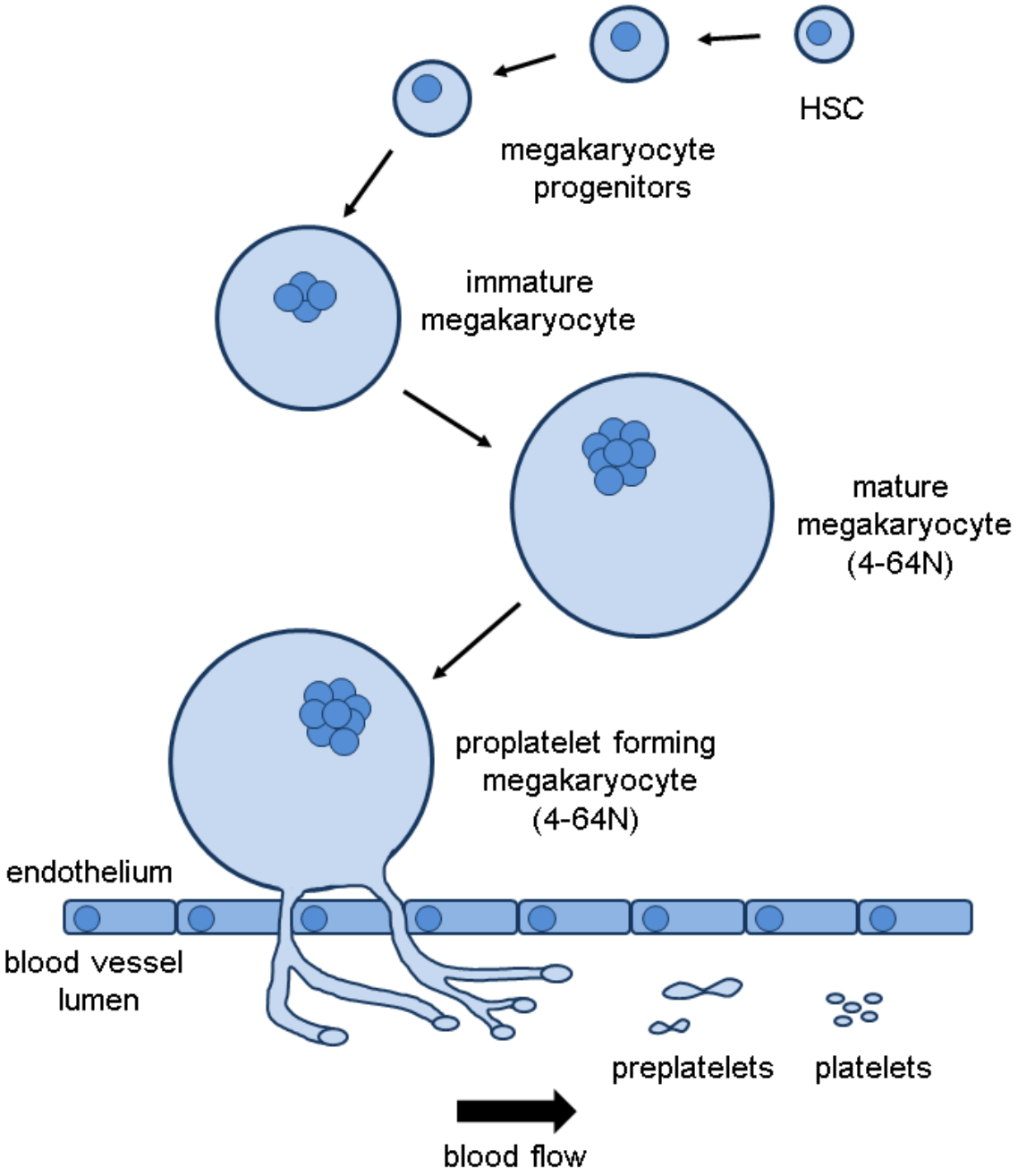

Figure 1. 1. Megakaryocyte maturation and platelet release. Megakaryocytes develop from haematopoietic stem cells (HSCs) residing in the bone marrow. Megakaryocytes become polyploid through process of endomitosis – repeated cycles of DNA replication without cellular division. Once mature, megakaryocytes extend long protrusions, termed proplatelets, into the sinusoidal blood vessels in a process powered by the microtubule cytoskeleton. Blood vessel shear stress then fragments the ends of these proplatelets, releasing preplatelets into the circulation. Preplatelet fragments are typically larger than platelets and undergo further division within the circulation producing mature platelets.

1.3.4. Platelet clearance and turnover

Platelet production and clearance are balanced in order to strictly control the number of circulating platelets. In humans, platelet counts range form 150 – 450 x 10^6/ml (600 – 1200 x 10^6/ml in mice), and approximately 100 billion new platelets are produced each day with an average lifespan of 7-10 days (3-5 days in mice). However, only a small proportion of platelets, during steady state conditions, are consumed through haemostasis. Old, defective and pre-activated platelets are rapidly removed from the circulation by macrophages resident in the spleen and liver (Josefsson et al., 2013). Platelet clearance is mediated by multiple mechanisms (Hoffmeister and Falet, 2016). Platelet desiaylation leads to increased β-gal exposure which the Ashwell Morell receptor on surface of hepatocytes and liver macrophages recognises inducing platelet clearance (Quach et al., 2018, Grozovsky et al., 2015). Antibody mediated clearance where opsonisation by autoantibodies, usually against αIIbβ3 and GPIB-IX, stimulate Fc-dependent clearance of platelets via macrophages (Quach et al., 2018).

1.4. Platelets in haemostasis and thrombosis

1.4.1. Primary role platelets

In order for platelets to perform their primary role and prevent blood loss, they must be able to sense and block sites of vascular damage rapidly. Also they must be able achieve this at a range of physiological shear rates, and without obstructing or occluding vessel blood flow. Enabling platelets to succeed in this are the expression of multiple surface proteins which all contribute to the formation of a stable thrombus. The process of thrombus formation is described below and illustrated in **Figure 1.2**.

Rolling and initiation. Initiation of platelet plug formation begins with the tethering, rolling and arrest of moving platelets (Brass, 2003, Offermanns, 2006). vWF present in the plasma

binds to extracellular matrix (ECM) collagens (type I and III) exposed at sites of vascular injury (Reininger, 2008, Kanaji et al., 2012). A1 domain binding sites then become exposed as the vWF is stretched by shear stress, allowing the GPIbα receptor on the platelet surface to bind, causing the tethering and slowing of the platelet to arrest (Clemetson, 2012).

Activation and firm adhesion. GPO (glycine-proline-hydroxyproline) repeats on the exposed collagens interact with the GPVI-Fc receptor (FcR) γ-chain complex on platelets producing strong activation signals (Clemetson, 2012). This triggers inside-out signalling, switching the conformation of integrins αIIbβ3 and α2β1 from low to high affinity state, enabling them to bind fibrinogen/fibrin and collagen respectively, resulting in stable platelet adhesion (Watson et al., 2005, Nieswandt et al., 2009).

Spreading. The binding of integrin αIIbβ3 to fibrinogen produces outside-in signalling and subsequent cytoskeletal rearrangement and spreading of the platelet (Calaminus et al., 2008, Durrant et al., 2017). First by extension of pseudopodia/filopodia and then by extension of lamellipodia, flattening and increasing the platelets surface area (Durrant et al., 2017). More platelets are then able to attach to the surface of activated platelets and through formation of tight junctions prevent blood loss (Clemetson, 2012).

Secretion and aggregation. Recruitment of circulating platelets to propagate the thrombus once all the exposed collagen is covered is through the local accumulation of soluble secondary mediators. ADP present in platelet granules is secreted, along with fibrinogen and vWF from activated platelets, which also release thromboxane A2 (TxA_2) by diffusion (Golebiewska and Poole, 2015). ADP produces powerful platelet activation through the G-protein coupled receptors (GPCRs) P2Y1 and P2Y12, which along with thromboxane receptor activation by TxA_2 enables circulating platelets to cross-linking to the platelet aggregate via vWF and fibrinogen binding through integrin αIIbβ3 (Brass, 2003, Golebiewska and Poole, 2015).

Thrombin generation. Procoagulant enzyme complex assembly is promoted on the surface of activated platelets by exposure of phosphatidylserine (PS), and leads to localized generation of thrombin through the proteolytic cleavage of prothrombin, by factor Xa and Va of the coagulation cascade (Ruggeri and Jackson, 2013). Thrombin is a major platelet activator, acting through protease activated receptor (PAR)-1 and -4 GPCRs in human (PAR-3 and 4 in mice), as well as converting fibrinogen to fibrin (Chen et al., 1994, Coughlin, 2005, Coughlin et al., 1992, Ishihara et al., 1997).

Clot stabilisation and contraction. Thrombin catalyses cleavage of fibrinogen to fibrin, which polymerises at growing thombus core. Fibrin binds integrin αIIbβ3 and further activates GPVI stabilizing the clot, preventing embolism (Mammadova-Bach et al., 2015). Contraction forces generated by non-muscle myosin II on actin cytoskeleton pulls platelets towards each other, retracting the thrombus reducing its size and preventing vessel occlusion (Lam et al., 2011, Kim et al., 2017). Clot contraction leads to full wound closure after formation (Sorrentino et al., 2015).

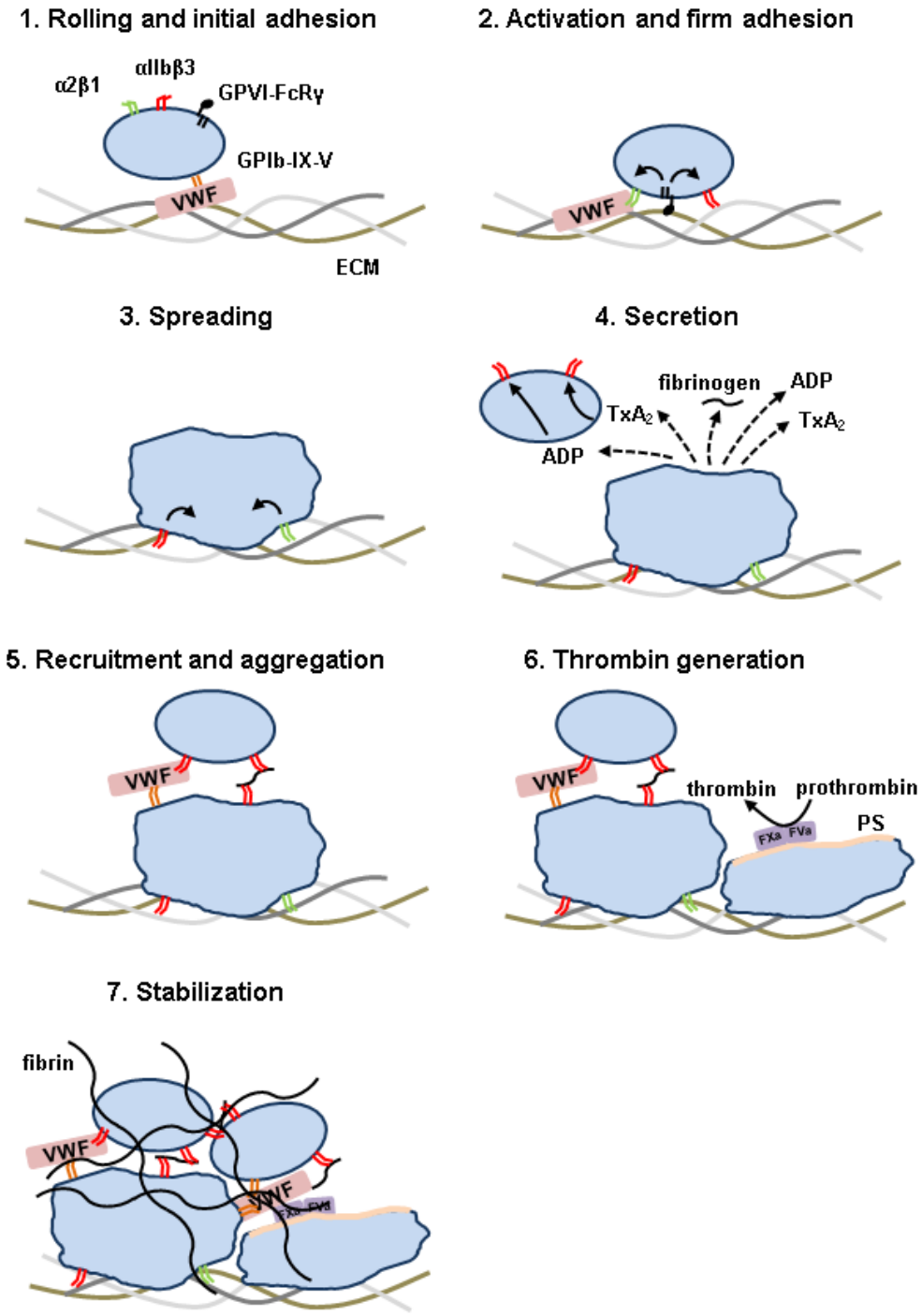

Figure 1. 2. Main stages of thrombus formation. Stages of primary of thrombus formation at sites of vascular injury. 1. Initial adhesion to the extracellular matrix (ECM); 2. Firm adhesion; 3. Integrin-mediated spreading; 4. Secretion of α- and dense granules; 5. Recruitment of platelets; 6. Thrombin generation and 7. Thrombus stabilisation by fibrin network generation.

1.5. Platelet activation

Platelet reactivity is determined by the interaction of their receptors with the range of agonists and adhesive proteins in their external environment. The major platelet surface receptors involved in haemostasis can be categorized as protein tyrosine kinase (PTK) linked receptors or GPCRs, with receptors involved at multiple stages of platelet function (Clemetson and Clemetson, 2013).

1.5.1. Adhesive PTK linked receptors

PTK linked receptors initiate primary platelet activation and mediate platelet adhesion.

1.5.1.1. GPIb-IX-V

Pivotal in initiating and propagating haemostasis and thrombosis, the vWF receptor complex GPIb-IX-V consists of GPIbα, GPIbβ, GPIX and GPV subunits. The largest of which, GPIbα, is involved in ligand binding, with vWF, P-selectin, thrombin and factor XII of the coagulation cascade among others all shown to interact (Andrews and Berndt, 2013, Berndt et al., 2001). Ligand binding produces intracellular signalling, with the cytoplasmic tail of GPIbα, filamin-1 and 14-3-ζ adaptor protein interacting with actin. The GPIbβ subunit also contributes to the signalling of the complex through 14-3-ζ binding and phosphorylation of a serine residue that regulates actin polymerisation (Dai et al., 2005).

1.5.1.2. Integrins αIIbβ3 and α2β1

Following vWF mediated tethering and arrest of platelets, integrins bind and stabilize platelet adhesion to ECM proteins. Uniquely expressed on platelets, αIIbβ3 is the major platelet adhesive integrin which binds fibrinogen, fibronectin and vWF through recognition of a

common RGD (Arg-Gly-Asp) sequence (Nieswandt et al., 2009, Bennett et al., 2009). The collagen receptor integrin α2β1, is also important, and along with supplemental binding of integrins α5β1 (fibronectin), α6β1 (laminin) and αVβ3 (vitronectin) results in firm platelet adhesion. Central to their function, integrins undergo activation by inside-out signalling, switching them from a low to a high affinity state (Clemetson and Clemetson, 2013, Bledzka et al., 2013). Initiation of this mechanism is triggered through engagement of various adhesion receptors and GPCRs.

Ligand binding to αIIbβ3 initiates outside-in signalling through SFKs or interaction with cytoskeletal proteins (Durrant et al., 2017). Activated integrin αIIbβ3 binding of divalent fibrinogen or multivalent vWF is also necessary for aggregate formation, cross-linking platelets together (Clemetson and Clemetson, 2013, Bledzka et al., 2013). Unlike αIIbβ3, α2β1 primary function is adhesion, and it mediates only weak activation signals.

1.5.2. ITAM signalling

More powerful activation signals are required than elicited through the vWF receptor complex GPIbα-IX-V and integrins for full platelet activation (Barrow and Trowsdale, 2006). Characterised by a conserved YxxL/Ix6-12YxxL/I motif in the cytoplasmic tail, ITAMs, first identified in antigen receptors of T-cells and B-cells, are found across all haematopoietic lineages (Reth, 1989). Expressed in human platelets are the ITAM-containing receptor complexes GPVI-FcRγ-chain and FcγRIIA, and the hemi-ITAM-containing C-type lectin-2 (CLEC-2) receptor (Gibbins et al., 1997). Although lacking any integral catalytic activity, ITAM-containing receptors mediate powerful activation of platelets through recruitment of PTKs following receptor cross-linking (Barrow and Trowsdale, 2006).

1.5.2.1. GPVI-FcR γ-chain

Exclusively expressed on megakaryocytes and platelets, GPVI is a type 1 transmembrane protein with two extracellular Ig domains, a transmembrane region and a short cytoplasmic tail. GPVI is found complexed through a salt-bridge in the transmembrane domain to the FcRγ-chain (Nieswandt et al., 2000). This association is essential for the surface expression and signalling of GPVI, which does not possess the ability to signal on its own (Pollitt et al., 2013, Nieswandt and Watson, 2003). The FcRγ-chain itself, is a covalently linked homodimer containing an ITAM in each cytoplasmic tail (Gibbins et al., 1997).

Classically thought of as a collagen receptor, GPVI has also been shown to bind laminins (but at much lower affinity), and more recently fibrin (Pollitt et al., 2013, Onselaer et al., 2017, Mammadova-Bach et al., 2015). Binding of the glycine-proline-hydroxyproline (GPO) repeats conserved within collagen fibres initiates signalling of the GPVI complex (Asselin et al., 1999). The two tyrosine residues conserved within the ITAMs of the FcRγ-chain are rapidly phosphorylated by the SFK Lyn, which is constitutively associated to the intracellular tail of GPVI via a proline rich region (PRR) (Suzuki-Inoue et al., 2002). Phosphorylation can also be performed by another SFK Fyn, however it is not constitutively associated with GPVI, and rather involved in prolonged activation of the receptor (Watson et al., 2010). The tyrosine kinase Syk, via its SH2 domains, is recruited to the phosphorylated ITAM and undergoes activation by autophosphorylation on tyrosines 525 and 526 (519 and 520 in mice). Activated Syk then phosphorylates numerous tyrosines on the adaptor protein linker for activation of T-cells (LAT), which recruits Grb2 and Gads plus its associated protein Slp76. Assembly of this signalosome activates PLCγ2 and PI3K. Activation of PI3K aids recruitment of PLCg2 to the membrane and supports its activation by Tec family kinases (Tec and Btk) which phosphorylate residues of the SH2-SH3 linker region of PLCγ2 (Humphries et al., 2004, Nieswandt and

Watson, 2003). Cleavage of phosphatidylinositol 4, 5-bisphosphate (PIP2) by PLCγ2 releases diacylglycerol (DAG) and inositol 1, 4, 5-trisphosphate (IP3), which subsequently initiate release of intracellular Ca^{2+} and activation of protein kinase C (PKC). This results in platelet integrin activation and granule secretion.

1.5.2.2. FcγRIIA

Consisting of two extracellular Ig-like domains, a transmembrane domain and an ITAM-containing intracellular tail, FcγRIIA is a low affinity receptor for the IgG Fc domain and is expressed on human, but not mouse platelets (Kasirer-Friede et al., 2007). Activation of the receptor through clustering induced by IgG binding, results in phosphorylation of the conserved tyrosine residues in its ITAM and signalling via the same pathway as the GPVI FcR γ-chain complex (Clemetson and Clemetson, 2013).

1.5.2.3. CLEC-2

CLEC-2 is a type-II transmembrane protein highly expressed in platelets. Consisting of an extracellular C-type lectin carbohydrate-like binding domain, a single transmembrane domain and an intracellular tail, CLEC-2 is expressed on the surface of platelets as a non-disulfide-linked homodimer (Hughes et al., 2010, Watson et al., 2009). The intracellular tail of CLEC-2 contains a conserved YxxL hemi-ITAM.

Rhodocytin, purified from the venom of the Malayan pit viper, was the first exogenous ligand identified for CLEC-2, with an endogenous ligand podoplanin since identified (Suzuki-Inoue et al., 2006, Suzuki-Inoue et al., 2007). Podoplanin is an extensively glycosylated cell surface protein with an extracellular domain of unknown structure. It is expressed at high levels in lung type 1 alveolar cells, kidney podocytes and lymphatic endothelial cells, as well as also being

upregulated on inflammatory macrophages and a variety of tumours and implicated in metastasis (Kato et al., 2003, Kerrigan et al., 2012). Interaction of platelet CLEC-2 with podoplanin is essential for separation of blood and lymphatic vascular systems (Osada et al., 2012, Lowe et al., 2015). However vascular endothelial cells and platelets do not express podoplanin, which suggests it is unlikely to play a general role in haemostasis (Watson et al., 2010). Instead CLEC-2 has significant roles in many non-classical functions of platelets, particularly vascular integrity and thrombosis during inflammation where podoplanin is upregulated and accessible to platelets (Suzuki-Inoue, 2017).

Dimerization of CLEC-2 is essential for commencement of receptor signalling, as binding of the two SH2-domains of Syk is key for its activation, and CLEC-2 only possesses a single tyrosine residue (Hughes et al., 2015). Crosslinking and further clustering of CLEC-2 induces more powerful stimulation (Hughes et al., 2010). Signalling events downstream of CLEC-2 are very similar to those of GPVI-FcR γ-chain complex, although there are some differences. In CLEC-2 signalling, SFK and Syk kinases appear to act more cooperatively, with Syk significantly contributing to hemi-ITAM phosphorylation, whereas during in GPVI signalling these kinases have a clearly defined hierarchy (Spalton et al., 2009, Severin et al., 2011). Also unlike GPVI, actin polymerisation and positive feedback by the secondary mediators ADP and TxA_2 are critical to phosphorylation of CLEC-2 following ligand engagement (Suzuki-Inoue et al., 2006).

1.5.3. G protein coupled receptors

Following activation platelets secrete secondary mediators which induce activation and recruitment of circulating platelets to the thrombus, as well as positively feeding back onto the

already activated platelets. TxA_2 and ADP are the chief mediators of this, activating platelets through GPCRs (Brass et al., 2013).

ADP is released from dense granules following platelet activation, and by damaged endothelial cells, it activates platelet P2Y1 and P2Y12 receptors (Clemetson and Clemetson, 2013, Brass et al., 2013). P2Y1 receptors are Gq coupled, leading to PLC activation and an increase in intracellular Ca^{2+} (Brass et al., 2013). The Gi-coupled P2Y12 receptors, inhibit cAMP formation by adenyl cyclase, reducing PKA activity allowing platelet activation, and also leads to phosphorylation of PKB/Akt downstream of PI3K (Cattaneo, 2013). The GTPase Rap1 is also activated downstream of PI3K, with Rap1 shown to contribute to integrin activation (Cattaneo, 2013).

Produced from arachidonic acid by cyclooxygenase and thromboxane synthase, TxA_2 is also released from platelets upon activation. TxA_2 activates the thromboxane receptor (TP), a Gq-coupled receptor with the same mechanism of platelet activation as P2Y1 (Clemetson and Clemetson, 2013).

Thrombin mediates powerful platelet activation via the protease-activated receptors (PARs) 1 and 4 (PAR4 only in mice)(Coughlin, 2005). These GPCRs require cleavage of their N-terminus by thrombin to expose a tethered ligand that produces activation signals via G_q and G_{13} (Clemetson, 2012, Brass et al., 2013, Chen et al., 1994). Downstream PLC and Rho activation then lead to intracellular Ca^{2+} increase and actin cytoskeletal rearrangement and shape change (Brass et al., 2013).

Cleavage of fibrinogen by thrombin stimulates fibrin polymerization which stabilizes the thrombus as well as activating GPVI (Mammadova-Bach et al., 2015, Onselaer et al., 2017). In humans, rapid cleavage of PAR1 by low thrombin concentrations provides early activation

before it is downregulated protecting platelet sensitivity. PAR4 responds more slowly, requiring higher concentration of thrombin for activation (Covic et al., 2000).

1.6. Inhibition of platelets

1.6.1. Cyclic nucleotides

Healthy undamaged endothelial cells release inhibitory mediators, prostacyclin (PGI_2) and nitric oxide (NO) to maintain circulating platelets in a quiescent state (Bye et al., 2016, Nagy and Smolenski, 2018). PGI_2 secreted by endothelial cells binds the prostaglandin receptor (IP receptor), a GPCR present on the platelet surface, activating the Gα subunit **(Figure 1.3)**. This stimulates the production of cAMP through activation of membrane bound adenyl cyclases. The cAMP then uncouples the catalytic subunits of the serine/threonine kinase PKA which phosphorylates its target substrates, resulting in inhibition of platelet activation (Bye et al., 2016). NO inhibits platelet activation in a similar manner, through the serine/threonine kinase PKG, which phosphorylates many of the same target substrates as PKA **(Figure 1.3)**. Generated by endothelial nitric oxide synthase in endothelial cells, NO diffuses across the cell membrane and into platelets where it activates soluble guanyl cyclase production of cGMP. cGMP uncouples the regulatory domain PKG, enabling phosphorylation of its substrates and inhibition of platelet activation (Nagy and Smolenski, 2018). The short half-lives of both PGI_2 and NO means inhibition is transient and only occurs close to the vessel wall. This enables platelets to respond rapidly to any endothelium damage.

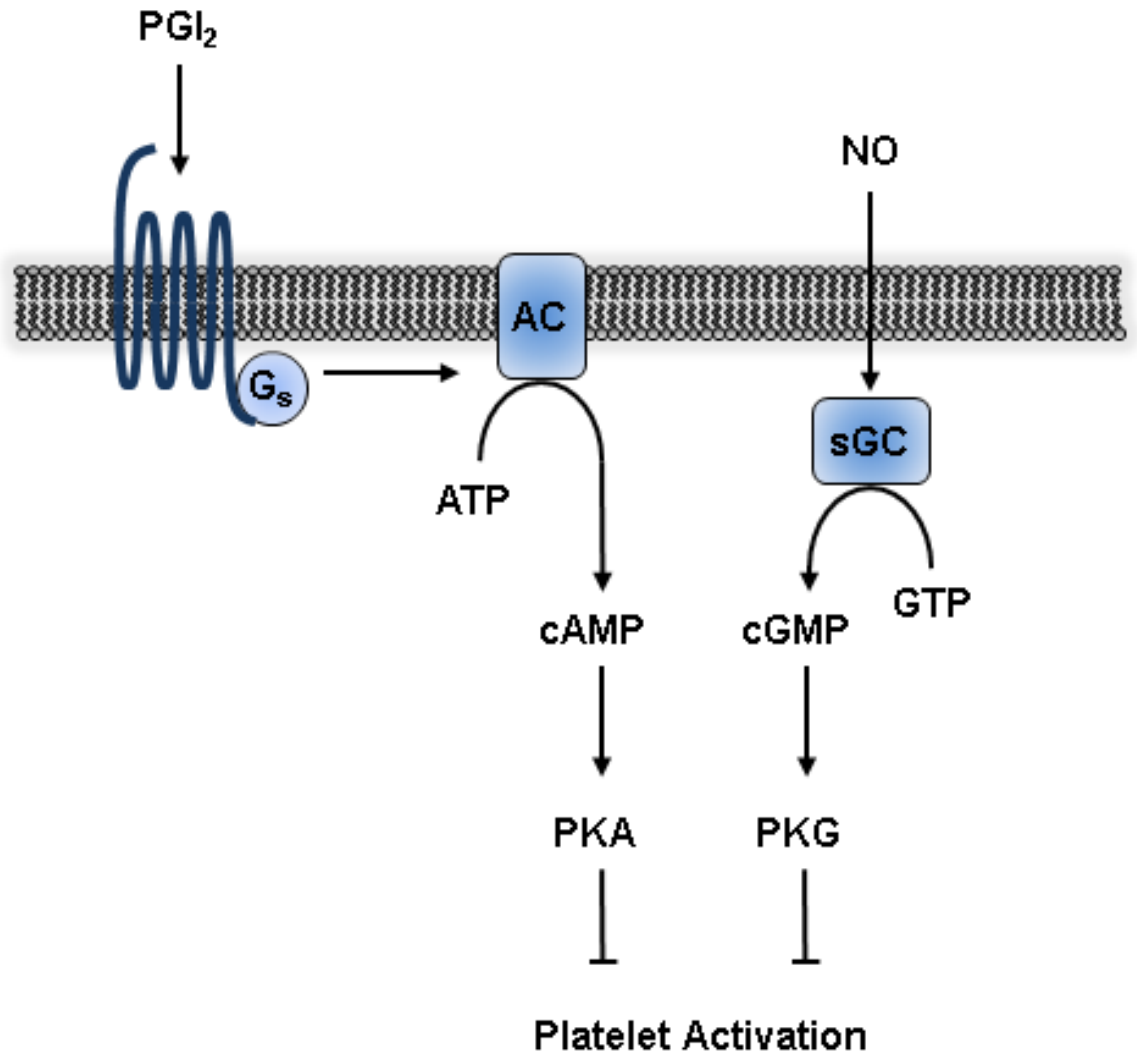

Figure 1. 3. Cyclic nucleotide-mediated inhibition of platelet activation. Prostacyclin (PGI_2) and nitric oxide (NO) stimulate adenyl and guanyl cyclase, respectively. Production of cyclic adenosine monophosphate (cAMP) and cyclic guanine monophosphate (cGMP) then activate protein kinase A (PKA) and protein kinase G (PKG), respectively. PKA and PKG phosphorylation of serine and threonine residues then prevent platelet activation.

1.6.2. ITIM-containing receptors

First identified in immune cells, immunoreceptor tyrosine base inhibition motif (ITIM)-containing receptors mediate intracellular inhibition of ITAM-containing receptor signalling (Daeron et al., 2008, Muta et al., 1994, Daeron et al., 1995). Defined as the consensus sequence (I/V/L/S)-x-Y-x-x-(L/V), ITIMs are present in the cytoplasmic tail of receptors, usually in pairs separated by approximately 20 amino acids. Platelet inhibition mediated by ITIM-containing receptors, unlike cyclic nucleotides which maintain platelets in a quiescent state, occurs following initiation of platelet activation, restraining activation signalling and preventing excessive thrombus growth (Bye et al., 2016, Coxon et al., 2017).

Phosphorylation of the conserved tyrosine residues within ITIMs provide docking sites for lipid and protein tyrosine phosphatases. These negative regulators of platelet activation, due to the receptors clustering with ITAM-containing receptors, are then able to dephosphorylation and inactivate key activation signalling pathway components (Bye et al., 2016, Du, 2014). Several ITIM-containing receptors have so far been identified in platelets and megakaryocytes (Coxon et al., 2017).

1.6.3. ITSM-containing receptors

Immunoreceptor tyrosine-based switch motifs (ITSMs) can also be found in tandem with ITIMs (Newman and Newman, 2013). Although the consensus sequence of ITSMs (T-x-Y-x-x-V-I) is similar to ITIMs, they are, depending on which proteins they recruit, able to produce either activation or inhibition signals (Ostrakhovitch and Li, 2006)(Cannons et al., 2011).

1.6.4. Canonical ITIM signalling

Once phosphorylated, usually by SFKs, the conserved tyrosine residues in ITIMs provide docking sites for Src homology 2 (SH2) domain containing inositol phosphatase-1 (SHIP-1) and the structurally similar SH2 domain containing tyrosine phosphatases Shp1 and Shp2. Due to the close proximity these phosphatases are then able to dephosphorylate and inactivate key signalling components of ITAM-containing receptor activation pathways **(Figure 1. 4)** (Bye 2016, Du 2014). C-terminal Src kinase (Csk) has also been shown to interact with some ITIM-containing receptors. Csk inhibits SFK activity through phosphorylation of their C-terminal tyrosine residue. This subsequently induces a conformational change through interaction with the SH2 domain, and obstructs the active site of the kinase (Senis et al., 2009).

1.6.4.1. PECAM-1

The first to be identified and most investigated platelet ITIM-containing receptor is PECAM-1. Also known as CD31, PECAM-1 is a 130 kDa glycoprotein consisting of 6 highly glycosylated extracellular Ig constant 2 (IgC2)-like domains, a transmembrane domain and a large intracellular tail containing an ITIM, ITSM, PRR and a transmembrane proximal palmitoylation site **(Figure 1. 5)** (Newman et al., 1990). PECAM-1 is expressed in haematopoietic and non-hematopoietic cells, and highly abundant in platelets and endothelial cells. Dependent on the two N-terminal IgC2-like ectodomains PECAM-1 primarily undergoes trans-homophilic interactions, although these domains have the capacity for cis-homophilic binding as well. PECAM-1 is also able to undergo heterophilic interactions with platelet αVβ3 and CD177 and CD38 on neutrophils (Buckley et al., 1996, Jones et al., 2012, Sachs et al., 2007, Deaglio et al., 1998).

Phosphorylation of the ITIM and ITSM conserved tyrosine residues mediated by SFKs, predominantly Lyn, is central to PECAM-1 signal transduction (Ming et al., 2011). The sequential phosphorylation of the ITSM by Lyn, enables Csk binding and phosphorylation of the ITIM (Tourdot et al., 2013). These phospho-tyrosines provide docking sites for Shp1 and Shp2 via their tandem SH2 domains, though it appears Shp2 is preferentially bound, localizing them to the plasma membrane and relieving their intramolecular inhibition, enhancing their catalytic activity (Edmead et al., 1999, Jackson et al., 1997, Hu et al., 2016). Interaction with other proteins (SHIP and SFKs) via their SH2 or SH3 domains have also been identified, but functional relevance in platelets is yet to be determined.

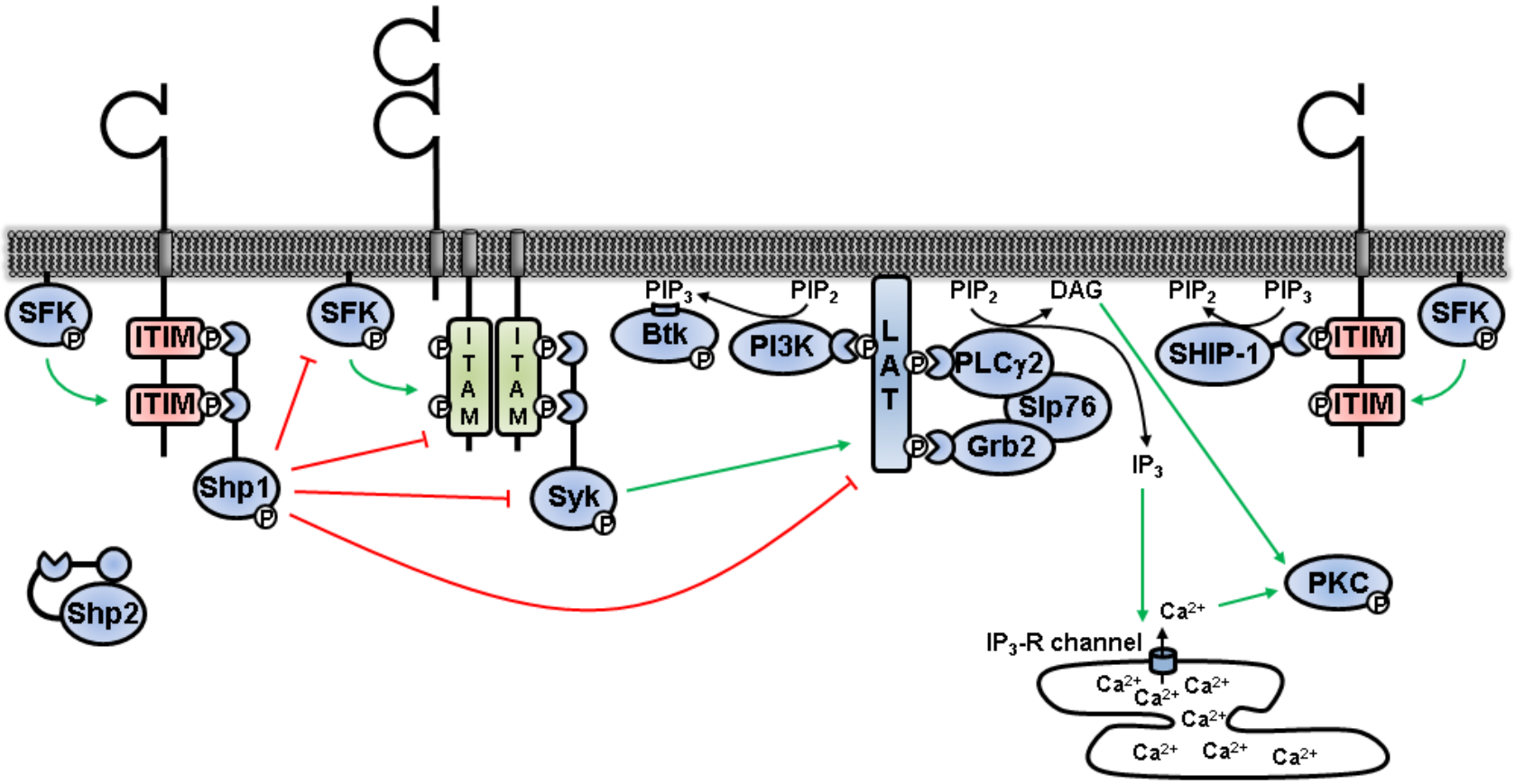

Figure 1. 4. Classical ITIM-mediated inhibition of ITAM signalling. Recruitment of Shp1, Shp2 and SHIP to ITIM-containing receptor inhibits cellular activation mediated by ITAM-containing receptors.

In resting cells, accessibility to the ITSM is controlled by interactions between cytoplasmic tail of PECAM-1 and the plasma membrane, which prevents phosphorylation and inhibitory signalling. Upon activation, phosphorylation of the lipid interacting segment C-terminal serine disrupts this membrane interaction. Subsequent exposure and phosphorylation of the C-terminal ITSM by the SFK Lyn completes plasma membrane dissociation, and enables phosphorylation of the N-terminal ITIM. Phosphorylation of both ITIMs is required for recruitment of Shp1 or Shp2 and inhibitory signalling (Paddock et al., 2011, Newman and Newman, 2013).

The role of PECAM-1 in platelets and megakaryocytes has been extensively characterised through use of a KO mouse model. PECAM-1 deficient platelets display enhanced aggregation and secretion responses to collagen and CRP, and subthreshold rhodocytin stimulation, but not thrombin or ADP (Patil et al., 2001, Wee and Jackson, 2005, Dhanjal et al., 2007b). Indicating PECAM-1 primarily inhibits ITAM (GPVI) and hemi-ITAM (CLEC-2) coupled receptor signalling; however at higher agonist concentrations enhancement is lost suggesting only a modulatory role.

Although normal platelet counts are observed in PECAM-1 KO mice (Mahooti et al., 2000), recovery following antibody-mediated depletion is delayed due to defective platelet production. Deficient megakaryocytes exhibit increased adhesion, and impaired SDF-1α migration which also contributes to the delayed recovery (Dhanjal et al., 2007a). The migration defect was found to be due to absence of CXCR4 (SDF-1α receptor) polarisation to the megakaryocytes leading edge and underlies the abnormal bone marrow distribution of megakaryocytes observed in KO mice (Dhanjal et al., 2007b, Wu et al., 2007).

In vivo thrombosis is also enhanced in absence of PECAM-1, with larger laser-induced thrombi and a modest increase in ferric chloride-induced thrombosis observed in deficient mice (Falati et al., 2006). Thrombosis to photochemical injury was however normal, with differences

probably owing to the different injury mechanisms (Vollmar et al., 2001). Further interrogation of the enhanced thrombosis using chimeric mice demonstrates the enhancement results from lack of platelet and leukocyte PECAM-1 rather than from endothelial cells. Tail bleeding time was also increased in PECAM-1 KO mice, and attributed somewhat paradoxically to absence of endothelial PECAM-1 (Falati et al., 2006, Mahooti et al., 2000).

PECAM-1 has also been suggested to play a role in platelet integrin responses, with delayed clot retraction, impaired cytoskeleton rearrangement and focal adhesion kinase (FAK) tyrosine phosphorylation reported in deficient platelets by some studies (Wee and Jackson, 2005). Yet normal clot retraction and mild increase in fibrinogen spreading reported by subsequent studies, with differences credited to the experimental methods used and genetic drift in the PECAM-1 KO mouse model (Dhanjal et al., 2007b).

1.6.4.2. G6b

G6b-B is specifically expressed on megakaryocytes and platelets and is the second most highly expressed ITIM-containing receptor (Zeiler et al., 2014, Burkhart et al., 2012, Senis et al., 2007, Newland et al., 2007). G6b-B consists of a single variable Ig-like (IgV) extracellular domain, a transmembrane region and an intracellular tail containing a PRR, an ITIM and ITSM **(Figure 1. 5)**. Although other G6b isoforms have been identified by transcriptomics, G6b-B is the only one conclusively shown to be expressed (Senis et al., 2007, Moebius et al., 2005).

The conserved tyrosine residues in the ITIM and ITSM of G6b-B are constitutively phosphorylated and associated with Shp1 and Shp2 (Senis et al., 2007, Mazharian et al., 2012). Phosphorylation is mediated by SFKs, with PTP binding primarily mediated by the ITIM. Shp2 binds G6b-B with higher affinity than Shp1, and is able to interact when only one motif is phosphorylated, whereas Shp1 interaction has an absolute requirement for both (Coxon et al.,

2012). There is no evidence for lipid phosphatase SHIP-1 binding, but although not confirmed in platelets, *in vitro* evidence suggests it can bind Fyn, Src, Syk which may facilitate Shp1/2 phosphorylation (Coxon et al., 2012). There is also no evidence for SH3 binding to the PRR of G6b-B.

Initial studies into the function of G6b-B revealed crosslinking of the receptor inhibited CRP and ADP-mediated platelet aggregations (Newland et al., 2007). This inhibitory role was verified in cell lines where co-expression of G6b-B with the (hemi)ITAM receptors GPVI-FcRγ chain and CLEC-2 inhibited activation in an NFAT-luciferase assay (Mori et al., 2008). The importance of this receptor was not however realised until the generation of a deficient mouse model.

Mice deficient in G6b present a severe phenotype unique among the platelet and megakaryocyte ITIM-containing receptors, with platelet count dramatically reduced by 80%, platelet volume increased 35% and altered reactivity (Mazharian et al., 2012). Reduced platelet production in combination with more rapid clearance of circulating platelets, due to their preactivated state, underlies the observed macrothrombocytopenia. G6b-deficient megakaryocytes undergo normal development and proliferation *ex vivo*, but fail to spread efficiently on fibrinogen, fibronectin and collagen, and have reduced capacity to form proplatelets (Mazharian et al., 2012). These findings establish G6b-B as important novel regulator of terminal stages platelet production.

G6b deficient platelets have impaired collagen reactivity, as GPVI-FcRγ chain expression is downregulated to temper tonic GPVI signalling (Mazharian et al., 2012). Altogether, this results in reduced thrombus formation and enhanced bleeding in G6b KO mice. Highlighting the critical role ITIM-containing receptor regulation has in platelets and megakaryocytes. Additional studies in mice expressing a mutant form of G6b-B, where tyrosine residues of the

ITIM/ITSM have been mutated to phenylalanine, preventing Shp1/2 docking and downstream signalling, report strikingly similar results (Geer et al., 2018). G6b diY/F were macrothrombocytopenic due to reduced platelet production and myelofibrosis was observed in bone marrow and spleens. Platelets from these mice also exhibited altered reactivity with collagen and thrombin responses reduced, but CLEC-2 responses potentiated. Recapitulation of the KO phenotype in these mice demonstrates the inhibitory effect of G6b is mediated via Shp1 and Shp2 binding to the ITIM/ITSM.

1.6.4.3. LAIR-1

LAIR-1 is a type 1 transmembrane glycoprotein consisting of a single IgC2 ectodomain, a transmembrane region and a cytoplasmic tail containing an ITIM and an ITSM **(Figure 1. 5)** (Brondijk 2010). Widely expressed on haematopoietic cells, including T cells, B cells and progenitor cells and immature MKs, LAIR-1 is however not expressed on platelets (Meyaard et al., 1997).

LAIR-1 is a collagen receptor, binding both transmembrane and extracellular collagens with high affinity (Lebbink et al., 2006, Lebbink et al., 2007). Like GPVI the interaction is dependent on the GPO repeats conserved in all collagen trimers, however LAIR-1 binds these repeats with much higher affinity, and has been shown to inhibit collagen induced GPVI signalling when they are expressed on the same cell (Brondijk et al., 2010, Lebbink et al., 2006).

Inhibition mediated by LAIR-1 was initially demonstrated through antibody mediated crosslinking of the receptor in immune cells. Crosslinking was able to potently inhibit NK cell from mediating lysis of target cells (Meyaard et al., 1997, Meyaard, 2008, Ouyang et al., 2003, Poggi et al., 1997), while in effector T cells it was able to diminish cytotoxic activity (Meyaard, 2008, Meyaard et al., 1997, Meyaard et al., 1999, Maasho et al., 2005, Poggi et al., 1997).

Density of surface expression was shown to correlate with inhibitory capacity of LAIR-1 in T cells (Saverino et al., 2002). Crosslinking on B cells, was also shown to decreased B cell receptor induced Ca^{2+} mobilization and cytokine production (Merlo et al., 2005).

LAIR-1 has also been implicated in negative regulation of megakaryopoiesis, with primary human CD34+ cell megakaryocyte production upon TPO stimulation decreased with antibody mediated LAIR-1 crosslinking (Xue et al., 2011). LAIR-1 has also been shown to play an essential role in the development of acute myeloid leukaemia (Kang et al., 2015).

Upon activation the conserved tyrosine residues in the ITIM and ITSM of LAIR-1's intracellular tail are phosphorylated by SFKs, with both required for full activation (Meyaard, 2008, Meyaard et al., 1997, Verbrugge et al., 2003, Xu et al., 2000). These phospho-tyrosines have been shown to facilitate interaction with the phosphatases Shp1 and Shp2 in humans, but not SHIP. In mice, LAIR-1 however does not interact with Shp1, interacting only with Shp2 (Lebbink et al., 2004). Csk has also been shown to interact with both mouse and human LAIR-1 (Meyaard, 2008, Verbrugge et al., 2006).

Co-expression of LAIR-1 with GPVI in transiently transfected DT40 chicken B cells results in powerful inhibition of collagen mediated activation of an NFAT reporter assay (Tomlinson et al., 2007). Both receptors have been shown to be expressed on a subset of megakaryoblasts during human megakaryocyte development, suggesting LAIR-1 may inhibit migration and proplatelet formation in immature megakaryocytes before expression is downregulated and lost upon mature megakaryocytes (Steevels et al., 2010).

LAIR-1 KO mice have been generated, the phenotype of which will be discussed in chapter 3.

1.6.4.4. CEACAM1/2 and PIR-B

Despite proteomic and transcriptomic studies questioning their expression in platelets, transgenic mouse studies have demonstrated functional roles for the ITIM-containing receptors CEACAM-1, CEACAM-2 and PIR-B in platelets **(Figure 1. 5)**.

While CECAM-1 is expressed in endothelial and hematopoitic cells, CECAM-2 is only present in mice kidney, testis, brain and select epithelial cells, with no human ortholog identified (Zebhauser et al., 2005). Constitutive KO models of the CEACAM-1 and CEACAM-2 receptors presented with similar phenotype; increased aggregation to subthreshold agonist concentrations, increased thrombus formation *in vivo*, and both receptors are implicated in positive regulation of αIIβ3 integrin function (Alshahrani et al., 2016, Alshahrani et al., 2014, Wong et al., 2009, Yip et al., 2016).

Containing an ITIM and 3 non-consensus ITIM-like motifs, PIR-B, the murine homolog of human LILRB2, is expressed in hematopoietic stem cells, myeloid B cells and platelets (Fan et al., 2014, Kubagawa et al., 1999, Zheng et al., 2012). Studies using a transgenic mouse model lacking the intracellular tail of PIR-B, suggest a role for PIR-B in megakaryocyte development as mice exhibited mild thrombocythemia and higher number of megakaryocytes. Platelets from this model were also hyper-responsive to low concentration CRP stimulation (Fan et al., 2014). Inability to detect these receptors by proteomics and genomics methods is likely due to low abundance and technique limitations, but does question the observed phenotypes.

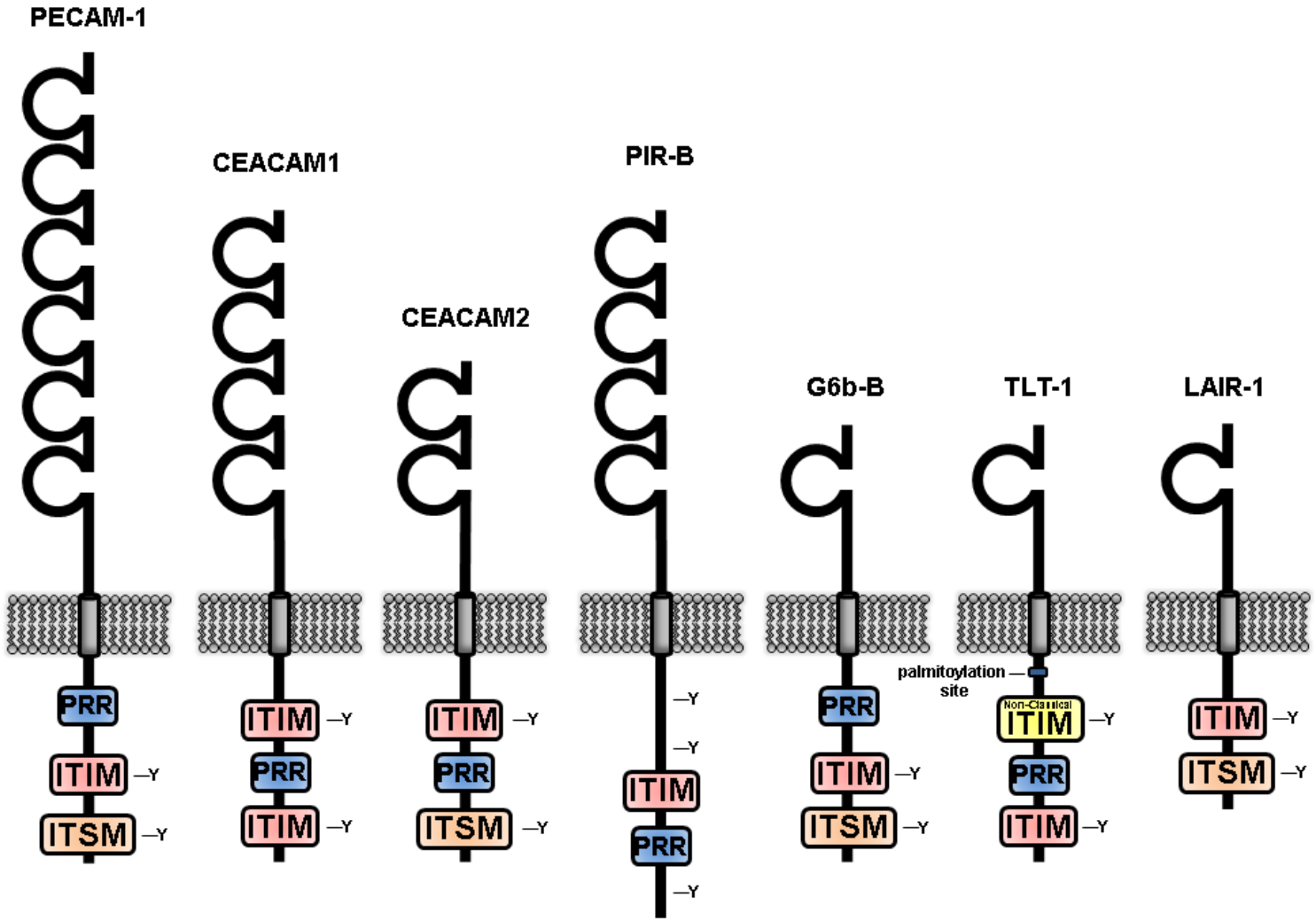

Figure 1. 5. ITIM-containing receptors expressed in mouse megakaryocytes and platelets. LAIR-1 is only expressed in immature megakaryocytes.

1.6.5. Non-canonical ITIM signalling

1.6.5.1. TLT-1

TLT-1 is the most highly abundant ITIM-containing receptor in both human and mouse platelets. Identified as the inhibitory analogue of TREM-1 immune receptor family, its expression is restricted to megakaryocytes and platelets. TLT-1 consists of a single extracellular V-set Ig domain, a transmembrane region and an intracellular tail containing an ITIM and ITSM. 3 splice variant isoforms of TLT-1 have been identified in platelets differing only in their intracellular tails. Full length TLT-1 has a 127aa intracellular tail containing 2 conserved Tyr residues and a proline rich region **(Figure 1. 5)**. The Tyr residues are present in a C-terminal classical ITIM and a membrane-proximal non-classical ITSM (Gattis et al., 2006). Whereas the shorter splice variant lacks these, instead its 18aa tail encodes a dileucine receptor sorting motif akin to variant chain MHC class II molecules (Gattis et al., 2006). The 3rd isoform lacks both the intracellular and transmembrane regions, only consisting of the extracellular domain (Washington et al., 2009). In addition, cleavage of TLT-1 from the surface by metalloproteinases is reported to produce a soluble form, consisting of the extracellular domain. The existence of a splice variant lacking the intracellular tail and soluble TLT-1 (sTLT-1) suggest some functional involvement of the extracellular domain independent of ITIM-signalling (Klesney-Tait et al., 2006). In resting megakaryocytes and platelets all these TLT-1 isoforms are localised in α-granules and upregulated to the surface following activation.

Details of the downstream signalling of TLT-1 are still not clear, with most of what is known to date coming from work in transfected cell lines. Following initial characterization as an ITIM-containing receptor, TLT-1 was assessed for interactions with the SH2-domain containing protein tyrosine phosphatases. Pervanadate treatment of transfected HEK293T cells demonstrated Shp1 interaction with the phosphorylated-ITIMs of TLT-1 (Washington et al.,

2002). Subsequent work in RBL-2H3 cell lines transfected with wtTLT-1 and mutant tyrosine to phenylalanine (Y>F) ITIMs demonstrated effective recruitment of Shp2 upon phosphorylation to the classical C-terminal ITIM, but not the non-classical membrane-proximal ITIM (Barrow et al., 2004). However, despite abundant expression interaction with Shp-1 or SHIP could not be detected.

Classical models of ITIM-mediated signalling would suggest TLT-1 might inhibit ITAM-containing receptor signalling. Interestingly, crosslinking of FcεRI with TLT-1 in these cells resulted unexpectedly in increased rather than inhibited intracellular calcium levels (Barrow et al., 2004). This indicates stimulation of TLT-1 actually enhances rather than inhibits activation, which was dependent on the C-terminal classical ITIM. Shp-2 has been implicated in both activation and inhibition signalling depending on conditions (Klesney-Tait et al., 2006).

Binding assays using Glutothione-S-transferase (GST) fusions of the cytoplasmic tail of TLT-1 found strong interaction with moesin and their other highly homologous ERM family members (ezrin and radixin), with moesin interactions subsequently confirmed in human platelets (Washington et al., 2009). ERM family proteins are known to link membrane bound proteins to the actin cytoskeleton and implicated in formation filopodia and lamellipodia in platelets suggesting TLT-1 may play a role in these processes (Washington et al., 2009).

Generation of a TLT-1 deficient mouse model has been utilized to interrogate the functional role of TLT-1 in platelet aggregation. Deficient mice are viable and fertile, with a decrease in platelet count of 20%. Aggregation responses to thrombin, collagen, ADP and U46619 were reduced in platelet rich plasma at all concentrations tested, with fibrinogen binding of deficient platelets showing a tendency to be decreased compared to wild type following suboptimal stimulation with ADP (Washington et al., 2009). *In vivo* tail bleeding time also showed null mice bled more than controls (Washington et al., 2009).

As TLT-1 is also a member of the TREM family of proteins, that play important roles in both adaptive and innate immunity, the role of TLT-1 has also been evaluated in various models of inflammation (Giomarelli et al., 2007). In mice, lipopolysaccharide (LPS)-induced sepsis led to detectable levels of plasma sTLT-1 within 2 hours, which continued to increase over 24 hours. This increase in sTLT-1 inversely mirrored the pattern of thrombocytopenia in these mice, suggesting sTLT-1 is released or shed as platelets leave the circulation during endotoxemia (Washington et al., 2009). TLT-1 deficient mice succumbed to LPS challenge faster than controls, and were also predisposed to haemorrhage associated with inflammatory lesions (Washington et al., 2009). Together findings advocate a protective role for TLT-1 during inflammation, dampening the inflammatory response and enhancing platelet aggregation at sites of vascular injury (Washington et al., 2009)

1.7. Phosphatases

One of the main ways activation signals are transmitted in platelets is through phosphorylation of signalling proteins on key tyrosine residues by PTKs. Regulation of these activation signals is achieved through protein tyrosine phosphatases (PTPs), which oppose the actions of PTKs by dephosphorylating these residues (Senis, 2013).

1.7.1. Protein tyrosine phosphatases

PTPs are a family of enzymes that modulate signal transduction within cells through the dephosphorylation of tyrosine residues (Senis, 2013). Depending on subcellular localisation and downstream targets, this can activate or inhibit cellular responses (Senis, 2013). There are two groups of PTPs, non-transmembrane, and receptor-like whose ectodomains vary in shape and size (Senis, 2013).

Platelets express only a few PTPs, with the receptor-like CD148 first to be identified (Senis et al., 2007). CD148 is master positive regulator of SFKs in platelets. In resting platelets CD148 is critical in maintaining a pool of active SFKs by dephosphorylating their C-terminal inhibitory tyrosine residues (Senis, 2013, Mori et al., 2012). However it also attenuates SFK activity by dephosphorylating their activation loop. CD148 is therefore a molecular switch modulating the optimal level of SFK activity in resting and activated states (Senis, 2013). The non-transmembrane PTP-1B is also highly expressed in platelets, and plays a specialized role in αIIbβ3 outside-in signalling through dephosphorylation of Src C-terminal inhibitory tyrosines (Senis, 2013).

1.7.2. Shp1 and Shp2

Consisting of tandem SH2 domains, a single PTP domain and a short C-terminal tail, the structurally related non-transmembrane PTPs Shp1 and Shp2 are crucial for ITIM-containing receptor signalling (Senis, 2013). The SH2 domains, via intra- and intermolecular interactions, regulate the activity and compartmentalisation of Shp1 and Shp2. The backside loop opposite the phosphotyrosine binding pocket of the N-terminal SH2 domain has been shown to obstruct the catalytic site of the PTP domain and disrupt the phosphotyrosine binding site of the N-terminal SH2 domain in the process (Barford and Neel, 1998, Hof et al., 1998). In this inactive conformation, the C-terminal SH2 domain is still free to interact with phosphotyrosines (Senis, 2013). Interactions of the tandem SH2 domains with the phosphor-tyrosines of tandem ITIMs, localizes Shp1/2 to the plasma membrane and strongly activates them.

Despite sharing structural similarity their physiological functions differ. Shp1 is mainly a negative regulator of intracellular signalling whereas Shp2 in contrast is a positive regulator of growth factor and cytokine signalling (Di Paola, 2013, Senis, 2013).

Megakaryocyte and platelet specific KO mouse models of Shp1 and Shp2 highlight the differences in their functions (Mazharian et al., 2013). Platelets deficient in Shp1 have reduced reactivity to CRP, as a result of downregulated GPVI surface expression and reduced SFK-Syk-PLCγ2 axis signalling, the reverse to what was predicted of an ITAM signalling negative regulator (Senis, 2013, Mazharian et al., 2013). Shp1 deficient platelets also exhibited reduced fibrinogen spreading and normal responses to anti-CLEC2 antibody. On the other hand, Shp2 deficient platelets responded normally to CRP, and were hyper responsive to fibrinogen and anti-CLEC2 antibody (Mazharian et al., 2013). Megakaryocytes of both KO mice showed impaired development, but only the Shp2 deficient megakaryocytes had reduced proplatelet formation and TPO and integrin signalling, resulting in Shp2 KO mice being macrothrombocytopenic (Senis, 2013, Mazharian et al., 2013).

1.8. Key questions

Although the abundance, structure and functional significance (for which transgenic mouse models have been pivotal) of several ITIM-containing receptors have been identified in megakaryocytes and platelets, many key questions still remain unanswered. Such as how despite all ITIM-containing receptors interacting with Shp1 and Shp2, dramatically different phenotypes are observed in mouse models. As well as how the phosphorylation of ITAM and ITIM-containing receptors is balanced upon SFK activation. In addition, it is not known whether the roles of ITIM-containing receptors are distinct or if there is redundancy between receptors. The mechanisms by which ITIM-containing receptors can modulate integrin signalling and GPCR-mediated responses are also yet to be defined (Coxon et al., 2017). Considerable work is therefore still required in order to fully understand how ITIM-containing receptor signalling is integrated within other platelet receptor signalling networks in order to

prevent life threatening thrombosis. Such physiological inhibitory mechanisms could be exploited as means to prevent or treat thrombosis.

1.9. Hypothesis and aims

The predominant hypotheses running throughout this thesis is that ITIM-containing receptors are critical regulators of megakaryocyte development and platelet production and function.

These hypotheses were explored through aiming to determine:

1. The role of LAIR-1 in platelet production and function
2. Whether the inhibitory function of LAIR-1 is discrete or if there is functional redundancy with inhibition mediated by PECAM-1
3. The role of TLT-1 in platelet production and function

CHAPTER 2

Materials and Methods

2.1. Materials

Antibodies, agonists and inhibitors used are listed in **Tables 2.1**, **2.2** and **2.3** respectively. All other reagents are from Sigma (Poole, UK) unless otherwise stated.

2.1.1. Mice

LAIR-1 KO mice were produced by Taconic (Cologne, Germany). Targeting strategy can be found in chapter 3 **(Figure 3.1)** (Smith et al., 2017). PECAM-1 KO mice were a generous gift from Dr Tak Mak (Amgen Institute, Toronto, Ontario, Canada), with targeting strategy as previously published (Duncan et al., 1999). LAIR-1/PECAM-1 double deficient mice were generated by crossing individual LAIR-1 KO and PECAM-1 KO mice strains. TLT-1 KO mice were provided by Dr Daniel McVicar (National Institute of Health, USA) / Dr Valance Washington (Universidad de Puerto Rico, Puerto Rico). Targeting strategy of TLT-1 can be found in Washington et al, (2009). All mice were on a C57BL/6 background and bred using heterozygous or homozygous breeding pairs. Control mice were either litter matched, or age matched WT mice from breeding pairs within the same colony. All procedures were carried out with United Kingdom Home Office approval in accordance with Animals (Scientific Procedures) Act 1986.

Table 2. 1. Antibodies

Antibody	Host species, conjugate (clone, catalogue number)	Source	Working concentration
α2 (mouse)	Rat, FITC-conjugated (Sam.C1, M071-1)	Emfret Analytics	FC: 1/100
αIIb (mouse)	Rat, PE-conjugated (MWReg30, 558040)	BD Biosciences	FC: 1/100
αIIbβ3, high affinity (mouse)	Rat, PE-conjugated (-, M023-2)	Emfret Analytics	MC: 1/20
CD11b+	Rat (M1/70, 13-0112)	eBioscience	MK: 3 µl/mouse
CD148	Syrian hamster (8A-1)	Custom antibody produced by Art Weiss (University of California San Francisco, USA)	WB: 1/1,000
CD16/32	Rat (2.4G2, 553142)	BD Bioscience	MK: 3 µl/mouse
CD45R/B220+	Rat (RA3-6B2, 553086)	BD Bioscience	MK: 3 µl/mouse
ChK (CtK)	Rabbit (C-20, sc470)	Santa Cruz	PS: 1/80
CLEC-2 (mouse)	Rat (17D9, MCA5700)	Bio-Rad Laboratories	AG: 10 µg/ml
CLEC-2 (mouse)	Rat, FITC-conjugated (17D9, MCA5700F)	Bio-Rad Laboratories	FC: 1/100
Csk	Rabbit (C-20, sc286)	Santa Cruz	WB: 1/1,000 PS: 1/10
ERK 1/2	Rabbit (K-23, sc-153)	Santa Cruz	WB: 1/1,000
ERK 1/2 -p	Mouse (E4, sc-7383)	Santa Cruz	WB: 1/200
Fyn	Rabbit (FYN3, sc-16)	Santa Cruz	WB: 1/1,000
Fyn p-Tyr-530	Rabbit (53690)	Abcam	WB: 1/1,000
G6b (mouse)	Rat (68-3, -)	Custom antibody produced by Biogenes	FC: 5 µg/ml
GAPDH	Rabbit (14C10, #2118)	Cell Signaling Technology	PS:1:10
GPIbβ (X488)	Rat, Dylight488-conjugated (-, X488)	Emfret Analytics	IV: 0.2 µg/g body weight
GPVI	Rat, FITC-conjugated (JAQ1, M011-1)	Emfret Analytics	FC: 5 µl per test
LAIR-1	Armenian hamster, PE-conjugated (113, 12-3051)	eBioscience	FC:10 µg/ml

Ly6G/Gr1+	Rat (RB6-8C5, 14-5931)	eBioscience	MK: 3 µl/mouse
Lyn	Rabbit (sc-15)	Santa Cruz	WB: 1/1,000
Lyn p-Tyr-507	Rabbit (2731)	Cell Signaling Technology	WB: 1/1,000
PLCγ2	Rabbit (DN84)	Custom antibody produced by Joseph Bolan (DNAX Research Institute, Palo Alto, USA)	WB: 1/1,000
PLCγ2 p-Tyr-1217	Rabbit (3871)	Cell Signaling Technology	WB: 1/500
PECAM-1	Rat, FITC-conjugated (MEC 13.3, 553372)	BD	FC: 10 µg/ml
P-selectin (human)	Mouse, FITC-conjugated (AK-4, 555523)	BD Pharmingen	FC: 5 µl per test
P-selectin (human)	Mouse, AF647-conjugated (CTB201, SC-8419)	Santa Cruz	IF: 1/250
P-selectin (mouse)	Rat, FITC-conjugated (Wug.E9, M130-1)	Emfret Analytics	FC: 5 µl per test
P-selectin (mouse)	Rat, AF647-conjugated (RB40.34, 563674)	BD	IF: 1/500 IV: 0.2 µg/g body weight
PTP1B	Rabbit (ABS40)	Millipoore	WB: 1/1,000
p-Tyr	Mouse (4G10, 5-321)	Sigma	WB: 1/1,000
Shp1	Rabbit (C14H6, 3759)	Cell Signaling Technology	WB: 1/1,000
Shp2	Rabbit (D50F2, 3397)	Cell Signaling Technology	WB: 1/1,000
Src	Rabbit (44656)	Invitrogen	WB: 1/1,000 PS: 1/50
Src p-Tyr-418	Rabbit (44660G)	Invitrogen	WB: 1/1,000 PS: 1/10
Src p-Tyr-529	Rabbit (44662)	Invitrogen	WB: 1/1,000
Syk	Rabbit (D1I5Q, 12358)	Cell Signaling Technology	WB: 1/1,000 PS: 1/10
Syk p-Tyr525/26	Rabbit (-, 2711)	Cell Signaling Technology	WB: 1/500 PS: 1/50

TLT-1 (human)	Rat, AF488-conjugated (268420, FAB 2394G)	Novus Biologicals	FC: 1 µg per test IF: 1/250
TLT-1 (Mouse)	Rat, AF488-conjugated (268529, NBP-248481)	R&D systems	FC: 1 µg per test IF: 1/500 IV: 0.2 µg/g body weight
TLT-1 (Mouse)	Rat, AF647-conjugated (268529, NBP-248481)	R&D systems	IV: 0.2 µg/g body weight
Tubulin	Mouse (DM1A, T6199)	Sigma	WB: 1/1,000
IgG isotypes			
IgG	Rat, FITC-conjugated (-, P190-1)	Emfret Analytics	FC: 1/100
IgG	Armenian hamster, PE-conjugated (eBio299Am, 12-4888)	eBioscience	FC:10 µg/ml
IgG1	Rat, FITC-conjugated (A85-1, 553443)	BD	FC:10 µg/ml
IgG2A	Rat, AF488-conjugated (54447, MAB006)	R&D systems	FC: 5 µg/ml
IgG2B	Rat, FITC-conjugated (-, MCA6006F)	Bio-Rad Laboratories	FC: 1/100
Secondary antibodies			
Donkey anti-rabbit IgG	Donkey, HRP-conjugated (-, NA934V)	GE Healthcare	WB: 1/5,000-10,000
Goat anti-mouse IgG	Goat, Alexa-488-conjugated (-, A-10680)	ThermoFisher	FC: 10 µg/ml
Rabbit anti-hamster IgG	Rabbit, HRO-conjugated (-, ab6783)	Abcam	WB:1/1,000

FC, flow cytometry; IF, immunofluorescence; WB, Western blotting; PS, ProteinSimple; IV, *in vivo*; MK, megakaryocyte culture; AG, aggregations

Table 2. 2. Agonists

Agonist	Receptor target	Source
ADP	P2Y12, P2Y1	Sigma (A2754)
Collagen (Horm)	GPVI, α2β1	Takeda (1130630)
Collagen-related peptide-cross-linked	GPVI	Provided by Prof. Richard Farndale, cross-linked in house
Convulxin	GPVI, GPIb-IX-V	Enzo Life Sciences (#ALX-350-100)
CLEC-2 antibody	CLEC-2	Bio-Rad Laboratories (MCA5700)
Fibrinogen	Integrin αIIbβ3	Enzyme Research (FIB 3)
PAR4 peptide	PAR4	Alta Biosciences (custom order)
Thrombin	PAR1, PAR4	Sigma (T4648)
U46619	TP	Sigma (D8174)

Table 2. 3. Inhibitors

Inhibitor	Target	Concentration	Source
AEBSF	Serine proteases	1 mM	Calbiochem (101500)
Aprotinin	Serine proteases	10 µg/ml	Sigma (A1153)
Apyrase	ATP	2 U/ml	Sigma (A6535)
EDTA	Divalent cation chelator	5 mM, 20 mM	Acros Organics (237205000)
Fragmin	Potentiates antithrombin III activity	50 U/ml	Pfizer (-)
GPRP	Fibrin polymerisation	10 µM	Sigma (G5779)
Heparin	Potentiates antithrombin III activity	FA: 5 U/ml PPF: 100 U/ml	Iduron (HEP001)
Indomethacin	Cycloxygenase	10 µM	Sigma (I7378)
Leupeptin	Cysteine, serine and threonine proteases	10 µg/ml	Enzo Life Sciences (260-009-M100)
Pepstatin	Aspartyl proteases	1 µg/ml	Sigma (P5318)
PPACK	Thrombin	40 µM	Cambridge Biosciences (FPRCK-01)
Sodium Orthovanadate	Tyrosine phosphatases	5 mM	Sigma (450243)

FA, flow adhesion; PPF, proplatelet formation

2.2. Molecular Biology

Polymerase chain reaction (PCR) was used to determine genotypes of genetically modified mice. Targeting primers are indicated in **Table 2.4** (Sigma, Poole, UK).

2.2.1. DNA isolation

DNA for genotyping was obtained from ear clips collected from preweaned 3-week old pups. Tissue was digested in lysis buffer (0.2% SDS, 100 nM Tris.HCl, 5 mM EDTA, 200 nM NaCl, pH 8.5) with proteinase K (650 µg/ml) overnight at 55^{o}C. Cell debris was pelleted by centrifugation (13,000 × g, 10 minutes, 4^{o}C) and ice cold 100% isopropanol used to precipitate DNA. DNA was then pelleted by centrifugation (13,000 × g, 20 minutes, 4^{o}C), dried and resuspended in sterile deionised water.

2.2.2. PCR

PCRs were performed using 10 µl ReadyMix REDTaq PCR reaction mix, 20 µM of primer and 1 µl purified DNA. Reactions were performed in a Tetrad 2 Peltier thermal Cycler (Bio-Rad Laboratories, Watford, UK), denaturing, annealing and extending cycles are shown in **Table 2.5**. PCR products were resolved on agarose gels containing 0.0001% ethidium bromide to detect DNA. Gels were run in TAE (40 mM tris, 20 mM acetic acid and 1 mM EDTA) at 120 V for 20-40 minutes, then imaged using a Gene Genius Gel Imaging System (Syngene, Cambridge, UK).

Table 2. 4. PCR Primers

Gene target	Forward primer	Reverse primer	
LAIR-1 WT	5'-TTTATGAGGAGG ACGACTGAGC-3'	5'-GGTTTGAGGACAG ACAGATGACC-3'	
LAIR-1 mutant	5'-TTTATGAGGAGG ACGACTGAGC-3'	5'-CCAGGTGCACATG ATCAGC-3'	
LAIR-1 control	5'-GAGACTCTGGCTA CTCATCC-3'	5'-CCTTCAGCAAGAG CTGGGGAC-3'	
PECAM-1	5'-CATGATGCC AAGTCT-3'	5'-GTGGGCTTATCTGTG AATGT-3'	
TLT-1	5'-GGGGTACCTTGA GAATCAGATGGCCCT G-3'	5'-CGGCACATGTGGCAGCTC GTCCATGCCGAGAGTG-3'	5'-GATCATCCTGC CTACAGTGG-3'

Table 2. 5. PCR Protocols

Gene target	PCR program			Product (bp)	Agarose gel
LAIR-1	95 ºC	5 min	× 35 cycles	WT: ~208 KO: ~284 Control: ~585	1.5%
	95 ºC	30 s			
	60 ºC	30 s			
	72 ºC	1 min			
	72 ºC	10 s			
PECAM-1	94 ºC	3 min	× 30 cycles	WT: ~165 KO: ~1500	1.5%
	94 ºC	30 s			
	54 ºC	30 s			
	72 ºC	1 min 30 secs			
	72 ºC	10 min			
TLT-1	95 ºC	2 min	× 40 cycles	WT: ~947 KO: ~1250	1%
	95 ºC	30 s			
	56 ºC	30 s			
	72 ºC	1 min			
	72 ºC	10 min			

bp, base pairs; min, minutes; s, seconds

2.3. Platelet isolation

2.3.1. Mouse washed platelet isolation

Blood was collected from the vena cava of CO_2 asphyxiated mice using a 25 gauge needle into 200 µl acid-citrate-dextrose (ACD) solution in a 1 ml syringe. Blood was then immediately diluted in 200 µl Tyrodes-HEPES buffer. Whole blood was centrifuged (2,000 rpm, 5 minutes, room temperature [RT]; Microcentaur, Sanyo) and platelet rich plasma (PRP) and third of erythrocytes collected. PRP was separated from erythrocytes by centrifugation (200 × g, 6 minutes, RT) in a swinging bucket centrifuge and collected. To maximise platelet yield an additional 200 µl Tyrodes-HEPES buffer was added to erythrocytes, mixed by inversion then centrifuged again (200 × g, 6 minutes, RT) and the PRP collected pooled. Collected PRP was made up to 1 ml by addition of Tyrodes-HEPES buffer and centrifuged (1,000 × g, 6 minutes, RT) in presence 10 µg/ml PGI_2 to pellet platelets. Platelets were resuspended in Tyrodes-HEPES buffer, counted (Coulter Z2 Particle Count and Size Analyzer, Beckman Coulter Ltd, High Wycombe, UK) and diluted to 2×10^7 for spreading assay, 2×10^8 for lumi-aggregometry and 5×10^8 for biochemistry. Washed platelets were allowed to rest for 30 minutes following isolation before beginning experiments.

2.3.2. Human washed platelet isolation

Blood was collected from drug free, healthy volunteers into sodium citrate (1:10, v:v). following collection acid citrate dextrose (97 mM sodium citrate, 111 mM glucose, 71 mM citric acid) was added to blood (1:9 , v:v). Anticoagulated blood was then centrifuged (200 × g, 20 minutes, RT) and PRP separated from red blood cells. Collected PRP was then centrifuged (1,000 × g, 10 minutes, RT) in presence 10 µg/ml PGI_2 to pellet platelets. Platelets were resuspended in modified Tyrodes-HEPES buffer with ACD (1:8, v:v) and centrifuged again

(1,000 × g, 10 minutes, RT). Platelet pellet was resuspended in Tyrodes-HEPES buffer, counted and diluted to 2×10^7 for spreading assay, 2×10^8 for lumi-aggregometry and 5×10^8 for biochemistry. Washed platelets were allowed to rest for 30 minutes following isolation before beginning experiments.

2.4. Platelet function assays

2.4.1. Lumi-aggregometry

Washed platelets (2×10^8/ml) were incubated (37ºC, 1 minute non-stirring, 1 minute stirring conditions, 1,200 revolutions per minute [rpm] in a Chrono-Log Lumi-aggregometer [Havertown, PA, USA]). Following incubation, agonists (1:100) were added and measurement started. Area under the curve (AUC) was calculated for 6 minutes following agonist addition by AGGRO/LINK8 software (Chrono-Log, Havertown, PA, USA).

ATP released from dense granules was measured using Chrono-lume (1:30 [v:v], Chrono-Log, Havertown, PA, USA). A calibration was performed with 2 nmol ATP standard (Chrono-Log, Havertown, PA, USA) for each channel at the start of experiments enabling AGGRO/LIK8 software to subsequently calculate ATP release and AUC.

2.4.2. Platelet spreading

Glass coverslips (13 mm diameter) were coated with fibrinogen (100 µg/ml, Enzyme Research, Swansea, UK) or collagen (10 µg/ml, Takeda, Tokyo, Japan) overnight, 4ºC. Coverslips were then blocked with denatured fatty acid free BSA (5 mg/ml) for 1 hour, RT. Washed platelets (2×10^8/ml) were then plated for 45 minutes, 37ºC. Adhered platelets were then fixed with 4% PFA for 10 minutes, RT. For differential interference contrast (DIC) microscopy, fixed coverslips were mounted directly onto microscope slides using Hydromount (National

Diagnostics, Hull, UK). For fluorescence microscopy, platelets were permeabilised and stained (as below) for actin cytoskeleton (6.6nM phalloidin-AF488, 1 hour, RT) before being mounted and imaged.

2.4.3. Flow adhesion

Glass coverslips (24 × 60 mm) were coated with collagen type I microscpots (100 µg/ml, Nycomed Pharma, Munich, Germany). Coated coverslips were blocked with Tyrodes-HEPES buffer containing 1% BSA and mounted into parallel plate flow chambers. Blood was collected from vena cava CO_2 asphyxiated mice into 40 µM PPack, 5 U/ml heparin and 50 U/ml fragmin (final concentrations) and perfused over coated coverslips for 3.5 minutes at 1,000 s^{-1} shear rate. Three brightfield and fluorescence images (P-selectin-FITC, JON/A-PE and Annexin A5-AF647) were captured per microspot. Images were blinded and analysed in Fiji Software (Laboratories for Optical and Computational Instrumentation, University of Wisconsin-Madison, USA), using semi-automated scripts to measure percentage surface area coverage (%SAC) of adhered platelets from brightfield images and fluorescence of each antibody.

2.4.4. Integrin activation and granule release

Whole blood was activated by indicated agonists in Tyrodes-HEPES buffer in presence of FITC-conjugated anti-P-selectin antibody or AF488-conjugated fibrinogen (Thermo Scientific, Loughborough, UK). GPRP (10 µM) was added to prevent clotting of thrombin stimulated samples. Following stimulation samples were fixed with ice-cold 1% PFA and analysed on Accuri C6 flow cytometer (BD Biosciences, Oxford, UK). Platelets were gated using forward- and side-scatter and median fluorescence intensity analysed from 10,000 events.

2.5. Megakaryocyte culture and function assays

2.5.1. Primary mouse bone marrow megakaryocyte culture

Bone marrow (BM)-cells were obtained from mice by flushing femurs and tibias with Dulbecco's Modified Eagle Medium (DMEM) containing 10% FBS, glutamine and penicillin/streptomycin. BM-cells were centrifuged (1,200 rpm, 5 minutes, 4^{o}C) and the pellet resuspended in ammonium chloride potassium lysing buffer (ACK, 150 nM NH_4Cl, 1 mM $KHCO_3$, 0.1 mM Na_2 EDTA) to lyse red blood cells and then filtered (70 µm nylon mesh filter). Filtered cells were centrifuged (1,200 rpm, 5 minutes, 4^{o}C) and resuspended in DMEM. Cells expressing non-megakaryocytic lineage markers (CD16/32, Gr1+, B220+ and CD11b+) were then depleted using immunogenic beads (sheep anti-rat IgG Dynabeads, Invitrogen, Carlsbad, USA). The remaining population was then cultured in Stempro medium (Invitrogen, Carlsbad, USA) supplemented with 2.6% serum, 2 mM L-glutamine and penicillin/streptomycin. For the first 2 days cells were cultured with 20 ng/ml murine stem cell factor (SCF, Peprotech, Rocky Hill, USA) and then in presence of SCF and 50 ng/ml TPO (Peprotech, Rocky Hill, USA) for a further 4 days. Mature megakaryocyte population was enriched using a 1.5%/3% BSA gradient under gravity (1 × g, 1 hour, RT).

2.5.2. Megakaryocyte ploidy

Cultured megakaryocytes were analysed using a FACSCalibur flow cytometer (BD Biosciences, Oxford, UK). Following enrichment, megakaryocytes were co-stained with ant-αIIb antibody and propidium iodide (PI). PI staining of αIIb-positive cells was then analysed in 50,000 events.

2.5.3. Megakaryocyte spreading and proplatelet formation

Coverslips were prepared as for platelet spreading. Enriched megakaryocytes were resuspended in complete Stempro medium with addition of SDF-1α (Peprotech Rocky Hill, USA) and heparin (100 U/ml) then plated on coverslips for 3 or 5 hours, at 37ºC, for spreading or proplatelet formation respectively. Adhered megakaryocytes were then fixed with 4% PFA (15 minutes, RT) before immunofluorescence staining and imaging.

2.6. Immunofluorescence staining, imaging and quantification

2.6.1. Immunofluorescence staining

PFA fixed platelets or megakaryocyte coverslips were quenched with NH_4Cl (50 mM, 10 minutes, RT), permeablised with Triton-X100 (0.2%, 5 minutes, RT). Coverslips were then blocked with 1% fatty acid free BSA with 2% goat serum and stained with conjugated antibody, or primary antibody followed by conjugated secondary. Antibodies can be found in **Table 2.1**. Following staining coverslips were mounted on microscope slides using Hydromount or Prolong Diamond Antifade Mountant with DAPI (Invitrogen, Carlsbad, USA).

2.6.2. Resting platelets and megakaryocytes

Washed platelets (4×10^8/ml) were fixed in suspension with 1% PFA (1:1 [v:v], 10 minutes, RT), plated onto poly-L-lysine coated coverslips and centrifuged (1,000 rpm, 10 minutes, RT). Megakaryocytes were plated on fibrinogen coated coverslips (100 µg/ml, 15 minutes, 37ºC), before fixing with 4% PFA. Coverslips were then immunofluorescently stained with anti-P-selectin, TLT-1 and phalloidin-rhodamine for 1 hour, RT **(Table 2.1)** then imaged.

2.6.3. Image acquisition

Images were captured using a Zeiss Axiovert 200M microscope (Cambridge, UK), Zeiss Observer 7 epifluorescent microscope, or Zeiss LSM880 confocal microscope with Airyscan processing (Cambridge, UK). Platelets were imaged using a 40× or 63× objectives, megakaryocytes using 20×, 40× or 63× objectives. 5 fields of view (FOV) per coverslip were captured for platelet spreading, and three 5×5 tiles captured per coverslip for megakaryocyte proplatelet formation. Images were acquired using Zen Pro V2.3 (Zeiss, Cambridge, UK).

2.6.4. Quantification spreading and proplatelet formation

Images were blinded before quantification. For platelets, quantification was either manually using Fiji (chapter 3) or using a semi-automated machine learning based KNIME workflow (details below) to measure number of adhered platelets, surface area and stages of spreading (unspread, forming filopodia, forming lamellipodia and fully spread, **Figure 2.1**). For megakaryocytes, quantification was carried out manually in Fiji (chapter 3) or using a semi-automated machine learning based KNIME workflow to measure number of proplatelet forming megakaryocytes and area of megakaryocyte spreading.

2.6.4.1 KNIME workflow

An Ilastik pixel classifier (Sommer et al., 2011) was used to produce a binary segmentation. To separate touching platelets and megakaryocytes the centre of individual cells were manually selected using KNIME (Berthold et al., 2009). These centre coordinates were then used as seeds for a watershed transform to produce the final segmentation result. Objects smaller than 5 μm^2 for platelet spreading and 100 μm^2 for megakaryocyte proplatelet formation were discarded and per cell measurements such as cell area were then calculated. A subset of cells were manually

assigned to one of the following classes: adhered, forming filopodia, forming lamellipodia and fully spread for platelets; or non-megakaryocyte, non-proplatelet forming or proplatelet forming for megakaryocytes. A decision tree based classifier was trained from this subset and used to assign classes to the full dataset. This method of analysis has previously been characterised and validated against manual spreading analysis by other members of the Birmingham Platelet Group.

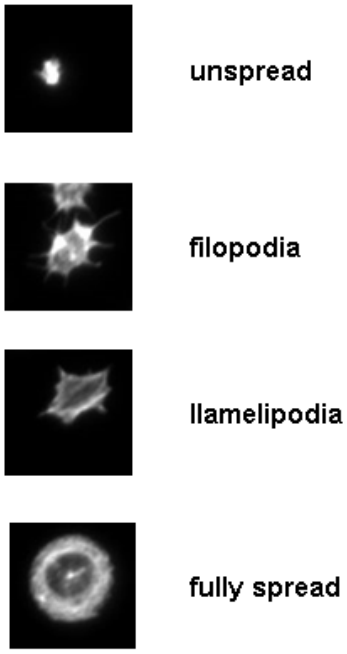

Figure 2. 1. Platelet spreading categories. Representative images of the four categories, unspread, filopodia forming, lamellipodia forming and fully spread, used to classify platelet spreading.

2.6.5. Colocalization

Analysis of receptor colocalization in platelets and megakaryocytes was performed on maximum intensity projections using Icy software (Quantitative Image Analysis Unit, Institut Pasteur, (de Chaumont et al.). Colocalization of 488 and 647 channels in platelets was determined by Manders overlap coefficient (Pike et al., 2017). Megakaryocyte images were processed using Icy's spot detector plugin (http:/icy.bioimageanalysis.org/plugin/Spot_Detector) to effectively threshold 488 and 647 channels and determine an object based measure of colocalization.

2.7. Biochemistry

2.7.1. Platelet sample preparation in solution

Washed platelets (2×10^8/ml) were prewarmed Chrono-Log aggregometer at 37^{o}C (1 minute non stirring followed by 1 minute stirring, 1,200 rpm). CRP stimulations were performed for 30, 90 and 180 seconds. Stimulations were stopped by adding 2× lysis buffer ((LB), 300mM NaCl, 20mM Tris, 2mM EGTA, 2mM EDTA and 2% NP-40 detergent) containing 5 mM Na_3VO_4, 1 mM AEBSF, 10 µg/ml aprotinin and 1 µg/ml pepstatin. Whole cell lysates (WCL) were precleared with protein-G sepharose (30 minutes, 4^{o}C, constant mixing). Cell debris and sepharose beads were pelleted by centrifugation (15,000 × g, 10 minutes, 4 ^{o}C). Reducing sample buffer (SB, 4% SDS, 20% glycerol, 1% stacking gel buffer, 10% β-mercaptoethanol) was then added to WCL and boiled for 5 minutes.

2.7.2. Sample preparation spread platelets

Six well plates or 10 cm diameter dishes were coated with 100 µg/ml fibrinogen (overnight, 4^{o}C), and blocked with 5 mg/ml denatured fatty acid free BSA (1 hour, RT). Washed platelets

(5×10^8) in Tyrodes-HEPES buffer with indomethacin (10 μM) and apyrase (2 U/ml) were plated on coated wells (45 minutes, 37°C). Non-adherent platelets were lysed with 1 × LB plus inhibitors on ice for 15 minutes. WCL protein concentrations were determined (Bio-Rad RC DC protein assay) and boiled in SB.

2.7.3. Megakaryocyte sample preparation

Following enrichment megakaryocytes were starved in serum free media (4 hours, 37°C). Megakaryocytes were then stimulated with indicated agonists (10 minutes, 37°C) and lysed with 2×LB with inhibitors. WCL samples were then precleared and protein levels normalised with reducing SB for immunoblotting, or following ProteinSimple Wes protocol.

2.7.4. SDS-PAGE and western blotting

Sodium dodecyl sulfate-polyacrylamide gel electrophoresis (SDS-PAGE) on 4-12% Bis-Tris gels (Life Technologies, Paisley, UK) was used to resolve proteins. Proteins were transferred to poly vinylidene difluoride membranes (Bio-Rad, Hemel Hempstead, UK) using a Bio-Rad semi-dry Turbo transfer system. Broad range unstained protein marker (2-212 kDa) and prestained protein standard (New England Biolabs, Hitchin, UK) were used to estimate molecular weight (MW).

Membranes were blocked following transfer with BSA blocking buffer (3% BSA [w:v], in 0.1% Tween-20 [v:v], Tris-buffered saline [TBS-T, 200 μM Tizma base, 1.37 M NaCl, 0.1% Tween-20]). Membranes were then incubated with indicated primary antibodies in blocking buffer (overnight, 4°C, constant mixing). Membranes were washed in TBS-T (1 × 10 minutes, 3 × 5 minutes) before incubation with horseradish peroxidase-conjugated secondary antibodies (1/10,000, 1 hour, RT) in TBS-T. Membranes were washed again in TBS-T and subsequently

proteins detected using Enhanced Chemiluminescence detection system (Life Technologies, Paisley, UK). Autoradiograph exposure was used to visualise chemiluminescence.

Bound antibodies were removed by membrane incubation (20 minutes, 80^{o}C) in stripping buffer (TBS-T containing 2% SDS) with 1% β-mercaptoethanol, followed by a second incubation (20 minutes, 80^{o}C) in stripping buffer without β-mercaptoethanol. Membranes were then washed in TBS-T and blocked with BSA before primary antibody incubation overnight.

2.7.5. Automated capillary-based immunoassay

Automated capillary-based immunoassay platform Wes (ProteinSimple, San Jose, USA) was used for quantitative protein analysis. WCLs were prepared according to manufacturer's instructions. Pre-filled microplates with Split Running Buffer (PS-MK14) were loaded with optimal concentrations of samples and primary antibodies **(Table 2.6)**. Separation time (31 minutes), stacking loading time (21 s) and sample loading time (9 s) was used for each 24 sample microplate, with primary antibody incubation time either 30 or 60 minutes and exposure detection profile set to high dynamic range. Results were analysed using Compass software (ProteinSimple, San Jose, USA).

Table 2. 6. ProteinSimple Wes Antibody conditions

Antibody	Source	Antibody dilution	Primary Incubation time (min)	Platelet concentration (mg/ml)	Megakaryocyte concentration (mg/ml)
GAPDH	Cell Signaling Technology (14C10)	1:10	60	0.05	-
Src p-Y418	Invitrogen (44660G)	1:10	60	0.05	-
Syk p-Y525/6	Cell Signaling Technologies (2711)	1:50	30	0.2	-
Csk (C20)	Santa Cruz (sc286)	1:10	30	0.025	0.05
Chk	Santa Cruz (sc470)	1:80	60	0.2	0.4

2.8. Immunohistochemistry

Spleens and femurs were isolated from CO_2 asphyxiated mice and fixed in 4% PFA. Before fixing, spleens were weighed and ends of femurs cut to expose bone marrow. Femurs were then decalcified and both tissues embedded in paraffin. Cut sections were mounted on glass microscope slides and stained with either haematoxylin an eosin, or reticulin (Pathology department, Queen Elizabeth Hospital, Birmingham, UK). Light microscopy images of slides were then taken with a Zeiss AxioScan Z1 (Carl Zeiss Ltd, Cambridge, UK). Number of megakaryocytes and reticulin staining in images were then assessed.

2.9. Ex vivo mouse assays

2.9.1. Haematology

Blood cell counts of whole mouse blood were measured using an ABX Pentra 60 Haematological counter (Horiba Medical, Northampton, UK).

2.9.2. Surface receptor levels

Surface receptor levels on platelets in whole blood and cultured megakaryocytes were assessed using flow cytometry. Samples were incubated with indicated FITC- or AF488-conjugated antibodies or IgG controls in combination with PE. Platelets and mature megakaryocyte fractions were gated by FSC-A and SSC-A and MFI of 10,000 and 50,000 events analysed for platelets and megakaryocytes respectively. Stained whole blood was analysed using an Accuri C6 flow cytometer. Megakaryocytes were analysed using a FACSCalibur.

2.10. *In vivo* mouse assays

2.10.1. Tail bleeding

Tail tips (3 mm) were excised using a scalpel from isoflurane anaesthetised mice and immediately placed in warmed saline (37ºC). Mice body temperature was maintained at 37ºC by heating mat. Time for bleeding to stop and any rebleeds was recorded. Mice were culled if bleeding was ceased for 1 minute or after total time reached 20 minutes.

2.10.2. Laser-injury thrombosis model

Experiments were conducted on male mice (20-30 g). Mice were anaesthetised by intraperitoneal injection with 125-240 mg/kg Avertin (Tribromoethanol dissolved in 2-Methyl-2-butanol, and diluted in sterile saline). Trachea tube inserted and either carotid artery or jugular vein cannulated for indicated antibody infusion prior to injuries. Cremaster muscle was then exteriorised over a glass coverslip and continually perfused with warmed bicarbonate buffered saline. Laser-induced thrombi were generated in arterioles. Thrombus formation was capture by simultaneous real-time brightfield and fluorescence confocal microscopy (Olympus BX61WI, upright spinning disk confocal microscope [40× 0.8NA water immersion lens] with a Photometrics Evolve camera).

2.10.3. Ferric chloride-injury thrombosis model

Experiments were conducted on mice (20-30 g). Mice were anaesthetised by intraperitoneal injection with Avertin. Trachea tube inserted and jugular vein cannulated for indicated antibody infusion prior to injury. Carotid artery (right side) was then exposed and ferric chloride-soaked filter paper applied (2 mm × 1 mm, 10% ferric chloride, 3 minutes). Injury site was then imaged

for 15 minutes by time lapse fluorescence confocal microscopy (Olympus BX61WI, upright spinning disk confocal microscope [4× 0.13NA air lens] with a Photometrics Evolve camera). All intravital data was collected and analysed using Slidebook 6 software (3i, Denver, USA).

2.11. Statistical analysis

All data presented as mean ± standard error of the mean (SEM) unless otherwise stated. Statistical significance was analysed by Students t-test, Analysis of Variance (ANOVA) or Mann-Whitney test. The appropriated parametric or non-parametric test was selected based on sample size, sample distribution, number of groups and if the measured variable is continuous. All statistical analysis was carried out using GraphPad Prism software (GraphPad Software Inc., La Jolla, CA, USA) unless otherwise stated.

Chapter 3

LAIR-1 deficient mouse model

3.1. Aim

The aim of this chapter was to investigate the physiological role of LAIR-1 in megakaryocyte development and platelet production and function. In order to do this, a constitutive LAIR-1 deficient murine model was generated and utilized. Mice lacking LAIR-1 were hypothesized to have hyper responsive megakaryocytes and platelets to collagen.

3.2. Introduction

ITIM-containing receptors have increasingly been shown to play an essential role in regulation of megakaryocyte and platelet reactivity. Several ITIM-containing receptors have been identified in megakaryocyte and platelets, with the majority of these receptors reported to inhibit ITAM-receptor mediated activation by the collagen receptor GPVI (Coxon et al., 2017). Widely expressed in haematopoietic cells, including megakaryocytes, but not in platelets (Steevels et al., 2010), the ITIM-containing receptor LAIR-1 has been shown to have an inhibitory function in immune cells, mediated via recruitment of Shp1 and Shp2 phosphatases, and Csk to the phosphorylated ITIMs of its cytoplasmic tail (Verbrugge et al., 2006). LAIR-1 has also been implicated as a negative regulator of haematopoiesis (Meyaard, 2010, Tang et al., 2012, Xue et al., 2011). Crosslinking LAIR-1 on primary human CD34+ cells has been shown to decrease generation of megakaryocytes in presence TPO (Xue et al., 2011). Furthermore, studies report LAIR-1 to be crucial for the development of acute myeloid leukaemia (Kang et al., 2015).

LAIR-1 is a collagen receptor, binding via the same repeated GPO motifs as GPVI but with a much higher affinity (Brondijk et al., 2010, Lebbink et al., 2006, Lebbink et al., 2009). When co-expressed in transiently transfected DT40 cells, LAIR-1 has been shown to strongly inhibit collagen mediated GPVI activation by an NFAT reporter assay (Tomlinson et al., 2007).

Due to the inhibitory nature of the receptor and the important role of collagens in their activation, the function of LAIR-1 in megakaryocytes and platelets has been investigated. Previous work has shown mice deficient in LAIR-1 present a mild phenotype, including thrombocythemia, prolonged platelet half-life *in vivo* and increased proplatelet formation *in vitro* (Smith et al., 2017). Interestingly despite platelets not ordinarily expressing LAIR-1, platelets from deficient mice show enhanced reactivity to GPVI receptor agonists and greater spreading on fibrinogen, suggesting transfer of activation signals from megakaryocytes to platelets. This enhanced reactivity of megakaryocytes and platelets from LAIR-1 deficient mice was attributed to the observed increase in SFK activity, amplifying GPVI-FcRγ-chain and integrin αIIbβ3 downstream signalling (Smith et al., 2017).

In this chapter, megakaryocytes and platelets from LAIR-1 deficient mice were further characterised in order to determine the underlying cause of the enhanced SFK activity previously observed. It also examines if enhanced responsiveness of LAIR-1 deficient platelets, as previously observed to ITAM-mediated activation, also occurs to hemi-ITAM and GPCR receptor activation. In addition, it determines if the enhanced reactivity of LAIR-1 deficient platelets observed *in vitro* translates to enhanced thrombosis *in vivo*.

3.3. Results

3.3.1. Generation of LAIR-1 KO mice

To investigate the physiological function of LAIR-1, a constitutive KO mouse model was generated (Taconic Biosciences, Cologne, Germany). The strategy to generate this mouse model is displayed in **Figure 3.1**. A targeting vector containing a puromycin resistance cassette (PuroR) flanked with flippase (Flp) recognition sites was produced. Homology arms of 4 kb and 6 kb were cloned into the targeting vector to allow Lair1 exons 1 and 2 to be effectively targeted and replaced with the PuroR cassette through homologous recombination in C57Bl/6NTac embryonic stem cells. Homologous recombinant clones, isolated using PuroR positive and thymidine kinase negative selection, were then injected into mouse blastocysts and transplanted into psudopregnant female mice. Replacement of the proximal promoter and exons 1 and 2 results in loss of Lair1 gene function through deletion of translation initiation codon and signal peptide sequence. In addition, deletion of proximal promoter and 5'UTR prevent transcription of LAIR-1 mRNA. Removal of PuroR positive selection cassette, mediated by crossing with Flp recombinase expressing mice, which excise the Flp target sites, results in constitutive KO. Further crossing with C57Bl5/NTac mice removed Flp recombinase. Mice were viable and fertile with no developmental or behavioural abnormalities. Mice were bred heterozygous and generated at Mendelian frequency, with litter matched WT mice were used as controls.

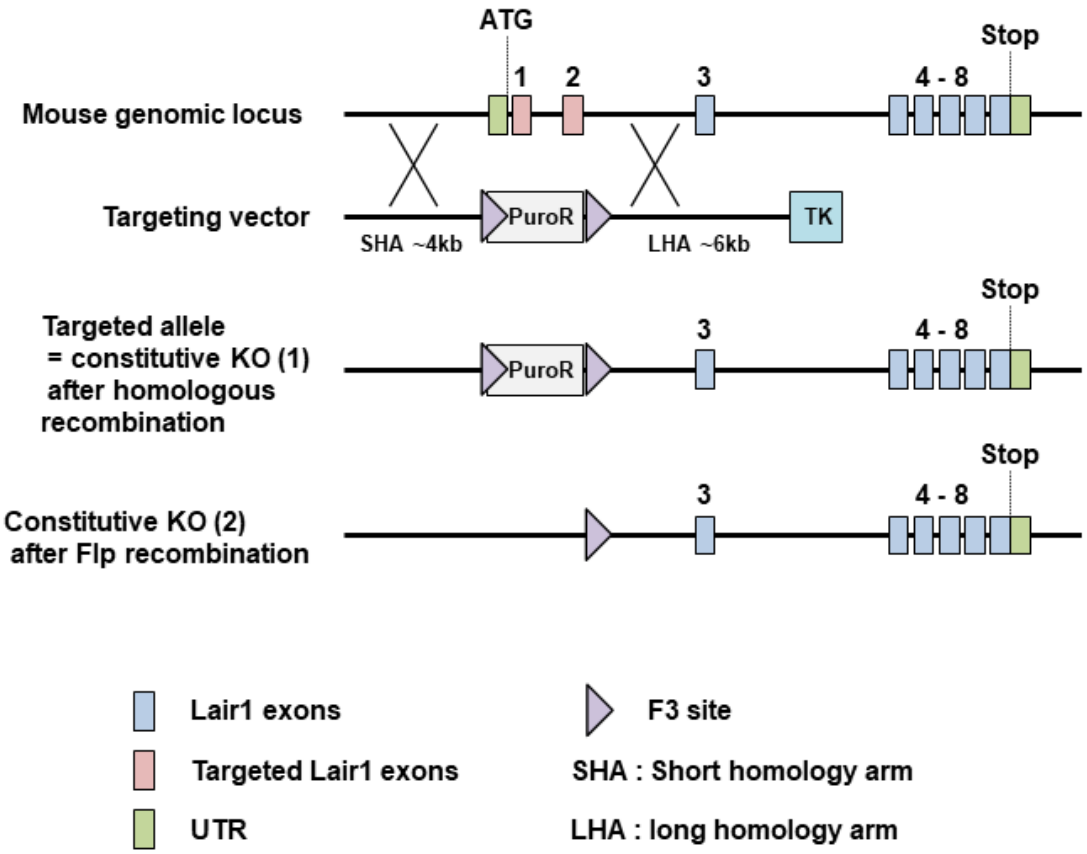

Figure 3. 1. Generation of LAIR-1 deficient mouse model. Targeting strategy used to generate LAIR-1 deficient mouse model showing mouse LAIR-1 genomic locus, targeting vector and mouse genome following vector insertion by homologous recombination and after subsequent removal of selection cassette. Targeting vector consists of puromycin resistance cassette (PuroR) and thymidine kinase (TK) for positive and negative selection respectively. PuroR is flanked with flippase recognition sites to allow subsequent removal by Flp recombinase. Homology arms allow for targeted homologous recombination. Replacement of proximal promoter and exons 1 and 2 results in loss of LAIR-1 gene function by deletion of translation initiation codon and signal peptide sequence. In addition, deletion of proximal promoter and 5'UTR should prevent transcription of LAIR-1 mRNA.

3.3.2. LAIR-1 deficient megakaryocyte spreading unaltered on collagen

Having previously been demonstrated that megakaryocytes from mice deficient in LAIR-1 exhibit a marked increase in spreading, and an increased number form proplatelets on fibrinogen (Smith et al., 2017), megakaryocyte spreading and proplatelet formation on collagen, the ligand of LAIR-1, was investigated. Megakaryocytes from LAIR-1 deficient mice and litter matched WT controls spread equally well on collagen, with neither forming proplatelets (**Figure 3.2**). No significant changes in collagen surface receptor expression were found on megakaryocytes from LAIR-1 deficient mice, compared to WT mice, by flow cytometry (**Table 3.1**).

3.3.3. Src activation proximal to GPVI in LAIR-1 deficient megakaryocytes

Signalling proximal to GPVI has previously been found to be elevated in LAIR-1 deficient megakaryocytes, with phosphorylation of Src, Syk and PLCγ2 activation sites increased at resting and following convulxin stimulation (Smith et al., 2017). A possible explanation for this finding is decreased inhibition of SFKs. Inhibitory site phosphorylation of Src Tyr529, Lyn Tyr507 and Fyn Tyr530 were therefore investigated in LAIR-1 deficient megakaryocytes. Phosphorylation levels of inhibitory tyrosines at both resting, and following convulxin stimulation, which strongly activates GPVI but not LAIR-1 (Tomlinson et al., 2007), were normal in LAIR-1 deficient megakaryocytes **(Figure 3.3).**

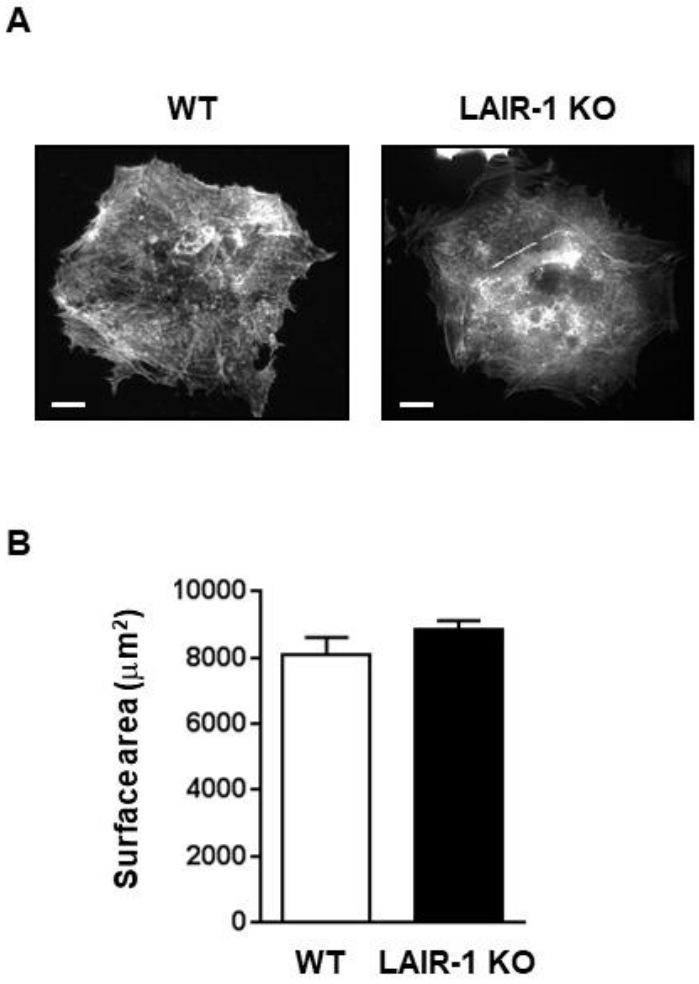

Figure 3. 2. LAIR-1 KO megakaryocyte spreading unaltered on collagen. Bone marrow-derived megakaryocytes from LAIR-1 KO and litter matched WT mice were plated on collagen (100 µg/ml) coated surface for 5 hours at 37ºC. (A) Representative images of spread phalloidin stained megakaryocytes and (B) surface area (mean ± SEM). N = 20-50 megakaryocytes from 3 mice/genotype. Scale bar 20 µm; Student's t-test, non-significant.

Table 3. 1. Megakaryocyte surface receptor expression in LAIR-1 KO mice. Surface receptor expression of cultured bone marrow derived megakaryocytes from LAIR-1 deficient mice and WT controls were measured by flow cytometry.

Surface receptor	WT	LAIR-1 KO	*P* value
GPVI	29 ± 2.7	27 ± 3.1	ns
Integrin α2	38 ± 1.7	40 ± 3.6	ns
GPIbα	34 ± 4.7	28 ± 5.6	ns
Integrin αIIbβ3	214 ± 10	215 ± 29	ns
CLEC-2	76 ± 5	68 ± 5.6	ns
G6b-B	25 ± 6	21 ± 5	ns
PECAM-1	330 ± 28	263 ± 14	ns
LAIR-1	6 ± 1.5	0.4 ± 1.1 ***	<0.001

Data represents mean values of the mean fluorescent intensity ± SEM; n= 6-10; Student's t-test; ns, non-significant; *** $P < 0.001$

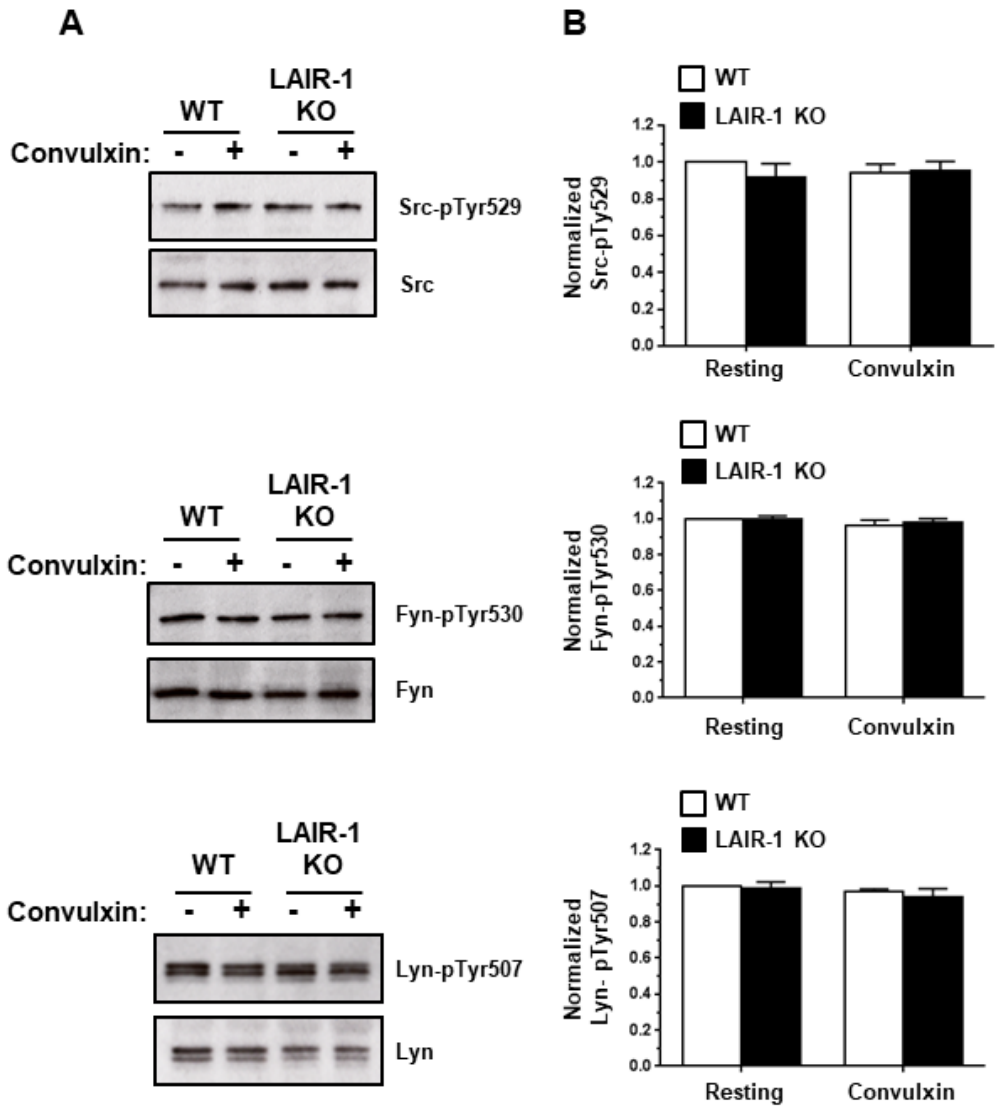

Figure 3. 3. GPVI-proximal signalling in LAIR-1 deficient megakaryocytes. Bone marrow-derived megakaryocytes from LAIR-1 KO and litter matched WT mice were stimulated with 30 µg/ml convulxin for 15 minutes at 37ºC. Whole cell lysates were Western blotted with anti-Src Tyr529, Fyn Tyr530 and Lyn Tyr507 antibodies. Membranes were stripped and reblotted with anti-Src, Fyn and Lyn antibodies. (A) Representative blots and (B) densitometry quantification (mean ± SEM) from 3 independent experiments/genotype. Two-way ANOVA with multiple comparisons.

3.3.4. LAIR-1 deficient mouse platelets response to non-GPVI agonists unaffected

Aggregation responses in platelets from LAIR-1 KO mice have previously been shown to be enhanced to collagen and CRP, which act through the ITAM-containing GPVI receptor (Smith et al., 2017). To determine if the absence of LAIR-1 affects signalling via other receptor pathways, aggregation and secretion responses to activation of the hemi-ITAM-containing receptor CLEC-2 and GPCR-coupled PAR receptors were investigated. Aggregation and secretion responses to CLEC-2 crosslinking were unaffected in platelets from LAIR-1 deficient mice**,** with aggregation to low dose thrombin stimulation also unaltered **(Figure 3.4).**

3.3.5. Src activation proximal to GPVI in LAIR-1 deficient mouse platelets

It has previously been shown platelets from LAIR-1 deficient mice exhibit elevated SFK activation, as measured by active site phosphorylation, at basal and following CRP stimulation, which strongly activates GPVI (Smith et al., 2017). This finding could potentially be explained by decreased inhibitory phosphorylation of SFKs. Src Tyr529, Lyn Tyr507 and Fyn Tyr530 inhibitory site phosphorylation was therefore investigated in resting and CRP stimulated platelets from LAIR-1 deficient mice. Phosphorylation levels of inhibitory tyrosines at both basal and following CRP stimulation were normal in platelets from LAIR-1 deficient mice **(Figure 3.5).**

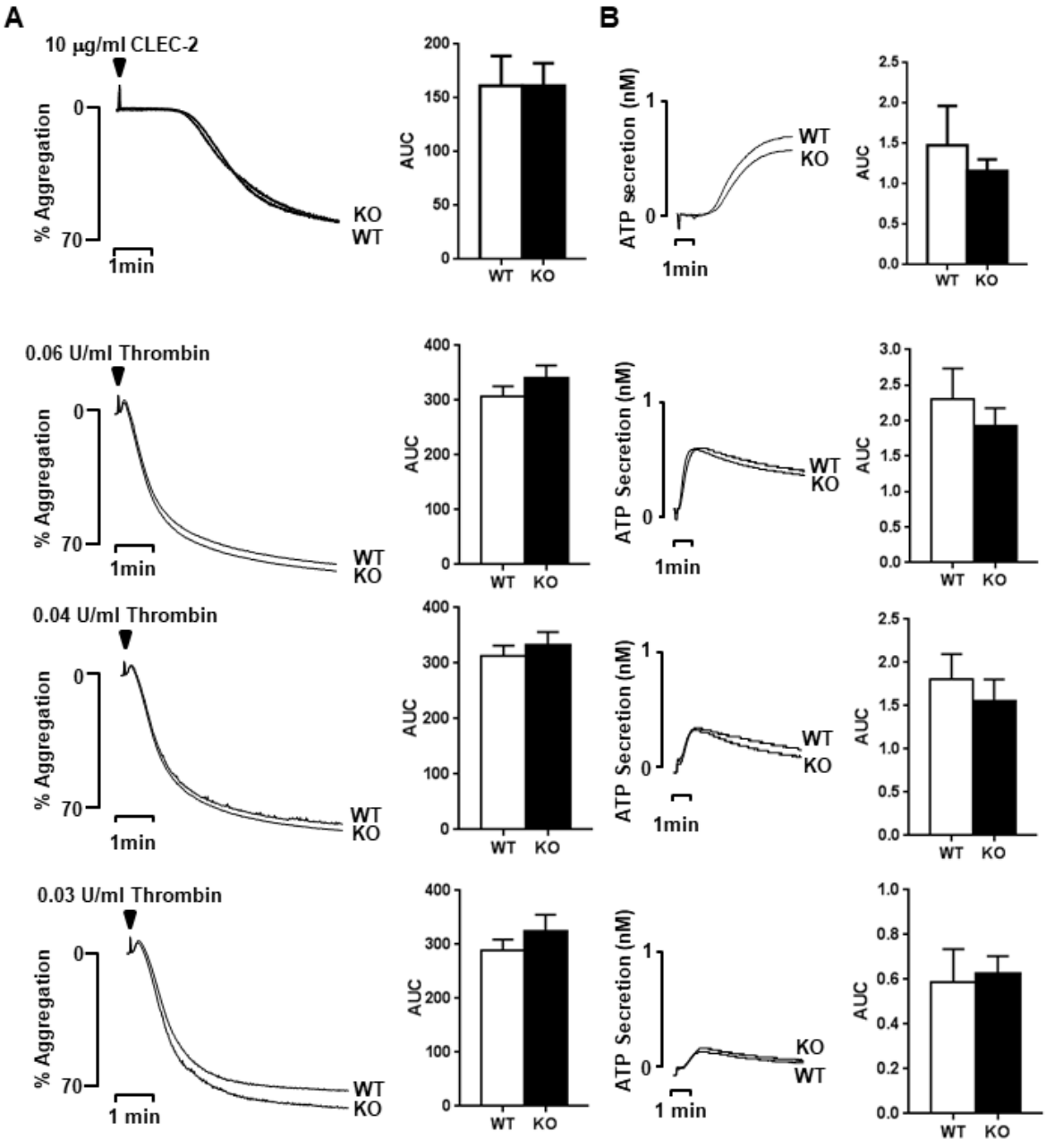

Figure 3. 4. Aggregation response to thrombin unaltered in platelets from LAIR-1 deficient mice. Aggregation and ATP secretion of washed platelets in response to 10 µg/ml anti-CLEC-2 antibody and 0.03, 0.04 and 0.06 U/ml thrombin. Representative traces and quantification of area under the curve (AUC) for aggregation (A) and secretion (B). Mean ± SEM; n=10-11 aggregations/condition; Student's t-test, non-significant.

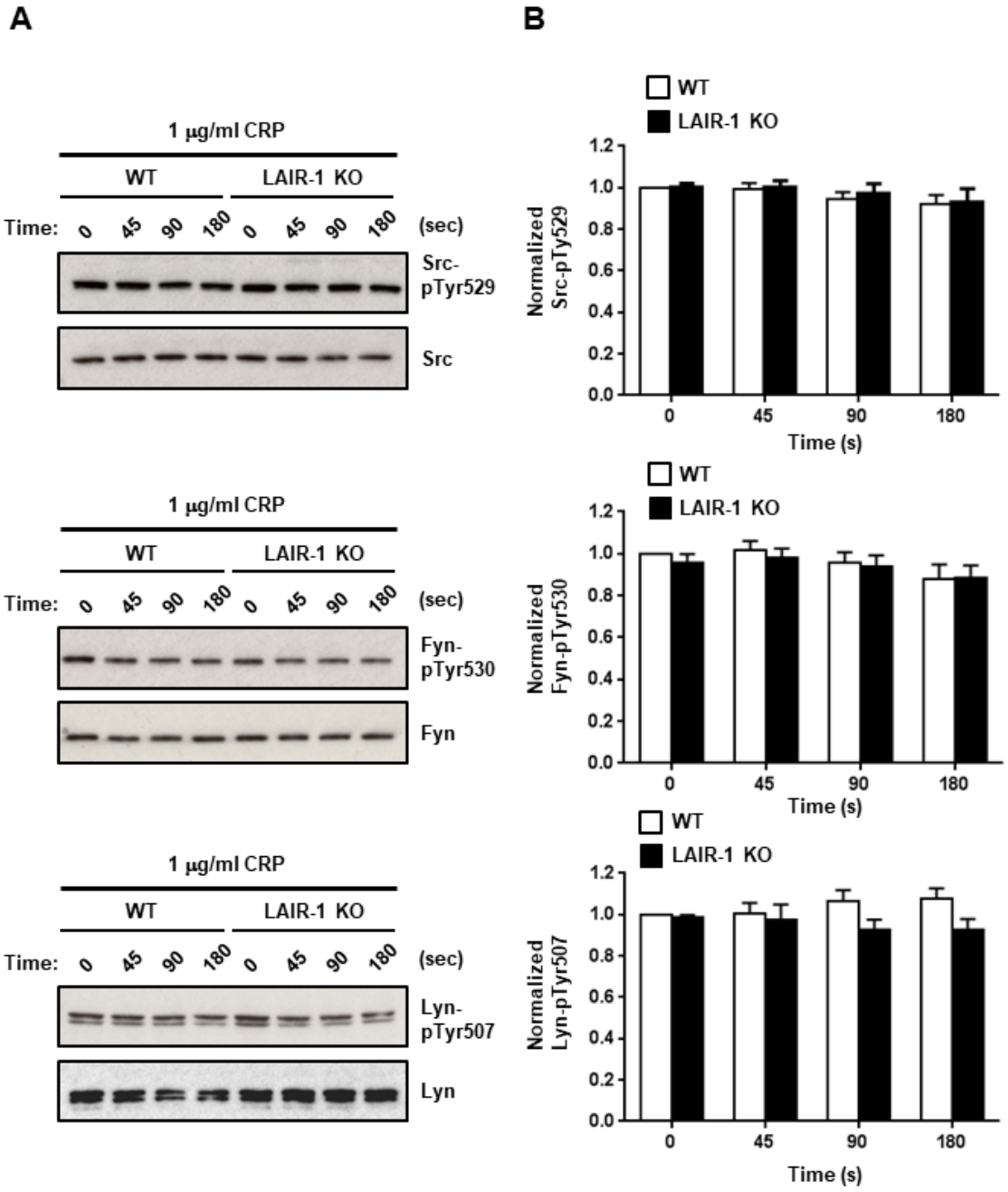

Figure 3. 5. GPVI-proximal signalling in platelets from LAIR-1 deficient mice. Whole cell lysates of resting and CRP stimulated washed platelets from LAIR-1 KO and litter matched WT mice were Western blotted with anti-Src Tyr529, Fyn Tyr530 and Lyn Tyr507 antibodies. Membranes were stripped and reblotted with anti-Src, Fyn and Lyn antibodies. (A) Representative blots and (B) densitometry quantification (mean ± SEM) from 3 independent experiments/genotype; Two-way ANOVA with multiple comparisons.

3.3.6. Increased integrin αIIbβ3 signalling in LAIR-1 deficient mouse platelets

Spreading on fibrinogen was previously shown to be enhanced in LAIR-1 deficient mouse platelets (Smith et al., 2017), despite levels of integrin αIIbβ3, as measured by flow cytometry, being the same as WT **(Table 3.2)**. Activation state of integrin αIIbβ3 downstream signalling proteins Src, Syk and PLCγ2 were therefore investigated upon fibrinogen adhesion as potential explanations for the observed enhancement. Phosphorylation of activation sites Src Tyr418 and Syk Tyr525/6 were increased in fibrinogen adherent cells, however PLCγ2 activation was not significantly increased, although this is potentially explained by the unreliable nature of the PLCγ2-pTyr1217 antibody **(Figure 3.6).** To explain the increased activity, SFK inhibitory site phosphorylation was assessed. LAIR-1 deficient mouse platelets show normal SFK inhibitory site phosphorylation in non- and fibrinogen adherent platelet lysates **(Figure 3.7)**.

3.3.7. Collagen spreading unaltered in LAIR-1 deficient mouse platelets

LAIR-1 deficient mouse platelets have previously shown enhanced spreading on fibrinogen (Smith et al., 2017). As LAIR-1 is an inhibitory collagen receptor, and deficient mouse platelets exhibit enhanced aggregation responses to collagen (Smith et al., 2017), spreading of LAIR-1 deficient mouse platelets on collagen was therefore evaluated. Interestingly, WT and LAIR-1 deficient mouse platelets spread equally well on collagen **(Figure 3.8)**.

3.3.8. Enhanced ferric chloride-induced thrombosis in LAIR-1 deficient mice

Platelets from LAIR-1 deficient mice have enhanced aggregation responses *in vitro*. Therefore the physiological role of LAIR-1 in arterial thrombosis *in vivo* was investigated. Utilizing the laser-injury model of thrombosis in mouse cremaster muscle arterioles, revealed thrombus formation was unaltered in LAIR-1 deficient mice **(Figure 3.9)**. Ferric chloride-induced

thrombosis in the carotid artery of mice did however show a significant increase in both the rate and extent of thrombosis **(Figure 3.10)**, correlating with the increased platelet reactivity to collagen *in vitro*.

Table 3. 2. Platelet surface receptor expression in LAIR-1 KO mice. Surface receptor expression of platelets from LAIR-1 deficient mice and WT controls were measured by flow cytometry.

Surface receptor	WT	LAIR-1 KO	*P* value
GPVI	1401 ± 118	1210 ± 82	ns
Integrin α2	821 ± 42	747 ± 52	ns
GPIbα	4305 ± 264	4260 ± 256	ns
Integrin αIIbβ3	3209 ± 111	3182 ± 167	ns
CLEC-2	6814 ± 205	6491 ± 466	ns
G6b-B	701 ± 77	902 ± 181	ns
PECAM-1	494 ± 35	535 ± 11	ns
LAIR-1	76 ± 10	72 ± 15	ns

Data represents mean values of the median fluorescent intensity ± SEM; n=8-12; Student's t-test; ns, non-significant.

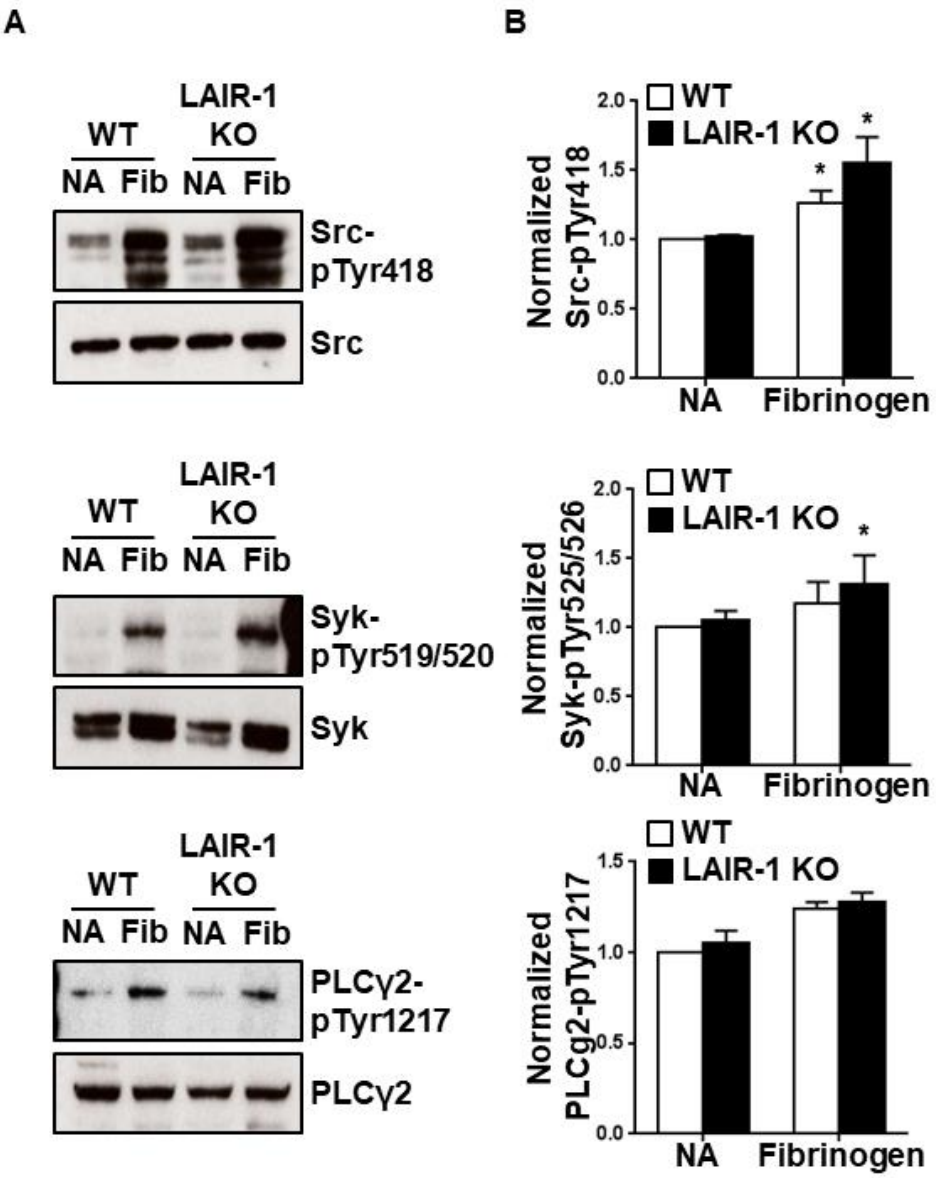

Figure 3. 6. Platelet integrin αIIbβ3 signalling from LAIR-1 deficient mice. Washed platelets from LAIR-1 KO and litter matched WT mice were plated on a fibrinogen coated surface (45 minutes, 37ºC). Whole cell lysates were prepared from non-adherent (NA) and adherent (fib) platelets and Western blotted with anti-Src Tyr418, Syk Tyr519/520 and PLCγ2 Tyr1217 antibodies. Membranes were stripped and reblotted with anti-Src, Syk and PLCγ2 antibodies. (A) Representative blots and (B) densitometry quantification (mean ± SEM) from 3 independent experiments/genotype; Two-way ANOVA with multiple comparisons, **P* < 0.05.

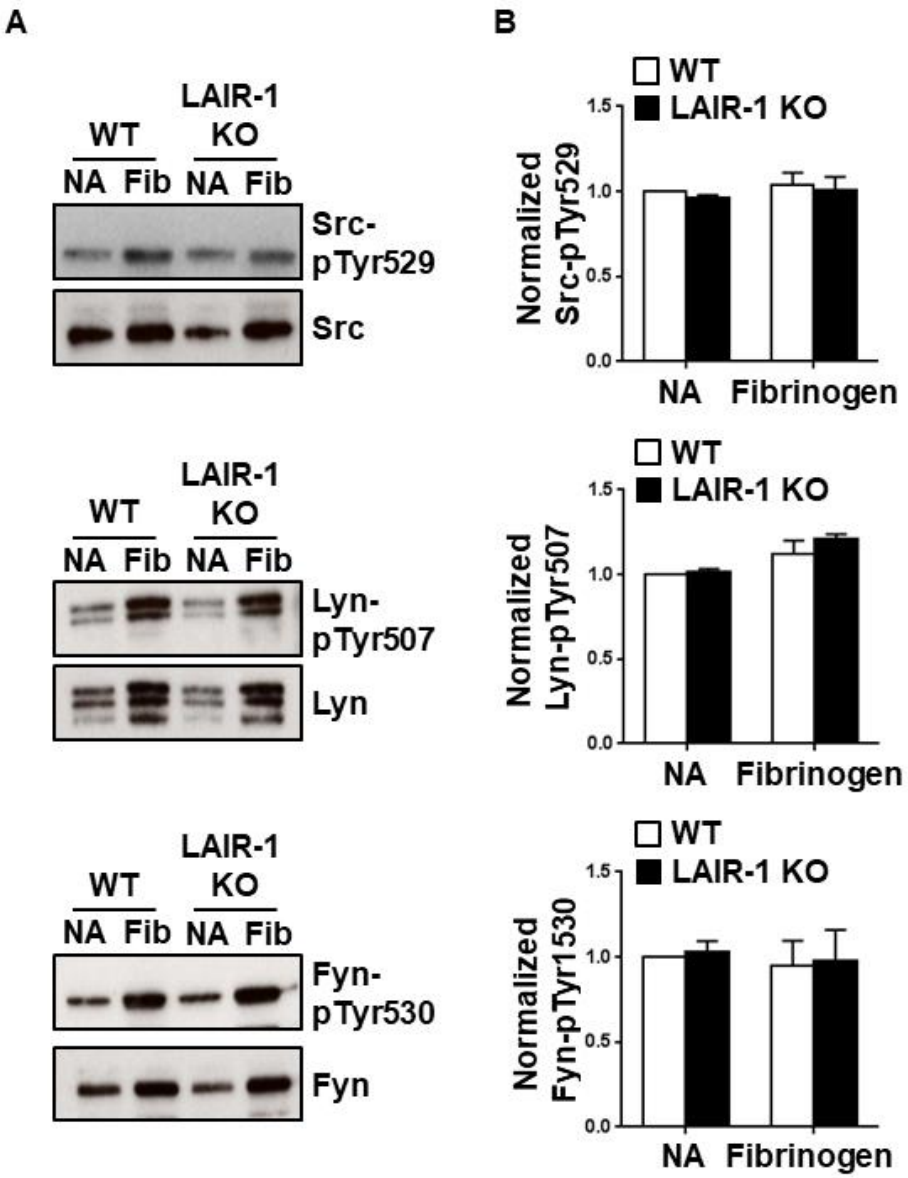

Figure 3. 7. Platelet integrin αIIbβ3 signalling from LAIR-1 deficient mice. Washed platelets from LAIR-1 KO and litter matched WT mice were plated on a fibrinogen coated surface (45 minutes, 37ºC). Whole cell lysates were prepared from non-adherent (NA) and adherent (fib) platelets and Western blotted with anti-Src Tyr529, Fyn Tyr530 and Lyn Tyr507 antibodies. Membranes were stripped and reblotted with anti-Src, Fyn and Lyn antibodies. (A) Representative blots and (B) densitometry quantification (mean ± SEM) from 3 independent experiments/genotype; Two-way ANOVA with multiple comparisons.

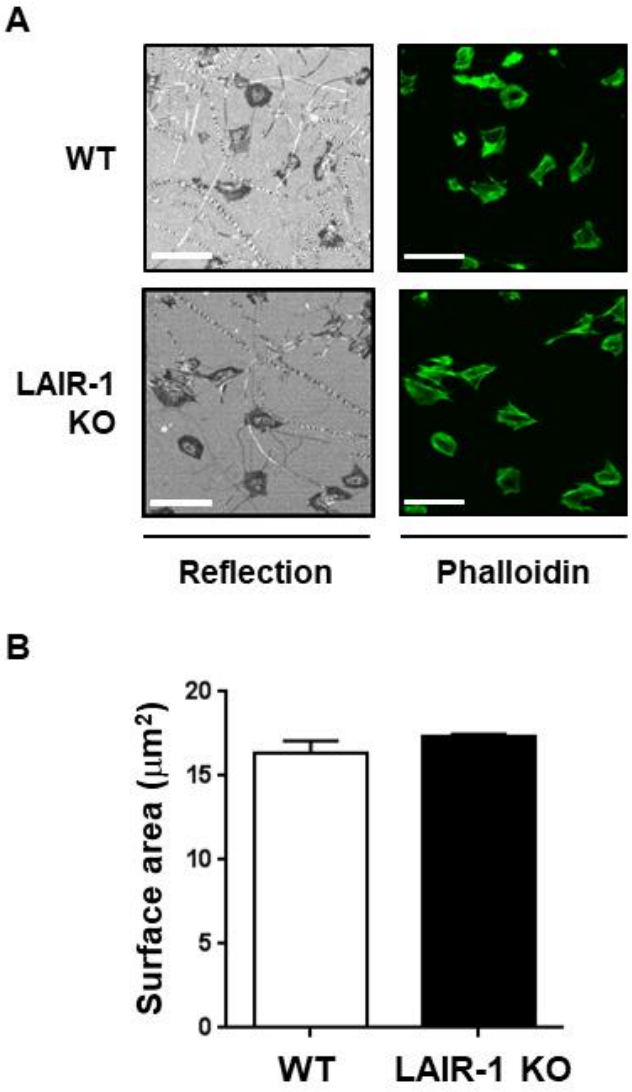

Figure 3. 8. Collagen spreading unaltered in platelets from LAIR-1 deficient mice. Platelets from LAIR-1 KO and litter matched WT mice were platelet on collagen-coated surface (45 minutes, 37ºC). (A) Representative phalloidin stained fluorescence and reflection images. Scale bar 10 μm. (B) Individual platelet surface area (mean ± SEM) from140-220 platelets, 5 mice/genotype; Students t-test, non-significant.

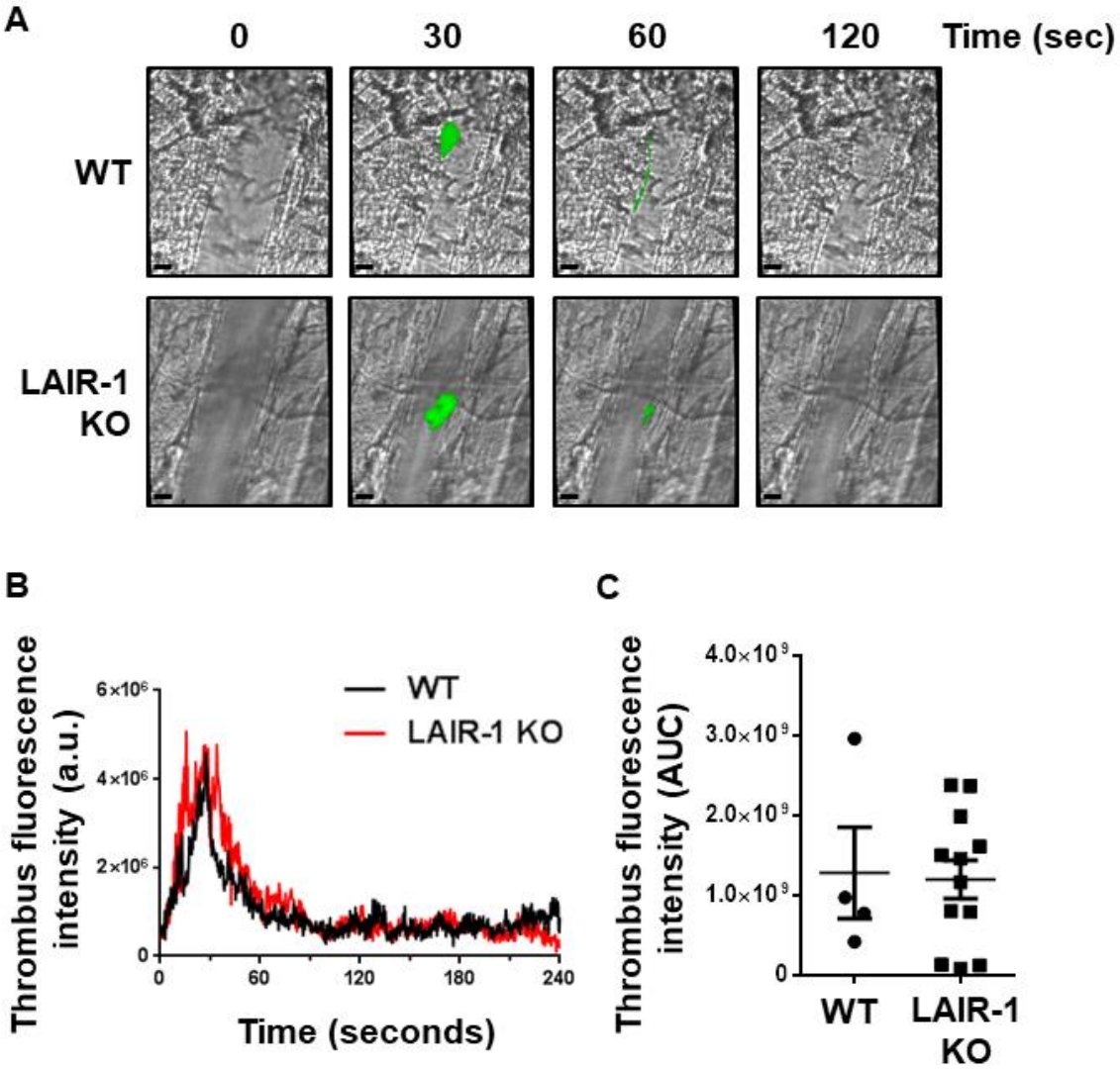

Figure 3. 9. Laser-injury induced thrombus formation *in vivo*. Mice were injected with anti-GPIbβ antibody (0.1µg/g body weight) and cremaster muscle arterioles subsequently injured by laser. Platelet accumulation in thrombi was assessed. (A) Representative composite brightfield and fluorescence images of thrombi are shown. Scale bar 10 µm. (B) Median integrated thrombi fluorescence intensity trace (arbitrary units, a.u.) and (C) area under the curve (mean ± SEM) are shown for 4-12 mice/genotype. Mann-Whitney U test, non-significant. See videos 3.I and 3.II.

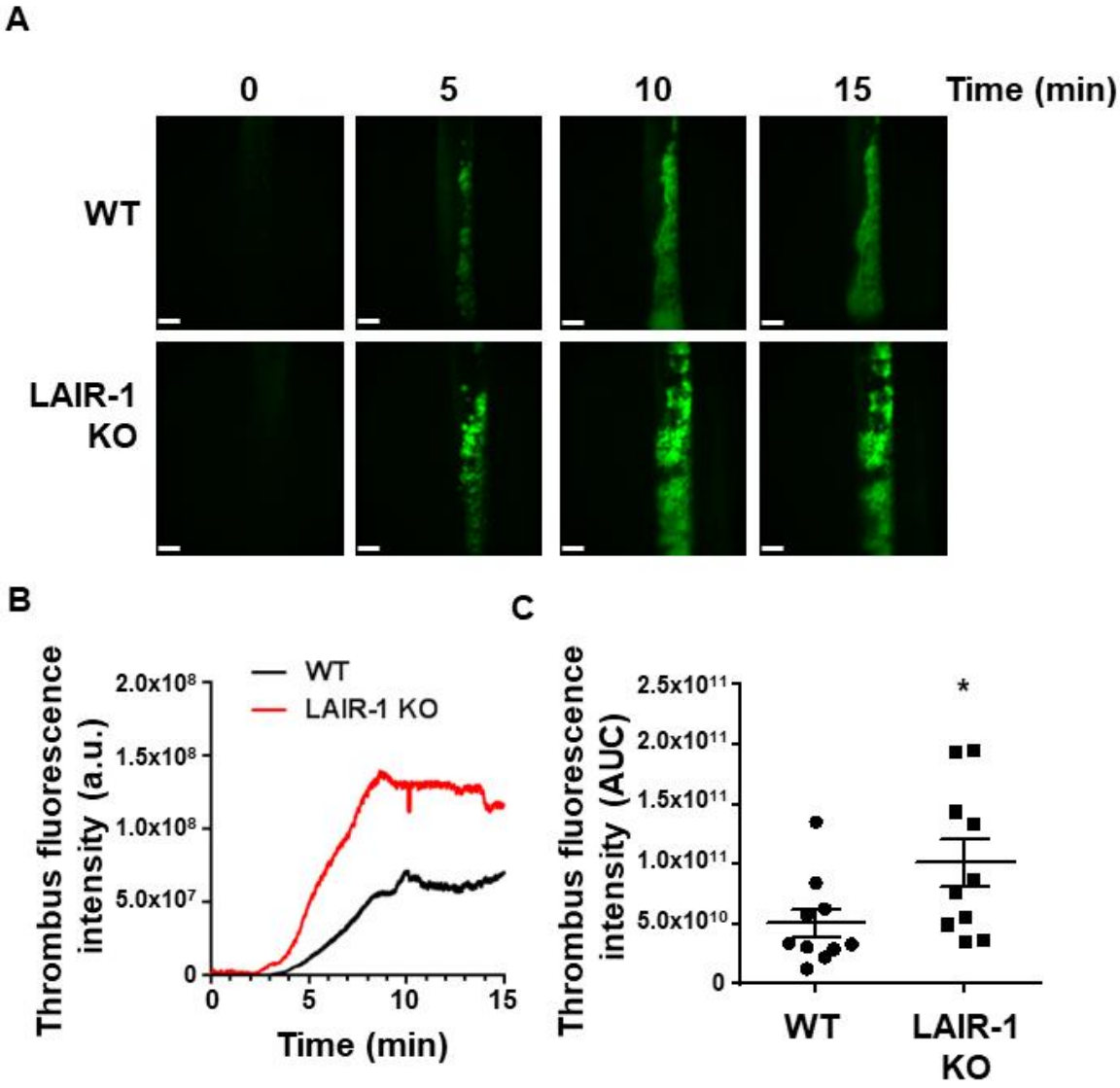

Figure 3. 10. Ferric chloride-induced thrombus formation *in vivo*. Mice were injected with anti-GPIbβ antibody (0.1µg/g body weight) and carotid arteries subsequently injured with ferric chloride-soaked filter paper (10%, 3 minutes). Platelet accumulation in thrombi was assessed. (A) Representative fluorescence images of thrombi are shown. Scale bar 200 µm. (B) Median fluorescence intensity traces (a.u.) and (C) area under the curve (mean ± SEM) are shown for 10 mice/genotype. *p<0.05 using Mann-Whitney U test. See also videos 3.III and 3.IV.

3.3.9. Unaltered levels of signalling proteins in LAIR-1 deficient mouse platelets

The enhanced signalling observed in LAIR-1 deficient mice may possible be the result of altered levels of LAIR-1 interacting proteins. Protein levels of tyrosine phosphatases CD148 and PTP1B, which together with Csk regulate activity of SFKs were assessed in platelets, along with the levels of Src itself, and of the important downstream activation protein PLCγ2. All protein levels were normal in LAIR-1 deficient mouse platelets **(Figure 3.11)**.

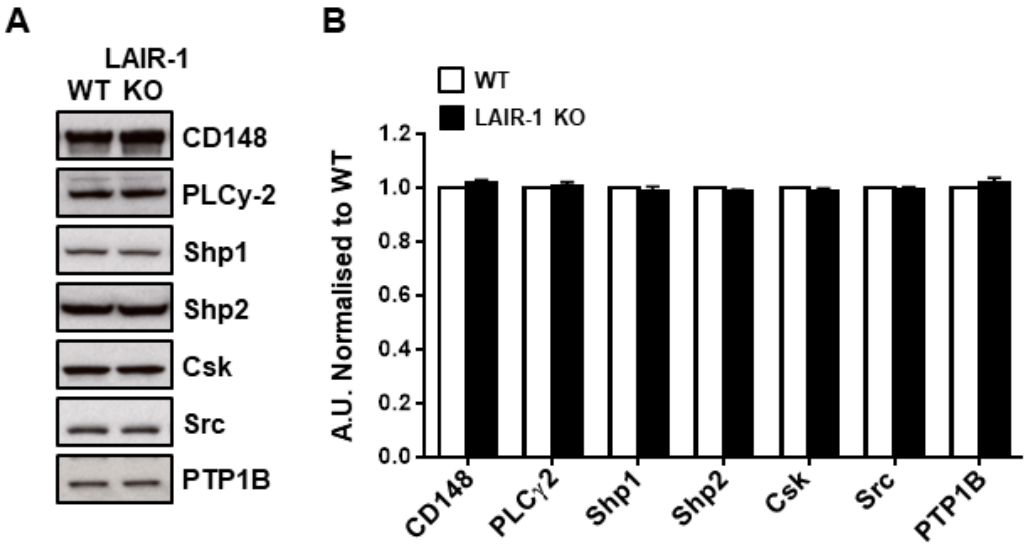

Figure 3. 11. Unaltered levels of Src, PLCγ2, CD148, Shp1, Shp2, Csk and PTP1B in platelets from LAIR-1 deficient mice. Washed platelet whole cell lysates from LAIR-1 KO and litter matched WT mice were Western blotted with anti-Src, PLCγ2, CD148, Shp1, Shp2, Csk and PTP1B antibodies. (A) Representative blots and (B) densitometry quantification (mean ± SEM) from 4 independent experiments. Student's t-test, non-significant.

3.4. Discussion

Findings presented in this chapter demonstrate a role for LAIR-1 in regulation of platelet reactivity. It also demonstrates platelet and megakaryocyte hyperactivity due to increased SFK activation is not a result of decreased levels or activity of Csk, but hypothesised to be due rather to uncoupling of SFK inhibition and altered compartmentalisation of signalling proteins.

Proplatelet formation is a cell autonomous process (Lecine et al., 1998) with the default setting appearing to be on, as megakaryocytes have been shown to immediately form proplatelets following migration out of bone marrow explants (Eckly et al., 2012). This suggests proplatelet formation may therefore be actively suppressed, potentially by several inhibitory signals acting in parallel. Collagen type-I mediated proplatelet inhibition surprisingly, has been demonstrated to be mainly arbitrated by GPVI (Semeniak et al., 2016). Through use of inhibitors and deficient mice, Semaniak et al revealed megakaryocytes form the same levels of proplatelets on collagen type-I in the absence of GPVI signalling as WT megakaryocytes form on surfaces (collagen type-IV and laminin) which are conducive to proplatelet formation (Semeniak et al., 2016). They also demonstrated a bimodal role for α2 integrin, enhancing proplatelet formation upon collagen type-IV binding, yet supporting GPVI-mediated inhibition at low collagen type-I levels (Semeniak et al., 2016). These studies were performed using foetal liver derived megakaryocytes, known to form proplatelets at a much higher rate than the bone-marrow derived megakaryocyte utilised in this chapter, which may explain the absence of any proplatelet formation on collagen (Balduini et al., 2008). Expression of GPVI during megakaryopoiesis has been shown to be inversely related, with LAIR-1 downregulated as GPVI is upregulated (Smith et al., 2017). This expression pattern therefore may potentially suggest LAIR-1 could be important in providing inhibitory signals to prevent proplatelet formation in immature megakaryocytes until they are expressing enough GPVI to mediate the inhibition.

Increased phosphorylation of Src Tyr418 and Syk Tyr525/6 in fibrinogen adherent platelet lysates from LAIR-1 deficient mice is consistent with the observed increase in spreading (Smith et al., 2017). Together with the unaltered phosphorylation of inhibitory sites is additional evidence of a proximal signalling defect.

Interestingly, despite LAIR-1 deficient mouse platelets displaying enhanced aggregation responses to collagen and CRP, and forming larger aggregates under shear, platelets from deficient mice underwent normal spreading on collagen. This is suspected to be due to the mild phenotype being masked by the synergistic effects of multiple receptors (GPVI and α2β1), and positive feedback pathways such as secondary mediators ADP and TxA_2, allowing WT platelets to achieve the same final degree of spreading.

The normal aggregation responses observed to thrombin were expected as SFKs are not involved in GPCR signalling. CLEC-2 however, is a hemi-ITAM containing receptor, which signals downstream via a similar pathway to GPVI. The normal aggregation responses upon CLEC-2 activation could be explained by the difference in phosphorylation of the (hemi)ITAM. Phosphorylation of CLEC-2 upon activation has been shown to be mediated by and dependent on Syk, with SFKs playing no role (Severin et al., 2012). GPVI phosphorylation upon activation in contrast is mediated by SFKs, which then allow subsequent binding and activation of Syk (Poole et al., 1997, Spalton et al., 2009). The enhanced SFK activity observed in LAIR-1 deficient mouse platelets would therefore enhance GPVI receptor phosphorylation, but not of CLEC-2.

LAIR-1 deficient mice demonstrate increased thrombosis *in vivo* to ferric chloride, but not laser-injury. This agrees with the observed platelet hyper responsiveness *in vitro* to GPVI, but not GPCR agonists. Both thrombosis models are well characterised; laser-injury induced thrombosis is highly dependent on tissue factor and thrombin generation, whereas ferric

chloride-induced thrombosis is more dependent on collagen exposure following endothelial denudation (Dubois et al., 2006). In addition to these mechanisms, the injuries were to vessels of differing size, composition and rheological characteristics. Laser-injury was performed on arterioles of the cremaster muscle, while ferric chloride-injury was to the much larger carotid artery, with these differences likely influencing the phenotype observed.

Change in SFK activity in megakaryocytes underlies increased platelet production and reactivity to GPVI and integrin activation in platelets. Enhanced SFK activity also underlies the hyper responsiveness of LARI-1 KO mouse platelets to collagen and fibrinogen **(Figure 3.12)**. It is therefore hypothesized that the enhanced SFK activity in megakaryocytes is transferred to platelets rendering them hyper responsive. This potentially represents a new paradigm of how platelet reactivity can be modulated.

C-terminal inhibitory site phosphorylation of SFKs was unaltered in both megakaryocytes and platelets from LAIR-1 deficient mice. Although, it should be noted that in contrast to activation loop tyrosine phosphorylation which correlates with SFK activity, inhibitory site phosphorylation does not. Phosphorylation of SFK inhibitory tyrosine residues induces a conformation change, blocking the active site and inhibiting SFKs. This however can be unclamped by interactions with proline rich or phosphor-tyrosine containing proteins **(Figure 3.13)**, which disrupt the intramolecular interactions of the SH2 C-terminal phosphor-tyrosine or SH3-proline rich linker, resulting in activation of the SFK despite phosphorylation of its C-terminal inhibitory tyrosine (Senis et al., 2014).

Levels of SFK proteins themselves or proteins involved in their regulation, such as the receptor phosphatase CD148 or kinase Csk, also do not explain the increase in SFK activity as were not altered in LAIR-1 deficient mouse platelets and megakaryocytes.

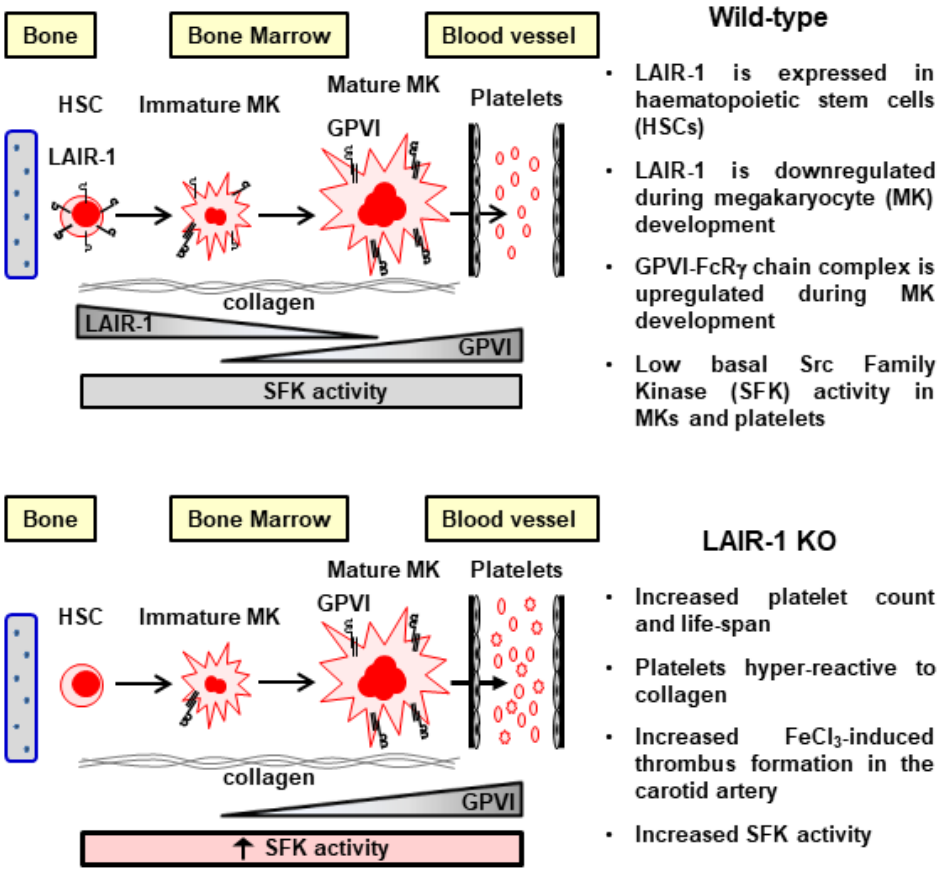

Figure 3. 12. Effect absence of LAIR-1 inhibition in megakaryocytes. Absence of LAIR-1 increases SFK activity in megakaryocytes, resulting increased platelet production. Enhanced SFK activity is transferred to circulating platelets rendering them hyper-responsive to collagen. Visual abstract from Smith et al., 2017.

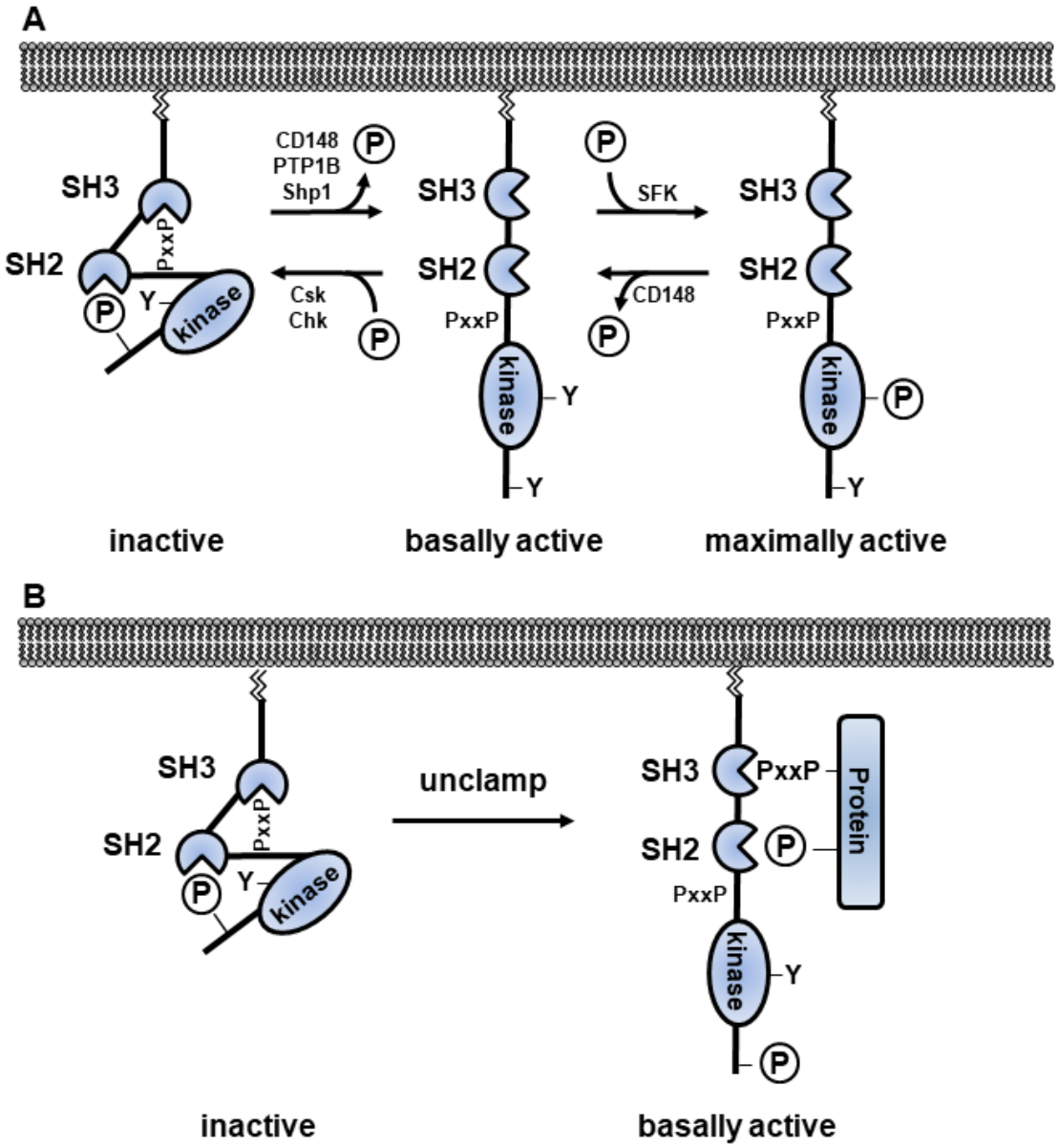

Figure 3. 13. SFK regulation and uncoupling. (A) Regulation of SFK activity. Phosphorylation of the C-terminal tyrosine residue mediates intramolecular interaction with the SH2 domain blocking the active site. The SFK is maintained in the inactive conformation by a second intramolecular interaction between the proline-rich (PxxP) SH2-kinase linker region and SH3 domain. C-terminal tyrosine dephosphorylation by protein tyrosine phosphatases CD148, PTP1B and Shp1 results in activation of the SFK. Trans-autophosphorylation of the activation loop tyrosine residue results in maximal SFK activation. Dephosphorylation of the activation by CD148 returns the SFK to basal activation state. Csk or Chk mediated phosphorylation of the inhibitory tyrosine residue returns SFK to inactive conformation. (B) Activation of SFKs by unclamping. Disruption of SH3-proline-rich linker or SH2-C-terminal phosphor-tyrosine intramolecular interactions by proteins containing proline-rich region or a phosphor-tyrosine facilitates SFK activation irrespective of C-terminal inhibitory tyrosine phosphorylation.

The inhibitory effects of LAIR-1 have been shown to be mediated through recruitment of the tyrosine phosphatases Shp1 and Shp2 and also the Src inhibitor Csk, to its ITIMs following phosphorylation upon activation (Verbrugge et al., 2006, Verbrugge et al., 2003). This brings them in close proximity to activation receptors whose signal transduction they can subsequently inhibit. It is therefore hypothesized that the increased activity of SFKs in megakaryocytes and platelets is due to decreased compartmentalization of the PTPs Shp1 and Shp2, and of Csk at the plasma membrane. Further work is needed to elucidate the exact mechanism underlying the increase in SFK activity and why it remains elevated in resting platelets.

Findings in this chapter add to the growing evidence that ITIM-containing receptors are crucial in the regulation of platelet production and function. Moreover this chapter demonstrates that alterations in the activation state in megakaryocytes can be transferred to their platelet progeny, and influence their functional response in the circulation. Opening up a new paradigm of how platelet reactivity can be modulated.

Chapter 4

LAIR-1/PECAM-1 double deficient mouse model

4.1. Aims

The aim of this chapter was to investigate the role of LAIR-1 alongside PECAM-1 in platelet production and function to determine if there is functional redundancy between these two ITIM-containing receptors or if they act through distinct pathways. A murine model deficient in both LAIR-1 and PECAM-1 was generated and characterized to achieve this.

4.2. Introduction

As demonstrated in chapter 3 and additional work in Smith et al (2017), LAIR-1 regulates megakaryocyte and platelet reactivity. The absence of LAIR-1 inhibition alters the activity of signalling proteins in megakaryocytes, this increased SFK activity within megakaryocytes results in increased proplatelet formation and release of platelets into the circulation. The enhanced signalling protein activation is then transferred to these platelet progeny, rendering them hyper responsive to GPVI and integrin αIIbβ3 mediated activation. Platelets from LAIR-1 deficient mice demonstrate enhanced responsiveness to GPVI activation, with aggregation responses to collagen and CRP and adhesion to collagen under shear all increased. Integrin αIIbβ3 mediated activation is also enhanced, with spreading increased on fibrinogen. This increased platelet reactivity is also observed in arterial thrombosis *in vivo*.

Similar regulation of platelet function has also been reported for another ITIM-containing receptor PECAM-1. PECAM-1 was the first identified and most extensively studied ITIM-containing receptor in platelets and megakaryocytes. Platelet aggregation and secretion responses following collagen and CRP activation of GPVI have been shown to be enhanced in PECAM-1 deficient platelets (Dhanjal et al., 2007b, Patil et al., 2001, Wee and Jackson, 2005). This modest enhancement is however only observed at low agonist doses, with the enhancement effect lost at higher concentrations. In agreement, antibody or recombinant ectodomain

mediated crosslinking of PECAM-1 on platelets inhibited calcium mobilisation, platelet aggregation and dense granule secretion to low doses of collagen, CRP and convulxin, which likewise could be overcome at higher concentrations (Cicmil et al., 2002, Dhanjal et al., 2007b, Jones et al., 2009). Interestingly, despite no effect on thrombin aggregation observed in the PECAM-1 KO mouse platelets, crosslinking PECAM-1 was shown to inhibit human platelet aggregation. This apparent discrepancy was attributed to differences in the PAR composition and expression in human (PAR-1, -3 and -4) and mouse (PAR-3 and -4 only) platelets, as thrombin primarily acts through PAR-1 in human, but through PAR-4 in mouse platelets (Wee and Jackson, 2005). Impaired outside-in integrin αIIbβ3 signalling with delayed clot retraction and reduced FAK phosphorylation have been reported in PECAM-1 deficient platelets, although fibrinogen spreading was unaffected (Wee and Jackson, 2005). However, a subsequent study demonstrated no difference in clot retraction and minor increase in fibrinogen spreading in PECAM-1 deficient platelets (Dhanjal et al., 2007b).

PECAM-1 mice also show enhanced thrombus formation *in vivo*, with larger thrombi observed in cremaster arterioles following laser-injury, and albeit modest an increase in ferric chloride-induced thrombosis of carotid arteries (Falati et al., 2006). Another model of photochemical induced thrombosis in cremaster arterioles was however found to be normal (Vollmar et al., 2001). Further experiments using bone marrow chimeric mice established the enhancement of thrombus formation detected in the laser-injury model was due to loss of platelet and leukocyte PECAM-1, rather than loss from the endothelium where PECAM-1 is also highly expressed (Falati et al., 2006).

Although deficient mice have normal platelet counts (Mahooti et al., 2000) and their megakaryocytes develop and form proplatelets normally *in vitro*, PECAM-1 has been shown to have a role in thrombopoiesis, through regulation of megakaryocyte migration (Dhanjal et al.,

2007a). Recovery of platelet counts following antibody mediated depletion of platelets in deficient mice was delayed, and attributed to increased megakaryocyte adhesion to the ECM and defective migration. The migration defect was due to the absence of SDF-1α receptor CXCR4 polarization to the leading edge of megakaryocytes (Dhanjal et al., 2007a), which is also thought to underlie the altered spatial localization of megakaryocytes within the bone marrow (Wu et al., 2007).

PECAM-1 inhibition is mediated principally via binding of Shp2 (and Shp1 to a lesser extent) to the phosphorylated ITIMs of its cytoplasmic tail. Shp2 then interacts with the p85 regulatory subunit of PI3K, disrupting its association with LAT and GAB1 in the signalling complex that forms following GPVI activation, thus preventing downstream recruitment of PLCγ2 (Moraes et al., 2010). Absence of PECAM-1 therefore enables uninhibited signalling downstream of GPVI resulting in enhanced responses. Phosphorylation of PECAM-1 ITIMs is dependent on SFKs, in platelets it has been shown to be dependent on Lyn phosphorylation of the C-terminal ITIM, with subsequent N-terminal phosphorylation by Csk (or Btk) (Tourdot et al., 2013).

Despite differences in the ligands of these two ITIM-containing receptors, the phenotypes of LAIR-1 KO and PECAM-1 KO mice share several similarities. Platelets from both KO strains display enhanced responsiveness to GPVI activation by low agonist concentrations that are lost at higher concentrations, and enhanced arterial thrombosis to ferric chloride *in vivo*. In addition, interaction of LAIR-1 and PECAM-1 with the same effector proteins (Shp1, Shp2 and Csk) that mediate the inhibition raises the possibility of redundancy between these receptors.

In this chapter, the role of LAIR-1 is investigated alongside PECAM-1, through characterisation a double deficient mouse model, in order to determine the distinct or redundant nature of these two ITIM-containing receptors in megakaryocyte development and platelet

production, as well as the effect absence of these receptors has on platelet function *in vitro* and *in vivo*.

4.3. Results

In order to investigate whether there is functional redundancy between the ITIM-containing receptors LAIR-1 and PECAM-1, a novel mouse model deficient in both receptors was generated through crossing of single KO strains (Smith et al., 2017, Duncan et al., 1999). LAIR-1/PECAM-1 DKO mice were bred as homozygous, with age matched WT mice used as controls. Megakaryocyte and platelet function from these LAIR-1/PECAM-1 double KO (DKO) mice were then assessed and characterized.

4.3.1. LAIR-1/PECAM-1 DKO mice are mildly thrombocythemic

LAIR-1 deficient mice have increased platelet counts, whereas counts are normal in PECAM-1 deficient mice (Smith et al., 2017, Mahooti et al., 2000). It was therefore of interest to investigate the effect on platelet count of absence of both these ITIM-containing receptors. DKO mice were found to have an increased platelet count (17%), although this was not as pronounced as the increase observed in LAIR-1 KO mice (27%; **Figure 4.1A)**. No effect on platelet volume was observed **(Figure 4.1B)**.

4.3.2. Megakaryocyte development unaffected in LAIR-1/PECAM-1 DKO mice

To determine if the absence of LAIR-1 and PECAM-1 effects megakaryocyte development, DNA content of primary bone marrow derived megakaryocytes differentiated *in vitro* was assessed. DKO megakaryocytes displayed normal ploidy profiles, suggesting megakaryocyte development and differentiation is not affected by ablation of the ITIM-containing receptors **(Figure 4.2)**. LAIR-1 and PECAM-1 single KO mice also display normal profiles as previously reported (Smith et al., 2017, Dhanjal et al., 2007a).

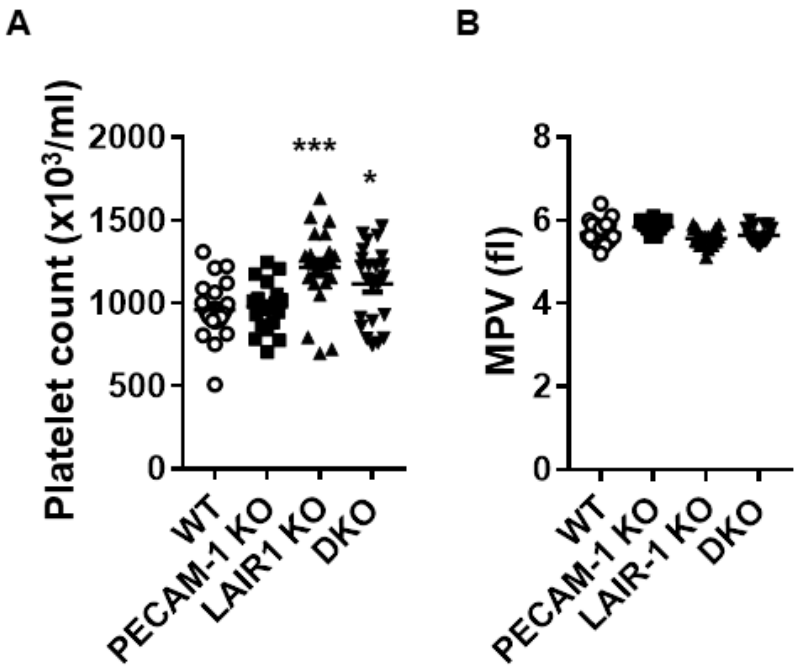

Figure 4. 1. LAIR-1 KO and LAIR-1/PECAM-1 DKO mice exhibit increased platelet count. (A) Platelet counts and (B) volumes from PECAM-1 KO, LAIR-1 KO, LAIR-1/PECAM-1 DKO and litter-matched wild-type mice (WT) were measured in whole blood using an ABX Pentra P60 blood counter. Mean ± SEM; n = 20-23 mice/genotype. One-way ANOVA with multiple comparisons, **P*<0.05, ****P*<0.001.

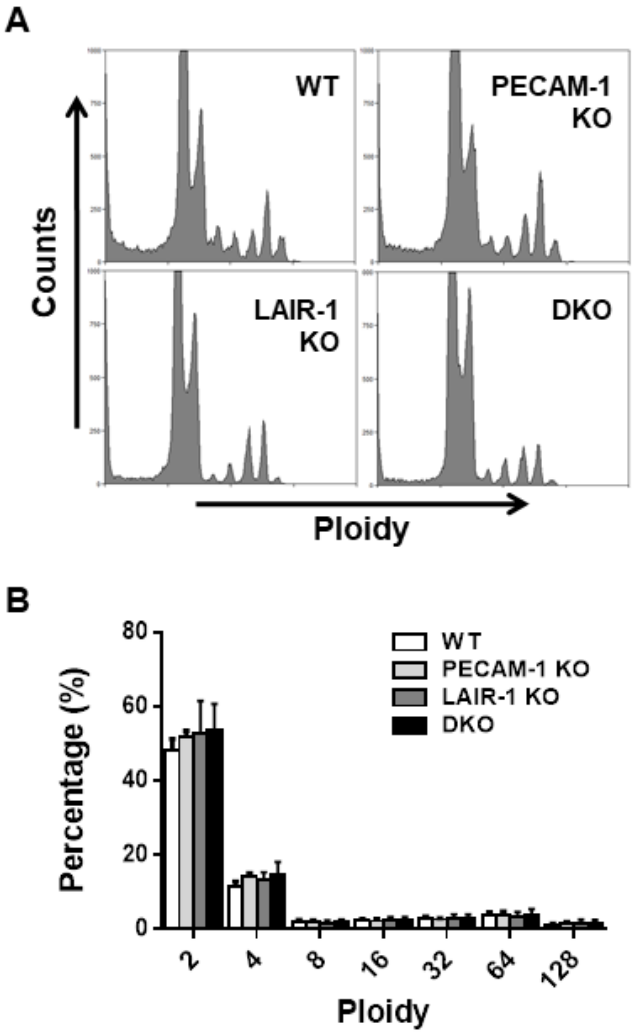

Figure 4. 2. Megakaryocyte differentiation unaltered in LAIR-1/PECAM-1 DKO megakaryocytes. Bone marrow-derived megakaryocytes from litter-matched WT, PECAM-1 KO, LAIR-1 KO and LAIR-1/PECAM-1 DKO mice were stained with propidium iodide and DNA content (ploidy) assessed by flow cytometry. (A) Representative profiles and (B) percentage of 2-128N ploidy cells was quantified. Mean ± SEM; n = 6 mice/genotype; Two-way ANOVA with multiple comparisons.

4.3.3. Proplatelet formation unaltered in LAIR-1/PECAM-1 DKO mouse megakaryocytes

The thrombocythemia observed in LAIR-1 deficient mice was due to a combination of enhanced proplatelet formation and increased platelet half-life. To determine whether the increased platelet count in DKO mice was due to enhanced platelet production, proplatelet formation on fibrinogen was investigated in bone marrow derived megakaryocytes. Megakaryocytes displayed normal proplatelet formation, with percentage of megakaryocytes forming proplatelets, number of proplatelet extensions and area of proplatelet extensions all unaltered in DKO mouse megakaryocytes **(Figure 4.3)**. Megakaryocyte surface receptor levels, as measured by flow cytometry, were also unaltered in DKO mice **(Table 4.1)**.

4.3.4. LAIR-1/PECAM-1 DKO mouse platelets are hyper responsive to GPVI activation

Both LAIR-1 and PECAM-1 single KO mice have been shown to have enhanced aggregation responses to GPVI receptor agonists, but not to PAR receptor activation (Smith et al., 2017, Dhanjal et al., 2007b, Wee and Jackson, 2005). Reactivity to (hemi)ITAM and GPCR mediated activation was therefore assessed in platelets from DKO mice by lumi-aggregometry. DKO mouse platelet aggregation was enhanced in response to low concentration collagen and CRP stimulation; however enhancement was not greater than observed in platelets from single KO mice **(Figure 4.4).** Enhanced aggregation responses of DKO mouse platelets to collagen and CRP were not observed at other concentrations tested (data not shown). Aggregation responses to CLEC-2 antibody and thrombin stimulation were normal in all genotypes at all concentrations tested **(Figure 4.4** and data not shown**)**. Assessment of surface receptor levels on DKO mouse platelets by flow cytometry revealed decreased α2 expression compared to WT, with all other receptors unaltered **(Table 4.2)**.

These findings are in agreement with previous reports, and indicate ITAM-containing receptor signalling, but not GPCR receptor signalling, is increased in the absence of LAIR-1 and PECAM-1. The lack of further enhancement in aggregation responses of DKO mouse platelets suggests functional redundancy in inhibition mediated by these receptors.

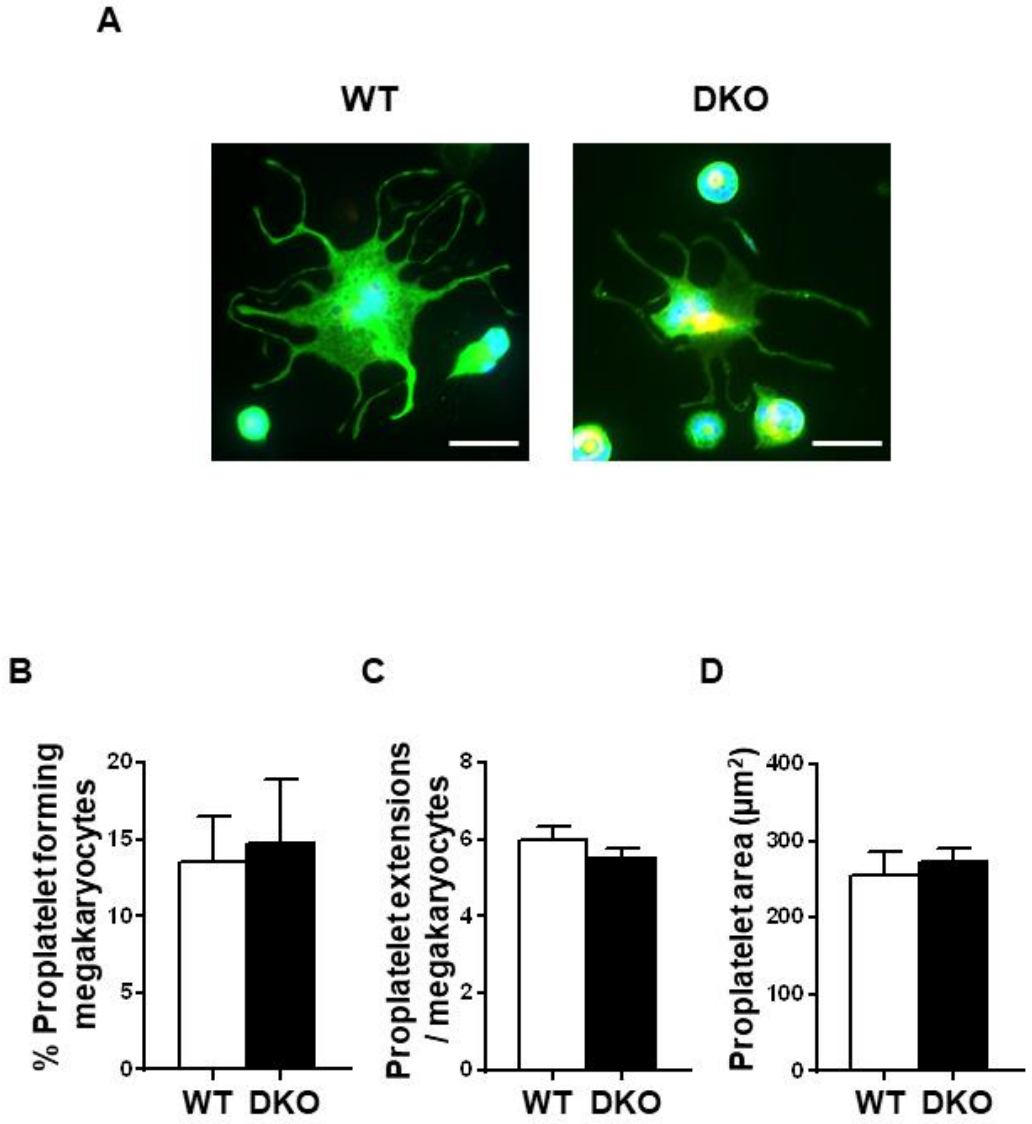

Figure 4. 3. Unaltered proplatelet formation in LAIR-1/PECAM-1 DKO megakaryocytes. Bone marrow-derived megakaryocytes from litter-matched WT and LAIR-1/PECAM-1 DKO mice were plated on fibrinogen-coated surfaces (5 hours, 37ºC, 5% CO_2) in the presence of SDF1α (300 ng/ml) and heparin (100 U/ml). (A) Representative images of tubulin stained proplatelet forming megakaryocytes. Scale bar: 50 µm. (B) Percent of megakaryocytes forming proplatelets, (C) number of extensions per proplatelet forming megakaryocyte and (D) proplatelet area. Mean ± SEM; n = 600-750 megakaryocytes from 3 mice/genotype; Students t-test, non-significant.

Table 4. 1. **Megakaryocyte surface receptor expression in LAIR-1/PECAM-1 DKO mice.** Surface receptor expression of cultured bone marrow derived megakaryocytes from PECAM-1 KO, LAIR-1 KO, LAIR-1/PECAM-1 DKO and WT control mice were measured by flow cytometry.

Surface receptor	WT	PECAM-1 KO	LAIR-1 KO	DKO
GPVI	21.8±3.7	12.5±6.0	22.2±3.6	20.6±3.8
Integrin α2	38.8±5.6	29.3±7.5	36.9±5.5	38.6±5.0
GPIbα	79.9±22.4	67.7±28.4	87.2±22.0	97.8±31.8
Integrin αIIbβ3	185.5±37.8	169.9±39.6	175.6±28.3	209.1±37.0
CLEC-2	131.8±16.8	117.1±18.2	141.0±15.5	141.1±16.3
G6b-B	44.5±11.6	28.7±6.1	44.3±9.4	28.2±7.6

Data represents mean values of the geometric mean fluorescence intensity ± SEM; n = 4-10; One-way ANOVA with multiple comparisons.

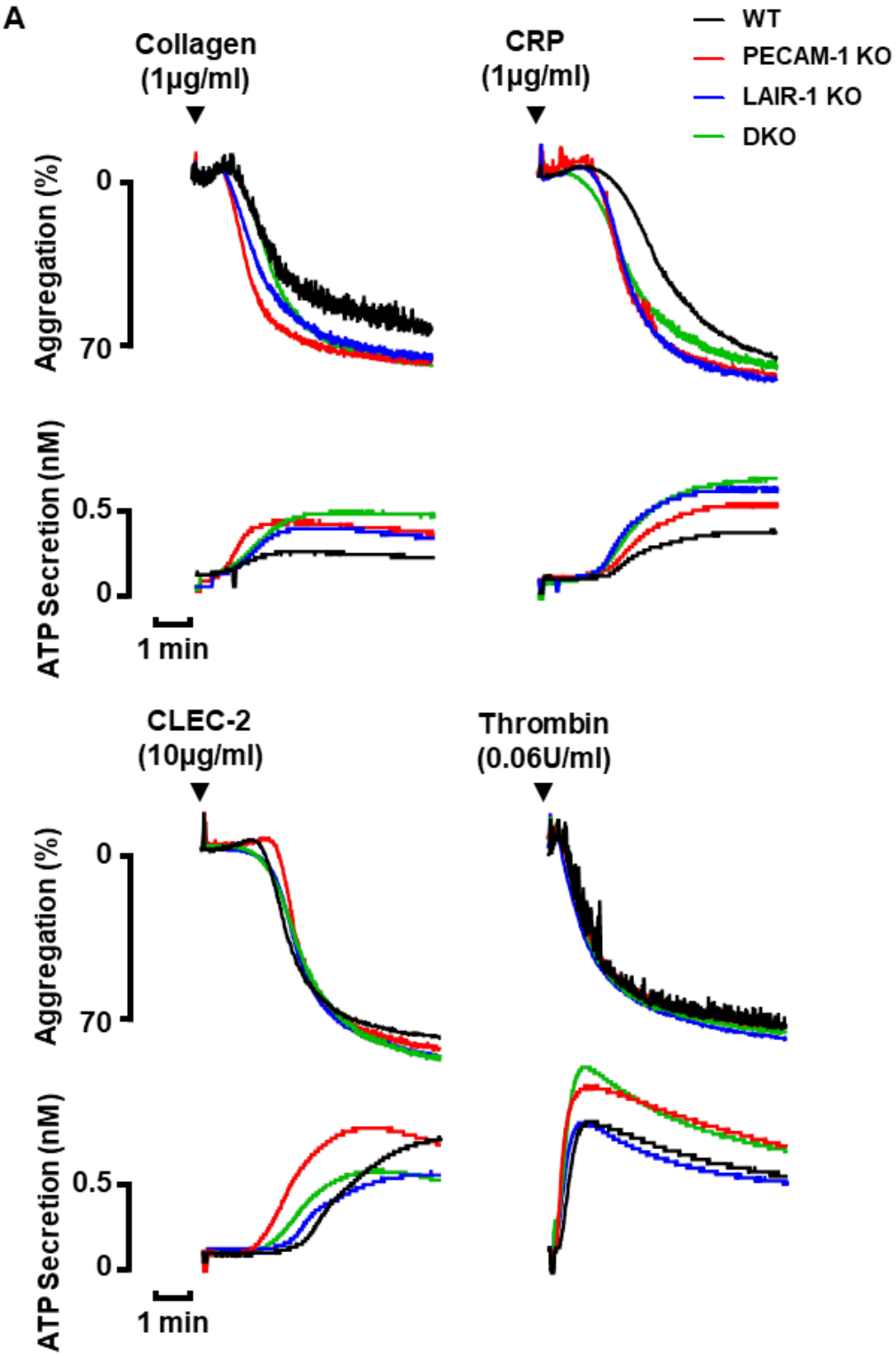
A
WT
PECAM-1 KO
LAIR-1 KO
DKO
Collagen
(1µg/ml)
CRP
(1µg/ml)
Aggregation (%)
0
70
ATP Secretion (nM)
0.5
0
1 min
CLEC-2
(10µg/ml)
Thrombin
(0.06U/ml)
Aggregation (%)
0
70
ATP Secretion (nM)
0.5
0
1 min

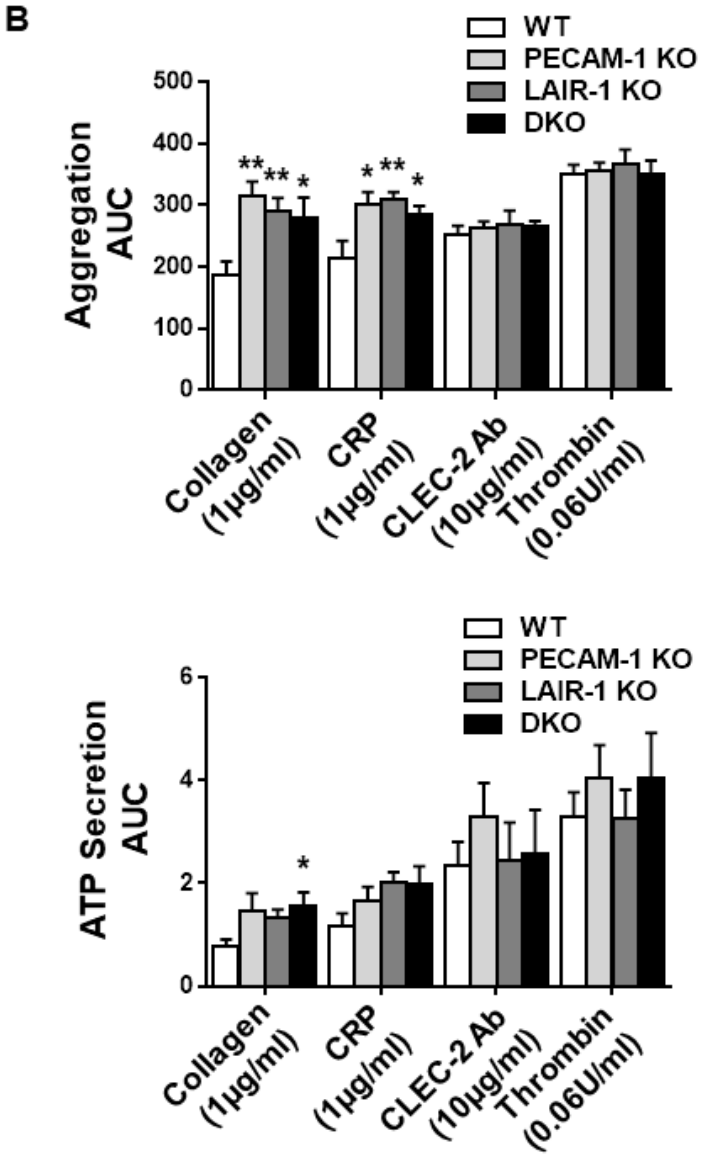

Figure 4. 4. Increased GPVI-mediated aggregation of LAIR-1/PECAM-1 DKO mouse platelets. Washed platelets (2×10^8/ml)from PECAM-1 KO, LAIR-1 KO, LAIR-1/PECAM-1 DKO and litter-matched WT mice were stimulated with 1 µg/ml collagen, 1 µg/ml collagen-related peptide (CRP), 10 µg/ml CLEC-2 antibody and 0.06 U/mL thrombin and platelet aggregation and secretion were measured using lumi-aggregometry. (A) Representative traces and (B) area under the curve (AUC) quantification of platelet aggregation and secretion. Mean ± SEM; n= 5-16; One-way ANOVA with multiple comparisons, **P*<0.05; ***P*<0.01.

Table 4. 2. Platelet surface receptor expression in LAIR-1/PECAM-1 DKO mice. Surface receptor expression of platelets PECAM-1 KO, LAIR-1 KO, LAIR-1/PECAM-1 DKO and WT control mice were measured by flow cytometry.

Surface receptor	WT	PECAM-1 KO	LAIR-1 KO	DKO
GPVI	1622±149	1460±158	1417±1252	1407±55
Integrin α2	938±26	870±22	909±16	847±6 *
GPIba	4715±384	4898±406	4702±349	4890±245
Integrin αIIbβ3	4886±1997	5312±2171	5180±2130	5185±2102
CLEC-2	6903±541	6533±217	7294±266	7143±155
G6b-B	582±128	559±128	505±121	525±102
PECAM-1	450±57	77±23 ***	544±34	71±19 ***

Data represents mean values of the median fluorescence intensity ± SEM; n = 4-5; One-way ANOVA with multiple comparisons, *P<0.05, ***P<0.001

4.3.5. Enhanced secretion and fibrinogen binding LAIR1/PECAM-1 DKO mouse platelets

Enhanced reactivity to ITAM-containing receptor agonists has previously been shown in platelets from LAIR-1 and PECAM-1 single KO mice (Smith et al., 2017, Jones et al., 2001, Dhanjal et al., 2007b, Patil et al., 2001). Platelet activation was assessed using flow cytometry to measure upregulation of the α-granule membrane receptor P-selectin following activation of platelets with CRP and thrombin. P-selectin surface expression was increased in DKO mouse platelets following activation by CRP, which gives robust activation of GPVI, and was mirrored by LAIR-1 KO mouse platelets. Thrombin activation also resulted in increased granule release in DKO mouse platelets; however this was not paralleled by platelets from either LAIR-1 or PECAM-1 single KO mice **(Figure 4.5)**. Increased α-granule secretion is suggestive of enhanced reactivity of DKO mouse platelet.

Activation of integrin αIIbβ3 was also measured using fluorescently labelled fibrinogen. Fibrinogen binding following activation with CRP was likewise increased in DKO mouse platelets **(Figure 4.5)**, which was copied in platelets from LAIR-1 deficient, but not PECAM-1 deficient mice in agreement with previous reports (Wee and Jackson, 2005, Smith et al., 2017). DKO mouse platelets fibrinogen binding was also increased following thrombin activation; this was mirrored by PECAM-1 KO platelets, but not those from LAIR-1 deficient mice **(Figure 4.5).** This suggests as previously reported LAIR-1 and PECAM-1 regulate integrin αIIbβ3 function, but via different mechanisms.

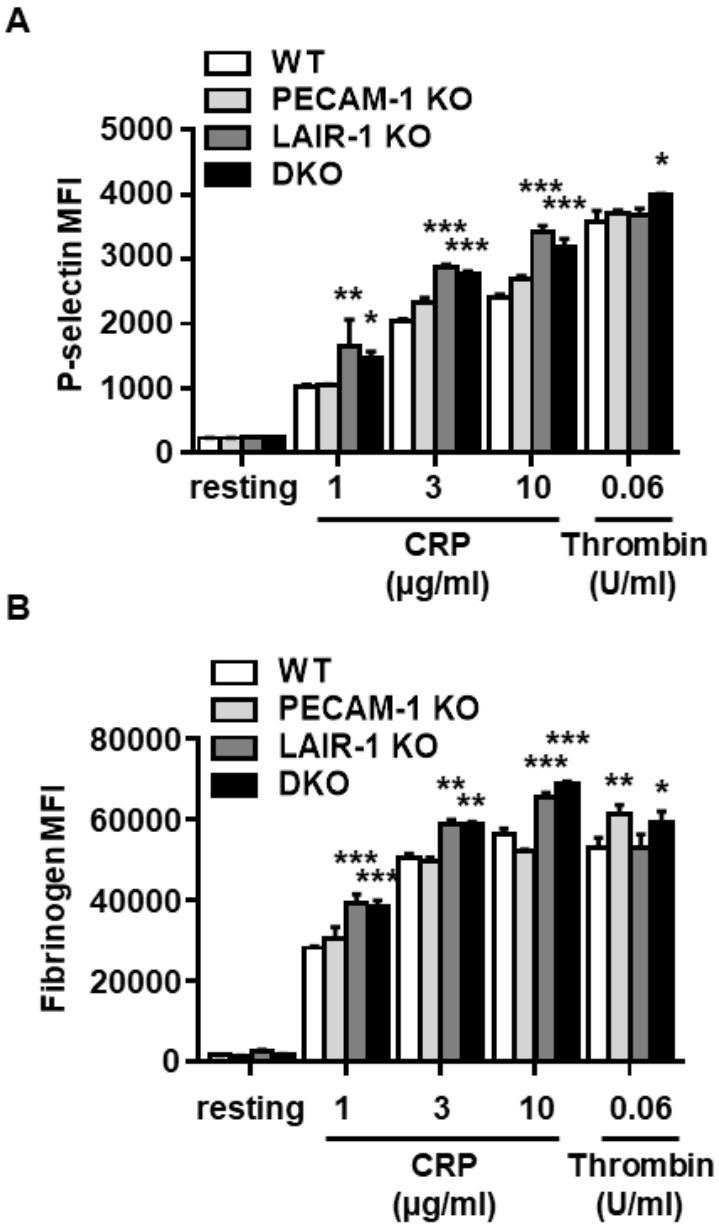

Figure 4. 5. Increased α-granule secretion and fibrinogen binding of LAIR-1/PECAM-1 DKO mouse platelets. (A) Platelet P-selectin surface expression and (B) AF488-fibrinogen binding were measured by flow cytometry in whole blood stimulated with 1, 3 and 10 µg/ml CRP and 0.06 U/ml thrombin. Thrombin stimulation was in presence GPRP to prevent aggregate formation. Median fluorescence intensity (MFI) ± SEM is represented; n = 6; Two-way ANOVA with multiple comparisons, **P*<0.05, ***P* < 0.01, ****P*<0.001.

4.3.6. LAIR-1/PECAM-1 DKO mouse platelet spreading on fibrinogen

ITIM-containing receptors are increasingly being implicated in regulation of integrin signalling (Coxon et al., 2017). Previous findings have shown LAIR-1 KO mouse platelets display increased spreading on fibrinogen, whereas spreading in PECAM-1 KO platelets was unaltered (Smith et al., 2017, Wee and Jackson, 2005). The ability of DKO mouse platelets to spread on fibrinogen coated coverslips was assessed at basal and following activation with 0.1 U/ml thrombin. Blinded fluorescence images were quantified using a semi-automated machine learning method to quantify platelet surface area, this analysis method has previously been characterised and its accuracy validated against manual analysis of spreading by members of the Birmingham Platelet Group. DKO mouse platelets adhered and spread normally on fibrinogen under basal conditions, but show increased spreading area following thrombin activation, although platelet adhesion was normal **(Figure 4.6)**. This is in agreement with fibrinogen binding results, and suggests enhanced integrin αIIbβ3 function in DKO mouse platelets.

4.3.7. Adhesion to collagen under shear unaltered in platelets from LAIR-1/PECAM-1 DKO mice

Following minor alterations in platelet function identified to GPVI activation *in vitro*, a more physiologically relevant *ex vivo* flow adhesion assay was used to investigate recruitment of DKO mouse platelets to collagen. Experiments were performed in collaboration with Johan Heemskerk, Johanna van Geffen and Marijke Kuijpers (Maastricht University, Netherlands), and both experiments and analysis were completed blind. Whole blood was flowed over collagen coated glass coverslips for 3.5 minutes at a shear rate of $1000s^{-1}$. Bright field and fluorescence images were then captured of thrombi. Platelet adhesion to collagen was normal

from DKO mice, as was integrin αIIbβ3 activation and phosphatidylserine exposure **(Figure 4.7)**. P-selectin surface expression showed a tendency to be increased in DKO mouse platelets **(Figure 4.7)**, though it did not reach significance it is suggestive of increased α-granule secretion and activation of DKO mouse platelets, as was observed by flow cytometry.

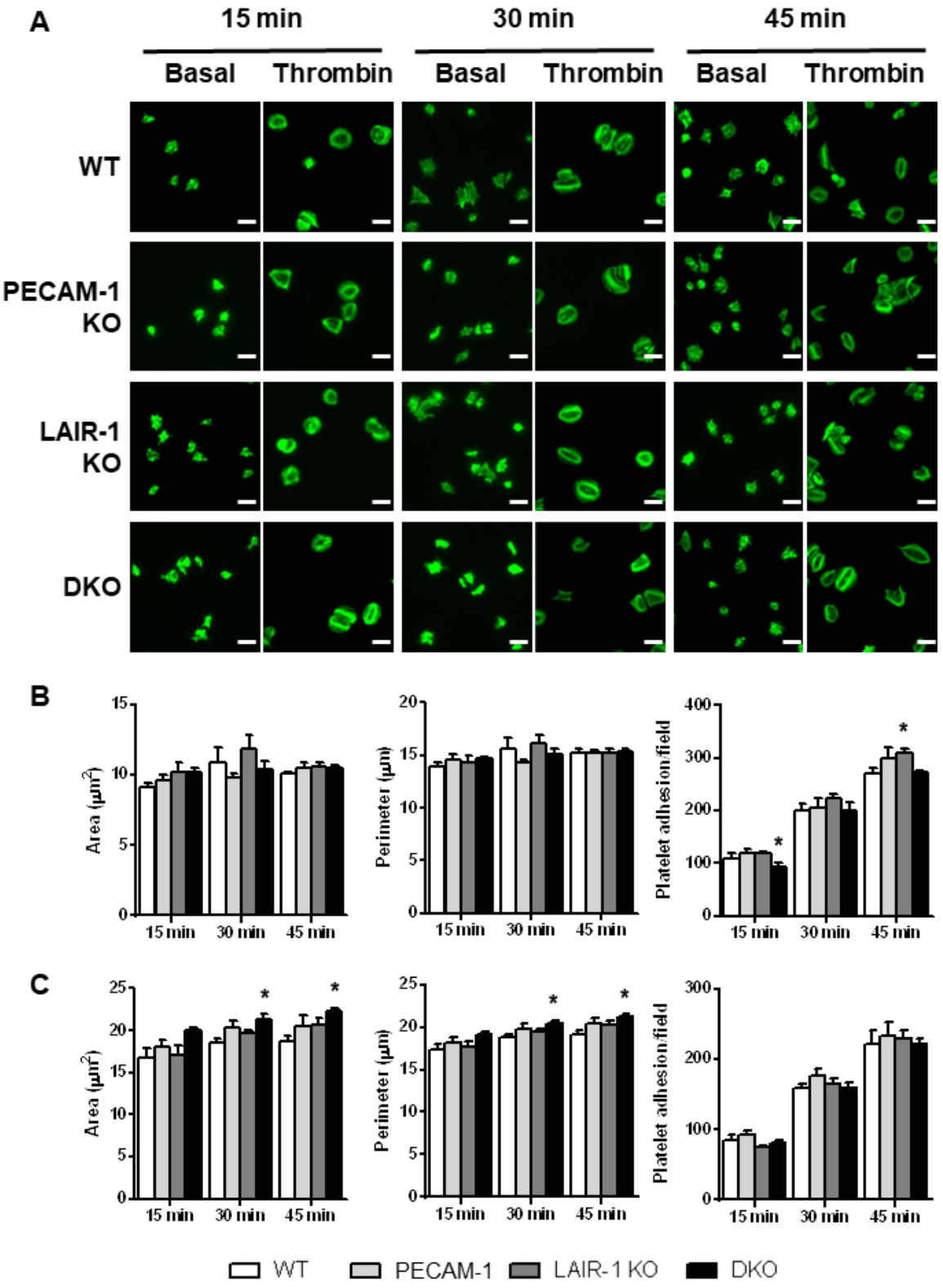
A
15 min
30 min
45 min
Basal
Thrombin
Basal
Thrombin
Basal
Thrombin
WT
PECAM-1 KO
LAIR-1 KO
DKO
B
Area (μm²)
Perimeter (μm)
Platelet adhesion/field
15 min
30 min
45 min
C
Area (μm²)
Perimeter (μm)
Platelet adhesion/field
15 min
30 min
45 min
WT
PECAM-1
LAIR-1 KO
DKO

Figure 4. 6. Fibrinogen spreading unaltered in LAIR-1/PECAM-1 DKO mouse platelets. Washed platelets from PECAM-1 KO, LAIR-1 KO, LAIR-1/PECAM-1 DKO and litter-matched WT mice were plated on fibrinogen (100 µg/ml) coated coverslips under basal and 0.1 U/ml thrombin pre-activated conditions for 15, 30 or 45 minutes at 37ºC. (A) Representative phalloidin stained fluorescence images and quantification of platelet surface area, platelet perimeter and number of adhered platelets for basal (B) and thrombin preactivated platelets (C). Mean ± SEM; n = 800-1000 platelets from 4 mice/genotype; Two-way ANOVA with multiple comparisons, **P*<0.05.

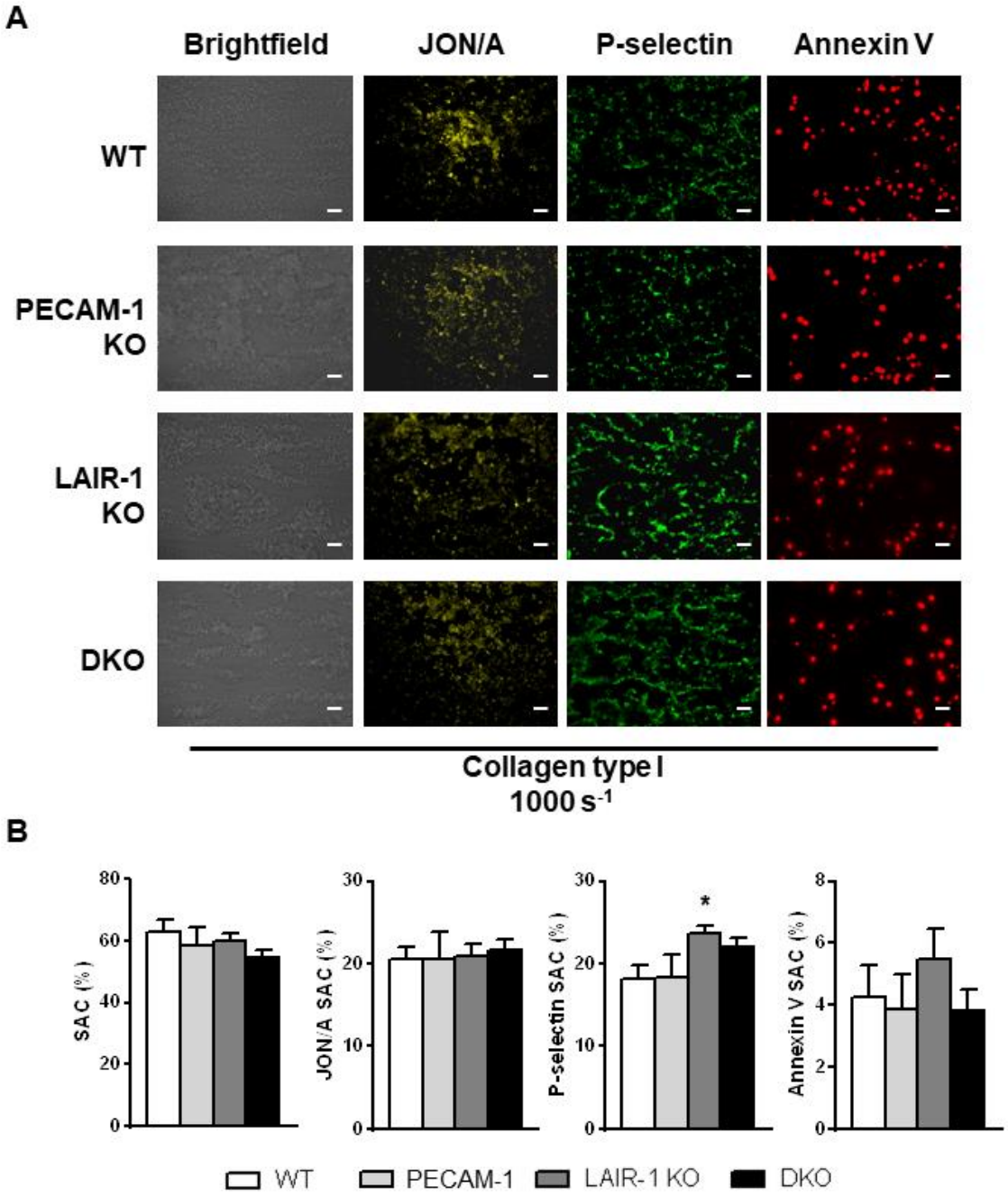

Figure 4. 7. Adhesion and activation under flow unaffected in LAIR-1/PECAM-1 DKO mouse platelets. Whole blood was flowed over collagen coated microspots at shear rate 1000 s^{-1} for 3.5 minutes. (A) Representative bright field and fluorescence images. (B) Quantification of surface area coverage (SAC) of adhered platelets, JON/A, P-selectin and annexin V staining. Mean ± SEM; n = 7-15 mice/genotype; One-way ANOVA with multiple comparisons, **P*<0.05. Experiments performed in collaboration with Johan Heemskerk, Johanna van Geffen and Marijke Kuijpers (Maastricht University, Netherlands).

4.3.8. *In vivo* thrombosis unaltered in LAIR-1/PECAM-1 DKO mice

Both LAIR-1 and PECAM-1 KO mice form larger thrombi in response to ferric chloride-injury (Smith et al., 2017, Falati et al., 2006), consequently this model was chosen to assess the physiological effect absence of both these receptors has on *in vivo* thrombosis. Interestingly, ferric chloride-injury induced thrombosis was normal in DKO mice **(Figure 4.8)** suggesting absence of both LAIR-1 and PECAM-1 has no physiological effect on platelet reactivity and thrombus formation.

4.3.9. Src activation unaltered in LAIR-1/PECAM-1 DKO mouse platelets

Increased Src activation was at the heart of the observed hyper reactivity of LAIR-1 KO mouse platelets. Activation of Src in platelets following collagen and CRP stimulation was therefore assessed in DKO mouse platelets. Platelets from DKO mice display normal levels of active loop phosphorylation on Src Tyr418 and Syk Tyr525/6 compared to litter-matched WT controls **(Figure 4.9)**. Lack of enhanced SFK activity in DKO mouse platelets to collagen potentially explains why no physiological effect of LAIR-1 and PECAM-1 absence was observed on thrombosis *in vivo*.

Csk plays an important role in regulation of SFK activity, expression of Csk and its homologous kinase Chk, which can also inactivate SFKs via phosphorylation of their C-terminal tyrosine residue, was therefore evaluated (Mori et al., 2018). Normal protein levels of Csk and Chk were detected in both megakaryocytes and platelets of DKO mice **(Figure 4.10)**; indicating Csk/Chk mediated inactivation of SFKs is unlikely to be responsible for the reduction in activity compared to LAIR-1 KO mouse platelets.

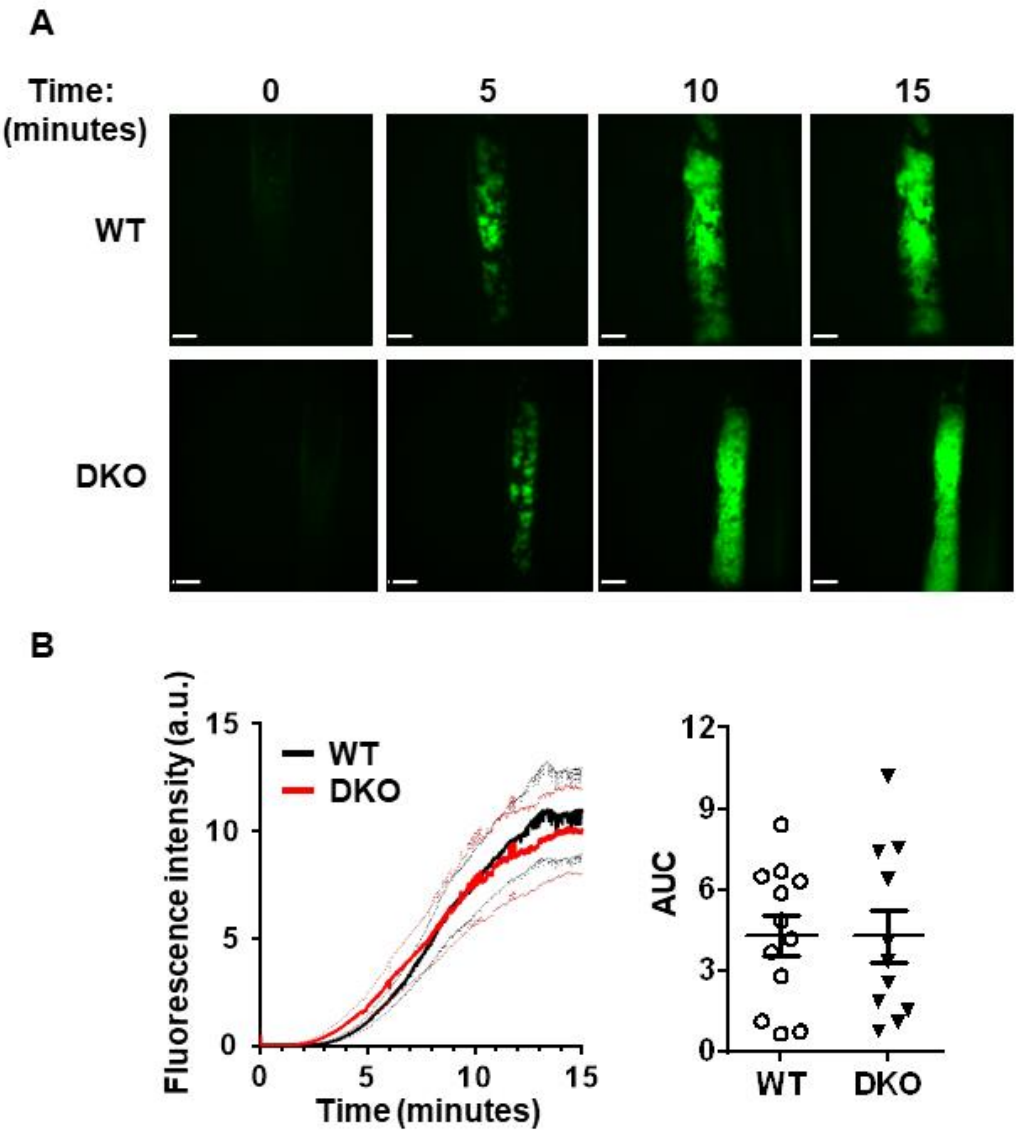

Figure 4. 8. Ferric chloride-induced thrombus formation *in vivo* unaltered in LAIR-1/PECAM-1 DKO mice. Mice were injected with DyLight488-conjugated anti-GPIbβ antibody (0.1 µg/g body weight). Exposed carotid arteries were injured with 10% ferric chloride for 3 minutes and the accumulation of platelets (green) into the thrombi was assessed. (A) Representative fluorescence images from GPIbβ -labeled platelets after ferric chloride-injury of carotid are shown. Scale bar: 200 µm. (B) Each curve represents the integrated fluorescence intensity in arbitrary units (a.u.) (C) Area under the curve of the integrated fluorescence density is represented. Mean ± SEM; n = 11-12 mice/genotype; Mann-Whitney U test, non-significant. See also videos 4.I and 4.II.

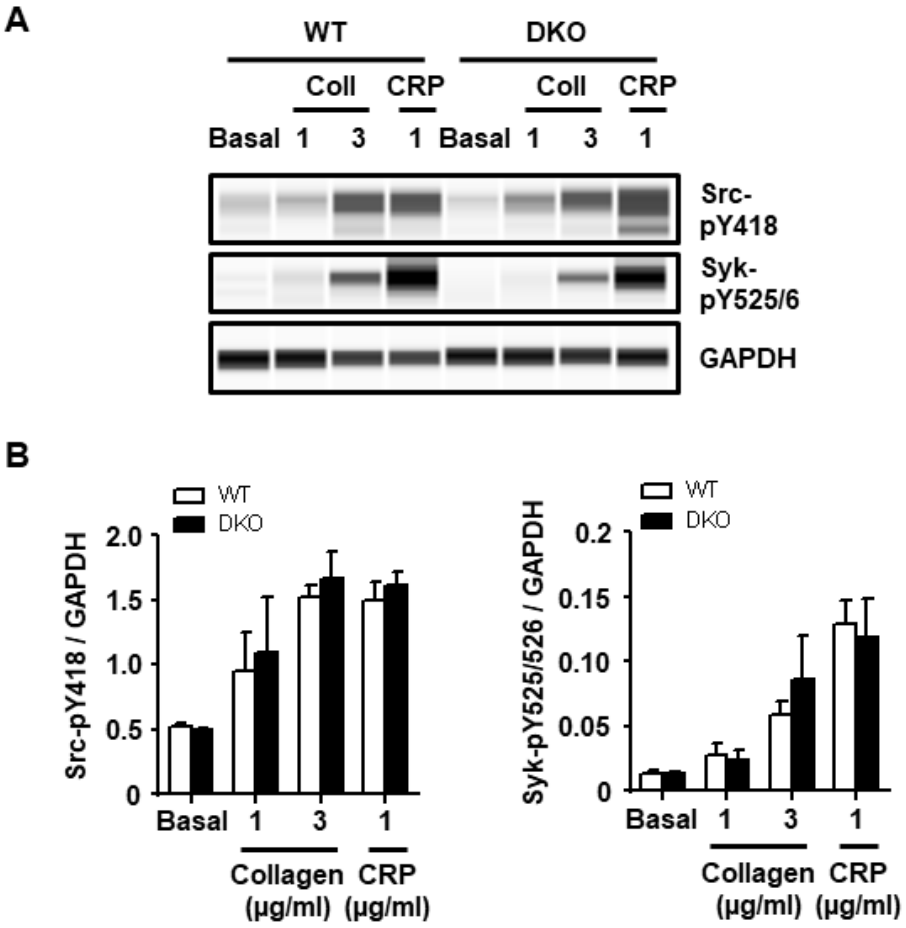

Figure 4. 9. Unaltered GPVI-mediated activation of Src and Syk in LAIR-1/PECAM-1 DKO mouse platelets. Washed platelets (5×10^8/ml) from DKO mice were stimulated with collagen and CRP. Phosphorylation of activation sites of Src and Syk were then assessed in whole cell lysates using a capillary based immunoassay (ProteinSimple). (A) Representative images and (B) Quantification of normalised peak area. Mean ± SEM; n = 3 independent experiments/genotype. Two-way ANOVA with multiple comparisons.

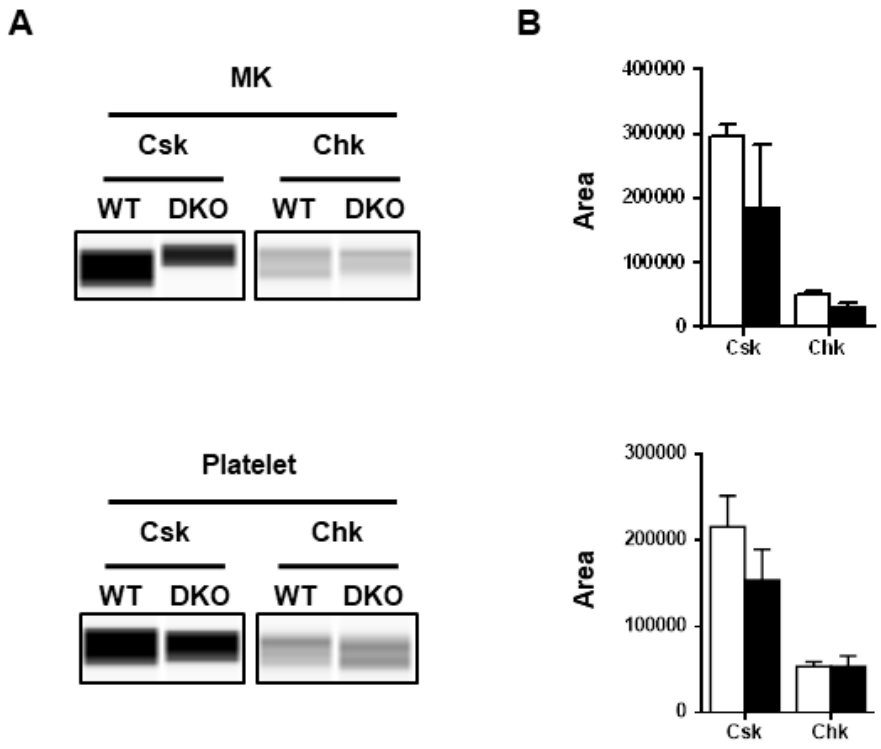

Figure 4. 10. Csk and Chk levels in LAIR-1/PECAM-1 DKO mouse megakaryocytes and platelets. Expression of Csk and Chk were assessed in whole cell lysates of WT and DKO mouse washed platelets (5×10^8) using a capillary based immunoassay (ProteinSimple). (A) Representative images and (B) Quantification of normalised peak area. Mean ± SEM; n = 3 independent experiments. Student's t-test, non-significant.

4.4. Discussion

Findings in this chapter reveal absence of PECAM-1 alongside LAIR-1 does not result in further enhancement of platelet reactivity. LAIR-1/PECAM-1 DKO mice have mild thrombocythemia, and platelets hyper responsive to GPVI-mediated activation *in vitro*, but interestingly lack the enhanced *in vivo* thrombosis phenotype observed in LAIR-1 and PECAM-1 single KO mice. The absence of further enhancement suggests the ITIM-containing receptors LAIR-1 and PECAM-1 regulate platelet reactivity via the same signalling pathways.

Platelet counts in DKO mice were increased, although not as much as those in LAIR-1 KO mice. In LAIR-1 KO mice the increase in circulating platelets was attributed to a combination of increased megakaryocyte platelet release and longer platelet half-life. Cultured DKO mouse megakaryocytes do not exhibit increased proplatelet formation suggesting platelet production *in vivo* is normal. Although not assessed in DKO mice increased half-life of platelets could account for the mild thrombocythemia, and together with the normal proplatelet formation in DKO mice would explain why the thrombocythemia observed is not as great as that in LAIR-1deficient mice. Clearance of circulating platelets is determined by multiple triggers which signal their removal, including modification of platelet surface glycoprotein glycans. Sialic acid loss occurs as platelets age, marking them for removal by hepatic Ashwell-Morrel receptors (Grozovsky et al., 2015). In platelets from LAIR-1 deficient mice no alteration in sialic acid staining was however observed, instead the increased lifespan was attributed to a change in prosurvival and proapoptotic signal interplay, which also regulates platelet survival, and is a possible explanation for the increased platelet counts in DKO mice (Smith et al., 2017).

Aggregation responses to GPVI-agonists collagen and CRP were enhanced in platelets from LAIR-1/PECAM-1 DKO mice with responses comparable to those of single KO mice. Lack of further enhancement in the DKO mouse platelets is suggestive of redundancy between the

inhibition of GPVI signalling mediated by LAIR-1 and PECAM-1. Normal responses to thrombin in LAIR-1/PECAM-1 DKO mouse platelets were expected, as although PECAM-1 has been shown to inhibit GPCR signalling this has only been observed in human platelets upon PECAM-1 crosslinking (Cicmil et al., 2002).

Despite previous reports of increased spreading on fibrinogen of LAIR-1 and controversially in PECAM-1 single KO mouse platelets (Smith et al., 2017, Dhanjal et al., 2007b, Wee and Jackson, 2005), normal spreading was observed in all genotypes, although adhesion was increased in single KO mice platelets. Differences in findings are likely due to differing methods of analysis. Normal platelet spreading on fibrinogen was observed in single KO mice following pre-activation with thrombin, in agreement with previous studies (Smith et al., 2017, Dhanjal et al., 2007b). Interestingly, DKO mouse platelets showed increased spreading, but not adhesion, on fibrinogen following thrombin pre-activation. This is a peculiar finding as thrombin mediated aggregation responses were normal, although flow cytometry did find activation and fibrinogen binding of DKO mouse platelets was increased to thrombin.

The normal platelet adhesion to collagen under flow conditions was not expected for DKO mice, as was the absence of larger platelet aggregates from LAIR-1 deficient mice which has previously been shown (Smith et al., 2017). There are conflicting reports regarding adhesion of PECAM-1 KO platelets to collagen under shear, with larger platelet aggregates and normal/slight reduction in aggregate size reported by different studies even though similar experimental conditions were used (Jones et al., 2001, Dhanjal et al., 2007b). Differences in experimental setup are likely the cause of results in this chapter being dissimilar to those previously published. Blood was flowed over a collagen micro spot coated flow chamber in this study, with a capillary based flow system previously utilised for assessment of LAIR-1 KO mice (Smith et al., 2017). The tendency for increased activation of platelet aggregates following

perfusion over collagen, as observed by P-selectin surface area coverage, agrees with flow cytometry data showing enhanced α-granule secretion in DKO mouse platelets.

Normal *in vivo* thrombosis in DKO mice was surprising given that both LAIR-1 and PECAM-1 single KO mice display enhanced thrombosis in the ferric chloride model (Smith et al., 2017, Falati et al., 2006). The 3 minute, 10% ferric chloride-soaked filter paper application was the same as utilized in both single KO mice studies, however thrombosis was assessed using a Doppler flow probe to measure time to 75% occlusion in PECAM-1 KO mice. The LAIR-1 KO, as was the case for the DKO, measured thrombus formation by assessment of fluorescence intensity following labelling of platelets with fluorescently conjugated antibody. Both of these methods of measuring *in vivo* thrombosis are well established but may contribute to the lack of enhancement.

LAIR-1 has been shown in immune cells to interact with Shp1, Shp2 and Csk to inhibit ITAM signalling. Expression of LAIR-1 however decreases throughout megakaryocyte development, and LAIR-1 is not present on platelets. The enhanced responsiveness of platelets from LAIR-1 deficient mice, unlike PECAM-1, is therefore not due to absence of inhibitory signalling. Instead enhancement is due to increased SFK activity which is present in the megakaryocytes and platelets of LAIR-1 deficient mice (Smith et al., 2017). The absence of enhanced SFK activity in DKO mice is consistent with the difference in phenotype to LAIR-1 deficient mice, as enhanced megakaryocyte proplatelet formation, platelet spreading and thrombus formation *in vivo* all returned to normal in DKO mice. SFKs are central to platelet activation responses propagating signals from a variety of platelet receptors including GPVI-FcR γ-chain complex and integrin αIIbβ3. SFKs are constitutively associated with the intracellular tail of GPVI and β3 subunit of integrin αIIbβ3. Upon GPVI activation, SFKs rapidly phosphorylate ITAMs of the FcR γ-chain, providing high affinity docking sites for Syk, which becomes activated by

autophosphorylation the further action of SFKs and together propagate downstream signalling (Senis et al., 2014, Poole et al., 1997). Integrin αIIbβ3 binding of fibrinogen activates associated SFK phosphorylation of β3 subunit. This provides docking sites for adaptor Shc and cytoskeletal proteins (vinculin and actinin), which themselves act as docking sites for assembly signalling complexes, tyrosine kinases FAK and Syk and lipid kinase PI3K that propagate the signal (Senis et al., 2014). Increased SFK activity, such as observed in LAIR-1 deficient mouse megakaryocytes and platelets, therefore results in enhanced reactivity to GPVI and integrin αIIbβ3 activation.

To explain the normal SFK activity in DKO mice, expression levels of Csk and its homologue Chk were investigated. Levels were however unaltered in DKO mice, further investigation of other known regulators of platelet SFK activity such as CD148, and known binding partners of LAIR-1 and PECAM-1 such as Shp1 and Shp2, may shed more light on the exact mechanism behind this change in signalling.

In conclusion, findings in this chapter show ablation of both LAIR-1 and PECAM-1 in megakaryocytes and platelets does not result in further enhancement of megakaryocyte and platelet hyper reactivity. Suggesting LAIR-1 and PECAM-1 mediate their inhibitory functions through the same signalling pathways, but are not functionally redundant.

Chapter 5

TLT-1: a novel platelet activation biomarker

5.1. Aims

The aim of this chapter was to determine if the ITIM-containing receptor TLT-1 is a more sensitive marker of α-granule secretion and irreversible platelet activation during thrombus formation *in vivo* than P-selectin.

5.2. Introduction

Observations *in vivo* have demonstrated that platelet activation throughout a developing thrombus is not uniform, with some platelets undergoing intracellular calcium mobilization and α-granule secretion while others retain a resting morphology (Stalker et al., 2013). Pioneering work by Stalker et al characterised the hierarchical structure of growing thrombi *in vivo,* demonstrating thrombi are made up of a tightly packed, irreversibly activated platelet core directly adjacent to the vascular injury site, surrounded by a loosely packed and minimally activated platelet shell (Stalker et al., 2013). The highly activated platelet core could be defined by surface expression of P-selectin, a commonly used marker of α-granule secretion and irreversible platelet activation (Maxwell et al., 2007, Nesbitt et al., 2009, Nishimura et al., 2012, van Gestel et al., 2002, Dubois et al., 2007, Gross et al., 2005, Vandendries et al., 2007, Hechler et al., 2010).

P-selectin is a type-1 transmembrane protein present in α-granules of platelets and megakaryocytes. Following platelet activation, α-granules fuse with the plasma membrane and expose P-selectin on the platelet surface. The primary role of P-selectin once on the platelet surface is to mediate interactions, via its ligand P-selectin glycoprotein ligand 1, with leukocytes (monocytes and neutrophils) to facilitate efficient recruitment to sites of vascular injury.

The platelet and megakaryocyte specific ITIM-containing receptor TLT-1 is also localized in α-granules and undergoes rapid translocation to the surface upon activation (Washington et al., 2009, Washington et al., 2004). In platelets, TLT-1 is highly abundant. Quantitative proteomics-based approaches estimate copy numbers of 14,200 in human and 154,780 in mouse platelets, making it more highly expressed than P-selectin (human: 8,900 copies; mouse: 35,970 copies) (Burkhart et al., 2012, Zeiler et al., 2014). Together with early findings that although TLT-1 and P-selectin are both present within α-granules, a proportion localized distinct to P-selectin, led to TLT-1 being investigated as a marker of platelet activation (Barrow et al., 2004). Following activation of both murine and human platelets with thrombin and the GPVI-specific agonist CRP, surface expression of TLT-1 and P-selectin was increased, though TLT-1 was upregulated to a much greater extent than P-selectin. Time course studies also showed more rapid upregulation of TLT-1, which could be detected earlier following platelet stimulation than P-selectin (**Figure 5.1**, Experiments performed by Lola Parfitt, Zaher Raslan and Alexandra Mazharian, University of Birmingham, UK) (Smith et al., 2018). Increased surface expression could also be detected on mouse bone marrow-derived megakaryocytes in response to collagen stimulation, which was not mirrored by P-selectin, suggesting TLT-1 could be used as a marker of megakaryocyte activation (**Figure 5.1**, Experiments performed by Alexandra Mazharian, University of Birmingham, UK) (Smith et al., 2018). These initial *in vitro* findings that TLT-1 is a more sensitive marker of platelet activation than P-selectin therefore led to assessment of TLT-1 during thrombus formation *in vivo*.

In this chapter, TLT-1 is investigated as a biomarker of platelet activation during thrombus formation *in vivo*. Upregulation and distribution of TLT-1 is compared to the current gold standard platelet activation marker P-selectin, in the laser and ferric chloride-injury models of thrombosis.

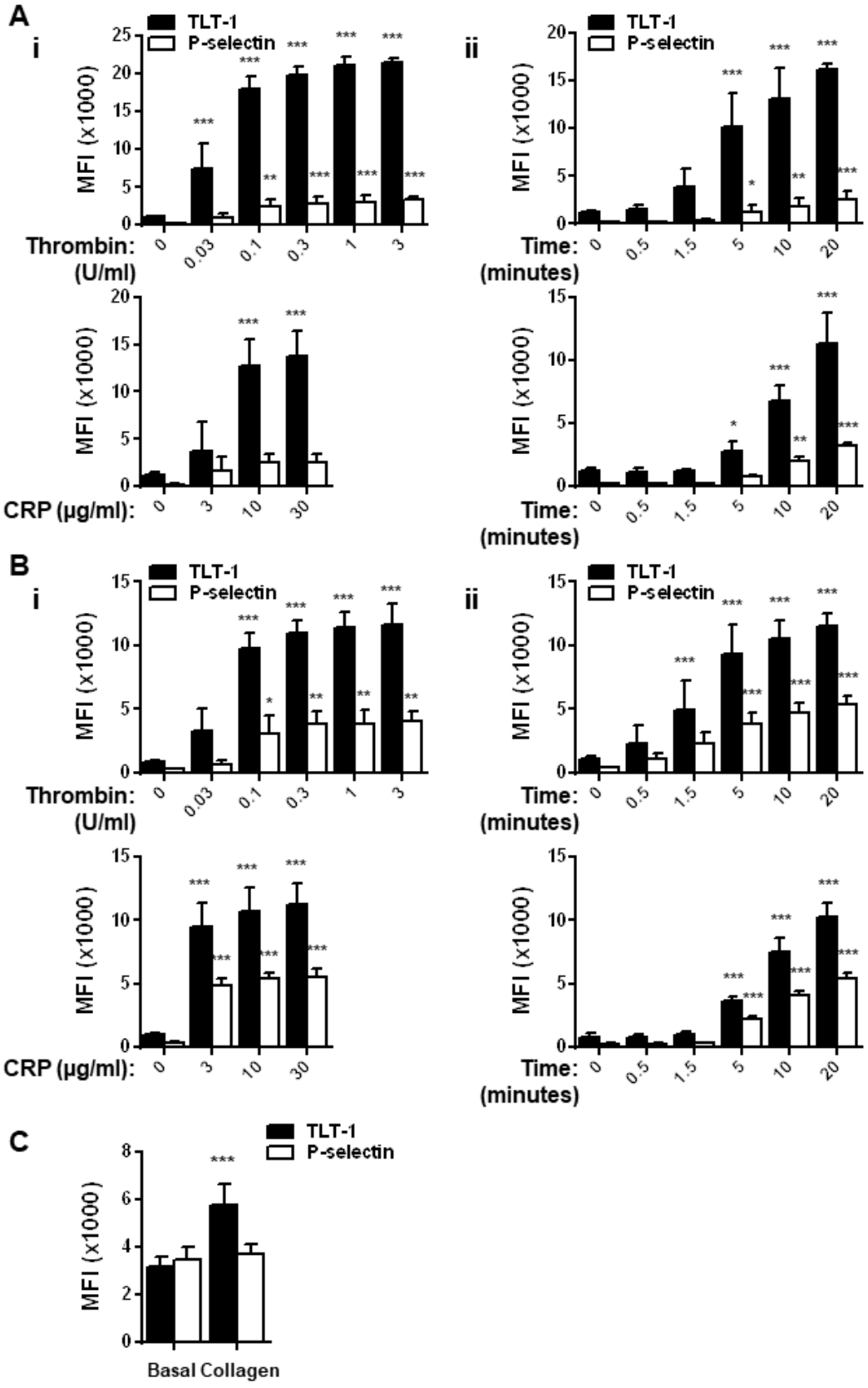
A
i
TLT-1
P-selectin
MFI (x1000)
Thrombin: (U/ml)
0
0.03
0.1
0.3
1
3
CRP (µg/ml):
0
3
10
30
ii
Time: (minutes)
0
0.5
1.5
5
10
20
B
i
ii
C
Basal
Collagen

Figure 5. 1. TLT-1 can be detected more easily than P-selectin on the surface of activated megakaryocytes and platelets *in vitro*. Platelet surface expression of TLT-1 and P-selectin were measured by flow cytometry in response to the PAR agonist thrombin and the GPVI-specific agonist collagen related peptide (CRP), in murine (A) and human (B) whole blood. (i) Dose-response (thrombin 0.03 - 3 U/ml and CRP 3 - 30 μg/ml) and (ii) time course (thrombin 0.1 U/ml, CRP 10 μg/ml). MFI ± SD; n = 3 - 6 independent experiments/condition. (C) Bone marrow-derived megakaryocyte surface expression of TLT-1 and P-selectin following collagen stimulation (30 μg/ml) for 20 minutes at 37ºC, MFI ± SD; n = 7 - 9. . **P*<0.05, ***P*<0.01 ****P*<0.001 vs basal. Experiments performed by Lola Parfitt, Zaher Raslan and Alexandra Mazharian, University of Birmingham, UK.

5.3. Results

5.3.1. TLT-1 is expressed throughout the core and shell of thrombi *in vivo*

In vitro findings show TLT-1 is a more sensitive marker of platelet activation than P-selectin (Smith et al., 2018). *In vivo* P-selectin surface expression only occurs on highly activated platelets in the thrombus core. TLT-1 surface upregulation was therefore investigated compared to P-selectin within thrombi *in vivo*. TLT-1 was detected more rapidly than P-selectin in thrombi following laser-induced injury of cremaster arterioles in WT mice. Interestingly, unlike P-selectin, TLT-1 was not restricted to the highly activated platelet core directly adjacent to the site of injury, but was present throughout both core and shell of thrombi **(Figure 5.2)**.

5.3.2. TLT-1 distribution throughout thrombi not due to non-specific binding

In order to confirm the observed rapid upregulation and distribution of TLT-1 throughout thrombi *in vivo* was not due to non-specific antibody binding, anti-TLT-1 antibody was infused into TLT-1 deficient mice and cremaster arterioles subsequently injured by laser. No anti-TLT-1 antibody signal could be detected in thrombi of TLT-1deficient mice **(Figure 5.3)**, demonstrating the rapid upregulation and distribution previously observed was due to detection of surface TLT-1, and not because of non-specific antibody binding.

5.3.3. TLT-1 is upregulated more rapidly than P-selectin during thrombosis *in vivo*

To determine if the rapid upregulation and distribution of TLT-1 is also observed in thrombi stimulated by other mechanisms, TLT-1 upregulation was assessed following ferric chloride-induced injury of the carotid arteries of WT mice. As expected due to the nature of the injury model a core and shell was not observed. Both TLT-1 and P-selectin were expressed throughout thrombi, however TLT-1 was detected more rapidly than P-selectin **(Figure 5.4)**.

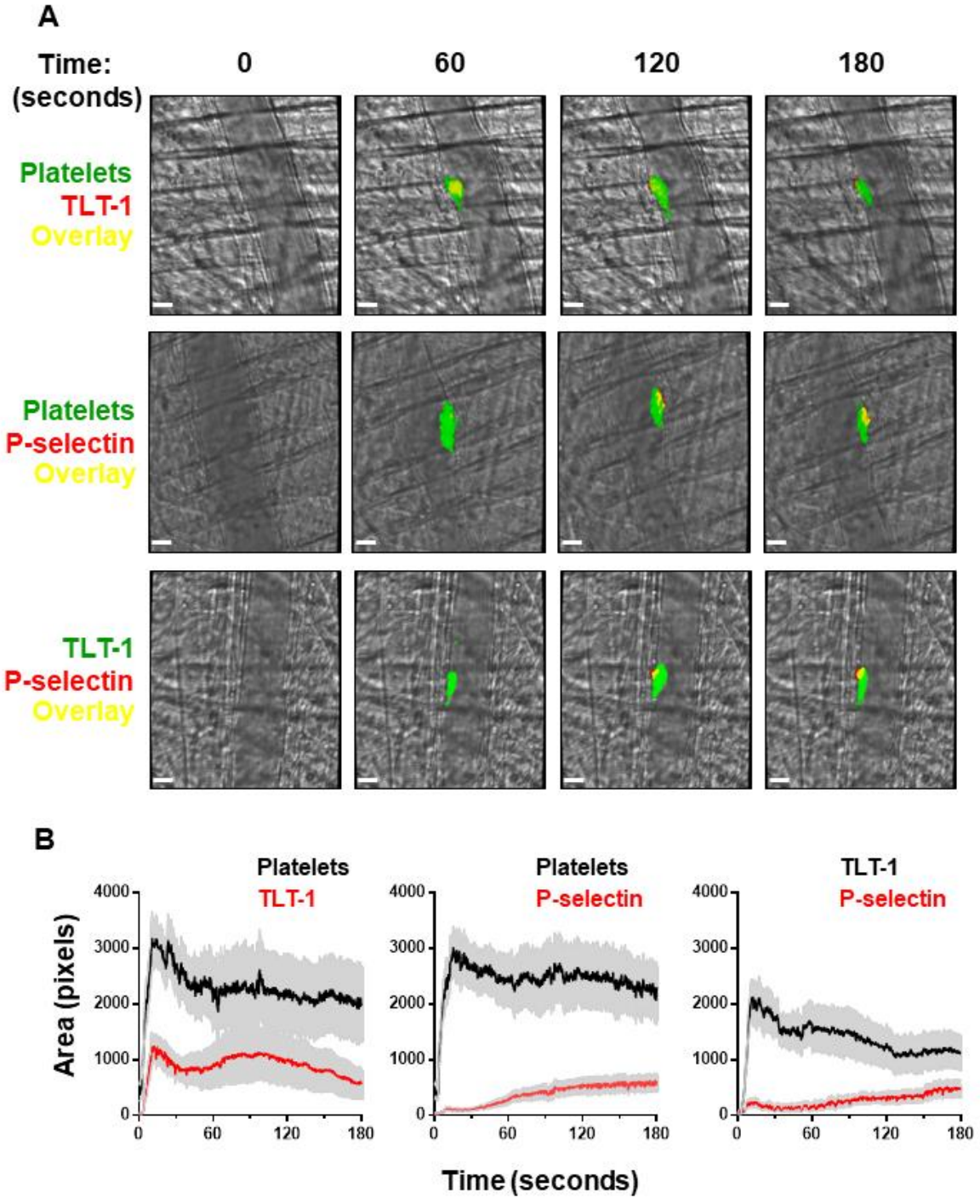

Figure 5. 2. TLT-1 appears more rapidly and is detected throughout laser-induced thrombi *in vivo*. Wild type mice were injected with anti-GPIbβ, -TLT-1 or –P-selectin antibody. Arterioles of cremaster muscles were subsequently injured by laser. (A) Representative composite brightfield and fluorescence images of platelets (GPIbβ), TLT-1 and P-selectin in thrombi. (B) Quantification of fluorescence area in pixels (mean ± SEM); n = 25 - 32 injuries from 4 - 6 mice. Scale bar 10 µm. See also videos 5.I – 5.III.

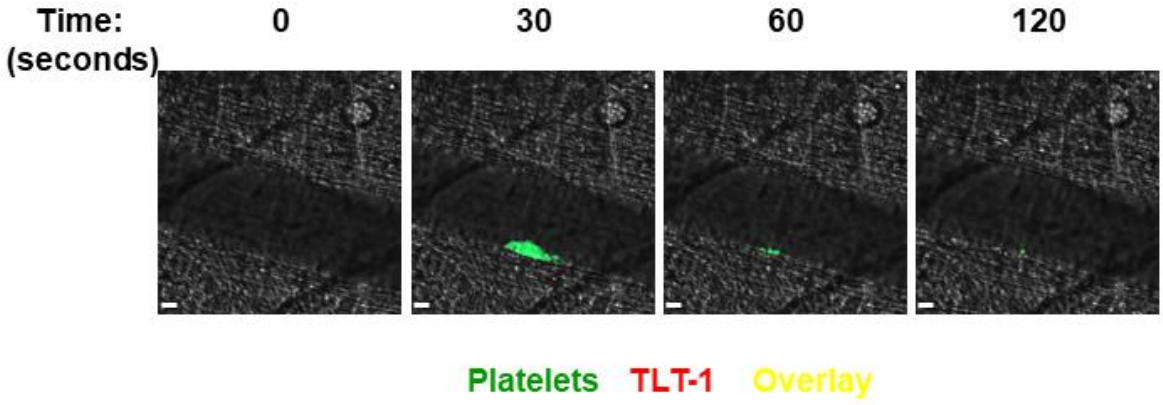

Figure 5. 3. Specificity of anti-TLT-1 antibody binding during thrombus formation *in vivo*. Anti-GPIbβ and TLT-1 antibody were injected into a TLT-1 deficient mouse. Arterioles of cremaster muscles were subsequently injured by laser. Representative composite brightfield and fluorescence images of platelets (GPIbβ) and TLT-1 in thrombi. n = 10 injuries from 1 mouse. Scale bar 10 μm. See also video 5.IV.

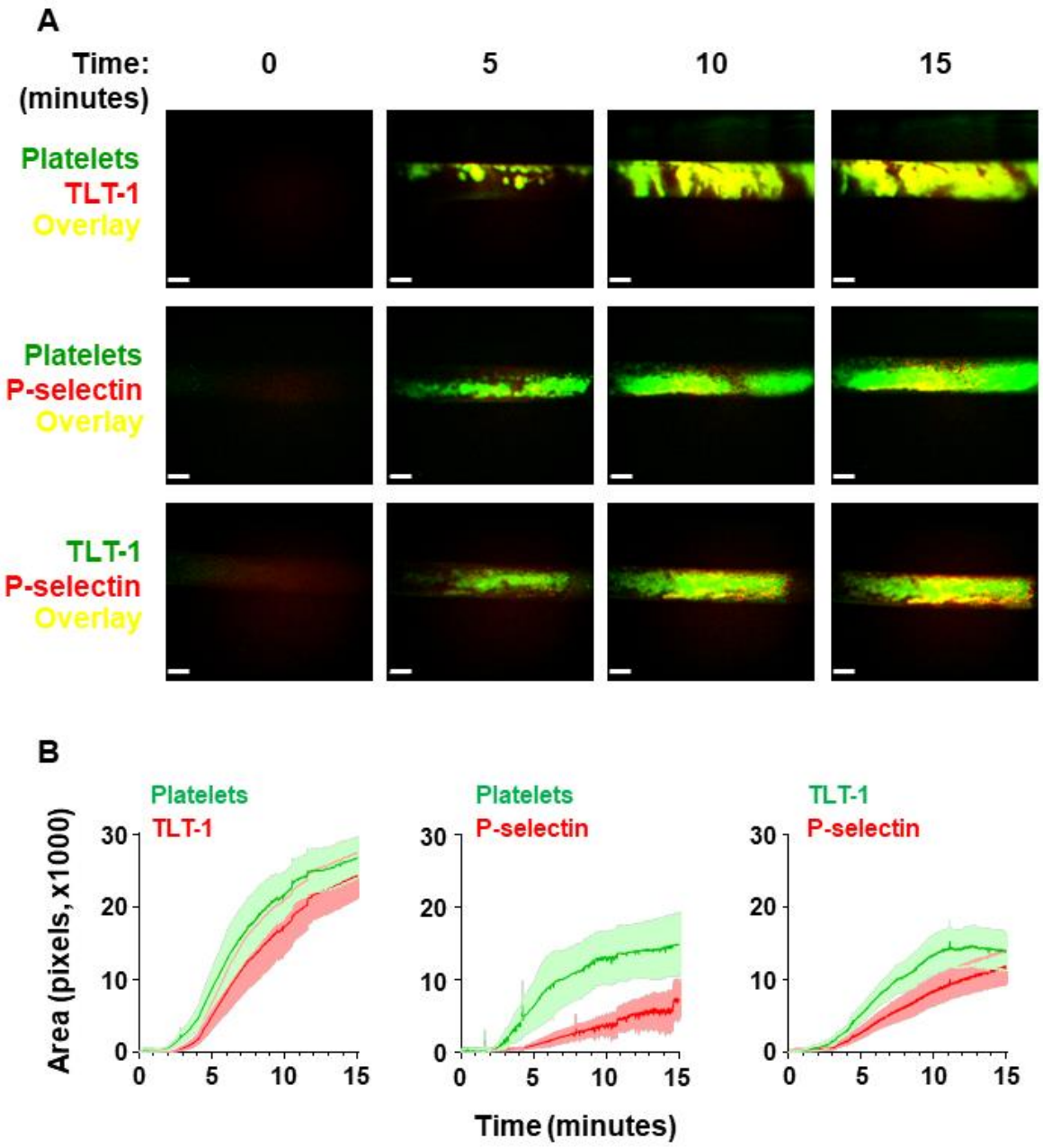

Figure 5. 4. Upregulation of TLT-1 and P-selectin during ferric chloride-induced thrombus formation in the carotid artery. Wild type mice were injected with anti-GPIbβ, TLT-1 or P-selectin antibody. Exposed carotid arteries were injured with 10% ferric chloride for 3 minutes and thrombi fluorescence area assessed. (A) Representative fluorescence images after ferric chloride-injury of carotid are shown. Scale bar: 200 μm. (B) Each curve represents the mean fluorescence area (± SEM) in pixels for 4-7 mice/condition. See also videos 5.V – 5.VII.

5.3.4. Distinct and overlapping staining of TLT-1 and P-selectin in platelets and megakaryocytes

To explain the difference in TLT-1 and P-selectin upregulation observed *in vivo* and *in vitro* (Smith et al., 2018), immunofluorescence microscopy was performed on resting human and WT mouse platelets and primary bone marrow derived megakaryocytes. TLT-1 colocalized with P-selectin within α-granules. A proportion however localized to distinct granules as determine by Manders overlap coefficient in platelets **(Figure 5.5)** and object based colocalization in megakaryocytes **(Figure 5.5)**, which suggests differential distribution or localization of a proportion of TLT-1 to other as-yet-unidentified compartments.

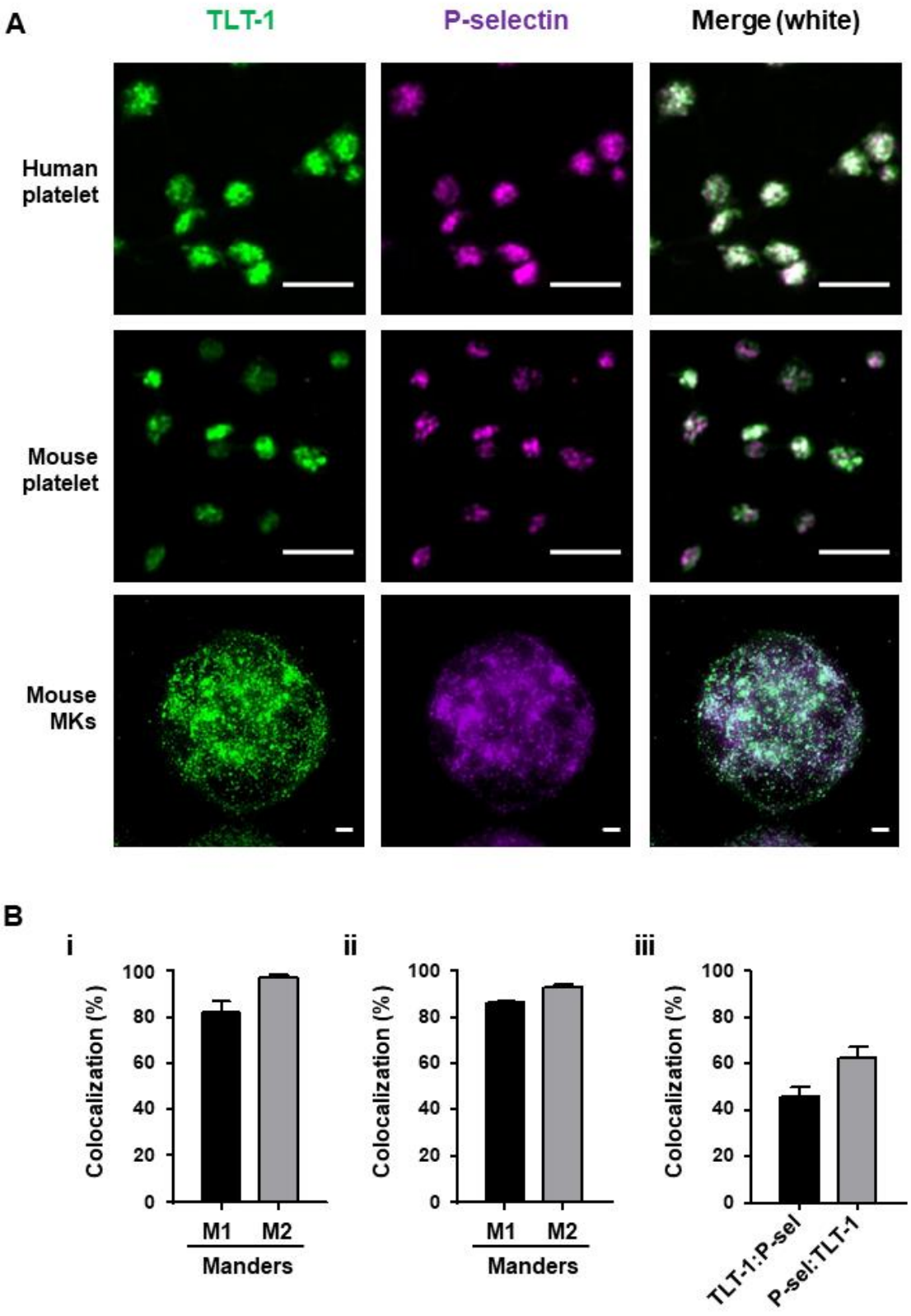
A
TLT-1
P-selectin
Merge (white)
Human platelet
Mouse platelet
Mouse MKs
B
i
ii
iii
Colocalization (%)
100
80
60
40
20
0
M1
M2
Manders
TLT-1:P-sel
P-sel:TLT-1

Figure 5. 5. Distinct and overlapping staining of TLT-1 and P-selectin in platelets and megakaryocytes. (A) Resting human and WT mouse platelets on poly-L-lysine and primary mouse bone marrow (BM)-derived megakaryocytes (MKs) spread on fibrinogen matrix for 15 minutes at 37°C were fixed, permeabilised and stained with anti-TLT-1 and -P-selectin antibodies. The right column represented an overlay of both images. Images are representative of 3-4 independent experiments. Scale bar 5 μm. (B) Degree of TLT-1 and P-selectin colocalization. Determined by the Manders overlap coefficient in (i) resting human and (ii) mouse platelets, and object based colocalization in (iii) BM-derived mouse MKs. N=3-4 independent experiments/condition, 400-600 platelets or 25-35 MKs/experiment.

5.4. Discussion

TLT-1 was found to more rapidly translocate to the surface of activated platelets compared with P-selectin during laser-induced thrombus formation in mouse cremaster arterioles. TLT-1 expression was detected throughout the entire thrombi whereas P-selectin was only observed in a highly localized region within the thrombus core, directly adjacent to the site of injury. While TLT-1 distribution does not suggest the core, which has additional defining characteristics, is larger than previously thought, it does demonstrate for the first time the presence of activated platelets in the thrombus shell **(Figure 5.6)**.

The rapid upregulation of TLT-1 compared with P-selectin during *in vivo* thrombosis is most likely due to the greater abundance of TLT-1 than P-selectin in mouse platelets. However, differential compartmentalization of the 2 receptors and differences in binding affinities of the antibodies may also contribute. Although all antibodies tested irrespective of staining yielded the same results, area rather than fluorescence intensity was assessed to avoid any differences in fluorophores.

Although both receptors are reportedly localized in α-granules, differences in the surface translocation rates and distribution within thrombi suggest distinct mechanisms of upregulation. Another possibility is TLT-1 is present in an early release granule, either an α-granule subpopulation or distinct granule type, that is devoid of P-selectin.

It has previously been reported that stimulation of platelets with different agonists results in differential α-granule cargo release. This led to the proposal of distinct α-granule subpopulations which undergo specific release to specific agonists (Chatterjee et al., 2011, Italiano et al., 2008, Jonnalagadda et al., 2012, Ma et al., 2005). Alternatively differential release has been suggested to result from segregation of randomly distributed cargo into sub regions within each α-granule, and partial activation producing release of some but not all cargo

sub regions (Sehgal and Storrie, 2007, van Nispen tot Pannerden et al., 2010). Tubular α-granules have also been identified, which raises the possibility of α-granule secretion being polarised.

These mechanisms could explain the differences in distribution of TLT-1 and P-selectin throughout thrombi, as agonists and extent of platelet activation are stratified at sites of vascular damage (Stalker et al., 2013, Jonnalagadda et al., 2012, Chatterjee et al., 2011). In the core, full platelet activation is driven by thrombin generation from the site of injury, though due to the packing density of platelets this only propagates a limited distance from the vessel wall (Stalker et al., 2013). ADP and TxA_2 released by the activated platelets though are able to extend further, driving accumulation of platelets which form the shell region (Stalker et al., 2013). Positive feedback pathways reinforce this architecture through additional signalling pathways, such as contact dependent signalling (Stalker et al., 2013).

Consistent with the hypothesis that rapid TLT-1 upregulation is due to its presence in an early release granule, immunofluorescence demonstrated distinct pattern of TLT-1 and P-selectin staining that suggests a proportion of these 2 receptors are localised differentially within platelets and megakaryocytes (Barrow et al., 2004). Additional work is required to characterise these distinct P-selectin negative granules and the mechanism of translocation to the surface.

In conclusion, this chapter demonstrates TLT-1 is a more sensitive platelet activation marker than current gold standard P-selectin that can be detected throughout both the core and shell of *in vivo* thrombi. Findings also raise important questions about platelet activation in the shell region of thrombi, and how proteins are compartmentalized within secretory granules of megakaryocytes and platelets. This opens the possibility of TLT-1 being used clinically as a biomarker for early detection of platelet activation in various pathologies, including coronary

artery disease and deep vein thrombosis, as well as megakaryocyte activation in bone marrow in myeloproliferative disorders and myelofibrosis.

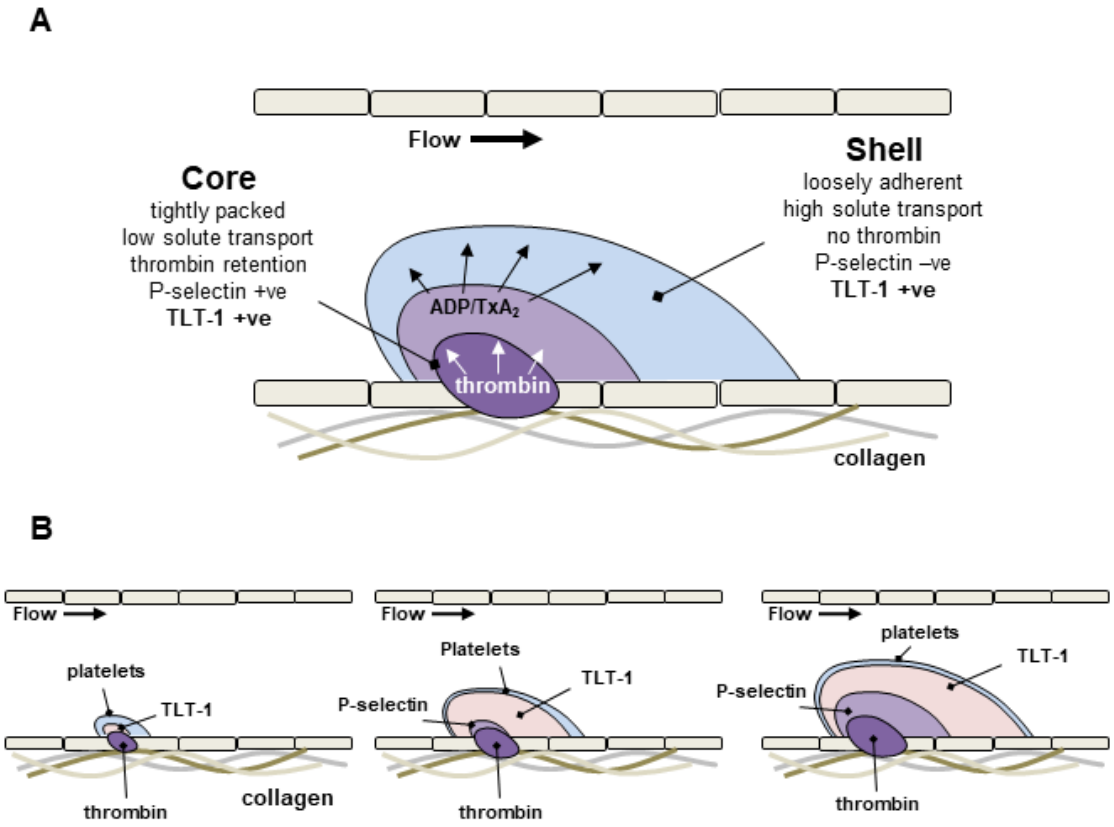

Figure 5. 6. Updated Core-shell thrombus model. (A) Architecture of a growing thrombus. Core tightly packed P-selectin and TLT-1 positive platelets directly adjacent to the site of injury. Surrounded by a loosely adherent P-selectin negative, TLT-1 positive platelet shell. (B) TLT-1 distribution throughout a growing thrombus. TLT-1 appears rapidly before P-selectin and is present in both core and shell regions of growing thrombus.

Chapter 6

TLT-1 deficient mouse model

6.1. Aims

The aim of this chapter was to determine the physiological function of the non-conventional ITIM-containing receptor TLT-1 in megakaryocyte development, platelet production, and function in haemostasis and thrombosis. This was achieved through characterisation of a TLT-1 deficient mouse model.

6.2. Introduction

TLT-1 is an ITIM-containing receptor exclusively expressed in the megakaryocyte lineage. Sequestered in α-granules TLT-1 is upregulated to the surface following activation. Intriguingly, TLT-1 is a non-conventional receptor shown to enhance rather than inhibit platelet activation like other conventional platelet ITIM-containing receptors. The specificity and abundance of TLT-1 suggests that it may play a unique role in vascular haemostasis, yet at the same time TLT-1 is also a member of the TREM family of proteins that play important roles in both adaptive and innate immunity (Giomarelli et al., 2007). Previous investigations into the function of TLT-1 have therefore been in respect to both platelet aggregation and inflammation. The function of TLT-1 during platelet aggregation has been interrogated through the generation of human single-chain Fv antibody fragments (scFv) and recombinant soluble TLT-1 (rsTLT-1). Anti-TLT-1 scFvs inhibited thrombin, but not GPVI-mediated platelet aggregation. This inhibition was reversible and could be overcome with higher doses of thrombin, suggesting anti-TLT-1 scFv affects the threshold of thrombin-mediated responsiveness rather than complete blockade (Giomarelli et al., 2007). The inhibition mediated by the scFvs comes after shape change, with the likely explanation that scFvs block TLT-1-ligand interactions during aggregation (Giomarelli et al., 2007). Recombinant soluble TLT-1 (rsTLT-1) enhanced human platelet aggregation to the thromboxane A_2-mimetic U46619, and to suboptimal doses of ADP

and collagen (Washington et al., 2009). This suggests TLT-1 maybe a platelet specific secondary activation factor, promoting aggregation in the presence of low levels of agonists (Washington et al., 2009). Recombinant sTLT-1 has also been shown to increase platelet adherence and spreading on fibrinogen (Morales et al., 2010) and is consistent with a model of sTLT-1 and TLT-1 on the platelet surface cross-linking the fibrinogen secreted upon platelet activation and thereby facilitating higher order platelet aggregation (Washington et al., 2009).

Generation of a TLT-1 deficient mouse model has also been utilized to interrogate the functional role of TLT-1 in platelet aggregation. Deficient mice are viable and fertile, with a mild decrease in platelet count. Aggregation responses to thrombin, collagen, ADP and U46619 were reduced in platelet rich plasma at all concentrations tested, with fibrinogen binding of deficient platelets showing a tendency to be decreased compared to wild type following suboptimal stimulation with ADP (Washington et al., 2009). *In vivo* tail bleeding time show deficient mice bleed more than controls, which is consistent with the decreased aggregation response of TLT-1 deficient platelets. Together these results suggest a role for TLT-1 in potentiating haemostasis (Washington et al., 2009).

The role of TLT-1 has also been evaluated in various models of inflammation. In mice, lipopolysaccharide (LPS)-induced sepsis led to detectable levels of plasma sTLT-1 within 2 hours, which continued to increase over 24 hours. This increase in sTLT-1 inversely mirrored the pattern of thrombocytopenia in these mice, suggesting sTLT-1 is released or shed as platelets leave the circulation during endotoxemia (Washington et al., 2009). TLT-1 deficient mice also succumb to LPS challenge faster than controls, and were predisposed to haemorrhage associated with inflammatory lesions (Washington et al., 2009). Together findings advocate a protective role for TLT-1 during inflammation, dampening the inflammatory response and enhancing platelet aggregation at sites of vascular injury (Washington et al., 2009).

This chapter investigates the role of TLT-1 in megakaryocytes and platelets. Utilizing a TLT-1 deficient mouse model, the absence of TLT-1 was assessed on megakaryocyte development, as well as platelet reactivity to a range of agonists, including the putatative ligand fibrinogen. In addition, the effect of TLT-1 absence on haemostasis and thrombosis *in vivo* were assessed.

6.3. Results

The TLT-1 deficient mouse model used in this chapter was provided by Dr Daniel McVicar (National Institute of Health, USA) / Dr Valance Washington (Universidad de Puerto Rico, Puerto Rico), the targeting strategy used can be found in Washington et al (2009). TLT-1 deficient mice were bred homozygous and with age matched WT mice used as controls.

6.3.1. Reduced platelet count TLT-1 deficient mice

TLT-1 deficient mice have previously been reported to have a mild thrombocytopenia (Washington et al., 2009); platelet count was therefore investigated in the TLT-1 deficient mice used in this study. TLT-1 deficient mice exhibited a mild reduction (15 %) in platelet count **(Figure 6.1 A)**. Platelet volume however remained unaltered **(Figure 6.1 B)**.

6.3.2. Increased spleen size TLT-1 deficient mice

To prevent inappropriate thrombus formation, activated platelets are cleared rapidly from the circulation by the spleen and liver. Reduced platelet production can increase plasma levels of TPO, which can result in expansion of the spleen megakaryocyte population. Release of cytokines from these megakaryocytes within the spleen can cause myelofibrosis by triggering stromal cell expansion and collagen deposition. Spleen size was therefore investigated in these thrombocytopenic mice. Spleens from TLT-1 deficient mice were larger than WT by 16 % **(Figure 6.2)**. Further investigation into spleen morphology was conducted on fixed and sectioned spleens, revealing normal megakaryocyte counts after Haematoxylin and Eosin staining **(Figure 6.2)**, and no evidence of myelofibrosis (reticulin staining) in TLT-1 deficient mice **(Figure 6.2)**. Similar sectioning and staining of mouse femurs also revealed unaltered megakaryocyte counts and absence of myelofibrosis within bone marrow **(Figure 6.2)**. This

suggests the enlarged spleens of these mice are not due to increased numbers of megakaryocytes and myelofibrosis, but possibly due to increased platelet clearance.

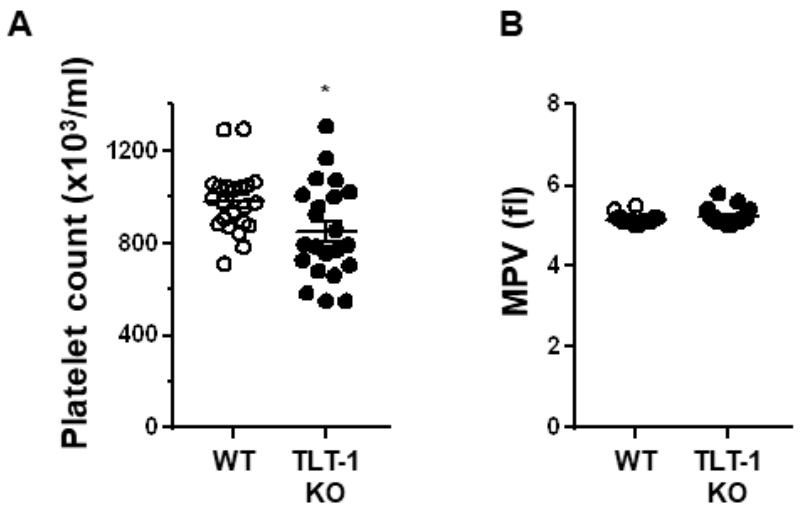

Figure 6. 1. Decreased platelet count TLT-1 deficient mice. (A) Platelet counts and (B) volumes from TLT-1 deficient and litter-matched wild-type mice (WT) were measured in whole blood using an ABX Pentra P60 blood counter. Mean ± SEM; **P* < 0.05; n = 22 mice/genotype. Student's t-test, **P*<0.05.

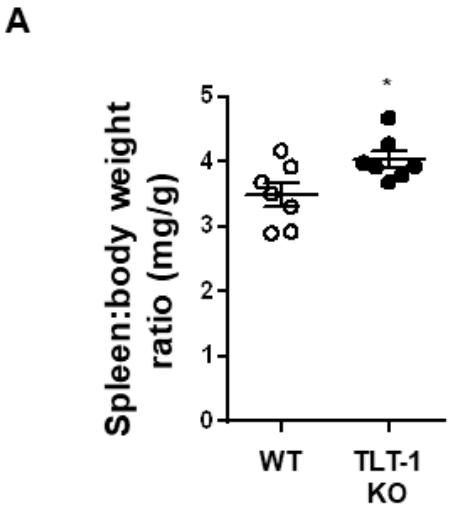

Figure 6. 2. Increased spleen size TLT-1 deficient mice. (A) Spleens from TLT-1 deficient and litter-matched WT mice were collected and spleen weight to bodyweight ratio calculated. Mean ± SEM; n = 6 mice/genotype; Student's t-test, **P* < 0.05. (B) Representative images of femurs and spleens stained with haematoxylin and eosin (H&E) and reticulin, after fixation, paraffin embedding and sectioning. Femurs were decalcified after fixation. (C) Quantification of megakaryocytes in blinded H&E sections. Scale bar 20 μm. Mean ± SEM, n = 3.

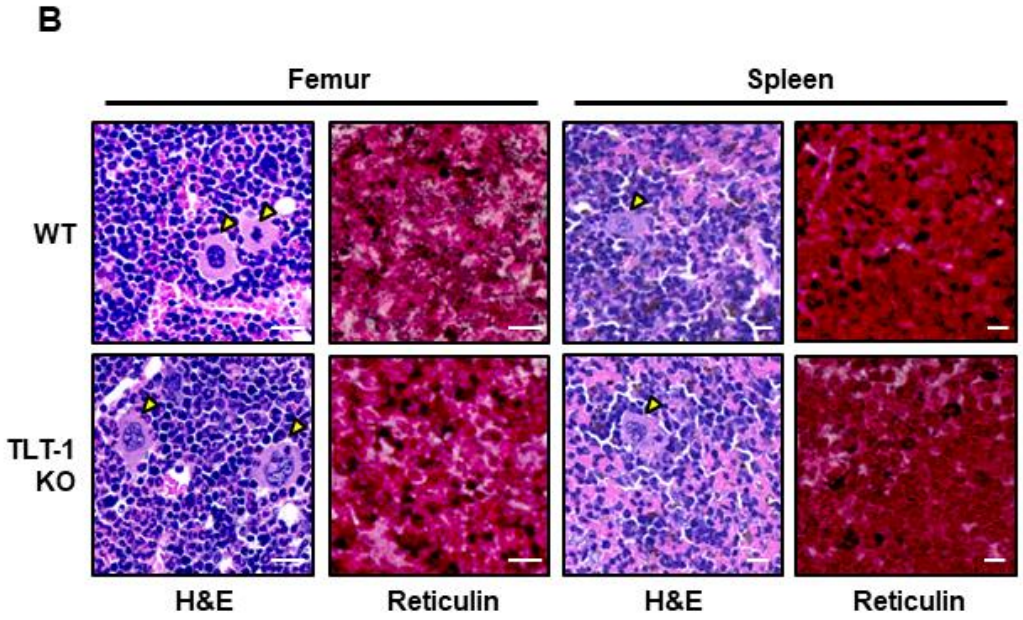
B
Femur
Spleen
WT
TLT-1 KO
H&E
Reticulin
H&E
Reticulin

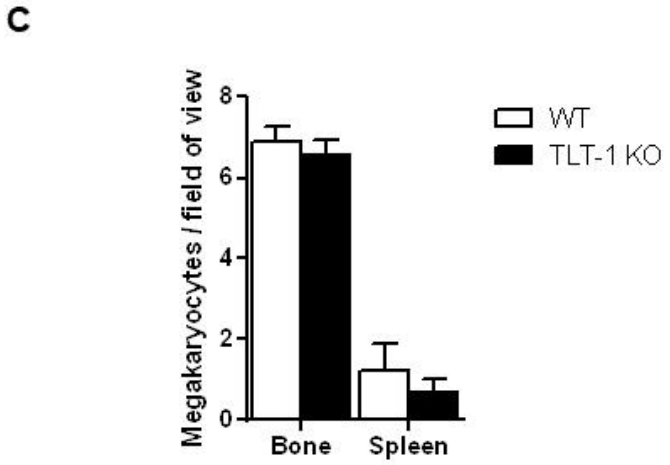
C
Megakaryocytes / field of view
0
2
4
6
8
Bone
Spleen
WT
TLT-1 KO

6.3.3. Development unaltered in TLT-1 deficient megakaryocytes

The effect of TLT-1 absence on megakaryocyte development was investigated by assessing DNA content of primary bone marrow derived megakaryocytes differentiated *in vitro*. TLT-1 deficient megakaryocytes developed normally *in vitro* as shown by the normal ploidy profiles **(Figure 6.3)**.

ERK1/2 have been shown to play a critical role in differentiation of megakaryocytes and platelet production (Mazharian et al., 2009). Mature bone marrow-derived megakaryocytes were stimulated with TPO for 10 minutes at 37^{o}C, cells were lysed and phosphorylation of ERK1/2 and Src were assessed by Western blot. Phosphorylation of ERK1/2 and the activation loop of Src were normal at resting and following stimulation in TLT-1 deficient megakaryocytes **(Figure 6.4)**, consistent with the normal growth and ploidy of these cells, indicating TLT-1 is not involved in regulation of megakaryocyte development. Future studies are required to investigate the cause of the thrombocytopenia of the TLT-1 deficient mice, likely due to defective proplatelet formation and/or increased platelet clearance.

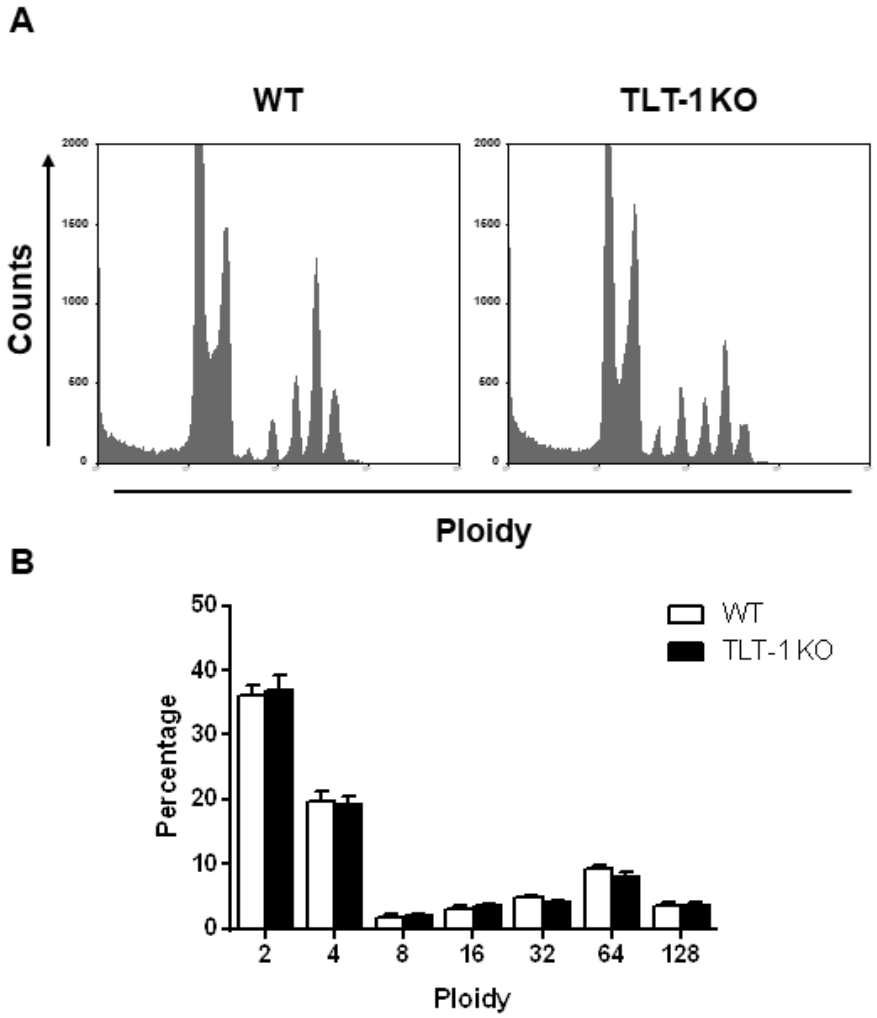

Figure 6. 3. Unaltered development of TLT-1 deficient megakaryocytes. Bone marrow-derived megakaryocytes from litter-matched WT and TLT-1 deficient mice were stained with propidium iodide and ploidy assessed by flow cytometry. (A) Representative profiles and (B) percentage of 2-128N ploidy cells was quantified. Mean ± SEM; n = 6 mice/genotype. Two-way ANOVA with multiple comparisons.

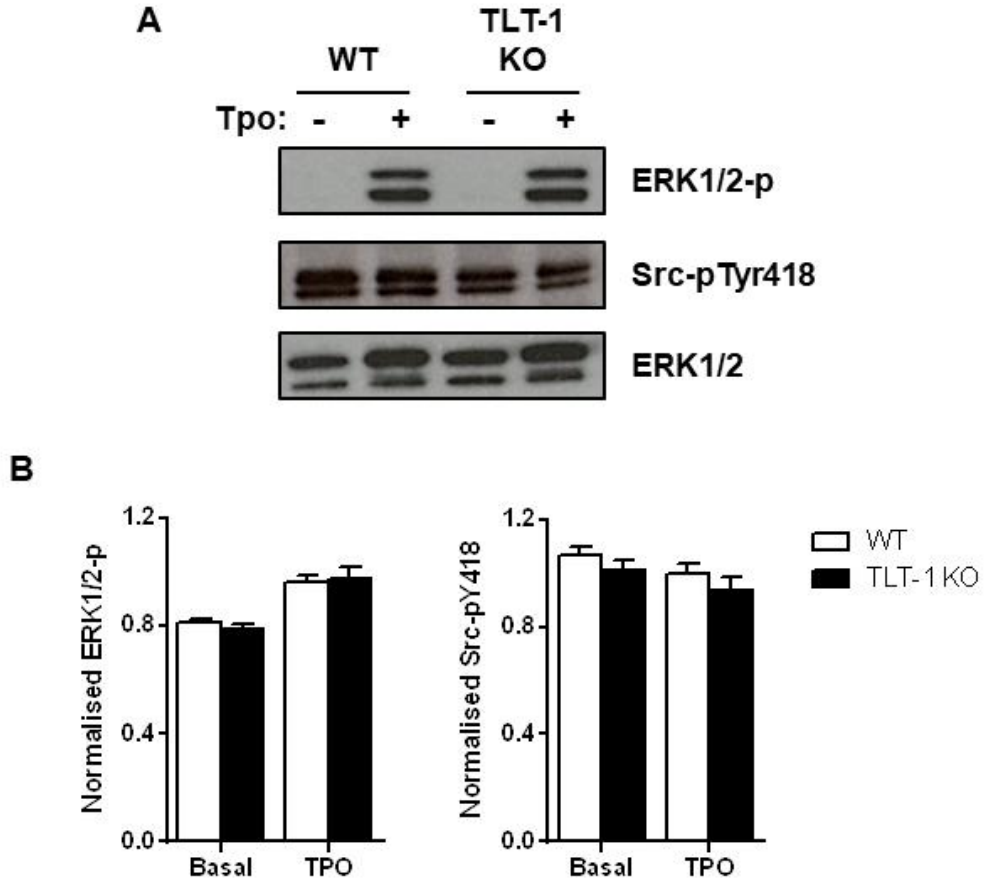

Figure 6. 4. TPO signalling unaltered in TLT-1 deficient megakaryocytes. Bone marrow-derived megakaryocytes from litter-matched WT and TLT-1 deficient mice were stimulated with TPO (10 minutes, 37^{o}C). Whole cell lysates were then Western blotted with anti-ERK1/2-p and Src-pTyr418 and ERK1/2. (A) Representative blots and (B) densitometry quantification. Mean ± SEM from 3 independent experiments. Two-way ANOVA with multiple comparisons.

6.3.4. Aggregation responses unaltered in TLT-1 deficient platelets

TLT-1 deficient platelets have previously been shown to aggregate less than WT in platelet rich plasma (Washington et al., 2009). Aggregation and dense granule secretion of washed TLT-1 deficient platelets was assessed by lumi-aggregometry. Aggregation responses to the GPVI receptor agonists collagen and CRP and to hemi-ITAM-containing receptor CLEC-2 activation were normal, as were responses to the GPCR agonists thrombin and thromboxane A_2 mimetic U46619 **(Figure 6.5)**. Dense granule secretion measured by ATP release was increased in response to high, but not low, concentrations CRP, with all other agonists displaying normal ADP release **(Figure 6.5)**. No alteration in surface receptor levels of TLT-1 deficient platelets were observed by flow cytometry **(Table 6.1)**. Normal aggregation responses to a wide range of agonists suggest TLT-1 has no role in platelet aggregation.

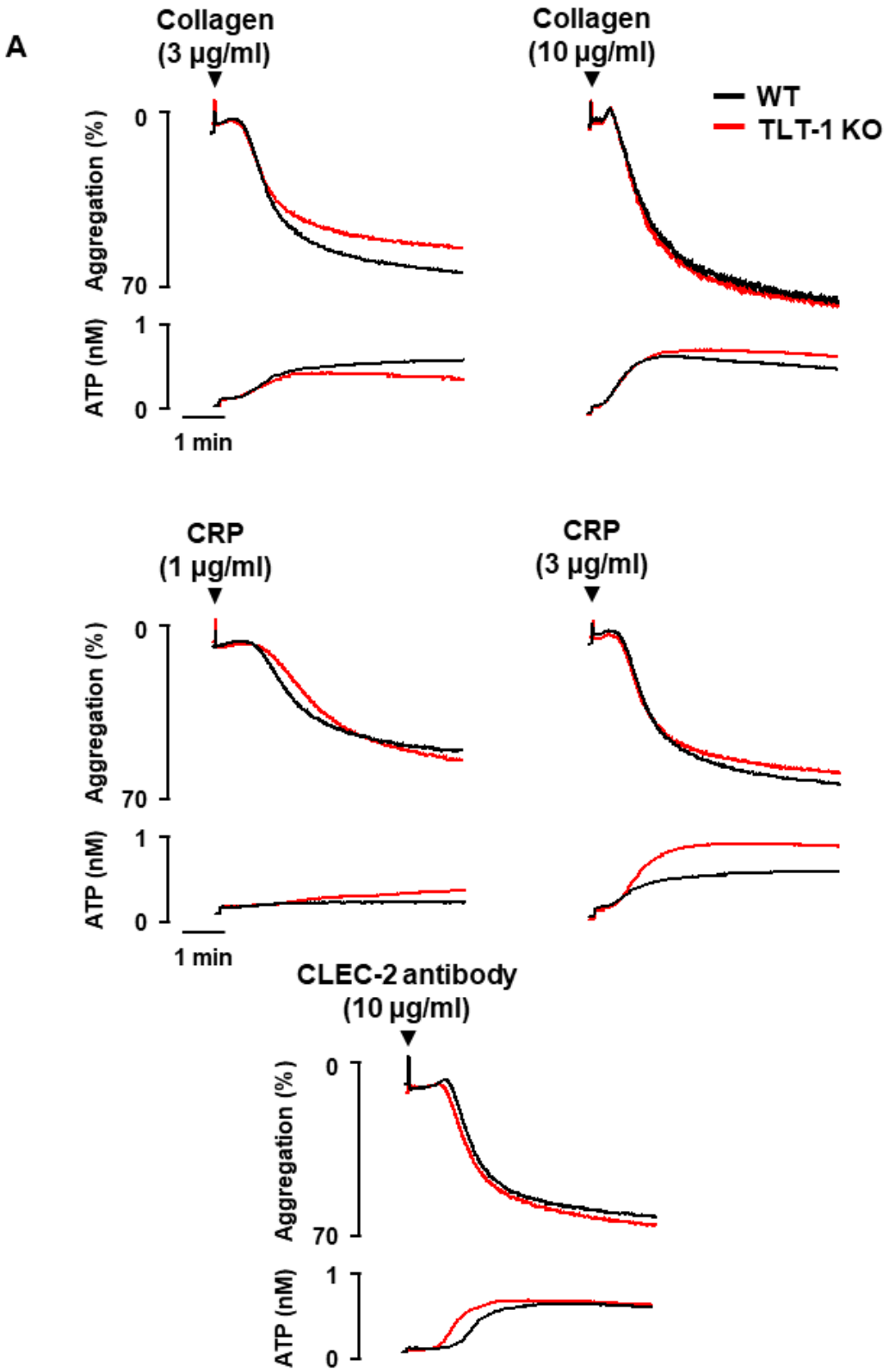
A
Collagen
(3 µg/ml)
Collagen
(10 µg/ml)
WT
TLT-1 KO
Aggregation (%)
0
70
ATP (nM)
1
0
1 min
CRP
(1 µg/ml)
CRP
(3 µg/ml)
CLEC-2 antibody
(10 µg/ml)

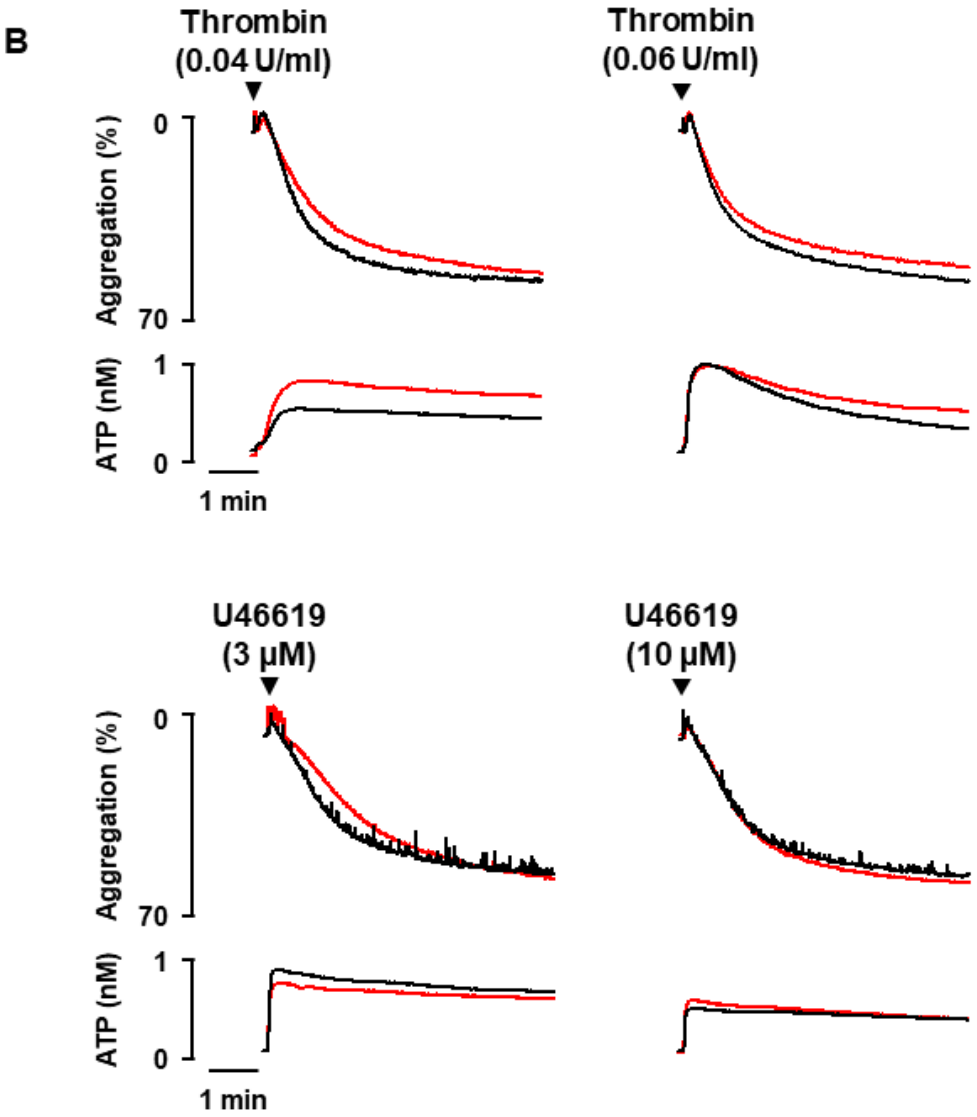
B
Thrombin
(0.04 U/ml)
Thrombin
(0.06 U/ml)
Aggregation (%)
0
70
ATP (nM)
1
0
1 min
U46619
(3 µM)
U46619
(10 µM)
Aggregation (%)
0
70
ATP (nM)
1
0
1 min

C

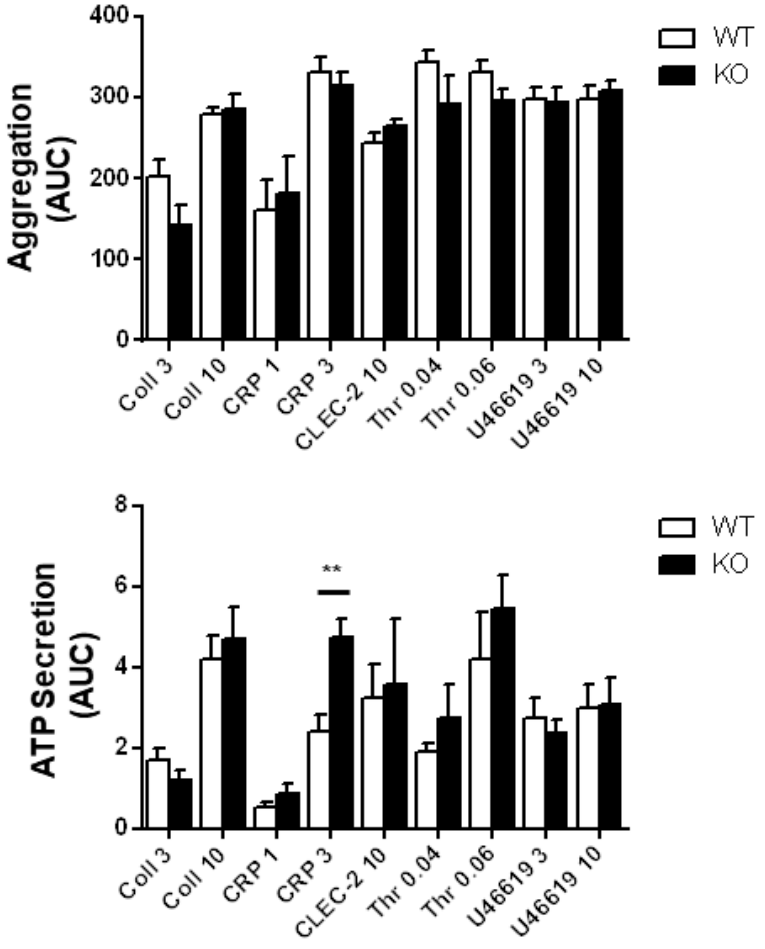

Figure 6. 5. Aggregation responses unaltered in TLT-1 deficient mouse platelets. Washed platelets (2×10^8/ml) from TLT-1 deficient and litter-matched WT mice were stimulated with collagen (3 and 10 µg/ml), collagen-related peptide (CRP; 1 and 3 µg/ml), CLEC-2 antibody (10 µg/ml), thrombin (0.04 and 0.06 U/ml) and thromboxane A_2 mimetic U46619 (3 and 10 µM) and platelet aggregation and secretion measured by lumi-aggregometry. Representative traces of (A) (hemi)ITAM and (B) GPCR agonist induced aggregation and secretion response. (C) Area under the curve (AUC) quantification of platelet aggregation and secretion. Mean ± SEM; n = 4-8 / condition; Student's t-test, $^{**}P<0.01$.

Table 6. 1. Platelet surface receptor expression in TLT-1 KO mice. Surface receptor expression of platelets from TLT-1 KO and WT control mice were measured by flow cytometry.

Surface receptor	WT	TLT-1 KO	*P* value
GPVI	1563 ± 263	1470 ± 228	ns
α2	731 ± 200	645 ± 160	ns
αIIBβ3	7070 ± 2460	7500 ± 2633	ns
GPIbα	5774 ± 214	3634 ± 962	ns
CLEC-2	8616 ± 304	7662 ± 427	ns
PECAM-1	654 ± 88	635 ± 98	ns
G6b-B	1451 ±362	1239 ±314	ns

Data represents mean values of the median fluorescence intensity ± SEM; n = 5-9. Student's t-test; ns, non-significant.

6.3.5. Reduced α-granule secretion in TLT-1 deficient platelets

TLT-1 is an α-granule protein requiring platelet activation and granule secretion before being expressed on the surface of platelets. α-granule secretion (P-selectin surface expression) was assessed in TLT-1 deficient platelets in response to various platelet agonists. Interestingly, α-granule secretion was reduced in response to stimulation by both (hemi)ITAM and GPCR agonists **(Figure 6.6)**. Decreased secretion response to all agonists advocates a role for TLT-1 in regulating α-granules secretion.

Fibrinogen has been proposed as a ligand for TLT-1. Binding of fluorescently labelled fibrinogen by TLT-1 deficient platelets was therefore assessed following stimulation with (hemi)ITAM and GPCR agonists. However, fibrinogen binding was normal in TLT-1 deficient mice following stimulation with all agonists tested **(Figure 6.6)**, suggesting TLT-1 does not significantly contribute to fibrinogen binding of platelets.

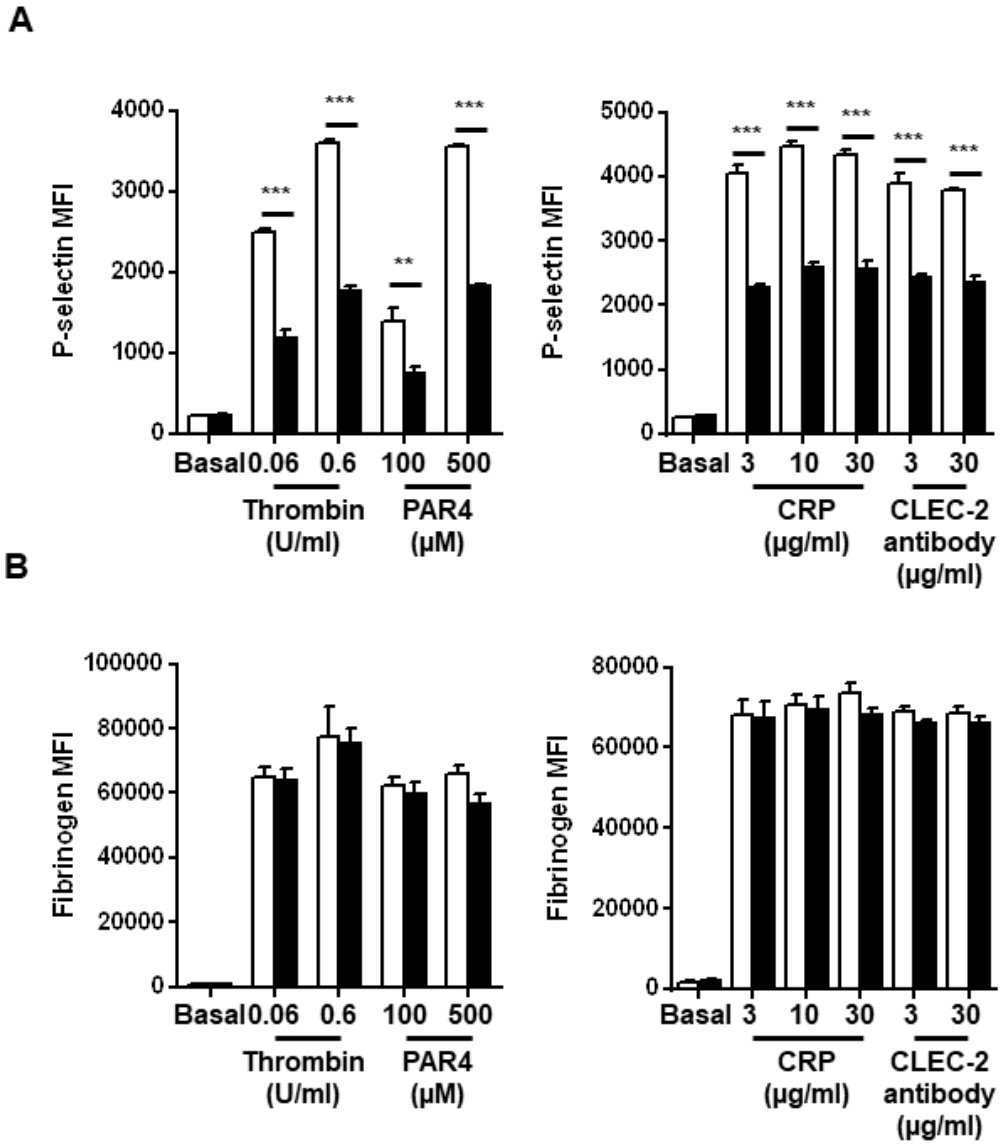

Figure 6. 6. Decreased α-granule secretion TLT-1 deficient platelets. (A) Platelet P-selectin surface expression and (B) AF488-fibrinogen binding were measured in whole blood stimulated with thrombin (0.06 and 0.6 U/ml), PAR4 peptide (100 and 500 μM), collagen related peptide (CRP; 3, 10 and 30 μg/ml) and CLEC-2 antibody (3 and 30 μg/ml). Median fluorescence intensity (MFI) ± SEM is represented; n = 6 mice/genotype; Two-way ANOVA with multiple comparisons, $^{**}P < 0.01$, $^{***}P<0.001$.

6.3.6. Spreading unaltered in TLT-1 deficient platelets

The cytoplasmic tail of TLT-1 has been shown to interact with the ERM family of actin cytoskeleton binding proteins (Morales et al., 2010, Washington et al., 2009); consequently TLT-1 deficient platelets were assessed for defects in platelet spreading. Washed platelets from WT and TLT-1 deficient mice were allowed to spread on coverslips coated with fibrinogen or collagen under basal conditions and on fibrinogen following pre-activation with thrombin. Following spreading, coverslips were washed, fixed and stained with phalloidin (actin cytoskeleton). Blinded fluorescence images were then quantified by a semi-automated machine learning method to quantify platelet surface area and assessment of four different classes of spreading (unspread, filopodia, lamellipodia and fully spread), this analysis method has previously been characterised and its accuracy validated against manual analysis of spreading by members of the Birmingham Platelet Group. No differences in platelet adhesion, surface area, perimeter or morphology were identified compared to WT platelets on collagen or fibrinogen under basal conditions **(Figure 6.7)**. Pre-activation with thrombin resulted in a minor decrease in perimeter of TLT-1 deficient platelets spread on fibrinogen, but surface area was not altered. Platelet adhesion and morphology were also normal **(Figure 6.7)**.

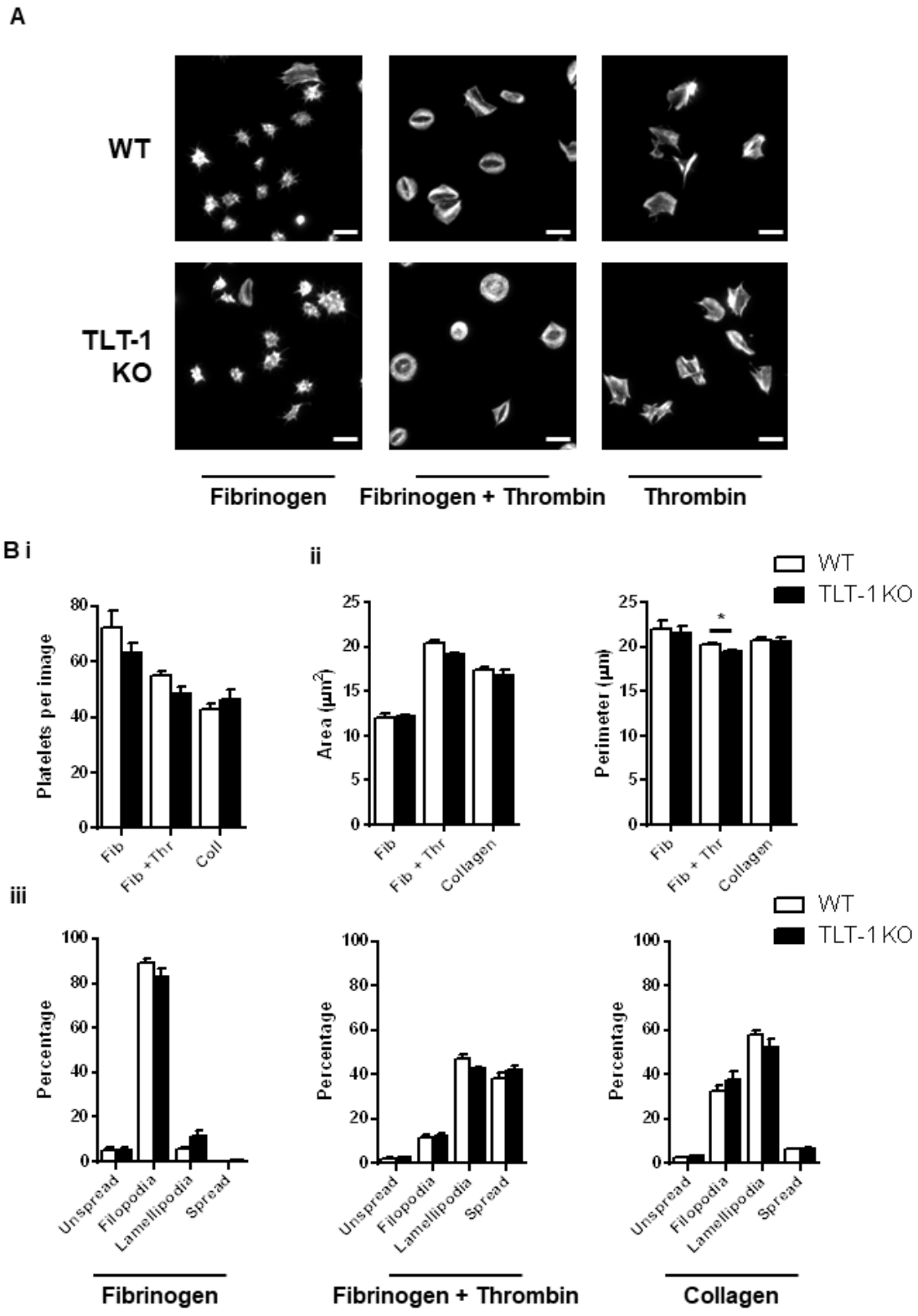
A
WT
TLT-1 KO
Fibrinogen
Fibrinogen + Thrombin
Thrombin
B i
Platelets per image
Fib
Fib +Thr
Coll
ii
Area (µm²)
Fib
Fib + Thr
Collagen
Perimeter (µm)
*
WT
TLT-1 KO
iii
Percentage
Unspread
Filopodia
Lamellipodia
Spread
Fibrinogen
Fibrinogen + Thrombin
Collagen

Figure 6. 7. Spreading unaltered in TLT-1 deficient platelets. Washed platelets from TLT-1 deficient and litter-matched WT mice were plated on fibrinogen (100 µg/ml) and collagen (10 µg/ml) coated coverslips under basal conditions, and on fibrinogen following pre-activation with 0.1 U/ml thrombin, for 45 minutes at 37^{o}C. (A) Representative phalloidin (actin cytoskeleton) stained fluorescence images. (B) Quantification of number of adhered platelets (i), platelet surface area and platelet perimeter (ii), and platelet morphology (iii). Mean ± SEM; n = 196-393 platelets from 3 mice/genotype; Student's t-test,*P<0.05.

6.3.7. Aggregate formation on von Willebrand factor under shear unaltered in TLT-1 deficient platelets

Studies by the McKinnon group have shown recombinant sTLT-1 binds vWF with high affinity, and propose it as a physiological ligand for TLT-1 (Doerr A., 2017). They have also shown that antibody mediated blocking of TLT-1 ligand interactions reduces aggregate formation on collagen type-1 under shear (Doerr A., 2017). In order to assess this, TLT-1 deficient mouse blood was flowed over collagen type-1 and vWF coated surfaces for 4 minutes at $1500s^{-1}$ and surface area coverage of platelets assessed. Experiments were performed blinded in collaboration with Tom McKinnon and Angela Doerr (Imperial College London, London, UK). TLT-1 deficient platelets demonstrate a tendency for reduced aggregate formation on collagen **(Figure 6.8 A)**; although this did not reach significance, it is suggestive of a role for TLT-1 in platelet aggregate formation on collagen. On vWF however TLT-1 deficient platelets aggregate normally compared to WT under flow **(Figure 6.8 B).**

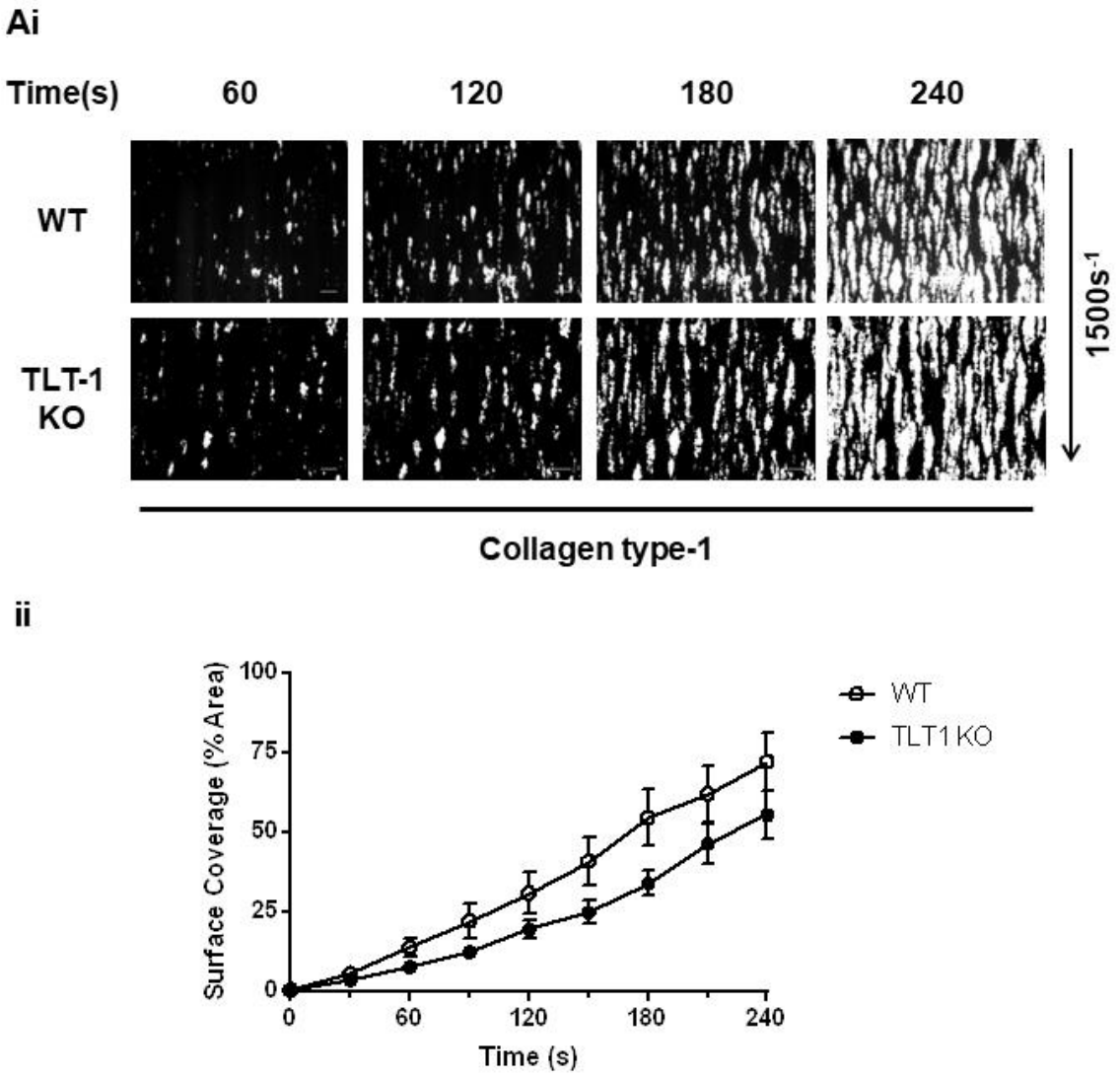

Figure 6. 8. Platelet adhesion under flow unaltered in TLT-1 deficient mouse platelets. Whole blood was flowed over (A) collagen and (B) von Willebrand factor (vWF) coated coverslips at shear rate 1500 s^{-1} for 4 minutes. (i) Representative bright field images. (ii) Quantification of surface area coverage (SAC) of adhered platelets. Mean ± SEM; n = 6-7 mice/genotype; Two-way ANOVA with multiple comparisons, **P*<0.05. Experiments performed in collaboration with Tom McKinnon and Angela Doerr (Imperial College London, UK).

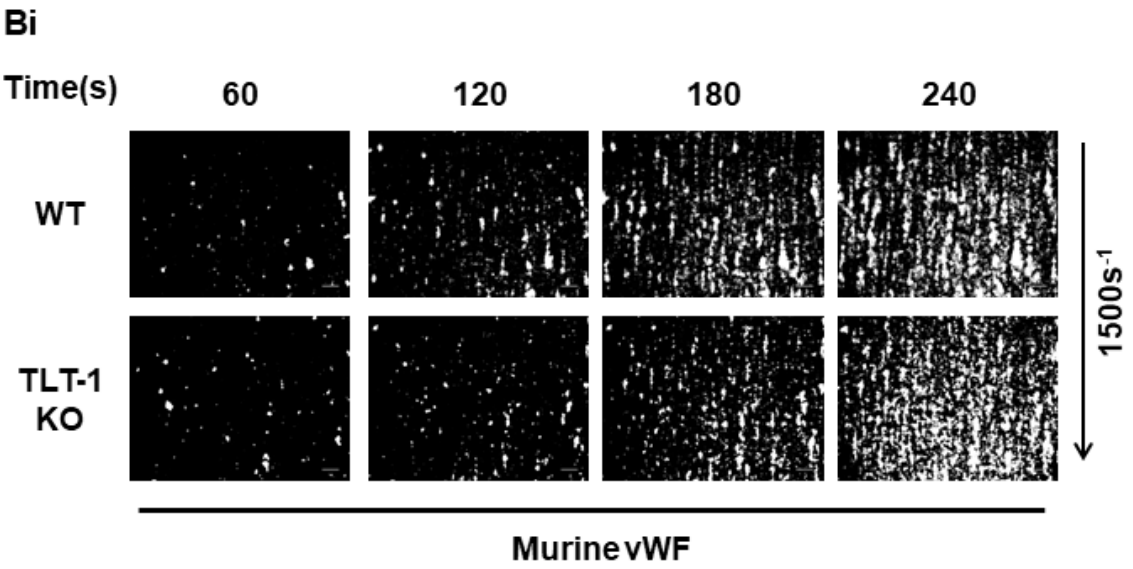
Bi
Time(s)
60
120
180
240
WT
TLT-1 KO
1500s-1
Murine vWF

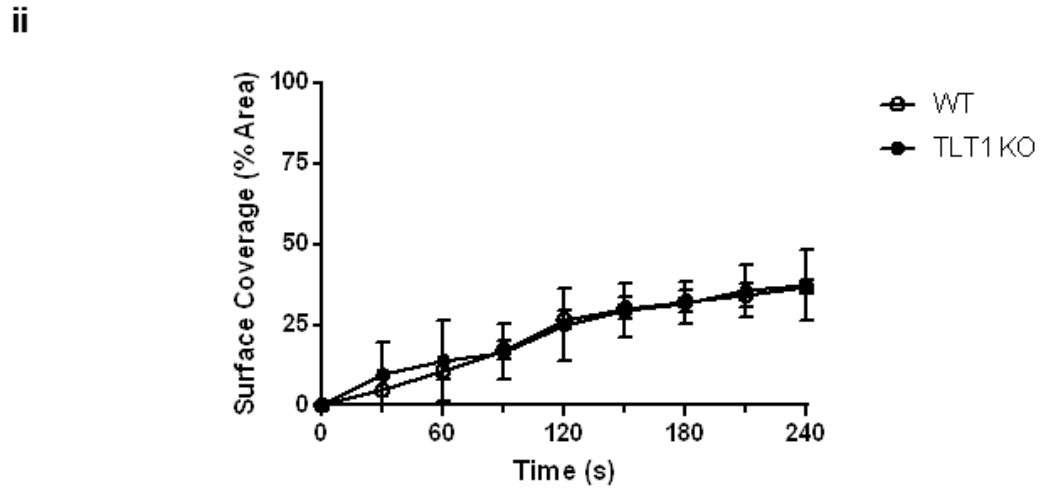
ii
Surface Coverage (% Area)
100
75
50
25
0
0
60
120
180
240
Time (s)
WT
TLT1 KO

6.3.8. Haemostatic response unaltered in TLT-1 deficient mice

To determine if TLT-1 has a role in haemostasis, time for bleeding to stop following tail tip excision and immersion in saline was assessed. Haemostatic response of TLT-1 deficient mice was normal **(Figure 6.9)** suggesting TLT-1 plays no role in haemostasis. This is in contrast to the extended bleeding times previously reported in TLT-1 deficient mice (Washington et al., 2009).

6.3.9. Decreased stability of laser-injury induced thrombi *in vivo*

The effect of TLT-1 absence on thrombus formation *in vivo* was assessed using the ferric chloride-induced injury and laser-induced injury models. Thrombus formation in TLT-1 deficient mice was normal following application of ferric chloride-soaked filter paper to the carotid artery **(Figure 6.10)**. However, thrombi formed following laser-injury displayed altered kinetics **(Figure 6.11)**. Although peak thrombus size was normal, thrombi formed faster than WT and had reduced stability **(Figure 6.11 C)**.

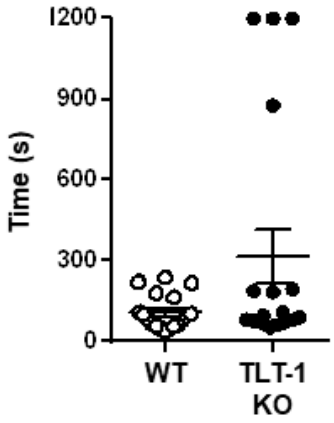

Figure 6. 9. Haemostatic response unaltered in TLT-1 deficient mice. TLT-1 KO and litter matched WT mice were anaesthetised and 3 mm of tail tip excised and immersed in warmed saline. Time for bleeding to stop was then recorded for up to a maximum 20 minutes. Bleeding was considered stopped when no blood was observed from tail tip for 1 minute. Total bleeding time was then calculated. Mean ± SEM; n = 18-19; Mann-Whitney U test, non-significant.

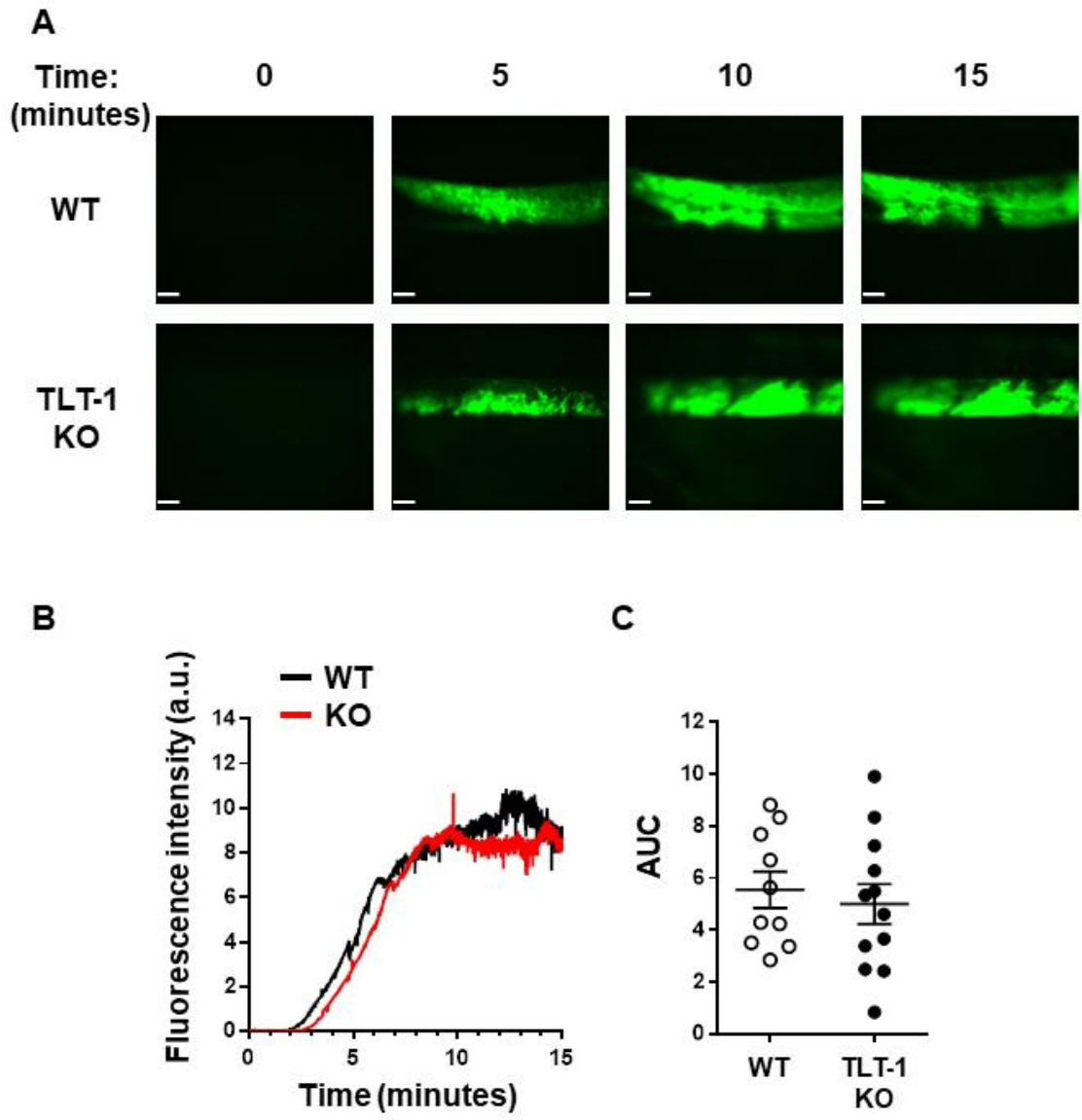

Figure 6. 10. Ferric chloride induced thrombosis unaltered in TLT-1 deficient mice. Mice were injected with DyLight488-conjugated anti-GPIbβ antibody (0.1 µg/g body weight). Exposed carotid arteries were injured with 10% ferric chloride for 3 minutes and the accumulation of platelets (green) into the thrombi was assessed. (A) Representative fluorescence images from GPIbβ-labeled platelets after ferric chloride-injury of carotid are shown. Scale bar: 200 µm. (B) Each curve represents the median integrated fluorescence intensity in arbitrary units (a.u.) for 10-12 mice/genotype. (C) Area under the curve of the integrated fluorescence density is represented (mean ± SEM); Mann-Whitney test, non-significant. See also videos 6.I and 6.II.

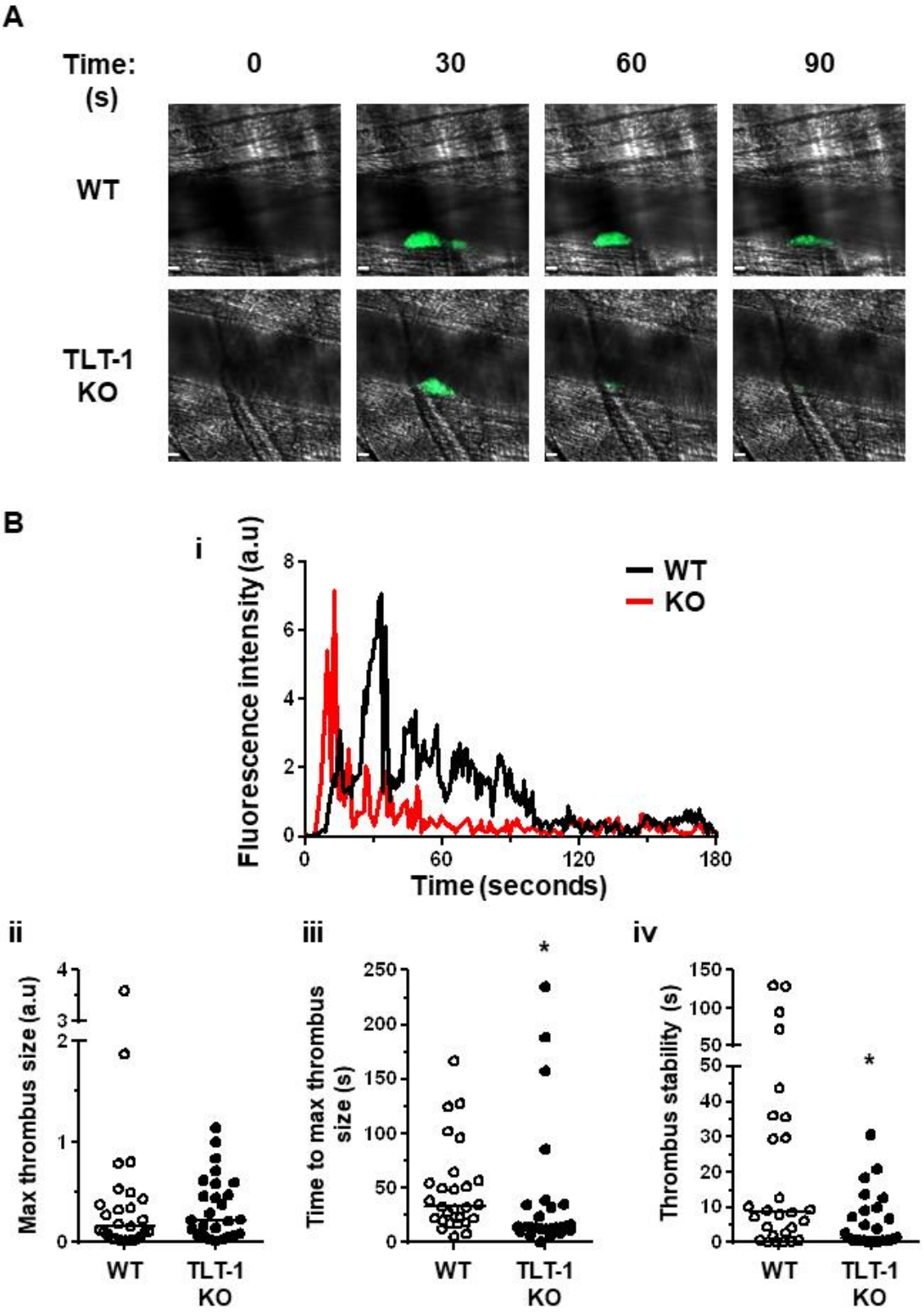
A
Time: (s)
0
30
60
90
WT
TLT-1 KO
B
i
Fluorescence intensity (a.u)
Time (seconds)
WT
KO
ii
Max thrombus size (a.u)
iii
Time to max thrombus size (s)
iv
Thrombus stability (s)
WT
TLT-1 KO

Figure 6. 11. Decreased thrombus stability TLT-1 deficient mice. Mice were injected with DyLight488-conjugated anti-GPIbβ antibody (0.1 μg/g body weight). Arterioles of cremaster muscles were subsequently injured by laser. (A) Representative composite brightfield and fluorescence images of platelets (GPIbβ). Scale bar: 10 μm. (B) Each curve represents the median integrated fluorescence intensity in arbitrary units (a.u.). (C) Distribution of (i) max thrombus size (a.u.), (ii) time to max thrombus size in seconds and (iii) thrombus stability. Thrombus stability was assessed as time (s) for thrombi after maximal fluorescence intensity to reduce by 50%. Mean ± SEM, 25-26 injuries in 4-5 mice mice/genotype; Mann-Whitney test, **P* = 0.05. See also videos 6.III and S6.IV.

6.4. Discussion

Findings presented in this chapter demonstrate ablation of the megakaryocyte and platelet specific ITIM-containing receptor TLT-1 has only a minor effect on platelet function in thrombosis and haemostasis. Deficient mice were mildly thrombocytopenic, likely due to increased platelet clearance as megakaryocyte development was normal. Interestingly, responses to putative ligands of TLT-1 were unaltered in deficient platelets. Haemostatic response *in vivo* was likewise normal; however stability of laser, but not ferric chloride-induced thrombi was reduced in deficient mice. Findings suggest the role of this highly abundant and specific protein is more likely mediating interactions with immune cells during thrombo-inflammation rather than in primary haemostasis.

As previously reported, TLT-1 deficient mice in this study exhibited a mild reduction in platelet count (Washington et al., 2009). Decreased platelet count can be a product of reduced platelet production or increased clearance of platelets. Normal megakaryocyte development and distribution within spleens and bones and no myelofibrosis in TLT-1 deficient mice, suggests platelet production is unaffected. Spleen weight was however increased in deficient mice, suggesting increased platelet clearance is the likely cause of the mild thrombocytopenia. Further studies to examine platelet half-life and recovery of platelet count following depletion, as well as megakaryocyte proplatelet formation are required in order to elucidate the exact underlying mechanisms of the mild thrombocytopenia.

Despite previous reports from the Washington Group of reduced aggregation responses in platelet rich plasma of TLT-1 deficient mice, aggregation responses in washed platelets were normal to all agonists tested (Washington et al., 2009). The absence of reduced aggregation responses in washed platelets suggests a component of the blood plasma is able to interact with TLT-1 and enhance aggregation. sTLT-1 which has been detected in blood plasma, has been

shown to enhance aggregation responses in washed human platelets (Washington et al., 2009). Although sTLT-1 does not interact directly with the platelet surface, it is instead proposed to bind fibrinogen and in partnership with surface TLT-1 mediates higher order platelet aggregation (Washington et al., 2009).

Surprisingly, in platelet rich plasma the strongest reduction in aggregation response of TLT-1 deficient mice was to ADP stimulation (Washington et al., 2009). The method of washed platelet isolation used in this chapter, however, renders platelets insensitive to ADP. The requirement of TLT-1 to be upregulated to the surface before mediating any effect negates the possibility of any effect on primary aggregation response, but would fit with enhancement of secondary feedback pathways such as ADP.

Interestingly, experiments performed in washed human platelets showed reduced aggregation responses when TLT-1-ligand interactions were blocked by anti-TLT-1 sv antibodies (Giomarelli et al., 2007). The inhibition mediated occurred after shape change, and was attributed to blocking of TLT-1-ligand interactions during aggregation (Giomarelli et al., 2007).

The most interesting result in this chapter is the reduction in α-granule secretion observed in TLT-1 deficient platelets following activation with both (hemi)ITAM and GPCR receptor agonists. This suggests TLT-1 is not just simply an α-granule cargo protein but rather has some regulatory role. This is not the first result leading to this speculation, a role for TLT-1 in granule formation has previously been put forward following observed differences in distribution patterns of TLT-1 and P-selectin on spread platelets (Washington et al., 2004). Both TLT-1 and P-selectin are synthesised in megakaryocyte ER and subsequently exported and sorted in the trans-Golgi network (Blair and Flaumenhaft, 2009). However, the receptors differ greatly in their cytoplasmic domains. TLT-1 has a much larger cytoplasmic tail (118 residues to P-selectins' 35) and contains multiple domains for protein interactions. TLT-1 may therefore

function in production, movement or regulation of α-granules rather than simply cargo (Washington et al., 2004). Alternatively, TLT-1 could play a role in secretion of α-granules rather than their packaging. TLT-1 mediated regulation of granule release could help explain the differences in speed of TLT-1 and P-selectin surface upregulation observed in chapter 5 and Smith et al (2018). Either way further investigation is required before any conclusions can be drawn on this interesting observation.

No alteration in platelet spreading was observed in TLT-1 deficient platelets on fibrinogen with or without pre-activation or on collagen coated surfaces. This result is surprising given fibrinogen has been identified as a physiological ligand for TLT-1, and the cytoplasmic tail of TLT-1 shown to interact with the ERM family of actin binding proteins. In agreement with spreading results, binding of fluorescently labelled fibrinogen was also normal in deficient mice. Previous studies with TLT-1 deficient platelets demonstrated a reduction in fibrinogen binding following activation with sub optimal doses of ADP, although it did not reach significance (Washington et al., 2009). The absence of alteration in fibrinogen spreading and binding of TLT-1 deficient platelets is likely explained by the presence of other surface receptors that bind fibrinogen, such as integrin αIIbβ3, masking any phenotype.

Recent work by the McKinnon group has shown recombinant sTLT-1 binds vWF with high affinity, and blocking the TLT-1-vWF interaction reduces platelet aggregate formation under shear on collagen type-1 (Doerr A., 2017). In collaboration, flow adhesion experiments on both collagen type-1 and murine vWF were performed with TLT-1 deficient mouse blood. TLT-1 deficient mouse blood had a tendency for reduced platelet adhesion to collagen type-1 but did not reach significance, nevertheless is suggestive of a minor role for TLT-1 in aggregate formation on collagen under shear. Platelet adhesion to vWF was normal under flow in TLT-1 deficient mouse blood. This is probably due to the fact TLT-1 is stored in α-granules and

requires upregulation to the platelet surface. vWF is only a weak platelet agonist (Tomaiuolo et al., 2017), and likely normal platelet adhesion is observed as vWF fails to stimulate α-granule release and exposure of TLT-1 on the platelet surface. Further experiments with pre-activation of platelets before flow over vWF may yield different results.

Although previously shown to have a decreased haemostatic response following excision of tail tip (Washington et al., 2009), normal tail bleeding times were observed in this study. Differences in observed findings may be due to the inherent variability of this crude assay, as the increase in bleeding time previously observed was only minor (Washington et al., 2009). Alternatively slight differences in experimental procedure may account for the lack of agreement between studies.

Altered thrombus kinetics were observed in TLT-1 deficient mice following laser, but not ferric chloride-injury, with differences likely reflecting the models different mechanisms. The reduced stability of laser-induced thrombi is potentially explained by the marked reduction in α-granule secretion observed in TLT-1 deficient platelets. α-granules contain many proteins that contribute to thrombus stability, including fibrinogen, thrombospondin-1 and integrin αIIbβ3, which mediates firm adhesion and ½ - ⅔ of integrin αIIbβ3 resides in α-granules (Blair and Flaumenhaft, 2009, Kuijpers et al., 2014). In addition, leukocytes contribute to fibrin deposition within thrombi (Palabrica et al., 1992). Reduced surface exposure of P-selectin which mediates platelet-leukocyte interactions will thus reduce fibrin deposition within the thrombus. P-selectin has also been shown to stabilize integrin αIIbβ3-fibrinogen interactions and aggregate formation *in vitro* (Merten and Thiagarajan, 2000, Prakash et al., 2017). Furthermore, TLT-1 has been shown to mediate interactions with leukocytes including neutrophils (Derive et al., 2012). Absence of TLT-1 interactions with these cells types within thrombi may similarly contribute to reduced stability. Recently, platelet secretion has been

shown to differentially contribute to thrombosis and haemostasis, with normal thrombosis having a greater requirement for platelet secretion (Joshi et al., 2018), which might explain why no effect on haemostasis was observed.

Alternatively, TLT-1 has been put forward to bind fibrinogen and mediate higher order platelet interactions (Morales et al., 2010, Washington et al., 2009). Absence of these interactions could possibly explain the decreased stability in TLT-1 deficient thrombi. However, no reduction in spreading or binding of fibrinogen was observed in TLT-1 deficient platelets in this study.

In conclusion, despite its specificity to platelets and megakaryocytes and abundant expression suggesting an important role in thrombosis and haemostasis, findings demonstrate TLT-1 plays only a minor role in classical platelet function. Previous work from other groups has shown a role for TLT-1 in thrombo-inflammation, suggesting the function of TLT-1, similar to another α-granule protein P-selectin, is mediating interaction with immune cells such as leukocytes at sites of vascular inflammation. Further work is needed to elucidate the exact role of this highly abundant platelet protein.

Chapter 7

General Discussion

7.1. Summary of results

The work presented in this thesis further establishes ITIM-containing receptors in the regulation of platelet production and function. Absence of LAIR-1 from megakaryocytes was found to alter platelet reactivity to GPVI activation *in vitro* and *in vivo*. Absence of PECAM-1 alongside LAIR-1 did not result in further enhancement of GPVI-mediated platelet activation, suggesting redundancy between these receptors. Absence of TLT-1 was found to alter platelet count with reduced numbers circulating in deficient mice. TLT-1 absence also altered α-granule secretion, and reduced thrombus stability *in vivo*, however had no effect on *in vivo* haemostasis. Finally, TLT-1 was shown to be a highly sensitive marker of platelet activation, shedding new light on the level of platelet activation in growing thrombi *in vivo*.

7.2. ITIM-containing receptor regulation of megakaryocyte development and platelet production

Investigations carried out in this thesis provide further evidence that ITIM-containing receptors have a critical role in megakaryocytes, regulating platelet production. This is clearly demonstrated by the altered platelet counts of the LAIR-1, LAIR-1/PECAM-1 and TLT-1 deficient mice used in this thesis, in addition to those previously published for G6b and PIR-B (Smith et al., 2017, Washington et al., 2009, Mazharian et al., 2012, Fan et al., 2014). Interestingly absence of ITIM-containing receptor signalling can result in increased (LAIR-1 and PIR-B) or decreased (TLT-1 and G6b) platelet count, indicating these receptors regulate multiple signalling pathways involved in thrombopoiesis.

LAIR-1 KO mice demonstrate a 25% increase in platelet count, due to an increase in both production and platelet half-life (Smith et al., 2017). Underlying the increase in proplatelet formation was elevated SFK activity (Smith et al., 2017). Inhibition of SFK activity has

previously been shown to cause mild reduction of platelet count *in vivo*, and abolish megakaryocyte proplatelet formation *in vitro* (Mazharian et al., 2011, Mazharian et al., 2010), highlighting the importance of SFKs in this process. In addition to inhibiting proplatelet formation, SFK inhibition also altered megakaryocyte development, increasing megakaryocyte ploidy (Mazharian et al., 2011). Csk and receptor phosphatase CD148 are major regulators of SFK activity in platelets (Mori et al., 2018). Interestingly deletion of Csk, a major SFK inhibitor, in the megakaryocyte lineage was reported to result in reduced platelet count (65%). Although proplatelet formation was not directly assessed in this study, extramedullary haematopoiesis was observed and circulating platelets in these mice were 35% larger and a greater proportion were immature, suggesting defective thrombopoiesis (Mori et al., 2018).

Platelet counts in mice lacking the intracellular tail and thus signalling of PIR-B are also thrombocythemic with counts increased by nearly 50% (Fan et al., 2014). In these mutant mice, increased numbers of megakaryocytes are observed in the bone marrow and credited for the increase in platelet count (Fan et al., 2014). This is not surprising given PIR-B is known to support self-renewal of HSCs and inhibit differentiation of acute myeloid leukaemia cells (Zheng et al., 2012).

The mechanism underlying the decreased platelet counts in TLT-1 deficient mice were not determined. Reduction in platelet count could be due to a decrease in platelet production or increase in platelet clearance. But it is interesting to think how a protein present in α-granules would be able to influence platelet production. Activation of megakaryocytes and surface exposure of TLT-1 during proplatelet formation is unlikely, as the inactivated circulating platelets released would be expected to have high levels of TLT-1 on their surface which is not the case (Smith et al., 2018, Washington et al., 2004). Alternatively releasate from activated platelets has been shown to increase megakaryocyte proplatelet production (Machlus et al.,

2016). It is therefore possible that sTLT-1 which is known to be released upon platelet activation may have a role facilitating platelet production. Further studies are required to define if absence of TLT-1 does indeed effect megakaryocyte platelet production.

The strongest megakaryocyte phenotype and effect on platelet count is by deletion of ITIM-containing receptor G6b, with KO mouse platelet count decreased by 80% (Mazharian et al., 2012). Megakaryocytes in these mice develop normally but fail to produce proplatelets to the same extent as WT. Increased clearance of the presumably pre-activated platelets was also thought to contribute, however more recent investigation in a loss of function model, which recapitulates the platelet count of the KO, was found to have normal rates of platelet clearance suggesting this may not be the case (Mazharian et al., 2012, Geer et al., 2018). In these mice circulating Tpo levels result in increased megakaryopoiesis causing myelofibrosis and destruction of the bone marrow (Geer et al., 2018, Mazharian et al., 2012). G6b-B is constitutively associated with the phosphatases Shp1 and Shp2, both of which have significant roles in megakaryocyte development (Mazharian et al., 2013). Megakaryocytes deficient in Shp1 or Shp2 have defective development, with partial block at 2/4N ploidy. Platelet counts are however normal in Shp1 deficient mice and only mild thrombocytopenia observed in Shp2 deficient, due to Shp2, but not Shp1, deficient megakaryocytes exhibiting reduced proplatelet formation (Mazharian et al., 2013). Deletion of both these phosphatases is required to phenocopy the absence of G6b-B. These studies established Shp1 and Shp2 as major regulators of megakaryocyte development and platelet production, and G6b-B as a major regulator of Shp1/2 (Mazharian et al., 2013, Mazharian et al., 2012).

Recently, four distinct G6b mutations in five consanguineous families, which result in loss or severe reduction in expression have been identified (Hofmann et al., 2018, Melhem et al., 2017). These patients are all macrothrombocytopenic with focal myelofibrosis, similar to mouse

models of G6b, confirming the pathophysiological function of G6b and role of ITIM-containing receptors in human platelet production.

The other ITIM-containing receptors identified in megakaryocytes do not appear to effect platelet production, as normal platelet counts are observed. However, reduced recovery of platelet count following immune induced depletion was observed in PECAM-1 deficient mice (Dhanjal et al., 2007a). This is due to defective polarization of the SDF1α receptor CXCR4 preventing migration and results in abnormal megakaryocyte distribution (Dhanjal et al., 2007a, Wu et al., 2007).

ITIM-containing receptors may therefore have potentially significant implications for the megakaryocyte biology field. Although great advances in the mechanism of megakaryocyte maturation, proplatelet elongation and platelet release have been made (Machlus and Italiano, 2013), the mechanism initiating proplatelet formation remains elusive. ITIM-containing receptors are known to interact with the Shp phosphatases and SFKs, so are likely contributing to regulation of proplatelet formation.

7.3. ITIM-containing receptor regulation of platelet function

Platelet reactivity must be tightly regulated, maintaining a balance between positive and negative signals as too much results in either thrombosis or bleeding (Gibbins, 2002). The classical role of ITIM-containing receptors in platelets is inhibition of ITAM signalling downstream of GPVI-FcRγ chain. Mice deficient in LAIR-1 exhibit the enhanced platelet reactivity to collagen and CRP stimulation associated with this classical inhibitory function. Platelets from LAIR-1 deficient mice also show a role for LAIR-1 inhibiting αIIβ3 function, another receptor whose function is increasingly shown to be under ITIM-containing receptor regulation (Coxon et al., 2017). The detection of any platelet function defects from LAIR-1

deficient mice is surprising, given LAIR-1 is not normally expressed in platelets; but further demonstrates alterations in megakaryocyte phenotype can affect the platelet progeny they produce. It has previously been reported that transfer of altered megakaryocyte mRNA to platelets can affect their function (Rondina and Weyrich, 2015). Similar to this in LAIR-1 deficient mice transmission of active SFKs and altered compartmentalization of binding partners from megakaryocytes underlies the observed platelet phenotype, and adds to the growing number of ways megakaryocytes influence platelet reactivity.

Characterisation of the LAIR-1/PECAM-1 DKO mice, the first mouse model where two ITIM-containing receptors have been simultaneously ablated, demonstrated no further enhancement of platelet hyper responsiveness, suggesting redundancy between these receptors. Given the strength of platelet activation elicited by GPVI-FcRγ chain stimulation, it would be expected to be highly regulated. Redundancy between ITIM-containing receptor mediated inhibition of this pathway is likely a mechanism to prevent GPVI activation going unchecked and the serious consequence of excessive thrombosis if this occurs. The inhibition mediated by LAIR-1 and PECAM-1 is however only mild, with more profound inhibition of GPVI mediated by G6b-B. In the absence of G6b-B signalling, surface levels of GPVI are significantly reduced by cleavage in order to prevent constant activation of the receptor (Geer et al., 2018, Mazharian et al., 2012).

Interest in the role of LAIR-1 in megakaryocytes and platelets was based around the importance of collagens in proplatelet formation and platelet activation. Assessment of LAIR-1 deficiency revealed only a minor role of the receptor in megakaryocyte and platelet function. The expression profile of LAIR-1 is broad; indeed LAIR-1 was first discovered in immune cells (leukocytes and NK cells) where it potently inhibits cell lysis (Meyaard et al., 1997, Poggi et al., 2008). The LAIR-1 deficient transgenic mouse model utilised in chapter 3 was a global

knockout, lacking the receptor from all cells. It is possible that observed differences *in vivo* may in part be due to absence of LAIR-1 from immune cells which are known to contribute to thrombosis. More recently, LAIR-1 has been shown to negatively control osteoclastogenesis, inhibiting osteoclast formation in the presence of collagen degradation fragments (Boraschi-Diaz et al., 2018). Like LAIR-1, PECAM-1 is also widely expressed. PECAM-1 has been shown to maintain endothelial cell junction integrity and a role in circulating leukocytes, as well as its minor inhibitory role in platelets (Lertkiatmongkol et al., 2016). The broad specificity of these receptors clearly indicates they possess a general inhibitory function. In megakaryocytes and platelets, inhibitory signalling from LAIR-1 and PECAM-1 does contribute to regulation of platelet production and function, but is not critical in the same way as inhibitory signalling from the megakaryocyte lineage specific ITIM-containing receptor G6b.

More powerful and global inhibition of platelet activation is mediated by PGI2 and NO to limit platelet activation (Nagy and Smolenski, 2018). Inhibition mediated by ITIM-containing receptors should be thought of more as fine tuning of platelet reactivity, setting a threshold for platelet response to specific agonists.

The specificity and abundance of TLT-1 in megakaryocytes and platelets suggested an important role in haemostasis and thrombosis. Interestingly, no defects in aggregation and spreading *in vitro*, or haemostasis *in vivo* were observed. Decreased thrombus stability was observed following laser-injury, and attributed to the decreased α-granule secretion observed in TLT-1deficient platelets. However, ferric chloride-induced thrombosis was normal, likely reflecting the differing mechanisms of the models. In addition to being an ITIM-containing receptor, TLT-1 is also a member of the TREM family of proteins that have important roles in

both adaptive and innate immunity (Giomarelli et al., 2007). The function of TLT-1 has therefore also been investigated in respect to thrombo-inflammation.

Sepsis is a systemic inflammatory response to severe infection. Sepsis is caused by the mechanisms meant to fight infection and can be accompanied by thrombocytopenia and often associated with disseminated intravascular coagulation (DIC), where platelets become systemically active resulting in increased fibrin deposition. Inflammation and coagulation are intrinsically linked in this setting as consumption of coagulation factors leads to simultaneous clotting and haemorrhage (Ferrer-Acosta et al., 2014). Mice deficient in TLT-1 were found to succumb in an LPS induced sepsis model faster and in greater numbers than WT mice. In another model which recapitulates the mechanisms of DIC in localized form, TLT-1 deficient mice were predisposed to haemorrhage at inflammatory lesions (Washington et al., 2009, Ferrer-Acosta et al., 2014). A protective role for TLT-1 was also shown in LPS induced acute lung injury. Increased alveolar bleeding and pulmonary tissue damage and decreased fibrinogen deposition were observed in TLT-1 deficient mice (Morales-Ortiz et al., 2018a). Fibrinogen deposition could be restored, and haemorrhage and tissue damage reduced by infusion of sTLT-1 (Morales-Ortiz et al., 2018a). These findings suggest a protective role for TLT-1 during thrombo-inflammation.

Further studies have also shown mice deficient in TLT-1 have increased susceptibility to bacterial infection (Derive et al., 2012). Outcomes were improved in TLT-1 deficient mice through administration of 17 amino acid peptide (LR17) derived from the extracellular domain of TLT-1 (Derive et al., 2012). The anti-inflammatory activity of this sequence, and TLT-1, is mediated through dampening of TREM-1 signalling. This is achieved through binding of TREM-1 ligand, thereby inhibiting TREM-1 activation (Derive et al., 2012). Similar improvements in outcomes have also been observed in a faecal peritonitis model in mini pigs

and LPS challenged non-human primates following TLT-1 derived peptide LR12 (LR17 minus 5 amino acids) administration (Derive et al., 2013, Derive et al., 2014). Preclinical trials administering LR12 during acute myocardial infarction have shown it was able to control leukocyte recruitment, limit inflammation, excessive cardiac remodelling and infarct size (Boufenzer et al., 2015). The ability of TLT-1 to inhibit inflammatory TREM-1 signalling in these studies therefore implicates TLT-1 in regulation of leukocyte recruitment and activation (Derive et al., 2012).

Primarily expressed on neutrophils and monocytes, and recently shown to be expressed in platelet α-granules, TREM-1 acts synergistically with pathogen-associated molecular patterns (PAMPs) amplifying inflammatory signals (Ford and McVicar, 2009, Jolly et al., 2017). The natural ligand of TREM-1 remains unknown (Thomas and Storey, 2015, Ford and McVicar, 2009). During systemic inflammation endothelial dysfunction leads to platelet activation. P-selectin exposure and interaction with PSGL-1 then initiate platelet-neutrophil binding, with the interaction stabilized by Mac-1-GPIb-α (Derive et al., 2012, Thomas and Storey, 2015). Neutrophils are then activated through membrane bound and soluble receptor interaction, including that of TREM-1 (Haselmayer et al., 2007, Derive et al., 2012). The above study findings suggest TLT-1 (both membrane bound and soluble forms) are able to inhibit this interaction through competing with TREM-1 to bind TREM-1 ligand and thus prevent neutrophil activation (Derive et al., 2012).

Platelets have also been shown to recognize LPS directly, interestingly this does not induce aggregation or P-selectin exposure instead leading to intense platelet-neutrophil binding and release of neutrophil extracellular traps (NETs) (Thomas and Storey, 2015, Clark et al., 2007, McDonald et al., 2012). It would be interesting to see if TLT-1 is present on the surface under these conditions, as although TLT-1 is an α-granule protein, differential upregulation of TLT-

1 and P-selectin has been observed (Smith et al., 2018). Although fibrinogen and vWF have been identified as ligands for TLT-1, the lack of functional response observed suggests other binding partners of TLT-1 are yet to be identified which may point towards the physiological role of this receptor.

7.4. TLT-1 as a more sensitive marker of platelet activation

Another aim of this thesis was to investigate TLT-1 as a marker of platelet activation. Findings from chapter 5 demonstrate TLT-1 is a more sensitive marker of platelet activation than P-selectin. This finding has important implications for future studies of platelet activation and thrombosis models, as well as potential clinical use.

Although extensive work was carried out by the Brass group characterising the architecture of growing thrombi, it was thought that platelets in the shell region were minimally active, only enough to tether them to the growing thrombi. This was based around the lack of the platelet activation marker P-selectin and observation that these platelets undergo embolization. P-selectin-positive platelets within the core do not embolize and remained attached; leading to the suggestion that firm attachment requires a level of platelet activation sufficient to cause α-granule secretion (Stalker et al., 2013).

The identification of TLT-1 expression in the shell region of thrombi, however suggests these platelets are more than minimally activated, as TLT-1 is an α-granule protein requiring platelet activation and granule secretion before being exposed upon the platelet surface. The presence of TLT-1 in the shell therefore suggests these platelets have undergone α-granule secretion, which is thought to be an irreversible platelet activation event. TLT-1-positive platelets in the shell, in contrast to the P-selectin-positive platelets in the core, can embolize and therefore are not firmly attached despite α-granule secretion. Further investigation is needed to understand

the differences in TLT-1 and P-selectin positive platelet activation. Whether TLT-1 surface exposure indicates reversible activation, or if differences are due to differential granule secretion as observed in resting platelets and megakaryocytes. Experiments utilising P2Y12 antagonists such as Cangrelor and thrombin inhibitor hirudin may help explain differences in the upregulation of TLT-1 and P-selectin *in vivo*.

The work in chapter 5 was carried out in the small arterioles of cremaster microcirculation, yet should be applicable to much larger arteries which have recently been shown to have the same thrombus architecture (Welsh et al., 2017). It is not readily possible to study human platelets *in vivo*, however microfluidic devices that incorporate collagen and tissue factor can form a core-shell architecture like that observed in mice *in vivo* (Muthard and Diamond, 2013, Zhu et al., 2015, Sakurai et al., 2018). Using such a system to assess TLT-1 distribution across human platelets, where abundance is more comparable to that of P-selectin, would give some indication how applicable *in vivo* mouse findings are to human thrombi. Based on flow cytometry observations of more rapid and greater surface upregulation of TLT-1 on human platelets (Smith et al., 2018), TLT-1 distribution throughout thrombi would be expected to be similar to that in mice thrombi *in vivo*.

The increased sensitivity of TLT-1 over P-selectin opens the possibility of use to detect activation level of circulating platelets. To this end, it is currently being used within the Birmingham Platelet Group to assess the level of pre-activated platelets in transgenic mouse models known to have increased platelet clearance, with very promising initial results.

In addition to research uses, TLT-1 as a platelet activation marker may have clinical application, where activation of circulating platelets has increasingly been associated to various disease states. TLT-1 could possibly be used as a clinical biomarker to detect early platelet activation in various disease pathologies such as coronary artery disease and deep vein thrombosis. Patient

response to antiplatelet therapy varies widely; with high on-treatment platelet reactivity associated with adverse cardiovascular events (Thomas and Storey, 2015). TLT-1 could possibly therefore be used to not only identify those patients at higher risk of cardiovascular events before P-selectin, but also assist with monitoring and dosing of antiplatelet therapies (Thomas and Storey, 2015).

Detection of sTLT-1 has already been shown to correlate with sepsis and high levels associated with acute respiratory distress syndrome which is common among sepsis patients (Morales-Ortiz et al., 2018a, Washington et al., 2009, Morales-Ortiz et al., 2018b). Elevated sTLT-1 levels have likewise been detected in acute coronary syndrome (ACS) patients, which covers a range of heart conditions. A study by Esponda et al (2015) showed elevated levels of sTLT-1 compared to healthy controls could be detected in the plasma of ACS patients admitted to hospital with chest pain. A later study conducted by Fu et al (2018) showing serum levels of sTLT-1 increased with severity of ACS, and could be decreased with effective treatment. Although detection of sTLT-1 in plasma and serum has been associated with these disease states, a direct marker on platelet activation is likely to provee a better indicator of degree of platelet activation. Only time will tell the usefulness of this new tool for assessing platelet activation.

7.5. Summary and future directions

Findings presented in this thesis add further evidence of the role ITIM-containing receptors play in regulation of platelet production and function, as well as demonstrate a new more sensitive biomarker of platelet activation, TLT-1. Although TLT-1 showed minor role in thrombosis and haemostasis, further studies into inflammation and infection are likely to return a significant role for this highly abundant and specific receptor mediating platelet-leukocytes

interactions. Use of TLT-1 as a biomarker has various research applications in the study of platelet biology, and has the potential for translation into clinical use in patients.

References

ADOLFSSON, J., BORGE, O. J., BRYDER, D., THEILGAARD-MONCH, K., ASTRAND-GRUNDSTROM, I., SITNICKA, E., SASAKI, Y. & JACOBSEN, S. E. 2001. Upregulation of Flt3 expression within the bone marrow Lin(-)Sca1(+)c-kit(+) stem cell compartment is accompanied by loss of self-renewal capacity. *Immunity,* 15**,** 659-69.

ALSHAHRANI, M. M., KYRIACOU, R. P., O'MALLEY, C. J., HEINRICH, G., NAJJAR, S. M. & JACKSON, D. E. 2016. CEACAM2 positively regulates integrin alphaIIbbeta3-mediated platelet functions. *Platelets,* 27**,** 743-750.

ALSHAHRANI, M. M., YANG, E., YIP, J., GHANEM, S. S., ABDALLAH, S. L., DEANGELIS, A. M., O'MALLEY, C. J., MOHEIMANI, F., NAJJAR, S. M. & JACKSON, D. E. 2014. CEACAM2 negatively regulates hemi (ITAM-bearing) GPVI and CLEC-2 pathways and thrombus growth in vitro and in vivo. *Blood,* 124**,** 2431-41.

ANDRE, P., NANNIZZI-ALAIMO, L., PRASAD, S. K. & PHILLIPS, D. R. 2002. Platelet-derived CD40L: the switch-hitting player of cardiovascular disease. *Circulation,* 106**,** 896-9.

ANDREWS, R. K. & BERNDT, M. C. 2013. Chapter 10 - The GPIb-IX-V Complex. *In:* MICHELSON, A. D. (ed.) *Platelets (Third Edition).* Academic Press.

ASLAN, J. E., ITAKURA, A., GERTZ, J. M. & MCCARTY, O. J. 2012. Platelet shape change and spreading. *Methods Mol Biol,* 788**,** 91-100.

ASSELIN, J., KNIGHT, C. G., FARNDALE, R. W., BARNES, M. J. & WATSON, S. P. 1999. Monomeric (glycine-proline-hydroxyproline)10 repeat sequence is a partial agonist of the platelet collagen receptor glycoprotein VI. *Biochem J,* 339 (Pt 2)**,** 413-8.

ASSINGER, A. 2014. Platelets and infection - an emerging role of platelets in viral infection. *Front Immunol,* 5**,** 649.

BALDUINI, A., PALLOTTA, I., MALARA, A., LOVA, P., PECCI, A., VIARENGO, G., BALDUINI, C. L. & TORTI, M. 2008. Adhesive receptors, extracellular proteins and myosin IIA orchestrate proplatelet formation by human megakaryocytes. *J Thromb Haemost,* 6**,** 1900-7.

BARFORD, D. & NEEL, B. G. 1998. Revealing mechanisms for SH2 domain mediated regulation of the protein tyrosine phosphatase SHP-2. *Structure,* 6**,** 249-54.

BARROW, A. D., ASTOUL, E., FLOTO, A., BROOKE, G., RELOU, I. A. M., JENNINGS, N. S., SMITH, K. G. C., OUWEHAND, W., FARNDALE, R. W., ALEXANDER, D. R. & TROWSDALE, A. 2004. Cutting edge: TREM-like transcript-1, a platelet immunoreceptor tyrosine-based inhibition motif encoding costimulatory immunoreceptor that enhances, rather than inhibits, calcium signaling via SHP-2. *Journal of Immunology,* 172**,** 5838-5842.

BARROW, A. D. & TROWSDALE, J. 2006. You say ITAM and I say ITIM, let's call the whole thing off: the ambiguity of immunoreceptor signalling. *Eur J Immunol,* 36**,** 1646-53.

BENDER, M., THON, J. N., EHRLICHER, A. J., WU, S., MAZUTIS, L., DESCHMANN, E., SOLA-VISNER, M., ITALIANO, J. E. & HARTWIG, J. H. 2015. Microtubule sliding drives proplatelet elongation and is dependent on cytoplasmic dynein. *Blood,* 125**,** 860-8.

BENNETT, J. S., BERGER, B. W. & BILLINGS, P. C. 2009. The structure and function of platelet integrins. *J Thromb Haemost,* 7 Suppl 1**,** 200-5.

BERNDT, M. C., SHEN, Y., DOPHEIDE, S. M., GARDINER, E. E. & ANDREWS, R. K. 2001. The vascular biology of the glycoprotein Ib-IX-V complex. *Thromb Haemost,* 86**,** 178-88.

BERTHOLD, M. R., CEBRON, N., DILL, F., GABRIEL, T. R., K\, T., \#246, TTER, MEINL, T., OHL, P., THIEL, K. & WISWEDEL, B. 2009. KNIME - the Konstanz information miner: version 2.0 and beyond. *SIGKDD Explor. Newsl.,* 11**,** 26-31.

BIZZOZERO, J. 1882. Ueber einen neuen Formbestandtheil des Blutes und dessen Rolle bei der Thrombose und der Blutgerinnung. *Archiv für pathologische Anatomie und Physiologie und für klinische Medicin,* 90**,** 261-332.

BLAIR, P. & FLAUMENHAFT, R. 2009. Platelet alpha-granules: basic biology and clinical correlates. *Blood Rev,* 23**,** 177-89.

BLEDZKA, K., PESHO, M. M., MA, Y.-Q. & PLOW, E. F. 2013. Chapter 12 - Integrin αIIbβ3. *In:* MICHELSON, A. D. (ed.) *Platelets (Third Edition).* Academic Press.

BORASCHI-DIAZ, I., MORT, J. S., BROMME, D., SENIS, Y. A., MAZHARIAN, A. & KOMAROVA, S. V. 2018. Collagen type I degradation fragments act through the collagen receptor LAIR-1 to provide a negative feedback for osteoclast formation. *Bone,* 117**,** 23-30.

BOUFENZER, A., LEMARIE, J., SIMON, T., DERIVE, M., BOUAZZA, Y., TRAN, N., MASKALI, F., GROUBATCH, F., BONNIN, P., BASTIEN, C., BRUNEVAL, P., MARIE, P. Y., COHEN, R., DANCHIN, N., SILVESTRE, J. S., AIT-OUFELLA, H. & GIBOT, S. 2015. TREM-1 Mediates Inflammatory Injury and Cardiac Remodeling Following Myocardial Infarction. *Circ Res,* 116**,** 1772-82.

BRASS, L. F. 2003. Thrombin and platelet activation. *Chest,* 124**,** 18s-25s.

BRASS, L. F., NEWMAN, D. K., WANNERMACHER, K. M., ZHU, L. & STALKER, T. J. 2013. Chapter 19 - Signal Transduction During Platelet Plug Formation. *In:* MICHELSON, A. D. (ed.) *Platelets (Third Edition).* Academic Press.

BRONDIJK, T. H., DE RUITER, T., BALLERING, J., WIENK, H., LEBBINK, R. J., VAN INGEN, H., BOELENS, R., FARNDALE, R. W., MEYAARD, L. & HUIZINGA, E. G. 2010. Crystal structure and collagen-binding site of immune inhibitory receptor LAIR-1: unexpected implications for collagen binding by platelet receptor GPVI. *Blood,* 115**,** 1364-73.

BUCKLEY, C. D., DOYONNAS, R., NEWTON, J. P., BLYSTONE, S. D., BROWN, E. J., WATT, S. M. & SIMMONS, D. L. 1996. Identification of alpha v beta 3 as a heterotypic ligand for CD31/PECAM-1. *J Cell Sci,* 109 (Pt 2)**,** 437-45.

BURKHART, J. M., VAUDEL, M., GAMBARYAN, S., RADAU, S., WALTER, U., MARTENS, L., GEIGER, J., SICKMANN, A. & ZAHEDI, R. P. 2012. The first comprehensive and quantitative analysis of human platelet protein composition allows the comparative analysis of structural and functional pathways. *Blood,* 120**,** e73-82.

BYE, A. P., UNSWORTH, A. J. & GIBBINS, J. M. 2016. Platelet signaling: a complex interplay between inhibitory and activatory networks. *J Thromb Haemost,* 14**,** 918-30.

CALAMINUS, S. D., THOMAS, S., MCCARTY, O. J., MACHESKY, L. M. & WATSON, S. P. 2008. Identification of a novel, actin-rich structure, the actin nodule, in the early stages of platelet spreading. *J Thromb Haemost,* 6**,** 1944-52.

CANNONS, J. L., TANGYE, S. G. & SCHWARTZBERG, P. L. 2011. SLAM family receptors and SAP adaptors in immunity. *Annu Rev Immunol,* 29**,** 665-705.

CATTANEO, M. 2013. Chapter 14 - The Platelet P2 Receptors. *In:* MICHELSON, A. D. (ed.) *Platelets (Third Edition).* Academic Press.

CHATTERJEE, M., HUANG, Z., ZHANG, W., JIANG, L., HULTENBY, K., ZHU, L., HU, H., NILSSON, G. P. & LI, N. 2011. Distinct platelet packaging, release, and surface expression of proangiogenic and antiangiogenic factors on different platelet stimuli. *Blood,* 117**,** 3907-11.

CHEN, J., ISHII, M., WANG, L., ISHII, K. & COUGHLIN, S. R. 1994. Thrombin receptor activation. Confirmation of the intramolecular tethered liganding hypothesis and discovery of an alternative intermolecular liganding mode. *J Biol Chem,* 269**,** 16041-5.

CICMIL, M., THOMAS, J. M., LEDUC, M., BON, C. & GIBBINS, J. M. 2002. Platelet endothelial cell adhesion molecule-1 signaling inhibits the activation of human platelets. *Blood,* 99**,** 137-44.

CLARK, S. R., MA, A. C., TAVENER, S. A., MCDONALD, B., GOODARZI, Z., KELLY, M. M., PATEL, K. D., CHAKRABARTI, S., MCAVOY, E., SINCLAIR, G. D., KEYS, E. M., ALLEN-VERCOE, E., DEVINNEY, R., DOIG, C. J., GREEN, F. H. & KUBES, P. 2007. Platelet TLR4 activates neutrophil extracellular traps to ensnare bacteria in septic blood. *Nat Med,* 13**,** 463-9.

CLEMETSON, K. J. 2012. Platelets and primary haemostasis. *Thromb Res,* 129**,** 220-4.

CLEMETSON, K. J. & CLEMETSON, J. M. 2013. Chapter 9 - Platelet Receptors. *In:* MICHELSON, A. D. (ed.) *Platelets (Third Edition).* Academic Press.

COUGHLIN, S. R. 2005. Protease-activated receptors in hemostasis, thrombosis and vascular biology. *J Thromb Haemost,* 3**,** 1800-14.

COUGHLIN, S. R., SCARBOROUGH, R. M., VU, T. K. & HUNG, D. T. 1992. Thrombin receptor structure and function. *Cold Spring Harb Symp Quant Biol,* 57**,** 149-54.

COVIC, L., GRESSER, A. L. & KULIOPULOS, A. 2000. Biphasic kinetics of activation and signaling for PAR1 and PAR4 thrombin receptors in platelets. *Biochemistry,* 39**,** 5458-67.

COXON, C. H., GEER, M. J. & SENIS, Y. A. 2017. ITIM receptors: more than just inhibitors of platelet activation. *Blood,* 129**,** 3407-3418.

COXON, C. H., SADLER, A. J., HUO, J. & CAMPBELL, R. D. 2012. An investigation of hierachical protein recruitment to the inhibitory platelet receptor, G6B-b. *PLoS One,* 7**,** e49543.

CRAMER, E. M., NOROL, F., GUICHARD, J., BRETON-GORIUS, J., VAINCHENKER, W., MASSE, J. M. & DEBILI, N. 1997. Ultrastructure of platelet formation by human megakaryocytes cultured with the Mpl ligand. *Blood,* 89**,** 2336-46.

DAERON, M., JAEGER, S., DU PASQUIER, L. & VIVIER, E. 2008. Immunoreceptor tyrosine-based inhibition motifs: a quest in the past and future. *Immunol Rev,* 224**,** 11-43.

DAERON, M., LATOUR, S., MALBEC, O., ESPINOSA, E., PINA, P., PASMANS, S. & FRIDMAN, W. H. 1995. The same tyrosine-based inhibition motif, in the intracytoplasmic domain of Fc gamma RIIB, regulates negatively BCR-, TCR-, and FcR-dependent cell activation. *Immunity,* 3**,** 635-46.

DAI, K., BODNAR, R., BERNDT, M. C. & DU, X. 2005. A critical role for 14-3-3zeta protein in regulating the VWF binding function of platelet glycoprotein Ib-IX and its therapeutic implications. *Blood,* 106**,** 1975-81.

DE CHAUMONT, F., DALLONGEVILLE S FAU - CHENOUARD, N., CHENOUARD N FAU - HERVE, N., HERVE N FAU - POP, S., POP S FAU - PROVOOST, T., PROVOOST T FAU - MEAS-YEDID, V., MEAS-YEDID V FAU - PANKAJAKSHAN, P., PANKAJAKSHAN P FAU - LECOMTE, T., LECOMTE T FAU - LE MONTAGNER, Y., LE MONTAGNER Y FAU - LAGACHE, T., LAGACHE T FAU - DUFOUR, A., DUFOUR A FAU - OLIVO-MARIN, J.-C. & OLIVO-MARIN, J. C. Icy: an open bioimage informatics platform for extended reproducible research.

DE SAUVAGE, F. J., HASS, P. E., SPENCER, S. D., MALLOY, B. E., GURNEY, A. L., SPENCER, S. A., DARBONNE, W. C., HENZEL, W. J., WONG, S. C., KUANG, W. J. & ET AL. 1994. Stimulation of megakaryocytopoiesis and thrombopoiesis by the c-Mpl ligand. *Nature,* 369**,** 533-8.

DEAGLIO, S., MORRA, M., MALLONE, R., AUSIELLO, C. M., PRAGER, E., GARBARINO, G., DIANZANI, U., STOCKINGER, H. & MALAVASI, F. 1998. Human CD38 (ADP-ribosyl cyclase) is a counter-receptor of CD31, an Ig superfamily member. *J Immunol,* 160**,** 395-402.

DEBILI, N., COULOMBEL, L., CROISILLE, L., KATZ, A., GUICHARD, J., BRETON-GORIUS, J. & VAINCHENKER, W. 1996. Characterization of a bipotent erythro-megakaryocytic progenitor in human bone marrow. *Blood,* 88**,** 1284-96.

DERIVE, M., BOUAZZA, Y., SENNOUN, N., MARCHIONNI, S., QUIGLEY, L., WASHINGTON, V., MASSIN, F., MAX, J. P., FORD, J., ALAUZET, C., LEVY, B., MCVICAR, D. W. & GIBOT, S. 2012. Soluble TREM-like transcript-1 regulates leukocyte activation and controls microbial sepsis. *J Immunol,* 188**,** 5585-92.

DERIVE, M., BOUFENZER, A., BOUAZZA, Y., GROUBATCH, F., ALAUZET, C., BARRAUD, D., LOZNIEWSKI, A., LEROY, P., TRAN, N. & GIBOT, S. 2013. Effects of a TREM-like transcript 1-derived peptide during hypodynamic septic shock in pigs. *Shock,* 39**,** 176-82.

DERIVE, M., BOUFENZER, A. & GIBOT, S. 2014. Attenuation of responses to endotoxin by the triggering receptor expressed on myeloid cells-1 inhibitor LR12 in nonhuman primate. *Anesthesiology,* 120**,** 935-42.

DHANJAL, T. S., PENDARIES, C., ROSS, E. A., LARSON, M. K., PROTTY, M. B., BUCKLEY, C. D. & WATSON, S. P. 2007a. A novel role for PECAM-1 in megakaryocytokinesis and recovery of platelet counts in thrombocytopenic mice. *Blood,* 109**,** 4237-44.

DHANJAL, T. S., ROSS, E. A., AUGER, J. M., MCCARTY, O. J., HUGHES, C. E., SENIS, Y. A., BUCKLEY, C. D. & WATSON, S. P. 2007b. Minimal regulation of platelet activity by PECAM-1. *Platelets,* 18**,** 56-67.

DI PAOLA, J. 2013. SHPing in different directions in platelet production. *Blood,* 121**,** 4018-9.

DOERR A., G. C., LAFFAN M., MCKINNON T. 2017. Triggering receptor expressed on myeloid cells like transcript-1 (TLT-1) is a novel ligand for von Willebrand factor [Poster presentation, ISTH 2017 Congress]. *Research and Practice in Thrombosis and Haemostasis,* 1**,** 698-699.

DU, X. 2014. Self-control of platelets: a new ITIM story. *Blood,* 124**,** 2322-2323.

DUBOIS, C., PANICOT-DUBOIS, L., GAINOR, J. F., FURIE, B. C. & FURIE, B. 2007. Thrombin-initiated platelet activation in vivo is vWF independent during thrombus formation in a laser injury model. *J Clin Invest,* 117**,** 953-60.

DUBOIS, C., PANICOT-DUBOIS, L., MERRILL-SKOLOFF, G., FURIE, B. & FURIE, B. C. 2006. Glycoprotein VI-dependent and -independent pathways of thrombus formation in vivo. *Blood,* 107**,** 3902-6.

DUNCAN, G. S., ANDREW, D. P., TAKIMOTO, H., KAUFMAN, S. A., YOSHIDA, H., SPELLBERG, J., DE LA POMPA, J. L., ELIA, A., WAKEHAM, A., KARAN-TAMIR, B., MULLER, W. A., SENALDI, G., ZUKOWSKI, M. M. & MAK, T. W. 1999. Genetic evidence for functional redundancy of Platelet/Endothelial cell adhesion molecule-1 (PECAM-1): CD31-deficient mice reveal PECAM-1-dependent and PECAM-1-independent functions. *J Immunol,* 162**,** 3022-30.

DURRANT, T. N., VAN DEN BOSCH, M. T. & HERS, I. 2017. Integrin alphaIIbbeta3 outside-in signaling. *Blood,* 130**,** 1607-1619.

DUTTING, S., GAITS-IACOVONI, F., STEGNER, D., POPP, M., ANTKOWIAK, A., VAN EEUWIJK, J. M. M., NURDEN, P., STRITT, S., HEIB, T., AURBACH, K., ANGAY, O., CHERPOKOVA, D., HEINZ, N., BAIG, A. A., GORELASHVILI, M. G., GERNER, F., HEINZE, K. G., WARE, J., KROHNE, G., RUGGERI, Z. M., NURDEN, A. T., SCHULZE, H., MODLICH, U., PLEINES, I., BRAKEBUSCH, C. & NIESWANDT, B. 2017. A Cdc42/RhoA regulatory circuit downstream of glycoprotein Ib guides transendothelial platelet biogenesis. *Nat Commun,* 8**,** 15838.

ECKLY, A., HEIJNEN, H., PERTUY, F., GEERTS, W., PROAMER, F., RINCKEL, J. Y., LEON, C., LANZA, F. & GACHET, C. 2014. Biogenesis of the demarcation membrane system (DMS) in megakaryocytes. *Blood,* 123**,** 921-30.

ECKLY, A., STRASSEL, C., CAZENAVE, J. P., LANZA, F., LEON, C. & GACHET, C. 2012. Characterization of megakaryocyte development in the native bone marrow environment. *Methods Mol Biol,* 788**,** 175-92.

EDMEAD, C. E., CROSBY, D. A., SOUTHCOTT, M. & POOLE, A. W. 1999. Thrombin-induced association of SHP-2 with multiple tyrosine-phosphorylated proteins in human platelets. *FEBS Lett,* 459**,** 27-32.

ENGELMANN, B. & MASSBERG, S. 2013. Thrombosis as an intravascular effector of innate immunity. *Nat Rev Immunol,* 13**,** 34-45.

ESPONDA, O. L., HUNTER, R., DEL RIO, J. R. & WASHINGTON, A. V. 2015. Levels of soluble TREM-like transcript 1 in patients presenting to the emergency department with chest pain. *Clin Appl Thromb Hemost,* 21**,** 30-4.

FALATI, S., PATIL, S., GROSS, P. L., STAPLETON, M., MERRILL-SKOLOFF, G., BARRETT, N. E., PIXTON, K. L., WEILER, H., COOLEY, B., NEWMAN, D. K., NEWMAN, P. J., FURIE, B. C., FURIE, B. & GIBBINS, J. M. 2006. Platelet PECAM-1 inhibits thrombus formation in vivo. *Blood,* 107**,** 535-41.

FAN, X., SHI, P., DAI, J., LU, Y., CHEN, X., LIU, X., ZHANG, K., WU, X., SUN, Y., WANG, K., ZHU, L., ZHANG, C. C., ZHANG, J., CHEN, G. Q., ZHENG, J. & LIU, J. 2014. Paired immunoglobulin-like receptor B regulates platelet activation. *Blood,* 124**,** 2421-30.

FERRER-ACOSTA, Y., GONZALEZ, M., FERNANDEZ, M. & VALANCE, W. A. 2014. Emerging Roles for Platelets in Inflammation and Disease. *J Infect Dis Ther,* 2.

FLAUJAC, C., BOUKOUR, S. & CRAMER-BORDE, E. 2010. Platelets and viruses: an ambivalent relationship. *Cell Mol Life Sci,* 67**,** 545-56.

FLAUMENHAFT, R. 2013. Chapter 18 - Platelet Secretion. *In:* MICHELSON, A. D. (ed.) *Platelets (Third Edition).* Academic Press.

FORD, J. W. & MCVICAR, D. W. 2009. TREM and TREM-like receptors in inflammation and disease. *Curr Opin Immunol,* 21**,** 38-46.

FRANCO, A. T., CORKEN, A. & WARE, J. 2015. Platelets at the interface of thrombosis, inflammation, and cancer. *Blood,* 126**,** 582-8.

FU, R., SONG, X., SU, D., LI, S., GAO, L. & JI, C. 2018. Serum STLT-1 and bilirubin levels in patients with acute coronary syndrome and correlation with prognosis. *Exp Ther Med,* 16**,** 241-245.

GATTIS, J. L., WASHINGTON, A. V., CHISHOLM, M. M., QUIGLEY, L., SZYK, A., MCVICAR, D. W. & LUBKOWSKI, J. 2006. The structure of the extracellular domain of triggering receptor expressed on myeloid cells like transcript-1 and evidence for a naturally occurring soluble fragment. *J Biol Chem,* 281**,** 13396-403.

GEER, M. J., VAN GEFFEN, J. P., GOPALASINGAM, P., VOGTLE, T., SMITH, C. W., HEISING, S., KUIJPERS, M. J. E., TULLEMANS, B. M. E., JARVIS, G. E., EBLE, J. A., JEEVES, M., OVERDUIN, M., HEEMSKERK, J. W. M., MAZHARIAN, A. & SENIS, Y. A. 2018. Uncoupling ITIM receptor G6b-B from tyrosine phosphatases Shp1 and Shp2 disrupts murine platelet homeostasis. *Blood,* 132**,** 1413-1425.

GIBBINS, J. M. 2002. The negative regulation of platelet function: extending the role of the ITIM. *Trends Cardiovasc Med,* 12**,** 213-9.

GIBBINS, J. M., OKUMA, M., FARNDALE, R., BARNES, M. & WATSON, S. P. 1997. Glycoprotein VI is the collagen receptor in platelets which underlies tyrosine phosphorylation of the Fc receptor gamma-chain. *FEBS Lett,* 413**,** 255-9.

GIOMARELLI, B., WASHINGTON, V. A., CHISHOLM, M. M., QUIGLEY, L., MCMAHON, J. B., MORI, T. & MCVICAR, D. W. 2007. Inhibition of thrombin-induced platelet aggregation using human single-chain Fv antibodies specific for TREM-like transcript-1. *Thrombosis and Haemostasis*.

GOLEBIEWSKA, E. M. & POOLE, A. W. 2015. Platelet secretion: From haemostasis to wound healing and beyond. *Blood Rev,* 29**,** 153-62.

GRINENKO, T., ARNDT, K., PORTZ, M., MENDE, N., GUNTHER, M., COSGUN, K. N., ALEXOPOULOU, D., LAKSHMANAPERUMAL, N., HENRY, I., DAHL, A. & WASKOW, C. 2014. Clonal expansion capacity defines two consecutive developmental stages of long-term hematopoietic stem cells. *J Exp Med,* 211**,** 209-15.

GROSS, P. L., FURIE, B. C., MERRILL-SKOLOFF, G., CHOU, J. & FURIE, B. 2005. Leukocyte-versus microparticle-mediated tissue factor transfer during arteriolar thrombus development. *J Leukoc Biol,* 78**,** 1318-26.

GROZOVSKY, R., BEGONJA, A. J., LIU, K., VISNER, G., HARTWIG, J. H., FALET, H. & HOFFMEISTER, K. M. 2015. The Ashwell-Morell receptor regulates hepatic thrombopoietin production via JAK2-STAT3 signaling. *Nat Med,* 21**,** 47-54.

GURNEY, A. L., CARVER-MOORE, K., DE SAUVAGE, F. J. & MOORE, M. W. 1994. Thrombocytopenia in c-mpl-deficient mice. *Science,* 265**,** 1445-7.

HAAS, S., HANSSON, J., KLIMMECK, D., LOEFFLER, D., VELTEN, L., UCKELMANN, H., WURZER, S., PRENDERGAST, A. M., SCHNELL, A., HEXEL, K., SANTARELLA-MELLWIG, R., BLASZKIEWICZ, S., KUCK, A., GEIGER, H., MILSOM, M. D., STEINMETZ, L. M., SCHROEDER, T., TRUMPP, A., KRIJGSVELD, J. & ESSERS, M. A. 2015. Inflammation-Induced Emergency Megakaryopoiesis Driven by Hematopoietic Stem Cell-like Megakaryocyte Progenitors. *Cell Stem Cell,* 17**,** 422-34.

HANDAGAMA, P., RAPPOLEE, D. A., WERB, Z., LEVIN, J. & BAINTON, D. F. 1990. Platelet alpha-granule fibrinogen, albumin, and immunoglobulin G are not synthesized by rat and mouse megakaryocytes. *J Clin Invest,* 86**,** 1364-8.

HARRISON, P. & CRAMER, E. M. 1993. Platelet alpha-granules. *Blood Rev,* 7**,** 52-62.

HARTWIG, J. H. 2013. Chapter 8 - The Platelet Cytoskeleton. *In:* MICHELSON, A. D. (ed.) *Platelets (Third Edition).* Academic Press.

HASELMAYER, P., GROSSE-HOVEST, L., VON LANDENBERG, P., SCHILD, H. & RADSAK, M. P. 2007. TREM-1 ligand expression on platelets enhances neutrophil activation. *Blood,* 110**,** 1029-35.

HECHLER, B., NONNE, C., ECKLY, A., MAGNENAT, S., RINCKEL, J. Y., DENIS, C. V., FREUND, M., CAZENAVE, J. P., LANZA, F. & GACHET, C. 2010. Arterial thrombosis: relevance of a model with two levels of severity assessed by histologic, ultrastructural and functional characterization. *J Thromb Haemost,* 8**,** 173-84.

HEIJNEN, H. & VAN DER SLUIJS, P. 2015. Platelet secretory behaviour: as diverse as the granules ... or not? *J Thromb Haemost,* 13**,** 2141-51.

HITCHCOCK, I. S. & KAUSHANSKY, K. 2014. Thrombopoietin from beginning to end. *Br J Haematol,* 165**,** 259-68.

HO-TIN-NOE, B., DEMERS, M. & WAGNER, D. D. 2011. How platelets safeguard vascular integrity. *J Thromb Haemost,* 9 Suppl 1**,** 56-65.

HOF, P., PLUSKEY, S., DHE-PAGANON, S., ECK, M. J. & SHOELSON, S. E. 1998. Crystal structure of the tyrosine phosphatase SHP-2. *Cell,* 92**,** 441-50.

HOFFMEISTER, K. M. & FALET, H. 2016. Platelet clearance by the hepatic Ashwell-Morrell receptor: mechanisms and biological significance. *Thromb Res,* 141 Suppl 2**,** S68-72.

HOFMANN, I., GEER, M. J., VOGTLE, T., CRISPIN, A., CAMPAGNA, D. R., BARR, A., CALICCHIO, M. L., HEISING, S., VAN GEFFEN, J. P., KUIJPERS, M. J. E., HEEMSKERK, J. W. M., EBLE, J. A., SCHMITZ-ABE, K., OBENG, E. A., DOUGLAS, M., FRESON, K., PONDARRE, C., FAVIER, R., JARVIS, G. E., MARKIANOS, K., TURRO, E., OUWEHAND, W. H., MAZHARIAN, A., FLEMING, M. D. & SENIS, Y. A. 2018. Congenital macrothrombocytopenia with focal myelofibrosis due to mutations in human G6b-B is rescued in humanized mice. *Blood,* 132**,** 1399-1412.

HU, M., ZHANG, H., LIU, Q. & HAO, Q. 2016. Structural Basis for Human PECAM-1-Mediated Trans-homophilic Cell Adhesion. *Sci Rep,* 6**,** 38655.

HUGHES, C. E., FINNEY, B. A., KOENTGEN, F., LOWE, K. L. & WATSON, S. P. 2015. The N-terminal SH2 domain of Syk is required for (hem)ITAM, but not integrin, signaling in mouse platelets. *Blood,* 125**,** 144-54.

HUGHES, C. E., POLLITT, A. Y., MORI, J., EBLE, J. A., TOMLINSON, M. G., HARTWIG, J. H., O'CALLAGHAN, C. A., FUTTERER, K. & WATSON, S. P. 2010. CLEC-2 activates Syk through dimerization. *Blood,* 115**,** 2947-55.

HUMPHRIES, L. A., DANGELMAIER, C., SOMMER, K., KIPP, K., KATO, R. M., GRIFFITH, N., BAKMAN, I., TURK, C. W., DANIEL, J. L. & RAWLINGS, D. J. 2004. Tec kinases mediate sustained calcium influx via site-specific tyrosine phosphorylation of the phospholipase Cgamma Src homology 2-Src homology 3 linker. *J Biol Chem,* 279**,** 37651-61.

HUNT, P. 1995. A bipotential megakaryocyte/erythrocyte progenitor cell: the link between erythropiesis and megakaryopoiesis becomes stronger. *J Lab Clin Med,* 125**,** 303-4.

ISHIHARA, H., CONNOLLY, A. J., ZENG, D., KAHN, M. L., ZHENG, Y. W., TIMMONS, C., TRAM, T. & COUGHLIN, S. R. 1997. Protease-activated receptor 3 is a second thrombin receptor in humans. *Nature,* 386**,** 502-6.

ITALIANO, J. E., JR., LECINE, P., SHIVDASANI, R. A. & HARTWIG, J. H. 1999. Blood platelets are assembled principally at the ends of proplatelet processes produced by differentiated megakaryocytes. *J Cell Biol,* 147**,** 1299-312.

ITALIANO, J. E., JR., RICHARDSON, J. L., PATEL-HETT, S., BATTINELLI, E., ZASLAVSKY, A., SHORT, S., RYEOM, S., FOLKMAN, J. & KLEMENT, G. L. 2008. Angiogenesis is regulated by a novel mechanism: pro- and antiangiogenic proteins are organized into separate platelet alpha granules and differentially released. *Blood,* 111**,** 1227-33.

JACKSON, D. E., WARD, C. M., WANG, R. & NEWMAN, P. J. 1997. The protein-tyrosine phosphatase SHP-2 binds platelet/endothelial cell adhesion molecule-1 (PECAM-1) and forms a distinct signaling complex during platelet aggregation. Evidence for a mechanistic link between PECAM-1- and integrin-mediated cellular signaling. *J Biol Chem,* 272**,** 6986-93.

JENNE, C. N. & KUBES, P. 2015. Platelets in inflammation and infection. *Platelets,* 26**,** 286-92.

JOLLY, L., LEMARIE, J., CARRASCO, K., POPOVIC, B., DERIVE, M., BOUFENZER, A. & GIBOT, S. 2017. Triggering Receptor Expressed on Myeloid cells-1: a new player in platelet aggregation. *Thromb Haemost,* 117**,** 1772-1781.

JONES, C. I., GARNER, S. F., MORAES, L. A., KAISER, W. J., RANKIN, A., OUWEHAND, W. H., GOODALL, A. H. & GIBBINS, J. M. 2009. PECAM-1 expression and activity negatively regulate multiple platelet signaling pathways. *FEBS Lett,* 583**,** 3618-24.

JONES, C. I., MORAES, L. A. & GIBBINS, J. M. 2012. Regulation of platelet biology by platelet endothelial cell adhesion molecule-1. *Platelets,* 23**,** 331-5.

JONES, K. L., HUGHAN, S. C., DOPHEIDE, S. M., FARNDALE, R. W., JACKSON, S. P. & JACKSON, D. E. 2001. Platelet endothelial cell adhesion molecule-1 is a negative regulator of platelet-collagen interactions. *Blood,* 98**,** 1456-63.

JONNALAGADDA, D., IZU, L. T. & WHITEHEART, S. W. 2012. Platelet secretion is kinetically heterogeneous in an agonist-responsive manner. *Blood,* 120**,** 5209-16.

JOSEFSSON, E. C., DOWLING, M. R., LEBOIS, M. & KILE, B. T. 2013. Chapter 3 - The Regulation of Platelet Life Span. *In:* MICHELSON, A. D. (ed.) *Platelets (Third Edition).* Academic Press.

JOSHI, S., BANERJEE, M., ZHANG, J., KESARAJU, A., POKROVSKAYA, I. D., STORRIE, B. & WHITEHEART, S. W. 2018. Alterations in platelet secretion differentially affect thrombosis and hemostasis. *Blood Adv,* 2**,** 2187-2198.

JUNT, T., SCHULZE, H., CHEN, Z., MASSBERG, S., GOERGE, T., KRUEGER, A., WAGNER, D. D., GRAF, T., ITALIANO, J. E., JR., SHIVDASANI, R. A. & VON ANDRIAN, U. H. 2007. Dynamic visualization of thrombopoiesis within bone marrow. *Science,* 317**,** 1767-70.

KAHR, W. H., LO, R. W., LI, L., PLUTHERO, F. G., CHRISTENSEN, H., NI, R., VAEZZADEH, N., HAWKINS, C. E., WEYRICH, A. S., DI PAOLA, J., LANDOLT-MARTICORENA, C. & GROSS, P. L. 2013. Abnormal megakaryocyte development and platelet function in Nbeal2(-/-) mice. *Blood,* 122**,** 3349-58.

KANAJI, S., FAHS, S. A., SHI, Q., HABERICHTER, S. L. & MONTGOMERY, R. R. 2012. Contribution of platelet vs. endothelial VWF to platelet adhesion and hemostasis. *J Thromb Haemost,* 10**,** 1646-52.

KANG, X., LU, Z., CUI, C., DENG, M., FAN, Y., DONG, B., HAN, X., XIE, F., TYNER, J. W., COLIGAN, J. E., COLLINS, R. H., XIAO, X., YOU, M. J. & ZHANG, C. C. 2015. The ITIM-containing receptor LAIR1 is essential for acute myeloid leukaemia development. *Nat Cell Biol,* 17**,** 665-77.

KAPUR, R. & SEMPLE, J. W. 2016. The nonhemostatic immune functions of platelets. *Semin Hematol,* 53 Suppl 1**,** S2-6.

KASIRER-FRIEDE, A., KAHN, M. L. & SHATTIL, S. J. 2007. Platelet integrins and immunoreceptors. *Immunol Rev,* 218**,** 247-64.

KATO, Y., FUJITA, N., KUNITA, A., SATO, S., KANEKO, M., OSAWA, M. & TSURUO, T. 2003. Molecular identification of Aggrus/T1alpha as a platelet aggregation-inducing factor expressed in colorectal tumors. *J Biol Chem,* 278**,** 51599-605.

KAUSHANSKY, K. 2005. The molecular mechanisms that control thrombopoiesis. *J Clin Invest,* 115**,** 3339-47.

KERRIGAN, A. M., NAVARRO-NUNEZ, L., PYZ, E., FINNEY, B. A., WILLMENT, J. A., WATSON, S. P. & BROWN, G. D. 2012. Podoplanin-expressing inflammatory macrophages activate murine platelets via CLEC-2. *J Thromb Haemost,* 10**,** 484-6.

KIM, O. V., LITVINOV, R. I., ALBER, M. S. & WEISEL, J. W. 2017. Quantitative structural mechanobiology of platelet-driven blood clot contraction. *Nat Commun,* 8**,** 1274.

KIM, S. J. & JENNE, C. N. 2016. Role of platelets in neutrophil extracellular trap (NET) production and tissue injury. *Semin Immunol,* 28**,** 546-554.

KLESNEY-TAIT, J., TURNBULL, I. R. & COLONNA, M. 2006. The TREM receptor family and signal integration. *Nat Immunol,* 7**,** 1266-73.

KUBAGAWA, H., CHEN, C. C., HO, L. H., SHIMADA, T. S., GARTLAND, L., MASHBURN, C., UEHARA, T., RAVETCH, J. V. & COOPER, M. D. 1999. Biochemical nature and cellular distribution of the paired immunoglobulin-like receptors, PIR-A and PIR-B. *J Exp Med,* 189**,** 309-18.

KUBES, P. 2016. The versatile platelet contributes to inflammation, infection, hemostasis, coagulation and cancer. *Semin Immunol,* 28**,** 535.

KUIJPERS, M. J., DE WITT, S., NERGIZ-UNAL, R., VAN KRUCHTEN, R., KORPORAAL, S. J., VERHAMME, P., FEBBRAIO, M., TJWA, M., VOSHOL, P. J., HOYLAERTS, M. F., COSEMANS, J. M. & HEEMSKERK, J. W. 2014. Supporting roles of platelet thrombospondin-1 and CD36 in thrombus formation on collagen. *Arterioscler Thromb Vasc Biol,* 34**,** 1187-92.

LAM, W. A., CHAUDHURI, O., CROW, A., WEBSTER, K. D., LI, T. D., KITA, A., HUANG, J. & FLETCHER, D. A. 2011. Mechanics and contraction dynamics of single platelets and implications for clot stiffening. *Nat Mater,* 10**,** 61-6.

LAURENTI, E. & GOTTGENS, B. 2018. From haematopoietic stem cells to complex differentiation landscapes. *Nature,* 553**,** 418-426.

LEBBINK, R. J., DE RUITER, T., ADELMEIJER, J., BRENKMAN, A. B., VAN HELVOORT, J. M., KOCH, M., FARNDALE, R. W., LISMAN, T., SONNENBERG, A., LENTING, P. J. & MEYAARD, L. 2006. Collagens are functional, high affinity ligands for the inhibitory immune receptor LAIR-1. *J Exp Med,* 203**,** 1419-25.

LEBBINK, R. J., DE RUITER, T., KAPTIJN, G. J., BIHAN, D. G., JANSEN, C. A., LENTING, P. J. & MEYAARD, L. 2007. Mouse leukocyte-associated Ig-like receptor-1 (mLAIR-1) functions as an inhibitory collagen-binding receptor on immune cells. *Int Immunol,* 19**,** 1011-9.

LEBBINK, R. J., DE RUITER, T., VERBRUGGE, A., BRIL, W. S. & MEYAARD, L. 2004. The mouse homologue of the leukocyte-associated Ig-like receptor-1 is an inhibitory receptor that recruits Src homology region 2-containing protein tyrosine phosphatase (SHP)-2, but not SHP-1. *J Immunol,* 172**,** 5535-43.

LEBBINK, R. J., RAYNAL, N., DE RUITER, T., BIHAN, D. G., FARNDALE, R. W. & MEYAARD, L. 2009. Identification of multiple potent binding sites for human leukocyte associated Ig-like receptor LAIR on collagens II and III. *Matrix Biol,* 28**,** 202-10.

LEBLANC, R. & PEYRUCHAUD, O. 2016. Metastasis: new functional implications of platelets and megakaryocytes. *Blood,* 128**,** 24-31.

LECINE, P., VILLEVAL, J. L., VYAS, P., SWENCKI, B., XU, Y. & SHIVDASANI, R. A. 1998. Mice lacking transcription factor NF-E2 provide in vivo validation of the proplatelet model of thrombocytopoiesis and show a platelet production defect that is intrinsic to megakaryocytes. *Blood,* 92**,** 1608-16.

LEFRANCAIS, E., ORTIZ-MUNOZ, G., CAUDRILLIER, A., MALLAVIA, B., LIU, F., SAYAH, D. M., THORNTON, E. E., HEADLEY, M. B., DAVID, T., COUGHLIN, S. R., KRUMMEL, M. F., LEAVITT, A. D., PASSEGUE, E. & LOONEY, M. R. 2017. The lung is a site of platelet biogenesis and a reservoir for haematopoietic progenitors. *Nature,* 544**,** 105-109.

LERTKIATMONGKOL, P., LIAO, D., MEI, H., HU, Y. & NEWMAN, P. J. 2016. Endothelial functions of platelet/endothelial cell adhesion molecule-1 (CD31). *Curr Opin Hematol,* 23**,** 253-9.

LI, Z., DELANEY, M. K., O'BRIEN, K. A. & DU, X. 2010. Signaling during platelet adhesion and activation. *Arterioscler Thromb Vasc Biol,* 30**,** 2341-9.

LIEVENS, D. & VON HUNDELSHAUSEN, P. 2011. Platelets in atherosclerosis. *Thromb Haemost,* 106**,** 827-38.

LINDEMANN, S., KRAMER, B., SEIZER, P. & GAWAZ, M. 2007. Platelets, inflammation and atherosclerosis. *J Thromb Haemost,* 5 Suppl 1**,** 203-11.

LOWE, K. L., FINNEY, B. A., DEPPERMANN, C., HAGERLING, R., GAZIT, S. L., FRAMPTON, J., BUCKLEY, C., CAMERER, E., NIESWANDT, B., KIEFER, F. & WATSON, S. P. 2015. Podoplanin and CLEC-2 drive cerebrovascular patterning and integrity during development. *Blood,* 125**,** 3769-77.

MA, L., PERINI, R., MCKNIGHT, W., DICAY, M., KLEIN, A., HOLLENBERG, M. D. & WALLACE, J. L. 2005. Proteinase-activated receptors 1 and 4 counter-regulate endostatin and VEGF release from human platelets. *Proc Natl Acad Sci U S A,* 102**,** 216-20.

MAASHO, K., MASILAMANI, M., VALAS, R., BASU, S., COLIGAN, J. E. & BORREGO, F. 2005. The inhibitory leukocyte-associated Ig-like receptor-1 (LAIR-1) is expressed at high levels by human naive T cells and inhibits TCR mediated activation. *Mol Immunol,* 42**,** 1521-30.

MACHLUS, K. R. & ITALIANO, J. E., JR. 2013. The incredible journey: From megakaryocyte development to platelet formation. *J Cell Biol,* 201**,** 785-96.

MACHLUS, K. R., JOHNSON, K. E., KULENTHIRARAJAN, R., FORWARD, J. A., TIPPY, M. D., SOUSSOU, T. S., EL-HUSAYNI, S. H., WU, S. K., WANG, S., WATNICK, R. S., ITALIANO, J. E., JR. & BATTINELLI, E. M. 2016. CCL5 derived from platelets increases megakaryocyte proplatelet formation. *Blood,* 127**,** 921-6.

MACHLUS, K. R., THON, J. N. & ITALIANO, J. E., JR. 2014. Interpreting the developmental dance of the megakaryocyte: a review of the cellular and molecular processes mediating platelet formation. *Br J Haematol,* 165**,** 227-36.

MAHOOTI, S., GRAESSER, D., PATIL, S., NEWMAN, P., DUNCAN, G., MAK, T. & MADRI, J. A. 2000. PECAM-1 (CD31) expression modulates bleeding time in vivo. *Am J Pathol,* 157**,** 75-81.

MAMMADOVA-BACH, E., OLLIVIER, V., LOYAU, S., SCHAFF, M., DUMONT, B., FAVIER, R., FREYBURGER, G., LATGER-CANNARD, V., NIESWANDT, B., GACHET, C., MANGIN, P. H. & JANDROT-PERRUS, M. 2015. Platelet glycoprotein VI binds to polymerized fibrin and promotes thrombin generation. *Blood,* 126**,** 683-91.

MAXWELL, M. J., WESTEIN, E., NESBITT, W. S., GIULIANO, S., DOPHEIDE, S. M. & JACKSON, S. P. 2007. Identification of a 2-stage platelet aggregation process mediating shear-dependent thrombus formation. *Blood,* 109**,** 566-76.

MAZHARIAN, A., GHEVAERT, C., ZHANG, L., MASSBERG, S. & WATSON, S. P. 2011. Dasatinib enhances megakaryocyte differentiation but inhibits platelet formation. *Blood,* 117**,** 5198-206.

MAZHARIAN, A., MORI, J., WANG, Y. J., HEISING, S., NEEL, B. G., WATSON, S. P. & SENIS, Y. A. 2013. Megakaryocyte-specific deletion of the protein-tyrosine phosphatases Shp1 and Shp2 causes abnormal megakaryocyte development, platelet production, and function. *Blood,* 121**,** 4205-20.

MAZHARIAN, A., THOMAS, S. G., DHANJAL, T. S., BUCKLEY, C. D. & WATSON, S. P. 2010. Critical role of Src-Syk-PLC{gamma}2 signaling in megakaryocyte migration and thrombopoiesis. *Blood,* 116**,** 793-800.

MAZHARIAN, A., WANG, Y. J., MORI, J., BEM, D., FINNEY, B., HEISING, S., GISSEN, P., WHITE, J. G., BERNDT, M. C., GARDINER, E. E., NIESWANDT, B., DOUGLAS, M. R., CAMPBELL, R. D., WATSON, S. P. & SENIS, Y. A. 2012. Mice lacking the ITIM-containing receptor G6b-B exhibit macrothrombocytopenia and aberrant platelet function. *Sci Signal,* 5**,** ra78.

MAZHARIAN, A., WATSON, S. P. & SEVERIN, S. 2009. Critical role for ERK1/2 in bone marrow and fetal liver-derived primary megakaryocyte differentiation, motility, and proplatelet formation. *Exp Hematol,* 37**,** 1238-1249.e5.

MAZZUCCO, L., BORZINI, P. & GOPE, R. 2010. Platelet-derived factors involved in tissue repair-from signal to function. *Transfus Med Rev,* 24**,** 218-34.

MCARTHUR, K., CHAPPAZ, S. & KILE, B. T. 2018. Apoptosis in megakaryocytes and platelets: the life and death of a lineage. *Blood,* 131**,** 605-610.

MCDONALD, B., URRUTIA, R., YIPP, B. G., JENNE, C. N. & KUBES, P. 2012. Intravascular neutrophil extracellular traps capture bacteria from the bloodstream during sepsis. *Cell Host Microbe,* 12**,** 324-33.

MELHEM, M., ABU-FARHA, M., ANTONY, D., MADHOUN, A. A., BACCHELLI, C., ALKAYAL, F., ALKHAIRI, I., JOHN, S., ALOMARI, M., BEALES, P. L. & ALSMADI, O. 2017. Novel G6B gene variant causes familial autosomal recessive thrombocytopenia and anemia. *Eur J Haematol,* 98**,** 218-227.

MENTER, D. G., KOPETZ, S., HAWK, E., SOOD, A. K., LOREE, J. M., GRESELE, P. & HONN, K. V. 2017. Platelet "first responders" in wound response, cancer, and metastasis. *Cancer Metastasis Rev,* 36**,** 199-213.

MERLO, A., TENCA, C., FAIS, F., BATTINI, L., CICCONE, E., GROSSI, C. E. & SAVERINO, D. 2005. Inhibitory receptors CD85j, LAIR-1, and CD152 down-regulate immunoglobulin and cytokine production by human B lymphocytes. *Clin Diagn Lab Immunol,* 12**,** 705-12.

MERTEN, M. & THIAGARAJAN, P. 2000. P-selectin expression on platelets determines size and stability of platelet aggregates. *Circulation,* 102**,** 1931-6.

MEYAARD, L. 2008. The inhibitory collagen receptor LAIR-1 (CD305). *J Leukoc Biol,* 83**,** 799-803.

MEYAARD, L. 2010. LAIR and collagens in immune regulation. *Immunol Lett,* 128**,** 26-8.

MEYAARD, L., ADEMA, G. J., CHANG, C., WOOLLATT, E., SUTHERLAND, G. R., LANIER, L. L. & PHILLIPS, J. H. 1997. LAIR-1, a novel inhibitory receptor expressed on human mononuclear leukocytes. *Immunity,* 7**,** 283-90.

MEYAARD, L., HURENKAMP, J., CLEVERS, H., LANIER, L. L. & PHILLIPS, J. H. 1999. Leukocyte-associated Ig-like receptor-1 functions as an inhibitory receptor on cytotoxic T cells. *J Immunol,* 162**,** 5800-4.

MING, Z., HU, Y., XIANG, J., POLEWSKI, P., NEWMAN, P. J. & NEWMAN, D. K. 2011. Lyn and PECAM-1 function as interdependent inhibitors of platelet aggregation. *Blood,* 117**,** 3903-6.

MOEBIUS, J., ZAHEDI, R. P., LEWANDROWSKI, U., BERGER, C., WALTER, U. & SICKMANN, A. 2005. The human platelet membrane proteome reveals several new potential membrane proteins. *Mol Cell Proteomics,* 4**,** 1754-61.

MORAES, L. A., BARRETT, N. E., JONES, C. I., HOLBROOK, L. M., SPYRIDON, M., SAGE, T., NEWMAN, D. K. & GIBBINS, J. M. 2010. Platelet endothelial cell adhesion molecule-1 regulates collagen-stimulated platelet function by modulating the association of phosphatidylinositol 3-kinase with Grb-2-associated binding protein-1 and linker for activation of T cells. *J Thromb Haemost,* 8**,** 2530-41.

MORALES-ORTIZ, J., DEAL, V., REYES, F., MALDONADO-MARTINEZ, G., LEDESMA, N., STABACK, F., CROFT, C., PACHECO, A., ORTIZ-ZUAZAGA, H., YOST, C. C., ROWLEY, J. W., MADERA, B., ST JOHN, A., CHEN, J., LOPEZ, J., RONDINA, M. T., HUNTER, R., GIBSON, A. & WASHINGTON, A. V. 2018a. TLT-1 is a Prognostic Indicator in ALI/ARDS and Prevents Tissue Damage in the Lungs in a Mouse model. *Blood*.

MORALES-ORTIZ, J., RONDINA, M. T., BROWN, S. M., GRISSOM, C. & WASHINGTON, A. V. 2018b. High Levels of Soluble Triggering Receptor Expressed on Myeloid Cells-Like Transcript (TLT)-1 Are Associated With Acute Respiratory Distress Syndrome. *Clin Appl Thromb Hemost,* 24**,** 1122-1127.

MORALES, J., VILLA, K., GATTIS, J., CASTRO, W., COLON, K., LUBKOWSKI, J., SANABRIA, P., HUNTER, R. & WASHINGTON, A. V. 2010. Soluble TLT-1 modulates platelet-endothelial cell interactions and actin polymerization. *Blood Coagul Fibrinolysis,* 21**,** 229-36.

MORI, J., NAGY, Z., DI NUNZIO, G., SMITH, C. W., GEER, M. J., AL GHAITHI, R., VAN GEFFEN, J. P., HEISING, S., BOOTHMAN, L., TULLEMANS, B. M. E., CORREIA, J. N., TEE, L., KUIJPERS, M. J. E., HARRISON, P., HEEMSKERK, J. W. M., JARVIS, G. E., TARAKHOVSKY, A., WEISS, A., MAZHARIAN, A. & SENIS, Y. A. 2018. Maintenance of murine platelet homeostasis by the kinase Csk and phosphatase CD148. *Blood,* 131**,** 1122-1144.

MORI, J., PEARCE, A. C., SPALTON, J. C., GRYGIELSKA, B., EBLE, J. A., TOMLINSON, M. G., SENIS, Y. A. & WATSON, S. P. 2008. G6b-B inhibits constitutive and agonist-induced signaling by glycoprotein VI and CLEC-2. *J Biol Chem,* 283**,** 35419-27.

MORI, J., WANG, Y. J., ELLISON, S., HEISING, S., NEEL, B. G., TREMBLAY, M. L., WATSON, S. P. & SENIS, Y. A. 2012. Dominant role of the protein-tyrosine phosphatase CD148 in regulating platelet activation relative to protein-tyrosine phosphatase-1B. *Arterioscler Thromb Vasc Biol,* 32**,** 2956-65.

MORRELL, C. N., AGGREY, A. A., CHAPMAN, L. M. & MODJESKI, K. L. 2014. Emerging roles for platelets as immune and inflammatory cells. *Blood,* 123**,** 2759-67.

MUTA, T., KUROSAKI, T., MISULOVIN, Z., SANCHEZ, M., NUSSENZWEIG, M. C. & RAVETCH, J. V. 1994. A 13-amino-acid motif in the cytoplasmic domain of Fc gamma RIIB modulates B-cell receptor signalling. *Nature,* 368**,** 70-3.

MUTHARD, R. W. & DIAMOND, S. L. 2013. Side view thrombosis microfluidic device with controllable wall shear rate and transthrombus pressure gradient. *Lab Chip,* 13**,** 1883-91.

NAGATA, Y., MURO, Y. & TODOKORO, K. 1997. Thrombopoietin-induced polyploidization of bone marrow megakaryocytes is due to a unique regulatory mechanism in late mitosis. *J Cell Biol,* 139**,** 449-57.

NAGY, Z. & SMOLENSKI, A. 2018. Cyclic nucleotide-dependent inhibitory signaling interweaves with activating pathways to determine platelet responses. *Res Pract Thromb Haemost,* 2**,** 558-571.

NESBITT, W. S., WESTEIN, E., TOVAR-LOPEZ, F. J., TOLOUEI, E., MITCHELL, A., FU, J., CARBERRY, J., FOURAS, A. & JACKSON, S. P. 2009. A shear gradient-dependent platelet aggregation mechanism drives thrombus formation. *Nat Med,* 15**,** 665-73.

NEWLAND, S. A., MACAULAY, I. C., FLOTO, A. R., DE VET, E. C., OUWEHAND, W. H., WATKINS, N. A., LYONS, P. A. & CAMPBELL, D. R. 2007. The novel inhibitory receptor G6B is expressed on the surface of platelets and attenuates platelet function in vitro. *Blood,* 109**,** 4806-9.

NEWMAN, P. J., BERNDT, M. C., GORSKI, J., WHITE, G. C., 2ND, LYMAN, S., PADDOCK, C. & MULLER, W. A. 1990. PECAM-1 (CD31) cloning and relation to adhesion molecules of the immunoglobulin gene superfamily. *Science,* 247**,** 1219-22.

NEWMAN, P. J. & NEWMAN, D. K. 2013. Chapter 15 - PECAM-1. *In:* MICHELSON, A. D. (ed.) *Platelets (Third Edition).* Academic Press.

NIESWANDT, B., BERGMEIER, W., SCHULTE, V., RACKEBRANDT, K., GESSNER, J. E. & ZIRNGIBL, H. 2000. Expression and function of the mouse collagen receptor glycoprotein VI is strictly dependent on its association with the FcRgamma chain. *J Biol Chem,* 275**,** 23998-4002.

NIESWANDT, B., VARGA-SZABO, D. & ELVERS, M. 2009. Integrins in platelet activation. *J Thromb Haemost,* 7 Suppl 1**,** 206-9.

NIESWANDT, B. & WATSON, S. P. 2003. Platelet-collagen interaction: is GPVI the central receptor? *Blood,* 102**,** 449-61.

NISHIMURA, S., MANABE, I., NAGASAKI, M., KAKUTA, S., IWAKURA, Y., TAKAYAMA, N., OOEHARA, J., OTSU, M., KAMIYA, A., PETRICH, B. G., URANO, T., KADONO, T., SATO, S., AIBA, A., YAMASHITA, H., SUGIURA, S., KADOWAKI, T., NAKAUCHI, H., ETO, K. & NAGAI, R. 2012. In vivo imaging visualizes discoid platelet aggregations without endothelium disruption and implicates contribution of inflammatory cytokine and integrin signaling. *Blood,* 119**,** e45-56.

NURDEN, A. T., NURDEN, P., SANCHEZ, M., ANDIA, I. & ANITUA, E. 2008. Platelets and wound healing. *Front Biosci,* 13**,** 3532-48.

OFFERMANNS, S. 2006. Activation of platelet function through G protein-coupled receptors. *Circ Res,* 99**,** 1293-304.

ONSELAER, M. B., HARDY, A. T., WILSON, C., SANCHEZ, X., BABAR, A. K., MILLER, J. L. C., WATSON, C. N., WATSON, S. K., BONNA, A., PHILIPPOU, H., HERR, A. B., MEZZANO, D., ARIENS, R. A. S. & WATSON, S. P. 2017. Fibrin and D-dimer bind to monomeric GPVI. *Blood Adv,* 1**,** 1495-1504.

OSADA, M., INOUE, O., DING, G., SHIRAI, T., ICHISE, H., HIRAYAMA, K., TAKANO, K., YATOMI, Y., HIRASHIMA, M., FUJII, H., SUZUKI-INOUE, K. & OZAKI, Y. 2012. Platelet activation receptor CLEC-2 regulates blood/lymphatic vessel separation by inhibiting proliferation, migration, and tube formation of lymphatic endothelial cells. *J Biol Chem,* 287**,** 22241-52.

OSTRAKHOVITCH, E. A. & LI, S. S. 2006. The role of SLAM family receptors in immune cell signaling. *Biochem Cell Biol,* 84**,** 832-43.

OUYANG, W., MA, D., LIN, D., SUN, Y., LIU, X., LI, Q., JIA, W., CAO, Y., ZHU, Y. & JIN, B. 2003. 9.1C3 is identical to LAIR-1, which is expressed on hematopoietic progenitors. *Biochem Biophys Res Commun,* 310**,** 1236-40.

PACKHAM, M. A. 1994. Role of platelets in thrombosis and hemostasis. *Can J Physiol Pharmacol,* 72**,** 278-84.

PADDOCK, C., LYTLE, B. L., PETERSON, F. C., HOLYST, T., NEWMAN, P. J., VOLKMAN, B. F. & NEWMAN, D. K. 2011. Residues within a lipid-associated segment of the PECAM-1 cytoplasmic domain are susceptible to inducible, sequential phosphorylation. *Blood,* 117**,** 6012-23.

PALABRICA, T., LOBB, R., FURIE, B. C., ARONOVITZ, M., BENJAMIN, C., HSU, Y. M., SAJER, S. A. & FURIE, B. 1992. Leukocyte accumulation promoting fibrin deposition is mediated in vivo by P-selectin on adherent platelets. *Nature,* 359**,** 848-51.

PATEL, S. R., RICHARDSON, J. L., SCHULZE, H., KAHLE, E., GALJART, N., DRABEK, K., SHIVDASANI, R. A., HARTWIG, J. H. & ITALIANO, J. E., JR. 2005. Differential roles of microtubule assembly and sliding in proplatelet formation by megakaryocytes. *Blood,* 106**,** 4076-85.

PATIL, S., NEWMAN, D. K. & NEWMAN, P. J. 2001. Platelet endothelial cell adhesion molecule-1 serves as an inhibitory receptor that modulates platelet responses to collagen. *Blood,* 97**,** 1727-32.

PIKE, J. A., STYLES, I. B., RAPPOPORT, J. Z. & HEATH, J. K. 2017. Quantifying receptor trafficking and colocalization with confocal microscopy. *Methods,* 115**,** 42-54.

POGGI, A., CATELLANI, S., BRUZZONE, A., CALIGARIS-CAPPIO, F., GOBBI, M. & ZOCCHI, M. R. 2008. Lack of the leukocyte-associated Ig-like receptor-1 expression in high-risk chronic lymphocytic leukaemia results in the absence of a negative signal regulating kinase activation and cell division. *Leukemia,* 22**,** 980-8.

POGGI, A., TOMASELLO, E., REVELLO, V., NANNI, L., COSTA, P. & MORETTA, L. 1997. p40 molecule regulates NK cell activation mediated by NK receptors for HLA class I antigens and TCR-mediated triggering of T lymphocytes. *Int Immunol,* 9**,** 1271-9.

POLLITT, A. Y., HUGHES, C. E. & WATSON, S. P. 2013. Chapter 11 - GPVI and CLEC-2. *In:* MICHELSON, A. D. (ed.) *Platelets (Third Edition).* Academic Press.

POOLE, A., GIBBINS, J. M., TURNER, M., VAN VUGT, M. J., VAN DE WINKEL, J. G., SAITO, T., TYBULEWICZ, V. L. & WATSON, S. P. 1997. The Fc receptor gamma-chain and the tyrosine kinase Syk are essential for activation of mouse platelets by collagen. *Embo j,* 16**,** 2333-41.

PRAKASH, P., NAYAK, M. K. & CHAUHAN, A. K. 2017. P-selectin can promote thrombus propagation independently of both von Willebrand factor and thrombospondin-1 in mice. *J Thromb Haemost,* 15**,** 388-394.

QUACH, M. E., CHEN, W. & LI, R. 2018. Mechanisms of platelet clearance and translation to improve platelet storage. *Blood,* 131**,** 1512-1521.

RADLEY, J. M. & HALLER, C. J. 1982. The demarcation membrane system of the megakaryocyte: a misnomer? *Blood,* 60**,** 213-9.

RADLEY, J. M. & HARTSHORN, M. A. 1987. Megakaryocyte fragments and the microtubule coil. *Blood Cells,* 12**,** 603-14.

RASLOVA, H., ROY, L., VOURC'H, C., LE COUEDIC, J. P., BRISON, O., METIVIER, D., FEUNTEUN, J., KROEMER, G., DEBILI, N. & VAINCHENKER, W. 2003. Megakaryocyte polyploidization is associated with a functional gene amplification. *Blood,* 101**,** 541-4.

RAVID, K., LU, J., ZIMMET, J. M. & JONES, M. R. 2002. Roads to polyploidy: the megakaryocyte example. *J Cell Physiol,* 190**,** 7-20.

REININGER, A. J. 2008. Function of von Willebrand factor in haemostasis and thrombosis. *Haemophilia,* 14 Suppl 5**,** 11-26.

RETH, M. 1989. Antigen receptor tail clue. *Nature,* 338**,** 383-4.

RICHARDSON, J. L., SHIVDASANI, R. A., BOERS, C., HARTWIG, J. H. & ITALIANO, J. E., JR. 2005. Mechanisms of organelle transport and capture along proplatelets during platelet production. *Blood,* 106**,** 4066-75.

RONDINA, M. T. & WEYRICH, A. S. 2015. Regulation of the genetic code in megakaryocytes and platelets. *J Thromb Haemost,* 13 Suppl 1**,** S26-32.

RUGGERI, Z. M. & JACKSON, S. P. 2013. Chapter 20 - Platelet Thrombus Formation in Flowing Blood. *In:* MICHELSON, A. D. (ed.) *Platelets (Third Edition).* Academic Press.

SABRI, S., FOUDI, A., BOUKOUR, S., FRANC, B., CHARRIER, S., JANDROT-PERRUS, M., FARNDALE, R. W., JALIL, A., BLUNDELL, M. P., CRAMER, E. M., LOUACHE, F., DEBILI, N., THRASHER, A. J. & VAINCHENKER, W. 2006. Deficiency in the Wiskott-Aldrich protein induces premature proplatelet formation and platelet production in the bone marrow compartment. *Blood,* 108**,** 134-40.

SABRI, S., JANDROT-PERRUS, M., BERTOGLIO, J., FARNDALE, R. W., MAS, V. M., DEBILI, N. & VAINCHENKER, W. 2004. Differential regulation of actin stress fiber assembly and proplatelet formation by alpha2beta1 integrin and GPVI in human megakaryocytes. *Blood,* 104**,** 3117-25.

SACHS, U. J., ANDREI-SELMER, C. L., MANIAR, A., WEISS, T., PADDOCK, C., ORLOVA, V. V., CHOI, E. Y., NEWMAN, P. J., PREISSNER, K. T., CHAVAKIS, T. & SANTOSO, S. 2007. The neutrophil-specific antigen CD177 is a counter-receptor for platelet endothelial cell adhesion molecule-1 (CD31). *J Biol Chem,* 282**,** 23603-12.

SAKURAI, Y., HARDY, E. T., AHN, B., TRAN, R., FAY, M. E., CICILIANO, J. C., MANNINO, R. G., MYERS, D. R., QIU, Y., CARDEN, M. A., BALDWIN, W. H., MEEKS, S. L., GILBERT, G. E., JOBE, S. M. & LAM, W. A. 2018. A microengineered vascularized bleeding model that integrates the principal components of hemostasis. *Nat Commun,* 9**,** 509.

SANJUAN-PLA, A., MACAULAY, I. C., JENSEN, C. T., WOLL, P. S., LUIS, T. C., MEAD, A., MOORE, S., CARELLA, C., MATSUOKA, S., BOURIEZ JONES, T., CHOWDHURY, O., STENSON, L., LUTTEROPP, M., GREEN, J. C., FACCHINI, R., BOUKARABILA, H., GROVER, A., GAMBARDELLA, A., THONGJUEA, S., CARRELHA, J., TARRANT, P., ATKINSON, D., CLARK, S. A., NERLOV, C. & JACOBSEN, S. E. 2013. Platelet-biased stem cells reside at the apex of the haematopoietic stem-cell hierarchy. *Nature,* 502**,** 232-6.

SAVERINO, D., FABBI, M., MERLO, A., RAVERA, G., GROSSI, C. E. & CICCONE, E. 2002. Surface density expression of the leukocyte-associated Ig-like receptor-1 is directly related to inhibition of human T-cell functions. *Hum Immunol,* 63**,** 534-46.

SCHMITT, A., GUICHARD, J., MASSE, J. M., DEBILI, N. & CRAMER, E. M. 2001. Of mice and men: comparison of the ultrastructure of megakaryocytes and platelets. *Exp Hematol,* 29**,** 1295-302.

SCHULZE, H., KORPAL, M., HUROV, J., KIM, S. W., ZHANG, J., CANTLEY, L. C., GRAF, T. & SHIVDASANI, R. A. 2006. Characterization of the megakaryocyte demarcation membrane system and its role in thrombopoiesis. *Blood,* 107**,** 3868-75.

SEHGAL, S. & STORRIE, B. 2007. Evidence that differential packaging of the major platelet granule proteins von Willebrand factor and fibrinogen can support their differential release. *J Thromb Haemost,* 5**,** 2009-16.

SEMENIAK, D., KULAWIG, R., STEGNER, D., MEYER, I., SCHWIEBERT, S., BOSING, H., ECKES, B., NIESWANDT, B. & SCHULZE, H. 2016. Proplatelet formation is selectively inhibited by collagen type I through Syk-independent GPVI signaling. *J Cell Sci,* 129**,** 3473-84.

SENIS, Y. A. 2013. Protein-tyrosine phosphatases: a new frontier in platelet signal transduction. *J Thromb Haemost,* 11**,** 1800-13.

SENIS, Y. A., MAZHARIAN, A. & MORI, J. 2014. Src family kinases: at the forefront of platelet activation. *Blood,* 124**,** 2013-24.

SENIS, Y. A., TOMLINSON, M. G., ELLISON, S., MAZHARIAN, A., LIM, J., ZHAO, Y., KORNERUP, K. N., AUGER, J. M., THOMAS, S. G., DHANJAL, T., KALIA, N., ZHU, J. W., WEISS, A. & WATSON, S. P. 2009. The tyrosine phosphatase CD148 is an essential positive regulator of platelet activation and thrombosis. *Blood,* 113**,** 4942-54.

SENIS, Y. A., TOMLINSON, M. G., GARCIA, A., DUMON, S., HEATH, V. L., HERBERT, J., COBBOLD, S. P., SPALTON, J. C., AYMAN, S., ANTROBUS, R., ZITZMANN, N., BICKNELL, R., FRAMPTON, J., AUTHI,

K. S., MARTIN, A., WAKELAM, M. J. & WATSON, S. P. 2007. A comprehensive proteomics and genomics analysis reveals novel transmembrane proteins in human platelets and mouse megakaryocytes including G6b-B, a novel immunoreceptor tyrosine-based inhibitory motif protein. *Mol Cell Proteomics,* 6**,** 548-64.

SEVERIN, S., NASH, C. A., MORI, J., ZHAO, Y., ABRAM, C., LOWELL, C. A., SENIS, Y. A. & WATSON, S. P. 2012. Distinct and overlapping functional roles of Src family kinases in mouse platelets. *J Thromb Haemost,* 10**,** 1631-45.

SEVERIN, S., POLLITT, A. Y., NAVARRO-NUNEZ, L., NASH, C. A., MOURAO-SA, D., EBLE, J. A., SENIS, Y. A. & WATSON, S. P. 2011. Syk-dependent phosphorylation of CLEC-2: a novel mechanism of hem-immunoreceptor tyrosine-based activation motif signaling. *J Biol Chem,* 286**,** 4107-16.

SHIN, J. Y., HU, W., NARAMURA, M. & PARK, C. Y. 2014. High c-Kit expression identifies hematopoietic stem cells with impaired self-renewal and megakaryocytic bias. *J Exp Med,* 211**,** 217-31.

SMITH, C. W., RASLAN, Z., PARFITT, L., KHAN, A. O., PATEL, P., SENIS, Y. A. & MAZHARIAN, A. 2018. TREM-like transcript 1: a more sensitive marker of platelet activation than P-selectin in humans and mice. *Blood Adv,* 2**,** 2072-2078.

SMITH, C. W., THOMAS, S. G., RASLAN, Z., PATEL, P., BYRNE, M., LORDKIPANIDZE, M., BEM, D., MEYAARD, L., SENIS, Y. A., WATSON, S. P. & MAZHARIAN, A. 2017. Mice Lacking the Inhibitory Collagen Receptor LAIR-1 Exhibit a Mild Thrombocytosis and Hyperactive Platelets. *Arterioscler Thromb Vasc Biol,* 37**,** 823-835.

SOMMER, C., STRAEHLE, C., KÖTHE, U. & HAMPRECHT, F. A. Ilastik: Interactive learning and segmentation toolkit. 2011 IEEE International Symposium on Biomedical Imaging: From Nano to Macro, 30 March-2 April 2011 2011. 230-233.

SORRENTINO, S., STUDT, J. D., MEDALIA, O. & TANUJ SAPRA, K. 2015. Roll, adhere, spread and contract: structural mechanics of platelet function. *Eur J Cell Biol,* 94**,** 129-38.

SPALTON, J. C., MORI, J., POLLITT, A. Y., HUGHES, C. E., EBLE, J. A. & WATSON, S. P. 2009. The novel Syk inhibitor R406 reveals mechanistic differences in the initiation of GPVI and CLEC-2 signaling in platelets. *J Thromb Haemost,* 7**,** 1192-9.

STALKER, T. J., TRAXLER, E. A., WU, J., WANNEMACHER, K. M., CERMIGNANO, S. L., VORONOV, R., DIAMOND, S. L. & BRASS, L. F. 2013. Hierarchical organization in the hemostatic response and its relationship to the platelet-signaling network. *Blood,* 121**,** 1875-85.

STEEVELS, T. A., WESTERLAKEN, G. H., TIJSSEN, M. R., COFFER, P. J., LENTING, P. J., AKKERMAN, J. W. & MEYAARD, L. 2010. Co-expression of the collagen receptors leukocyte-associated immunoglobulin-like receptor-1 and glycoprotein VI on a subset of megakaryoblasts. *Haematologica,* 95**,** 2005-12.

STEGNER, D., VANEEUWIJK, J. M. M., ANGAY, O., GORELASHVILI, M. G., SEMENIAK, D., PINNECKER, J., SCHMITHAUSEN, P., MEYER, I., FRIEDRICH, M., DUTTING, S., BREDE, C., BEILHACK, A., SCHULZE, H., NIESWANDT, B. & HEINZE, K. G. 2017. Thrombopoiesis is spatially regulated by the bone marrow vasculature. *Nat Commun,* 8**,** 127.

SUZUKI-INOUE, K. 2017. CLEC-2/podoplanin and thromboinflammation. *Blood,* 129**,** 1896-1898.

SUZUKI-INOUE, K., FULLER, G. L., GARCIA, A., EBLE, J. A., POHLMANN, S., INOUE, O., GARTNER, T. K., HUGHAN, S. C., PEARCE, A. C., LAING, G. D., THEAKSTON, R. D., SCHWEIGHOFFER, E., ZITZMANN, N., MORITA, T., TYBULEWICZ, V. L., OZAKI, Y. & WATSON, S. P. 2006. A novel Syk-dependent mechanism of platelet activation by the C-type lectin receptor CLEC-2. *Blood,* 107**,** 542-9.

SUZUKI-INOUE, K., KATO, Y., INOUE, O., KANEKO, M. K., MISHIMA, K., YATOMI, Y., YAMAZAKI, Y., NARIMATSU, H. & OZAKI, Y. 2007. Involvement of the snake toxin receptor CLEC-2, in podoplanin-mediated platelet activation, by cancer cells. *J Biol Chem,* 282**,** 25993-6001.

SUZUKI-INOUE, K., TULASNE, D., SHEN, Y., BORI-SANZ, T., INOUE, O., JUNG, S. M., MOROI, M., ANDREWS, R. K., BERNDT, M. C. & WATSON, S. P. 2002. Association of Fyn and Lyn with the

proline-rich domain of glycoprotein VI regulates intracellular signaling. *J Biol Chem,* 277**,** 21561-6.

TANENBAUM, M. E., VALE, R. D. & MCKENNEY, R. J. 2013. Cytoplasmic dynein crosslinks and slides anti-parallel microtubules using its two motor domains. *Elife,* 2**,** e00943.

TANG, X., TIAN, L., ESTESO, G., CHOI, S. C., BARROW, A. D., COLONNA, M., BORREGO, F. & COLIGAN, J. E. 2012. Leukocyte-associated Ig-like receptor-1-deficient mice have an altered immune cell phenotype. *J Immunol,* 188**,** 548-58.

TAVASSOLI, M. & AOKI, M. 1989. Localization of megakaryocytes in the bone marrow. *Blood Cells,* 15**,** 3-14.

THOMAS, M. R. & STOREY, R. F. 2015. The role of platelets in inflammation. *Thromb Haemost,* 114**,** 449-58.

THON, J. N., MACLEOD, H., BEGONJA, A. J., ZHU, J., LEE, K. C., MOGILNER, A., HARTWIG, J. H. & ITALIANO, J. E., JR. 2012. Microtubule and cortical forces determine platelet size during vascular platelet production. *Nat Commun,* 3**,** 852.

THON, J. N., MONTALVO, A., PATEL-HETT, S., DEVINE, M. T., RICHARDSON, J. L., EHRLICHER, A., LARSON, M. K., HOFFMEISTER, K., HARTWIG, J. H. & ITALIANO, J. E., JR. 2010. Cytoskeletal mechanics of proplatelet maturation and platelet release. *J Cell Biol,* 191**,** 861-74.

TOMAIUOLO, M., BRASS, L. F. & STALKER, T. J. 2017. Regulation of Platelet Activation and Coagulation and Its Role in Vascular Injury and Arterial Thrombosis. *Interv Cardiol Clin,* 6**,** 1-12.

TOMLINSON, M. G., CALAMINUS, S. D., BERLANGA, O., AUGER, J. M., BORI-SANZ, T., MEYAARD, L. & WATSON, S. P. 2007. Collagen promotes sustained glycoprotein VI signaling in platelets and cell lines. *J Thromb Haemost,* 5**,** 2274-83.

TOURDOT, B. E., BRENNER, M. K., KEOUGH, K. C., HOLYST, T., NEWMAN, P. J. & NEWMAN, D. K. 2013. Immunoreceptor tyrosine-based inhibitory motif (ITIM)-mediated inhibitory signaling is regulated by sequential phosphorylation mediated by distinct nonreceptor tyrosine kinases: a case study involving PECAM-1. *Biochemistry,* 52**,** 2597-608.

VAN GESTEL, M. A., HEEMSKERK, J. W., SLAAF, D. W., HEIJNEN, V. V., SAGE, S. O., RENEMAN, R. S. & OUDE EGBRINK, M. G. 2002. Real-time detection of activation patterns in individual platelets during thromboembolism in vivo: differences between thrombus growth and embolus formation. *J Vasc Res,* 39**,** 534-43.

VAN NISPEN TOT PANNERDEN, H., DE HAAS, F., GEERTS, W., POSTHUMA, G., VAN DIJK, S. & HEIJNEN, H. F. 2010. The platelet interior revisited: electron tomography reveals tubular alpha-granule subtypes. *Blood,* 116**,** 1147-56.

VANDENDRIES, E. R., HAMILTON, J. R., COUGHLIN, S. R., FURIE, B. & FURIE, B. C. 2007. Par4 is required for platelet thrombus propagation but not fibrin generation in a mouse model of thrombosis. *Proc Natl Acad Sci U S A,* 104**,** 288-92.

VERBRUGGE, A., RIJKERS, E. S., DE RUITER, T. & MEYAARD, L. 2006. Leukocyte-associated Ig-like receptor-1 has SH2 domain-containing phosphatase-independent function and recruits C-terminal Src kinase. *Eur J Immunol,* 36**,** 190-8.

VERBRUGGE, A., RUITER TD, T., CLEVERS, H. & MEYAARD, L. 2003. Differential contribution of the immunoreceptor tyrosine-based inhibitory motifs of human leukocyte-associated Ig-like receptor-1 to inhibitory function and phosphatase recruitment. *Int Immunol,* 15**,** 1349-58.

VITRAT, N., COHEN-SOLAL, K., PIQUE, C., LE COUEDIC, J. P., NOROL, F., LARSEN, A. K., KATZ, A., VAINCHENKER, W. & DEBILI, N. 1998. Endomitosis of human megakaryocytes are due to abortive mitosis. *Blood,* 91**,** 3711-23.

VOLLMAR, B., SCHMITS, R., KUNZ, D. & MENGER, M. D. 2001. Lack of in vivo function of CD31 in vascular thrombosis. *Thromb Haemost,* 85**,** 160-4.

WALSH, T. G., METHAROM, P. & BERNDT, M. C. 2015. The functional role of platelets in the regulation of angiogenesis. *Platelets,* 26**,** 199-211.

WASHINGTON, A. V., GIBOT, S., ACEVEDO, I., GATTIS, J., QUIGLEY, L., FELTZ, R., DE LA MOTA, A., SCHUBERT, R. L., GOMEZ-RODRIGUEZ, J., CHENG, J., DUTRA, A., PAK, E., CHERTOV, O., RIVERA, L., MORALES, J., LUBKOWSKI, J., HUNTER, R., SCHWARTZBERG, P. L. & MCVICAR, D. W. 2009. TREM-like transcript-1 protects against inflammation-associated hemorrhage by facilitating platelet aggregation in mice and humans. *J Clin Invest,* 119**,** 1489-501.

WASHINGTON, A. V., QUIGLEY, L. & MCVICAR, D. W. 2002. Initial characterization of TREM-like transcript (TLT)-1: a putative inhibitory receptor within the TREM cluster. *Blood,* 100**,** 3822-4.

WASHINGTON, A. V., SCHUBERT, R. L., QUIGLEY, L., DISIPIO, T., FELTZ, R., CHO, E. H. & MCVICAR, D. W. 2004. A TREM family member, TLT-1, is found exclusively in the alpha-granules of megakaryocytes and platelets. *Blood,* 104**,** 1042-7.

WATSON, A. A., CHRISTOU, C. M., JAMES, J. R., FENTON-MAY, A. E., MONCAYO, G. E., MISTRY, A. R., DAVIS, S. J., GILBERT, R. J. C., CHAKERA, A. & O'CALLAGHAN, C. A. 2009. The Platelet Receptor CLEC-2 Is Active as a Dimer. *Biochemistry,* 48**,** 10988-10996.

WATSON, S. P., AUGER, J. M., MCCARTY, O. J. & PEARCE, A. C. 2005. GPVI and integrin alphaIIb beta3 signaling in platelets. *J Thromb Haemost,* 3**,** 1752-62.

WATSON, S. P., HERBERT, J. M. & POLLITT, A. Y. 2010. GPVI and CLEC-2 in hemostasis and vascular integrity. *J Thromb Haemost,* 8**,** 1456-67.

WEE, J. L. & JACKSON, D. E. 2005. The Ig-ITIM superfamily member PECAM-1 regulates the "outside-in" signaling properties of integrin alpha(IIb)beta3 in platelets. *Blood,* 106**,** 3816-23.

WELSH, J. D., POVENTUD-FUENTES, I., SAMPIETRO, S., DIAMOND, S. L., STALKER, T. J. & BRASS, L. F. 2017. Hierarchical organization of the hemostatic response to penetrating injuries in the mouse macrovasculature. *J Thromb Haemost,* 15**,** 526-537.

WHITE, J. G. 1969. The dense bodies of human platelets: inherent electron opacity of the serotonin storage particles. *Blood,* 33**,** 598-606.

WHITE, J. G. 2013. Chapter 7 - Platelet Structure. *In:* MICHELSON, A. D. (ed.) *Platelets (Third Edition).* Academic Press.

WHITEHEART, S. W. 2011. Platelet granules: surprise packages. *Blood,* 118**,** 1190-1.

WONG, C., LIU, Y., YIP, J., CHAND, R., WEE, J. L., OATES, L., NIESWANDT, B., REHEMAN, A., NI, H., BEAUCHEMIN, N. & JACKSON, D. E. 2009. CEACAM1 negatively regulates platelet-collagen interactions and thrombus growth in vitro and in vivo. *Blood,* 113**,** 1818-28.

WOOLTHUIS, C. M. & PARK, C. Y. 2016. Hematopoietic stem/progenitor cell commitment to the megakaryocyte lineage. *Blood,* 127**,** 1242-8.

WU, Y., WELTE, T., MICHAUD, M. & MADRI, J. A. 2007. PECAM-1: a multifaceted regulator of megakaryocytopoiesis. *Blood,* 110**,** 851-9.

XU, M., ZHAO, R. & ZHAO, Z. J. 2000. Identification and characterization of leukocyte-associated Ig-like receptor-1 as a major anchor protein of tyrosine phosphatase SHP-1 in hematopoietic cells. *J Biol Chem,* 275**,** 17440-6.

XUE, J., ZHANG, X., ZHAO, H., FU, Q., CAO, Y., WANG, Y., FENG, X. & FU, A. 2011. Leukocyte-associated immunoglobulin-like receptor-1 is expressed on human megakaryocytes and negatively regulates the maturation of primary megakaryocytic progenitors and cell line. *Biochem Biophys Res Commun,* 405**,** 128-33.

YEAMAN, M. R. 2010a. Bacterial-platelet interactions: virulence meets host defense. *Future Microbiol,* 5**,** 471-506.

YEAMAN, M. R. 2010b. Platelets in defense against bacterial pathogens. *Cell Mol Life Sci,* 67**,** 525-44.

YIP, J., ALSHAHRANI, M., BEAUCHEMIN, N. & JACKSON, D. E. 2016. CEACAM1 regulates integrin alphaIIbbeta3-mediated functions in platelets. *Platelets,* 27**,** 168-77.

ZEBHAUSER, R., KAMMERER, R., EISENRIED, A., MCLELLAN, A., MOORE, T. & ZIMMERMANN, W. 2005. Identification of a novel group of evolutionarily conserved members within the rapidly diverging murine Cea family. *Genomics,* 86**,** 566-80.

ZEIGLER, F. C., DE SAUVAGE, F., WIDMER, H. R., KELLER, G. A., DONAHUE, C., SCHREIBER, R. D., MALLOY, B., HASS, P., EATON, D. & MATTHEWS, W. 1994. In vitro megakaryocytopoietic and thrombopoietic activity of c-mpl ligand (TPO) on purified murine hematopoietic stem cells. *Blood,* 84**,** 4045-52.

ZEILER, M., MOSER, M. & MANN, M. 2014. Copy number analysis of the murine platelet proteome spanning the complete abundance range. *Mol Cell Proteomics,* 13**,** 3435-45.

ZHANG, L., ORBAN, M., LORENZ, M., BAROCKE, V., BRAUN, D., URTZ, N., SCHULZ, C., VON BRUHL, M. L., TIRNICERIU, A., GAERTNER, F., PROIA, R. L., GRAF, T., BOLZ, S. S., MONTANEZ, E., PRINZ, M., MULLER, A., VON BAUMGARTEN, L., BILLICH, A., SIXT, M., FASSLER, R., VON ANDRIAN, U. H., JUNT, T. & MASSBERG, S. 2012. A novel role of sphingosine 1-phosphate receptor S1pr1 in mouse thrombopoiesis. *J Exp Med,* 209**,** 2165-81.

ZHENG, J., UMIKAWA, M., CUI, C., LI, J., CHEN, X., ZHANG, C., HUYNH, H., KANG, X., SILVANY, R., WAN, X., YE, J., CANTO, A. P., CHEN, S. H., WANG, H. Y., WARD, E. S. & ZHANG, C. C. 2012. Inhibitory receptors bind ANGPTLs and support blood stem cells and leukaemia development. *Nature,* 485**,** 656-60.

ZHU, S., HERBIG, B. A., LI, R., COLACE, T. V., MUTHARD, R. W., NEEVES, K. B. & DIAMOND, S. L. 2015. In microfluidico: Recreating in vivo hemodynamics using miniaturized devices. *Biorheology,* 52**,** 303-18.

ZOU, Z., SCHMAIER, A. A., CHENG, L., MERICKO, P., DICKESON, S. K., STRICKER, T. P., SANTORO, S. A. & KAHN, M. L. 2009. Negative regulation of activated alpha-2 integrins during thrombopoiesis. *Blood,* 113**,** 6428-39.